

---

**PLANT GENES WITH MEIOTIC  
FUNCTION: FROM THEIR  
IDENTIFICATION TOWARD  
BIOTECH EXPLOITATION**

---

**Riccardo Aiese Cigliano**

Dottorato in Scienze Biotechnologiche – XXIV ciclo  
Indirizzo Biotecnologie per le Produzioni Vegetali  
Università di Napoli Federico II





Dottorato in Scienze Biotecnologiche –XXIV ciclo  
Indirizzo Biotecnologie per le Produzioni Vegetali  
Università di Napoli Federico II



---

**PLANT GENES WITH MEIOTIC  
FUNCTION: FROM THEIR  
IDENTIFICATION TOWARD  
BIOTECH EXPLOITATION**

---

**Riccardo Aiese Cigliano**

Dottorando: Riccardo Aiese Cigliano

Relatore: Dott.ssa Clara Conicella

Correlatore: Dott.ssa Federica Consiglio

Coordinatore: Prof. Giovanni Sannia



*Alla mia famiglia*



## **INDEX**

### **PLANT GENES WITH MEIOTIC FUNCTION: FROM THEIR IDENTIFICATION TOWARD BIOTECH EXPLOITATION**

|  |           |
|--|-----------|
| <b>SUMMARY</b>   | <b>3</b>  |
| <b>RIASSUNTO</b>   | <b>9</b>  |
| <b>1. INTRODUCTION</b>   | <b>15</b> |
| 1.1. Preliminary Remarks   | 15        |
| 1.2. Meiosis and plant sexual reproduction   | 16        |
| 1.3. Identification of meiotic genes in plants   | 18        |
| 1.3.1. Meiotic genes as biotechnological tools for crop breeding                                       | 19        |
| 1.4. Chromatin structure and histone modifications   | 26        |
| 1.4.1. Histone modifications and meiosis   | 27        |
| 1.5. Aims and activities of PhD thesis   | 30        |
| <b>2. MATERIALS &amp; METHODS</b>  | <b>31</b> |
| 2.1. Plant materials and growth conditions   | 31        |
| 2.2. Selection of candidate meiotic genes in <i>Arabidopsis thaliana</i>                               | 31        |
| 2.2.1. Microarray data analysis  | 31        |
| 2.2.2. Identification of <i>Arabidopsis</i> HATs and HDACs most similar genes in other model organisms | 32        |
| 2.3. <i>HDA7 in silico</i> analysis  | 33        |
| 2.4. Analysis of gene coregulation   | 33        |
| 2.5. amiRNA design and plasmid construction  | 34        |
| 2.6. <i>Arabidopsis</i> transformation   | 35        |
| 2.7. Nucleic acid extraction   | 35        |
| 2.8. Expression analysis   | 35        |
| 2.9. Analysis of fertility associated traits   | 36        |
| 2.10. Potato <i>PSL</i> cloning and sequence analysis  | 36        |
| 2.11. Identification of unannotated <i>PSL</i> genes   | 37        |
| 2.12. <i>PSL</i> molecular phylogenetic analysis   | 38        |
| 2.13. <i>PSL</i> domain analysis   | 39        |
| 2.14. Comparison of dN-dS values between <i>PSL</i> sequences  | 39        |
| 2.15. Statistical analyses   | 39        |

|   |            |
|---|------------|
| <b>3. RESULTS</b>   | <b>40</b>  |
| <b>3.1. Identification of histone acetylases (HATs) and deacetylases (HDACs) with putative role in <i>Arabidopsis</i> meiosis/reproduction by <i>in silico</i> analysis</b> | <b>40</b>  |
| <b>3.2. Functional characterization of <i>Arabidopsis HDA7</i> gene by loss-of-function and gain-of-function strategies</b>   | <b>43</b>  |
| 3.2.1. <i>In silico</i> analysis of <i>HDA7</i>   | 44         |
| 3.2.2. Analysis of <i>HDA7</i> mutants  | 46         |
| <b>3.3. Reverse genetics of putative meiotic genes affected by histone acetylation by screening of insertional lines</b>  | <b>58</b>  |
| <b>3.4. Isolation of <i>PARALLEL SPINDLES LIKE (PSL)</i> genes in potato and evolutive analysis of PSLs in <i>Viridiplantae</i></b>   | <b>61</b>  |
| <b>4. DISCUSSION</b>  | <b>75</b>  |
| <b>4.1. Identification of HATs/HDACs with putative role in <i>Arabidopsis</i> meiosis/reproduction</b>  | <b>75</b>  |
| <b>4.2. Functional characterization of <i>Arabidopsis HDA7</i> gene</b>   | <b>77</b>  |
| <b>4.3. Reverse genetics of putative meiotic genes affected by histone acetylation</b>  | <b>85</b>  |
| <b>4.4. Evolution of <i>PARALLEL SPINDLES LIKE (PSL)</i> in potato and <i>Viridiplantae</i></b>   | <b>86</b>  |
| <b>5. CONCLUDING REMARKS</b>  | <b>91</b>  |
| <b>6. BIBLIOGRAPHY</b>  | <b>93</b>  |
| <b>RESEARCH ACTIVITY IN FOREIGN LABORATORIES</b>  | <b>110</b> |
| <b>APPENDIX</b>   | <b>111</b> |

## SUMMARY

Plant reproductive organs such as seeds and fruits represent the main source of food for human nutrition. The knowledge of the processes that ensure successful outcomes of plant reproduction is pivotal to guarantee higher and stable food production. Meiosis is a specialized cell division, consisting of two successive divisions without intervening DNA synthesis, that is crucial in the sexual reproduction. Peculiar features of meiosis are pairing and crossovers between homologous chromosomes, as well as random segregation of homologs. As a consequence, meiotic cells (meiocytes) give rise to four cells with haploid number of chromosomes and new set of allelic combinations. In contrast to animals, which form gametes directly by meiosis, plants form male and female spores by meiotic division during micro- and megasporogenesis, respectively. The spores develop by mitotic divisions and cell differentiation into the male and female gametophytes during micro- and megagametogenesis, respectively. The two morphologically distinct gametophytes, pollen and embryo sac, ultimately give rise to the gametes. Double fertilization of the female gametes by one sperm cell each produce embryo and endosperm initiating seed development.

The knowledge of the genetic control of meiosis is useful to provide new tools for plant breeding. Indeed, a deep understanding of the mechanisms controlling genetic recombination and chromosome assortment would allow breeders to manipulate genetic diversity and genetic uniformity. In particular, increase/decrease and redistribution of crossovers as well as meiotic nuclear restitution modes in  $2n$  gametes pave the way to control the transmission of valuable traits. Based on this premise, the PhD project points to the identification of genes that are involved in meiotic recombination and nuclear restitution in model organism *Arabidopsis thaliana* and in potato, respectively. The specific aims and activities of PhD project are summarized as follows:

- **To investigate the role of histone acetylation/deacetylation in plant meiosis through reverse genetics strategy in *Arabidopsis*;**

- To isolate **PARALLEL SPINDLES LIKE (PSL)** genes in potato and to study the evolutive history of PSLs in *Viridiplantae*.

### **Histone acetylation and reproduction in *Arabidopsis***

Histones constitute the fundamental unit of chromatin which is the nucleosome. Histones are characterized by a protruding N-terminal tail, which participates to the interaction with DNA and with other chromatin associated proteins, that can be target of a multitude of post-translational modifications among which acetylation is the most studied. In *Arabidopsis*, histone acetylation/deacetylation is performed by 12 predicted histone acetylases (HATs) and 18 predicted deacetylases (HDACs). Many of these genes were linked to several aspects of plant development such as gametogenesis, flowering time and flower organogenesis, root growth and development, embryo development and seedling growth, seed development, light signaling, RNA-directed DNA methylation, rDNA silencing and response to jasmonate and to abiotic and biotic stress. Mutations in different HATs and HDACs showed a low seed set thereby suggesting a role in reproduction. However, a meiotic function was attributed so far only to HAT *AtMCC1* and HDAC *AtHDA19*. *AtMCC1* overexpression and *AtHDA19* disruption, both leading to histone hyperacetylation, caused changes in meiotic recombination and defects in chromosome segregation. In particular, Perrella and colleagues (2010) showed in *Atmcc1* microsporocytes that crossovers increased in chromosome 4 while decreased in chromosome 1 and in chromosome 2. In the latter, the obligate crossover failed leading to unpaired homologs.

In this PhD project, *Arabidopsis* HATs and HDACs were firstly analyzed *in silico* in order to find the best candidates for a meiotic function. The adopted strategy aimed to the identification of genes overexpressed in reproductive respect to vegetative tissues and similar to genes involved in reproduction in other model organisms. By this way, *HAG2*, *HAG1*, *HAM1* and *HAF1* resulted the strongest HAT candidates while *HDA7*, *HDA6*, *HDA9* and *HDA19* were the strongest not only among HDACs but also among HATs. RNA interference mediated by artificial microRNA (amiRNA) was chosen as strategy to study the function of the meiotic candidates. In this work it is reported the functional analysis of *HDA7*, which resulted

highly expressed in flowers and to be similar to genes involved in reproduction in *S. cerevisiae*, *D. melanogaster* and *M. musculus*. The constitutive expression of amiRNA (amiHDA7) in *Arabidopsis* led to *HDA7* silencing. Moreover, analysis of the mutants showed altered expression levels of other histone deacetylases such as *HDA6* and *HDA9*, which resulted up-regulated, and *HDA19* which was only slightly down-regulated. The functional analysis reported in this work was performed through the characterization of amiHDA7 expressing mutant (*hda7-2*) and of a previous identified T-DNA mutant showing *HDA7* over-expression (*hda7<sup>oe</sup>*). By this way, *HDA7* revealed its role both in reproductive and vegetative development in *Arabidopsis*. Indeed, a significant reduction of 20% for seed set due to embryo sac collapse in *hda7-2* plants highlighted that *HDA7* has an important function in female gametophyte development. In addition, reduction of about 20% of germination rate, slower post-germination growth and delayed embryo development likely associated to shrunken seeds evidenced that *HDA7* down-regulation affects also vegetative growth. Interestingly, *HDA7* up-regulation had a different phenotype except for a reduction of about 20% of germination rate similarly to *hda7-2*. Indeed, female gametophyte was not affected by *HDA7* over-expression while seedlings showed both faster and slower post-germination growth respect to wild type. Given that no obvious alterations were observed in embryos we speculate that subtle defects occurring during germination cause germination rate decrease in *hda7<sup>oe</sup>*. *In silico* identification of *HDA7* co-regulated genes, both during embryo development and in flowers, allowed the identification of *AtAESP*, *AtUBP14* and *BRITTLE* as target candidates of *HDA7* regulation. These genes could likely explain the defects observed in *hda7-2*, which is also supported by the evidence of *AtAESP* downregulation in *hda7-2*. Together, these data reveal a general requirement of histone deacetylation for proper embryo development as previously showed through the functional analysis of other HDACs such as *HDA19*, *HDA6*, *HD2A* and *HD2C*. Moreover, for the first time we highlight that an HDAC is required for proper megagametophyte development. This work has been supported by EU7FP project “Systematic Analysis of Factors Controlling Meiotic Recombination in Higher Plants (MeioSys)”.

*Arabidopsis thaliana* was also used to investigate the causes of the meiotic defects observed in histone hyperacetylated mutant *Atmcc1*. Indeed, previous experiments identified 150 differentially expressed

genes in the microsporocytes of *Atmcc1* respect to the wild type. In this work, 16 candidate genes putatively involved in cell-cycle, protein metabolism and chromosome dynamics which were up-regulated in *Atmcc1* were chosen to assess their role in plant meiosis. For each gene one or more T-DNA insertional lines were obtained from Germplasm Stock Centers and screened for seed set phenotype. None of the selected lines showed a drop of fertility. Functional redundancy, partial knock-out as well as lack of T-DNA insertions should be ascertained in these lines.

### **Isolation of *PARALLEL SPINDLES* gene in potato**

Polyploidy represents the occurrence of more than two complete sets of chromosomes in an organism and has long been recognized as playing an important role in plant evolution. It is widely accepted that almost all angiosperms are ancient polyploids having experienced one or more round of whole genome duplication. Nowadays, the major route for polyploid formation is considered to be the production of  $2n$  gametes which were observed in several plant species including crops. Among them, the tuber-bearing potato (*Solanum tuberosum*) and its wild relatives are of particular interest for the study of polyploidization and many surveys to ascertain the genetic base of  $2n$  gametes production were conducted in these species. With regard to  $2n$  pollen production, Peloquin and colleagues (1975) reported that mutants showing parallel instead of perpendicular spindles in the second meiotic division are characterized by a recessive mutation in the gene *PARALLEL SPINDLES* (*PS*). Despite the genetic basis of  $2n$  pollen production has been widely investigated in potato, molecular insights into this phenomenon remained sketchy. Only recently, genes *PS1* and *JASON* isolated in *Arabidopsis* were showed to be involved in  $2n$  pollen production. *AtPS1* encodes a protein which contains contemporarily a ForkHead Associated domain (FHA), and a C-terminal PiIT N-terminus domain (PINc). The first has been found in thousands of different proteins from prokaryotes to higher eukaryotes being involved in several processes including cell cycle control, DNA repair, protein degradation, transcription and pre-mRNA splicing. PINc domain shows RNA nuclease activity and has been found in more than 3600 proteins in all life kingdoms. On the basis of the sequences of FHA and PINc encoding regions, a reverse genetics approach was carried out to identify the homologue of *AtPS1* in a potato clone which does

not produce  $2n$  pollen. Cloning and *in silico* analyses showed the presence of three *PS-Like* (*PSL1* to *PSL3*) genes. Among them, *PSL1* was the most similar to *AtPS1* as regards the PINc active sites and, therefore, it is the best candidate for future functional characterization and manipulation of  $2n$  pollen production in potato and likely other crops. Molecular analysis showed, in pre-bolting buds, that potato *PSL* genes encode splicing variants with Premature Termination Codons (PTC) which could be involved in the regulation of *PSL* expression through Nonsense Mediated mRNA Decay (NMD). When *PSL* sequences were blasted against the sequenced potato genome only one *PSL* gene, corresponding to *PSL1*, was identified. Analysis of available RNA-seq data highlighted that *PSL1* is mainly expressed in reproductive tissues. In order to investigate the evolution of *PSL* family, we retrieved *PSL* sequences in 20 *Viridiplantae*. One *PSL* locus was found in the analyzed species, except for *Glycine max*. Indeed, four different *PSL* loci were identified in soybean and three of them encode alternative transcripts. Differently from potato, the alternative transcripts of soybean do not show PTCs thus likely playing a different role respect to their potato counterparts. The analysis of FHA and PINc domains evidenced that, in terms of secondary structure, a major degree of variability occurred in PINc domain respect to FHA. In terms of specific active sites, both domains showed diversification among plant species that could be related to a functional diversification among *PSL* genes. Vice versa, some specific active sites were strongly conserved among plants as supported by sequence alignment and by evidence of negative selection evaluated as difference between non-synonymous and synonymous mutations. The results obtained on *PSL* genes were published on BMC Evolutionary Biology.

In conclusion, the present work provided candidate histone acetylases and deacetylases for a meiotic role in *Arabidopsis*. Moreover, the involvement of *HDA7* in proper megagametophyte development and in vegetative growth was showed for the first time in *Arabidopsis*. The meiotic function of *HDA7* is currently under investigation to assess if defects during megasporogenesis are the causes of embryo sac collapse and to verify if crossover distribution and/or frequency is changed in microsporocytes. The work conducted on *PSLs* family highlighted the importance of these genes in plant evolution and pave the way to the manipulation of nuclear

restitution mechanisms in potato which could be very useful for plant breeding.

## RIASSUNTO

La conoscenza dei processi che assicurano il successo riproduttivo delle piante è fondamentale poiché i prodotti finali della riproduzione, semi e frutti, rappresentano la fonte principale di cibo per l'alimentazione umana. La meiosi è l'evento cruciale della riproduzione sessuale e corrisponde ad un particolare programma di divisione cellulare costituito da due divisioni successive precedute da un solo ciclo di replicazione del DNA. Tra le caratteristiche peculiari della meiosi si ricordano l'appaiamento e la ricombinazione tra i cromosomi omologhi e la loro segregazione casuale. Le cellule meiotiche diploidi (meiociti) originano quattro cellule aploidi recanti nuove combinazioni di alleli. A differenza degli animali, in cui i gameti si originano direttamente dalla meiosi, le piante formano prima spore maschili e femminili durante i rispettivi processi di micro- e megasporogenesi. Successivamente le spore si sviluppano in gametofiti maschili e femminili attraverso una serie di divisioni mitotiche seguite dal differenziamento cellulare durante la micro- e la megagametogenesi, rispettivamente. Infine, i gametofiti che corrispondono al polline e al sacco embrionale originano i gameti. Il ciclo riproduttivo della pianta si conclude con la doppia fecondazione dei gameti femminili (cellula uovo e cellula centrale) da parte dei due nuclei spermatici che originano l'embrione e l'endosperma, avviando così lo sviluppo del seme che si associa a quello del frutto.

La conoscenza del controllo genetico della meiosi è anche di interesse per il miglioramento genetico delle piante. Infatti, una approfondita conoscenza dei meccanismi che controllano la ricombinazione meiotica e la segregazione dei cromosomi potrebbe consentire ai costitutori di nuovi materiali genetici di manipolare la diversità e/o l'uniformità genetica. In particolare, la possibilità di incrementare/ridurre il numero dei *crossing over* o di modificare la loro distribuzione così come la possibilità di manipolare i meccanismi di restituzione nucleare che producono gameti  $2n$  sono importanti per il controllo della trasmissione di caratteri utili. Sulla base di questi presupposti, il presente progetto di dottorato ha avuto lo scopo di identificare i geni che sono coinvolti nella ricombinazione meiotica e nella restituzione nucleare in un organismo modello, *Arabidopsis thaliana*, ed in patata, rispettivamente. Gli scopi specifici e le relative attività del progetto di dottorato sono riassunte di seguito:

- **Investigare il ruolo dell'acetilazione e della deacetilazione istonica in meiosi in *Arabidopsis* utilizzando un approccio di *reverse genetics*;**
- **isolare il gene *PARALLEL SPINDLES LIKE (PSL)* in patata ed analizzare l'evoluzione delle proteine PSLs delle *Viridiplantae*.**

### **Acetilazione istonica e riproduzione in *Arabidopsis***

Gli istoni costituiscono l'unità fondamentale della cromatina che è rappresentata dai nucleosomi. Gli istoni sono proteine caratterizzate da code N-terminali, che partecipano all'interazione con il DNA e con altre proteine associate alla cromatina, che possono essere soggette ad una moltitudine di modifiche post-traduzionali tra cui l'acetilazione è quella più studiata. In *Arabidopsis*, l'acetilazione e la deacetilazione istonica sono effettuate da 12 acetilasi (HAT) e 18 deacetilasi (HDAC) che sono state identificate in modo predittivo con analisi bioinformatiche. Quelle studiate sono risultate coinvolte in diversi aspetti dello sviluppo della pianta come nella gametogenesi, nel tempo di fioritura e nello sviluppo florale, nella crescita e nello sviluppo della radice, nello sviluppo embrionale, nella crescita dei germogli, nello sviluppo del seme, nella fotopercezione, nella metilazione del DNA diretta da RNA, nel silenziamento dell'rDNA e nella risposta al jasmonato ed agli stress biotici ed abiotici. Nonostante diversi mutanti in HAT e HDAC abbiano mostrato una riduzione della produzione di seme, suggerendo un loro coinvolgimento nella riproduzione, solo per l'acetilasi *AtMCC1* e la deacetilasi *AtHDA19* è stato dimostrato un ruolo in meiosi. Infatti, la sovraespressione di *AtMCC1* e l'inattivazione di *AtHDA19*, entrambe causanti iperacetilazione istonica, hanno indotto cambiamenti nella ricombinazione meiotica e difetti nella segregazione dei cromosomi. In particolare, Perrella e collaboratori (2010) hanno evidenziato un aumento dei *crossing over* per il cromosoma 4 ed una riduzione per i cromosomi 1 e 2 con conseguente perdita del *crossing over* obbligato per quest'ultimo nei microsporociti di *Atmcc1*.

Nel corso del presente progetto di dottorato, le HAT e le HDAC di *Arabidopsis* sono state prima analizzate *in silico* per identificare i migliori candidati per un ruolo in meiosi. A questo scopo sono stati identificati i geni sovraespressi in tessuti riproduttivi rispetto a quelli

vegetativi e quelli simili a geni coinvolti in riproduzione in altri organismi modello. In questo modo quattro HAT, *HAG2*, *HAG1*, *HAM1* e *HAF1*, e quattro HDAC, *HDA7*, *HDA6*, *HDA9* e *HDA19*, sono risultati i geni candidati più probabili. La strategia scelta per studiare la funzione dei candidati è stato l'*RNA interference* mediante microRNA artificiali (amiRNA). In particolare, nella presente tesi di dottorato è descritta l'analisi funzionale del gene *HDA7*, che è risultato non solo altamente espresso in fiori ma anche simile a geni coinvolti nella riproduzione di *S. cerevisiae*, *D. melanogaster* e *M. musculus*. L'espressione di un amiRNA specifico (amiHDA7) ha consentito di silenziare *HDA7* in linee mutanti di *Arabidopsis* che hanno inoltre evidenziato un'aumentata espressione dei geni *HDA6* e *HDA9* ed una leggera riduzione dell'espressione di *HDA19*. L'analisi funzionale è stata condotta oltre che sulla linea esprimente l'amiHDA7 (*hda7-2*) anche su una linea T-DNA, precedentemente identificata, caratterizzata dalla sovraespressione di *HDA7* (*hda7<sup>oe</sup>*). L'analisi di entrambe le linee ha evidenziato che *HDA7* ha un ruolo nello sviluppo riproduttivo e vegetativo di *Arabidopsis*. Infatti, una riduzione significativa del 20% di produzione del seme dovuta alla degenerazione di sacchi embrionali nelle piante *hda7-2* ha evidenziato la funzione di *HDA7* nello sviluppo del gametofito femminile. Inoltre, il silenziamento del gene ha determinato una riduzione del 20% del tasso di germinazione, un rallentamento della crescita post-germinativa ed un ritardo dello sviluppo embrionale con conseguente aborto di semi indicando che *HDA7* ha un ruolo anche nello sviluppo vegetativo. L'analisi della linea *hda7<sup>oe</sup>* ha evidenziato un fenotipo diverso rispetto alla linea *hda7-2* ad eccezione di una simile riduzione del 20% del tasso di germinazione. Infatti, lo sviluppo del gametofito femminile non è risultato influenzato dalla sovraespressione di *HDA7* mentre l'analisi della crescita post-germinativa ha mostrato plantule con velocità di crescita sia superiore che inferiore rispetto al controllo. Inoltre, non essendo stati riscontrati difetti evidenti nel corso dello sviluppo embrionale è stato ipotizzato che altre anomalie potrebbero essere la causa della riduzione della germinabilità osservata in *hda7<sup>oe</sup>*. Un'analisi bioinformatica dei geni co-regolati con *HDA7* nel corso dello sviluppo del fiore e dell'embrione ha inoltre consentito di identificare *AtAESP*, *AtUBP14* e *BRITTLE* come possibili bersagli della regolazione di *HDA7* coinvolti nei difetti osservati in *hda7-2*. Complessivamente l'analisi svolta ha evidenziato, per la prima volta, l'importanza della

deacetilazione istonica per lo sviluppo del megagametofito e, come già riportato per altre HDAC (*HDA19*, *HDA6*, *HD2A* e *HD2C*) per un corretto sviluppo embrionale. Questa attività è stata finanziata del progetto europeo “*Systematic Analysis of Factors Controlling Meiotic Recombination in Higher Plants (MeioSys)*” nell’ambito del 7° Programma Quadro.

Il sistema modello *Arabidopsis thaliana* è stato utilizzato nel corso dell’attività di dottorato anche per approfondire la cause dei difetti meiotici osservati nel mutante iperacetilato *Atmcc1*. Precedenti esperimenti di trascrittomica su singola cellula hanno consentito di identificare 150 geni differenzialmente espressi nei microsporociti di *Atmcc1* rispetto al controllo. In questo lavoro, 15 geni candidati, putativamente coinvolti nel ciclo cellulare, nel metabolismo proteico e nella dinamica dei cromosomi, che erano risultati sovrappresi in *Atmcc1* sono stati scelti per analizzarne il ruolo in meiosi. Per ogni gene sono state collezionate una o più linee T-DNA che sono state analizzate per la fertilità della siliqua. Nessuna delle linee selezionate ha però mostrato semisterilità il che potrebbe essere imputabile a diverse cause come la ridondanza funzionale dei geni analizzati, oppure parziale inattivazione dei geni nelle linee T-DNA o completa assenza del T-DNA nelle linee selezionate.

### **Isolamento del gene *PARALLEL SPINDLES LIKE (PSL)* in patata**

La poliploidia consiste nella presenza di più di due *set* completi di cromosomi in un organismo ed è considerata un importante fattore nell’evoluzione delle piante. Infatti, è ampiamente riconosciuto che la maggior parte delle angiosperme sono poliploidi ancestrali che hanno subito uno o più fenomeni di duplicazione completa del genoma. Attualmente si ritiene che la formazione di poliploidi avvenga principalmente attraverso la produzione di gameti  $2n$ , osservati in numerose specie vegetali incluse quelle coltivate. Tra queste, la patata (*Solanum tuberosum*) e le specie selvatiche affini sono di particolare interesse per lo studio della poliploidizzazione. Infatti sono stati condotti numerosi studi in queste specie per determinare la base genetica della produzione di gameti  $2n$ . Per quanto riguarda il polline  $2n$ , Peloquin e collaboratori (1975) hanno riportato che mutanti con fusi meiotici paralleli in meiosi II erano caratterizzati da una mutazione recessiva nel gene *PARALLEL SPINDLES (PS)* ma sconosciute sono rimaste le basi molecolari del

fenomeno. Recentemente in *Arabidopsis* sono stati identificati i geni *PS1* e *JASON* che sono risultati coinvolti nella produzione di polline *2n*. In particolare, *AtPS1* codifica una proteina che contiene un dominio *Forkhead Associated* (FHA) ed un dominio *C-terminal PiIT N-terminus* (PINc). Il dominio FHA descritto in migliaia di proteine codificate in organismi procarioti ed eucarioti superiori è coinvolto in numerosi processi come il controllo del ciclo cellulare, riparo del DNA, degradazione delle proteine, trascrizione e *splicing* del pre-mRNA. Il dominio PINc, invece, è implicato in attività degradativa dell'RNA ed è stato trovato in più di 3600 proteine in tutti gli organismi viventi. Sulla base delle sequenze codificanti i domini FHA e PINc, tramite una strategia di genetica inversa è stato identificato l'omologo di *AtPS1* in un clone di patata che non produce polline *2n*. Esperimenti di clonaggio ed analisi bioinformatiche hanno evidenziato la presenza di tre loci *PS-Like* in patata (*PSL1*, *PSL2* e *PSL3*), tra i quali *PSL1* è il più simile ad *AtPS1* dal punto di vista dei siti attivi del dominio PINc. Di conseguenza, *PSL1* è risultato il candidato più forte per procedere con la caratterizzazione funzionale. Successive analisi molecolari hanno evidenziato che i geni *PSL* codificano, in bocci in pre-antesi, trascritti alternativi caratterizzati da Codoni di Stop Prematuri (CSP) che potrebbero essere coinvolti nella regolazione dei geni *PSL* attraverso il processo *Nonsense Mediated mRNA Decay* (NMD). La ricerca dei geni *PSL* nel genoma sequenziato di patata ha evidenziato un solo locus, corrispondente a *PSL1*, la cui espressione è prevalente nei tessuti riproduttivi, come confermato dai dati di *RNA-seq*. Al fine di studiare l'evoluzione della famiglia *PSL*, è stata condotta una ricerca bioinformatica per identificare gli ortologhi in 20 *Viridiplantae*. Da questa analisi è emerso che in tutte le specie analizzate è presente un solo locus *PSL*, ad eccezione della soia (*Glycine max*) che invece mostra quattro loci *PSL* di cui tre codificano trascritti alternativi privi di CSP. L'analisi delle strutture secondarie predette dei domini FHA e PINc ha evidenziato una notevole variabilità tra le diverse specie analizzate, soprattutto per il dominio PINc. Inoltre, per quanto riguarda i siti attivi dei due domini sono stati evidenziati siti variabili tra le diverse specie, suggerendo una possibile diversificazione funzionale tra i geni *PSL*, mentre altri sono risultati fortemente conservati e soggetti a selezione negativa tra mutazioni sinonime e non.

In conclusione, la presente attività di tesi ha consentito di identificare *in silico* otto geni codificanti acetilasi e deacetilasi istoniche come

candidati per un ruolo meiotico in *Arabidopsis*. Tra questi, *HDA19* precedentemente analizzato aveva evidenziato una funzione meiotica confermando la validità dell'approccio bioinformatico messo a punto in questa tesi. E' stato, inoltre, dimostrato per la prima volta il ruolo funzionale di *HDA7* nello sviluppo del megagametofito. Ulteriori analisi sono in corso per analizzare la megasporogenesi e per verificare la ricombinazione nei microsporociti di *hda7*. Lo studio della famiglia *PSL* ha evidenziato l'importanza evolutiva di questi geni in pianta ponendo le premesse per la manipolazione dei meccanismi di restituzione nucleare meiotica, di notevole interesse per il miglioramento genetico.

# 1. INTRODUCTION

## 1.1. Preliminary Remarks

Plant foods contributing to human nutrition are mainly represented by seeds, fruits and tubers. The main crops cultivated in the world and their edible parts are listed in Table 1. Seeds and fruits are products of plant reproduction processes, sexual or asexual, while tubers deriving from modified stems or roots are products of asexual reproduction. Seeds consisting of both embryo developed from zygote and coat from ovule integuments conclude the plant reproduction cycle. Fruits defined from a botanical point of view as the ripened ovaries usually forming after fertilization (Lewis, 2002) are considered the fleshy seed-associated structures. Inevitably, the production of plant foods rely mostly on the success of plant sexual reproduction. Considering that the reproductive phase in flowering plants is often highly sensitive to environmental stresses (Zinn *et al.*, 2010, Kranner *et al.*, 2010), the impending global climate change, with predicted increment of temperatures ranging from 1.5 to 5.8°C within the present century, pose threats to agricultural production (Rosenzweig *et al.*, 2001). Furthermore, there is a need to dramatically increase food production for feeding the rapidly increasing human population, which is expected to be 9.2 billion by 2050 (<http://esa.un.org/unpd/wpp>). In this landscape, fundamental and applied research of plant reproduction is becoming pivotal to ensure high and stable food production by maintaining the current area of arable fields.

**Table 1. The world most cultivated crops for food. The crops are listed in descending order of Production (P). Botanical name, the Net Production Value (NPV) and the edible organ are reported for each crop. [Data from FAOStat (<http://faostat.fao.org>), 2009].**

| Crop           | Species                     | P (Million tonnes) | NPV (Million US\$) | Edible organ |
|----------------|-----------------------------|--------------------|--------------------|--------------|
| Maize          | <i>Zea mays</i>             | 818.82             | 51.16              | Seed         |
| Wheat          | <i>Triticum spp.</i>        | 685.61             | 86.72              | Seed         |
| Rice           | <i>Oryza sativa</i>         | 685.24             | 178.34             | Seed         |
| Potatoes       | <i>Solanum tuberosum</i>    | 329.58             | 44.13              | Tuber        |
| Cassava        | <i>Manihot esculenta</i>    | 233.80             | 22.71              | Tuber        |
| Soybeans       | <i>Glycine max</i>          | 223.18             | 57.59              | Seed         |
| Tomatoes       | <i>Solanum lycopersicum</i> | 152.96             | 55.89              | Fruit        |
| Sweet potatoes | <i>Ipomea batatas</i>       | 102.30             | 4.75               | Tuber        |
| Watermelons    | <i>Citrullus lanatus</i>    | 98.05              | 10.31              | Fruit        |
| Bananas        | <i>Musa spp.</i>            | 97.38              | 27.02              | Fruit        |

## 1.2. Meiosis and plant sexual reproduction

Meiosis is a specialized cell division program that is exploited by all sexually reproducing organisms for the production of gametes. Meiosis shows some crucial differences respect to mitosis. The first is that homologous chromosomes pair and associate in the early stages of meiosis. The second is that crossovers occur between homologous chromosomes thanks to meiotic recombination, which represents the physical exchange of genetic material between maternal and paternal chromosomes. Meiotic recombination is essential to ensure proper completion of meiosis as well as to produce new genetic combinations in the gametes. The third difference between meiosis and mitosis is the random segregation of homologous chromosomes. Finally, meiosis has a second division with no previous DNA synthesis. As a consequence, meiotic cells (meiocytes) give rise to four cells with haploid chromosome number (Ma, 2006). Differently from diplontic or haplontic organisms, many plant species are diplohaplontic showing an alternance of haploid and diploid generations. Indeed, plant meiosis, which is also called sporogenesis, gives rise to haploid spores (Bateman & DiMichele, 1994). Following mitotic divisions, which represent the gametogenesis, male and female gametes are produced inside the microgametophyte (i.e. pollen) and the megagametophyte (i.e. embryo sac), respectively. Both sporogenesis and gametogenesis take place in specific organs. Indeed, pollen and embryo sac form inside anthers and ovaries, where Pollen Mother Cells (PMCs) and Megaspore Mother Cells (MMCs) are committed to male and female meiosis, respectively (Osman *et al.*, 2011).

Plant meiosis is a tightly regulated process composed by perfect timed stages which are divided in first and second meiotic divisions, (MI and MII, respectively) (Armstrong & Jones, 2003). The meiotic process is very conserved among different organisms. However, some differences exist between monocots and dicots and, therefore, the following description is referred to a dicot such as *Arabidopsis thaliana*. Meiosis I and II are subdivided in prophase, metaphase, anaphase and telophase. The key meiotic steps occurring during prophase I allow the definition of five sub-phases. During leptotema, the homologous chromosomes, each composed by two sister chromatids linked at the centromere as a consequence of premeiotic DNA replication, start to condensate and to pair. ASY1 protein

forming filamentous structures (axial elements) along each chromosome is essential for completion of pairing occurring during zygonema. Axial elements are joined by a central element constituted by polymerized ZYP1 protein thus forming a tripartite Synaptonemal Complex (SC) which tether each pair of homologs (bivalents) (Page & Hawley, 2004). Pachynema is the substage of prophase I during which meiotic recombination occur and the homologs are so strictly paired that they appear as threads. During diplotema, the SC is disassembled and the homologs are visibly connected by chiasmata at the level of crossovers (CO). During diakinesis homolog pairs condense dramatically and move towards the equator of the cell. During metaphase I bivalents are aligned and linked to the meiotic spindle at centromeres so that in anaphase I the homologous chromosomes can segregate at opposite pole of the cell. During telophase I chromosomes partially decondense before starting meiosis II which is mostly similar to mitosis. Indeed, at prophase II chromosomes condense while at metaphase II the two groups of chromosomes are aligned separately at two division planes. During anaphase II sister chromatids segregate at opposite poles while in telophase II four haploid nuclei are formed marking the end of meiosis. At the end of male meiosis, microspores undergo microgametogenesis which is characterized by two haploid mitotic divisions producing two sperm nuclei (the male gametes) and one vegetative nucleus enclosed in the pollen grain (Ma, 2005). On the female side, only one of the four haploid megaspores survives while the others degenerate. The functional megaspore undergoing megagametogenesis develops into the haploid embryo sac (female gametophyte) through three successive mitotic divisions. The embryo sac consists of seven cells including two gametes (the haploid egg cell and the homo-diploid central cell), two synergids and three antipodals (Kägi & Gross-Hardt, 2007).

Following gamete production, double fertilization of female gametes by one sperm cell each occurs in plants to produce zygote and endosperm. Indeed, the pollen grain germinates after reaching the stigma and produces pollen tube which grows inside the stigma and the style and penetrates the embryo sac. One sperm cell fuses with the egg cell while the other one with the central cell giving rise to the diploid zygote and the triploid endosperm, respectively (Grossniklaus & Schneitz, 1998).

### 1.3. Identification of meiotic genes in plants

The model system for the study of plant meiosis is *Arabidopsis thaliana*. The advantages of using *A. thaliana* are its reduced size, the rapid life cycle and the high seed set. Moreover, *Arabidopsis* was the first plant genome sequenced, thanks to its reduced genome size (125 Mb), allowing the development of genetic, molecular and bioinformatic tools to study gene function (Arabidopsis Genome Initiative, 2000).

To date, about 70 meiotic genes have been described in *Arabidopsis* (Chen, *et al.*, 2010a). Most of them have been isolated through approach of forward genetics based on the screening of populations mutagenized by chemicals, physical and/or genetic agents for traits associated to meiotic defects such as silique sterility or semisterility (Hamant *et al.*, 2006). Map-based cloning (in case of chemical/physical mutagenesis) or PCR-based techniques (in case of T-DNA/transposon mutagenesis) combined with cytological analysis have been performed to identify the meiotic genes. Another approach was based on reverse genetics (Caryl *et al.*, 2003). Indeed, the conservation of meiotic process allowed the identification of plant meiotic genes by sequence similarity with other organisms, even those that are distantly related. Moreover, the availability of large datasets of *Arabidopsis* expression data (microarray and RNA-seq) allowed the selection of candidate genes which are preferentially expressed in reproductive tissues and/or coregulated with known meiotic genes (d'Erfurth *et al.*, 2008, d'Erfurth *et al.*, 2009). To ascertain the meiotic role, functional analysis of candidate genes was mostly performed by loss-of-function mutants available at Germplasm Stock Centers including insertional and RNA-silenced lines. So far, silencing of meiotic genes was obtained by expression of hairpin RNA (hpRNA) (Ma, 2006) while artificial miRNA (amiRNA) technology, recently developed to silence single genes as well as gene families (Schwab *et al.*, 2006), has not been applied to meiotic genes, yet. Easiness of cloning and higher specificity are distinctive features of amiRNAs respect to hpRNAs thus making them a valuable tool to study gene function. For this reason, amiRNA approach was performed to silence the candidate genes studied in the present thesis.

### **1.3.1. Meiotic genes as biotechnological tools for crop breeding**

The study of the genetic control of the meiotic process can be useful to provide new tools for plant breeding. Indeed, a deep understanding of the mechanisms controlling genetic recombination and nuclear division would allow breeders to manipulate combination and transmission of valuable traits (Martinez-Perez & Moore, 2008).

#### **1.3.1.1. Manipulating genetic recombination for plant breeding**

Plant breeding is dependent upon recombination for the generation of new genotypes through introgression of useful traits, selection for improved traits and dissociation of undesirable linkage combinations of alleles. The rate and position of meiotic crossovers are thus fundamental aspects that constrain the efficacy of plant breeding. Meiotic recombination is a complex multistep process which involves several proteins acting in a coordinated fashion as represented schematically in Figure 1 (Osman *et al.*, 2011). DNA double strand breaks are induced genome-wide immediately after pre-meiotic DNA replication by the topoisomerase AtSPO11-1/2, which is then removed leaving free DNA 5'-end. Successively, MRE11-RAD50-XRS2 (MRX) complex performs the resection of 5'-end thus leaving 3' protruding tails on the opposite strands. Then RecA homologues, AtRAD51C and AtDMC1, catalyze the invasion of one 3'-ssDNA filament into the homologous chromosome thus forming a D-loop. Either Homologous Recombination (HR) or Synthesis Dependent-Strand Annealing (SDSA) pathways can be used by the cell to process D-loops. The first pathway can lead to crossover (CO) or Non Crossover (NCO), the second produces only NCOs. In the SDSA pathway the invading 3'-end is firstly extended by DNA synthesis then it anneals again to its complementary strand without any exchange of DNA between the homologous chromosomes. Also in the HR pathway the invading 3'-end is firstly extended by DNA synthesis, however one DNA filament of the invaded chromosome anneals to the free strand of its homologue and the invading 3'-end is then captured again by its proper complementary strand. These filament exchanges produce a Double Holliday Junction that can be resolved either producing a CO or a NCO. Despite both HR and SDSA pathways can produce NCOs, an obligate chiasma is ensured for each pair of homologous chromosomes, being pivotal for correct alignment and segregation in metaphase I and anaphase I.

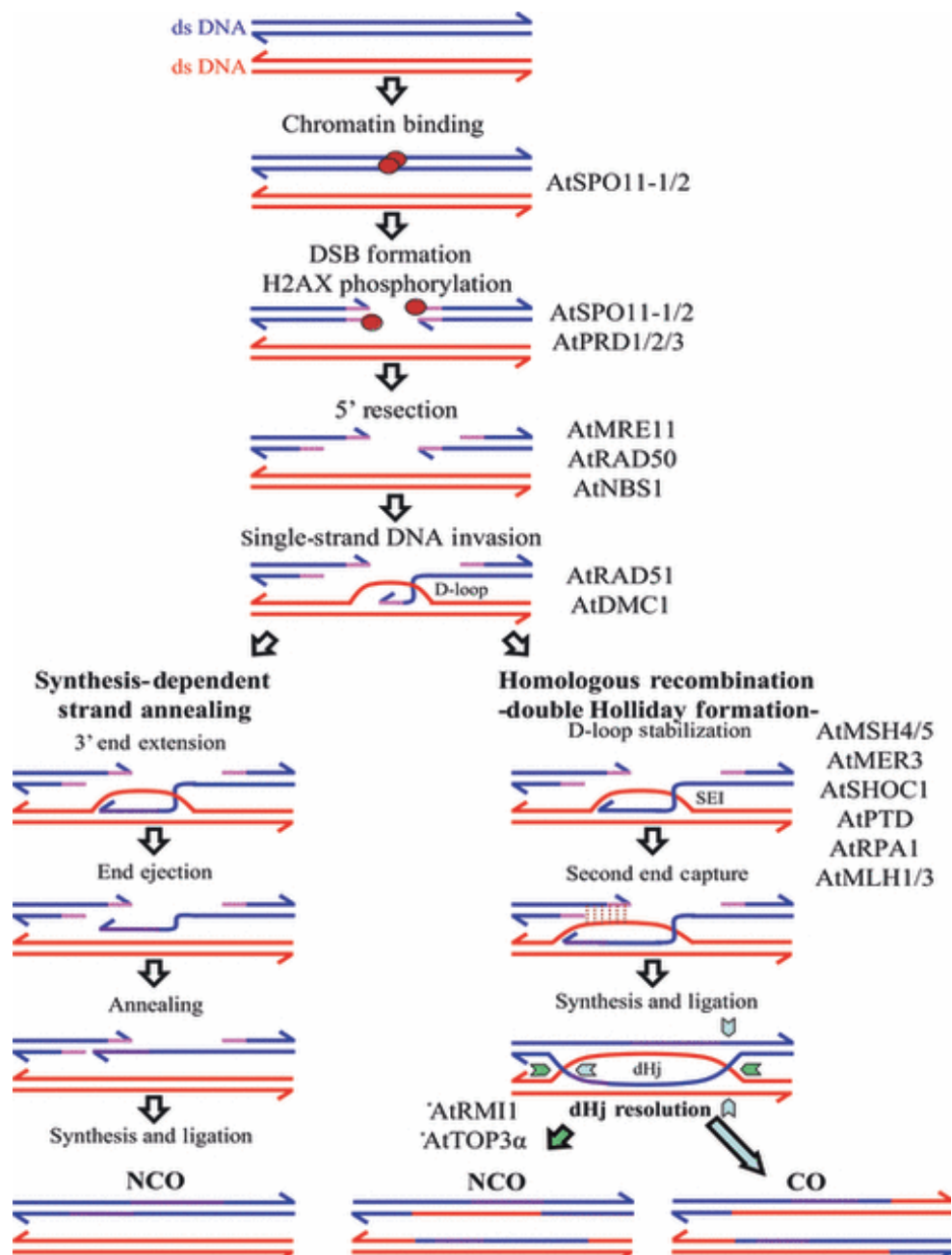
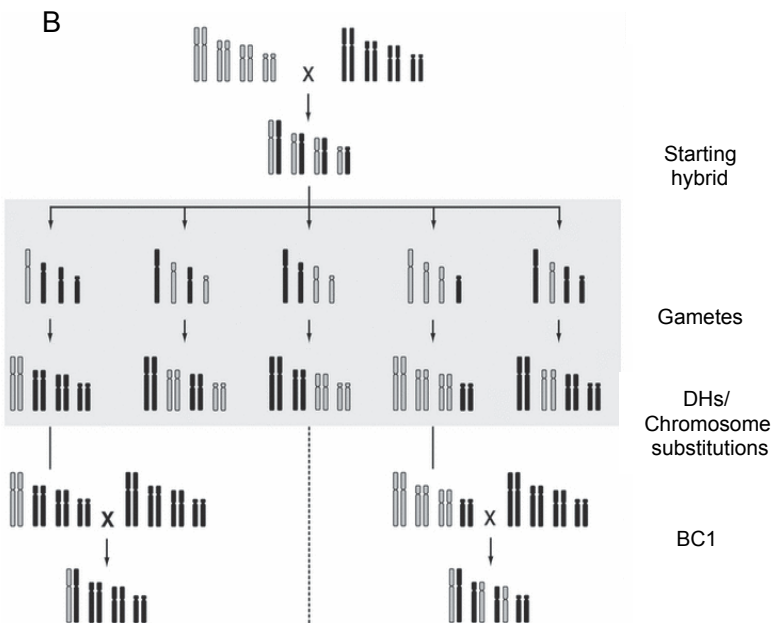
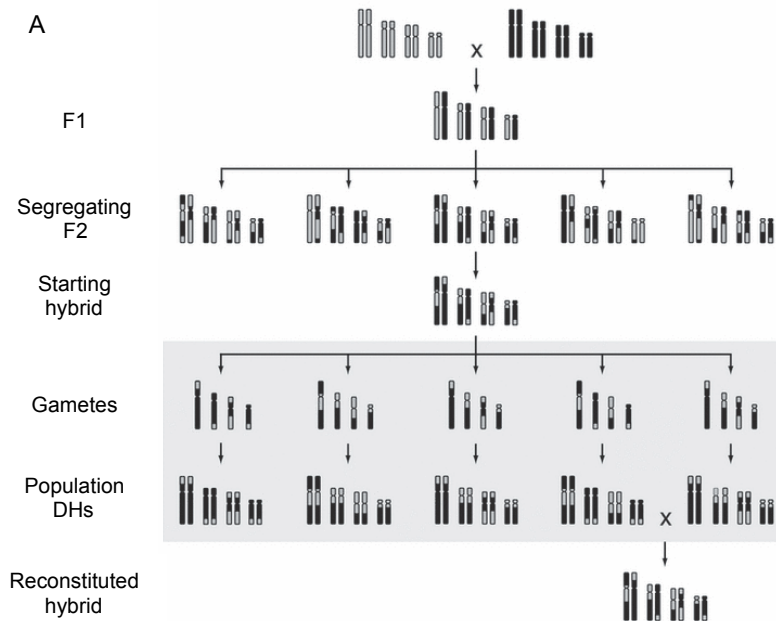


Figure 1. Schematic representation of meiotic recombination pathway in *Arabidopsis thaliana* with DSB site showed in pink (Osman *et al.*, 2011).

Interestingly, the number and the distribution of COs is not random in the genomes (Martinez-Perez & Moore, 2008). The factors which make some regions more suitable for meiotic recombination (hotspots) and others less recombinogenic (coldspots) are mostly unknown. In addition, complex phenomena, like the interference, regulate the positioning of nearby DSBs and COs (Kleckner, 1996). In this complex landscape plant breeders are interested in manipulating frequency and position of COs to increase variation for agronomic, environmental and economically important traits. Chemical/physical treatments in many species such as *Arabidopsis*, barley, *Vicia faba* and *Allium* (Wijnker & De Jong, 2008) allowed to increase CO frequencies.. The manipulation of genes involved in recombination is a promising alternative. Indeed, overexpression of *RAD51* as well as mutations in genes such as *XRAYS4* (*XRS4*) in *Arabidopsis* and overexpression of *MutL Homolog* (*MLH1*) in tomato increased the frequency of meiotic recombination (Wijnker & De Jong, 2008). The control of CO distribution would be equally useful in plant breeding considering that many species preferentially have either terminal (barley, maize, soybean and wheat) or proximal (*Allium* spp.) chiasmata (Ott *et al.*, 2011, Kik, 2002). Mapping studies revealed that in cereals recombination rate is not linearly related to gene content and biased distribution of COs results in substantial genetic blocks that rarely undergo recombination. These linkage blocks are estimated to constitute as much as 30-50% of the genes, effectively preventing access to much of the variability existing within current elite germplasm. However, the factors controlling the distribution of crossovers are far from being fully understood (Paigen *et al.*, 2010). Interestingly, Perrella and colleagues (2010) reported that histone hyperacetylation due to *AtMCC1* overexpression affects the number and distribution of crossover per chromosome without changing the total CO number per cell. In particular, reduction of COs on chromosomes 1 and 2 and increase on chromosome 4 were observed in male meiocytes highlighting that histone acetylation has an important role in plant meiotic recombination.

Reverse breeding is a technique, which relies on the complete absence of COs to propagate F1 hybrids by seeds (Dirks *et al.*, 2009). Total inhibition of COs can be obtained by knocking out genes involved in the early phases of HR such as *SPO11* or *DMC1*. Depending on the chromosome number of the species, a percentage of regular gametes are produced together with aneuploids as a

consequence of the lack of obligate chiasmata. Dihaploids (DHs) are then recovered through *in vitro* culture of anthers that are homozygous at all loci (Figure 2A). Genetically different DHs can be crossed to produce the original F1 hybrid. It is also possible to select DHs having a complete paternal chromosome set including only one maternal chromosome (chromosome substitution) or *viceversa* so that progeny homozygous and/or heterozygous only for one chromosome pair can be selected after crossing (Figure 2B).



**Figure 2. Reverse breeding technique applied to reconstitute F1 hybrids (A) or to induce chromosome substitutions in Back Cross (BC) lines. Modified from Dirks *et al.*, 2009.**

### 1.3.1.2. Manipulating gamete ploidy for plant breeding

Polyploidy represents the occurrence of more than two complete sets of chromosomes in an organism and has long been recognized as playing an important role in plant evolution (Tate *et al.*, 2005). Recent advances in genomic analysis revealed that almost all angiosperms are ancient polyploids. Nowadays, the major route for polyploid formation is considered to be the production of  $2n$  gametes (Bretagnolle & Thompson, 1995). Several crop species were reported to produce either  $2n$  pollen (*Secale cereale*, *Trifolium pratense*, *Arachis* spp., *Malus x domestica*, *Manihot esculenta*, *Ipomea batatas*) or  $2n$  ovules (*Solanum* spp.) or both (*Solanum* spp., *Hieracium pilosella*, *Vaccinium* spp., *Medicago sativa*). Several species including potato (*Solanum tuberosum*) and its wild relatives are of particular interest for the study of polyploidization. Indeed, these species show a series of ploidy levels ranging from  $2x$  to  $6x$  likely established through  $2n$  gametes (Ortiz *et al.*, 2009). Thus, it is not surprising that most of cytological and genetic studies on  $2n$  gametes were performed in potato mutants where micro- and/or megasporogenesis were affected. With regard to microsporogenesis, Peloquin and colleagues (1975) reported that mutants showing parallel instead of perpendicular spindles in the second meiotic division are characterized by a recessive mutation in the gene *PARALLEL SPINDLES (PS)* (Mok & Peloquin, 1975). As a consequence, non-sister chromatids are included in the same nucleus leading to the production of  $2n$  microspores by a mechanism equivalent to a First Division Restitution (FDR). On the other hand, in *premature cytokinesis (pc)* mutants, cytokinesis occurs after meiosis I while meiosis II is omitted and chromatids just fall apart. As a consequence, sister chromatids are in the same nucleus thus leading to the production of  $2n$  pollen with a Second Division Restitution mechanism (SDR). As regards the genetics of  $2n$  ovules, two mutants were described in potato (Peloquin *et al.*, 1999): *omission of the second meiotic division (os)* characterized by the lack of meiosis II while *failure of cytokinesis (fc)* is a post-meiotic mutation leading to nuclear fusion after meiosis II. Both *os* and *fc* are recognizable as SDR mechanisms of  $2n$  ovule production. The genetic consequences of FDR and SDR are different. Indeed, a heterozygous parental line, in absence of crossovers, transmit full heterozygosity or full homozygosity to the progenies depending on FDR and SDR mechanisms, respectively.

The molecular mechanisms leading to  $2n$  gametes have only recently begun to be uncovered (Brownfield & Köhler, 2011). In particular, d'Erfurth and colleagues (2008) isolated and characterized *Arabidopsis Parallel Spindle 1* gene (*AtPS1*) that controls diploid pollen formation through spindle orientation in the second division of meiosis (d'Erfurth *et al.*, 2008). Interestingly, *AtPS1* is a protein which contains contemporarily a ForkHead Associated domain (FHA), and a C-terminal PiIT N-terminus domain (PINc). So far, the FHA domain has been found in more than 5600 different proteins from prokaryotes to higher eukaryotes involved in several processes including cell cycle control, DNA repair, protein degradation, transcription and pre-mRNA splicing (Li *et al.*, 2000). PINc domain has been found in more than 3600 proteins in all life kingdoms. PINc domain has RNA nuclease activity (Lareau *et al.*, 2007). In eukaryotes, PINc-containing proteins, such as human SMG6 and SMG5, were linked to Nonsense Mediated mRNA Decay (NMD), that recognizes and rapidly degrades mRNAs containing Premature translation Termination Codons (PTCs). More recently, De Storme & Geelen (2011) described the mutant *jason* which produces  $2n$  pollen by *AtPS1* misregulation. Mutations in *OSD1* and in *CYCA1;2* cyclin (also termed *TAM*) cause omission of meiosis II leading to SDR male and female diploid gametes (d'Erfurth *et al.*, 2009, d'Erfurth *et al.*, 2010). When the authors combined *osd1* and *tam* with *AtSPO11-1* and *AtREC8* (which is involved in chromatid segregation) mutations, obtaining *osd1/Atspo11-1/Atrec8* and *tam/Atspo11-1/Atrec8* triple mutants,  $2n$  gametes were genetically identical to parent. Indeed, *Atspo11-1/Atrec8* double mutants are characterized by a mitotic-like meiosis I, due to the absence of meiotic recombination and bipolar orientation of sister kinetochores, but sister chromatids segregate randomly in meiosis II leading to gamete death. The introduction of *osd1* or *tam* in the *Atspo11-1/Atrec8* background abolish the effect of the random segregation of chromatids leading to viable  $2n$  gametes. This combination of different mutations is the first step toward the apomictic production of seeds and represents an interesting biotechnological application of meiotic genes for plant breeding.

Mutants producing  $2n$  gametes in crops have been proved useful to allow crosses between plants of different ploidy levels. For example, in potato, the use of  $2n$  gametes enabled the transfer of biotic stress resistance from the diploid species *Solanum vernei*, *Solanum tarijense*, and *Solanum chacoense* to tetraploid cultivated species

(Ortiz & Franco, 1997, Carputo *et al.*, 2000, Capo *et al.*, 2002). Gametes with somatic chromosome number are also valuable to produce plants with higher ploidy levels to exploit the potential enhancement of genetic diversity and the heterosis (Ramanna & Jacobsen, 2003, Consiglio *et al.*, 2004). In this landscape, the identification of genes involved in  $2n$  gamete production in model systems could allow the manipulation of their orthologues in crops.

#### **1.4. Chromatin structure and histone modifications**

Eukaryotic genomes are constituted by chromatin which has the double function of providing access to the DNA-encoded genetic information and of ensuring the stability of the genome and its segregation to daughter cells (Pawlowski, 2010). The fundamental unit of chromatin is represented by the nucleosome, which is composed of an octamer of the four core histones (H3, H4, H2A, H2B) around which 147 base pairs (bp) of DNA are wrapped. About 20–50 bp of linker DNA connects the nucleosomes, overall producing the so called “beads-on-a-string” configuration or 10 nm fiber. Chromatin higher order structures require additional proteins as histone H1 and Polycomb Group proteins (PcG) that can produce either ordered regions of 30 nm of diameter (“solenoid” configuration) or irregular arrangements of nucleosome aggregates (van Steensel, 2011). In this landscape the interaction between DNA and histones plays a fundamental role in determining both physical and functional properties of chromatin. Histones are basic proteins composed by a core domain, which is mainly involved in the interaction with the other histones, and protruding N-terminal tails participating to the interaction with DNA and with other chromatin associated proteins. Interestingly, both the histone tails and the core domains can be target of a multitude of post-translational modifications including acetylation, methylation, ubiquitination, phosphorylation and sumoylation which severely affect chromatin biology (Kouzarides, 2007). These histone modifications are carried out by specific enzymes which are evolutionary conserved among different organisms (Bannister & Kouzarides, 2011). Histone acetylation and deacetylation are performed by histone acetylases (HATs) and deacetylases (HDACs), respectively, while histone methylation and demethylation are catalyzed by histone methylases (HMTs) and histone demethylases (HDMs), respectively. Histone phosphorylation is performed by protein kinases while ubiquitination and sumoylation

both rely on the sequential activity of E1-activating, E2-conjugating and E3-ligating enzymes. The effect of histone modifications on chromatin biology is dependent on the modification of the interaction between histones and DNA through the alteration of the net charge of histone tails. Indeed, it was proposed that acetylation and phosphorylation can increase the negative charge of histones thus loosening the interaction with DNA (Clayton *et al.*, 2006). Moreover, the “histone code” theory suggests that different histone marks can be recognized by other proteins, such as DNA/RNA polymerases or transcription factors or DNA-repair proteins, thus promoting or preventing their interaction with chromatin (Strahl & Allis, 2000). More recently, an integrated view of the dynamics of histone modifications, small RNAs and protein-protein interactions suggested that the concept of “chromatin signalling pathway”, instead of the “histone code”, would be more suitable to describe the complex processes underlying chromatin biology (Smith & Shilatifard, 2010). The biological relevance of histone modifications is proved by their link with several DNA based processes such as transcriptional activation/repression (Fischer *et al.*, 2008), DNA-repair (van Attikum & Gasser, 2009), chromatin compaction (Prigent & Dimitrov, 2003), DNA replication (Iizuka *et al.*, 2006) and meiotic recombination (Petes, 2001).

#### **1.4.1. Histone modifications and meiosis**

Several histone modifications have been shown to be important for meiosis in different organisms. Yeast histone methyltransferase SET1 catalyzes the trimethylation of lysine 4 of histone H3 (H3K4me3) and is required for meiotic DNA replication and DSBs formation (Sollier *et al.*, 2004, Borde *et al.*, 2009). Similarly, MEISETZ and PRDM9, which catalyze H3K4me3 in mouse and human, respectively, were showed to be required for hotspot specification and DSB repair (Baudat *et al.*, 2010, Wahls & Davidson, 2010, Parvanov *et al.*, 2010, Hayashi *et al.*, 2005). In mice, mono- and dimethylation of H3K9, which are catalyzed by G9a, were proved to be required for synapsis, DSBs repair and SC formation (Tachibana *et al.*, 2007) while H3K9me3, which is catalyzed by SUV39h, was showed to be required for synapsis and segregation (Peters *et al.*, 2001). Dimethylation of H3K9 is required for DSBs formation also in *C. elegans* as showed by Reddy and Villeneuve (2004). In yeast, DOT1 catalyzed di- and trimethylation of H3K79

were showed to be important for pachytene checkpoint which prevents meiotic nuclear division in cells that fail to complete meiotic recombination and chromosome synapsis (San-Segundo & Roeder, 2000). Finally, reduced H3K36me3 produced by *SET2* knockout in yeast was showed to increase meiotic recombination at *HIS4* hotspot (Merker *et al.*, 2008). Histone ubiquitination (ub) plays also an important role in DSBs formation as showed in yeast. Indeed, H2BK123-ub mediated by the RAD6/BRE1/LGE1 complex is required for H3K4 and H3K79 trimethylation and therefore for DSBs formation in *S. cerevisiae* (Game & Chernikova, 2009, Yamashita *et al.*, 2004). Histone H3 phosphorylation on serine 10 (H3S10) is required for chromatin condensation before chromosome segregation in *Tetrahymena* (Wei *et al.*, 1999). On the other hand, H3S10 phosphorylation in maize is associated with the maintenance of sister chromatid cohesion during meiosis instead of chromatin condensation (Kaszás & Cande, 2000). Phosphorylated H2BS10 is associated with higher order chromatin structures during meiosis in yeast (Ahn *et al.*, 2005). Finally, phosphorylation of the histone variant H2AX is associated to DSBs formation and is triggered by DNA repair in mouse (Chicheportiche *et al.*, 2007).

As regards histone acetylation, several works showed its involvement in meiosis in mammals, yeast, nematode and plants. As showed by Merker and colleagues (2008) in yeast, RPD3 mediated H3K27 deacetylation, which is induced by H3K36 trimethylation by SET2, is involved in the repression of the meiotic cell cycle during vegetative growth and represses the recombination activity at *HIS4* hotspot. HDA1 mediated H3K18 deacetylation has been also linked to repression of recombination at *HIS4* hotspot and in telomeric regions (Mieczkowski *et al.*, 2007, Merker *et al.*, 2008). Mieczkowski and colleagues (2007) also reported that *SIR2* knockout mutants, which show H4K16 hyperacetylation, have an increase of 5% and a decrease of 7% of DSBs with the majority of the variations occurring close to telomeres. Interestingly, the authors hypothesized that the observed decrease of DSBs is linked to an increased activity of HDA1 caused by the absence of SIR2, thus suggesting that the two deacetylases compete for their target chromatin regions (Mieczkowski *et al.*, 2007). The histone acetylase GCN5 that is involved in H3K9, H3K14, H3K18 and H2B acetylation was showed to be required for induction of the meiotic cell cycle in *S. cerevisiae* (Burgess *et al.*, 1999). Moreover, its homologue in *S. pombe*,

SpGCN5, is required for the proper timing of the DSB formation and for recombinational activity of *M26* hotspot (Yamada *et al.*, 2004). In human, MOF is involved in H4K16 acetylation and knockout and knockdown mutants show delayed recruitment of proteins involved in DNA DSB repair and reduction of RAD51 foci in irradiated somatic cells (Sharma *et al.*, 2010). However, the authors suggest its role in meiosis on the basis of the association of MOF with the synaptonemal complex till late pachytene in mice testes. In *C. elegans*, XND-1 that is neither an histone acetylase (HAT) nor an histone deacetylase (HDAC), when mutated leads to H2AK5 hyperacetylation and to a shift of crossover distribution from terminal to proximal regions in autosomic chromosomes without affecting the total CO number (Wagner *et al.*, 2010). In contrast to autosomes, loss of XND-1 produced a twofold decrease in recombination frequency for X chromosome with consequent univalents and non-disjunction defects.

The involvement of histone acetylation in plant meiosis has been less studied respect to other organisms. Pandey and colleagues (2002) predicted 18 HDACs and 12 HATs in the *Arabidopsis* genome. Overall, *Arabidopsis* HATs and HDACs were linked to several aspects of plant development such as gametogenesis (Latrasse *et al.*, 2008), flowering time and flower organogenesis (Han *et al.*, 2007, Bertrand *et al.*, 2003, Vlachonasios *et al.*, 2003, Wu *et al.*, 2008, Cohen *et al.*, 2009, Tian & Chen, 2001, Tian *et al.*, 2003, Zhou *et al.*, 2004), root growth and development (Kornet & Scheres, 2009, Xu *et al.*, 2005), embryo development and seedling growth (Nelissen *et al.*, 2010, Long *et al.*, 2006, Tanaka *et al.*, 2008, Willmann *et al.*, 2011, Sridha & Wu, 2006), seed development (Wu *et al.*, 2000), light signaling (Benhamed *et al.*, 2006), RNA-directed DNA methylation (Aufsatz *et al.*, 2002), rDNA silencing (Earley *et al.*, 2006) and response to jasmonate and to abiotic and biotic stress (Wu *et al.*, 2008, Chen *et al.*, 2010b, To *et al.*, 2011a, Zhou *et al.*, 2005, Wang *et al.*, 2010). The involvement of *Arabidopsis* HATs and HDACs in plant meiosis was showed with the functional analysis of the putative histone acetylase *AtMCC1* (Perrella *et al.*, 2010) and of the histone deacetylase *AtHDA19* (Cremona, 2010). Perrella and colleagues (2010) showed that histone H3 hyperacetylation induced by *AtMCC1* overexpression leads to univalents both at meiosis I and meiosis II and unbalanced nuclei at the end of meiosis (Perrella *et al.*, 2010). The univalents observed in *Atmcc1* microsporocytes are explained

by a redistribution of crossovers (CO) leading to lack of the obligate CO on chromosome 2, CO reduction on chromosome 1 and CO increase on chromosome 4, without affecting the total number of COs per cell (Perrella *et al.*, 2010). Afterwards, Barra and colleagues (personal communication) through transcriptome profiling of *Atmcc1* microdissected microsporocytes evidenced the misregulation of 150 genes. Among them, the author proposed genes involved in protein metabolism, in cell cycle and in chromosome dynamics as the most interesting for a role in *Atmcc1* defects. Effects on microsporogenesis that are similar to those observed in *Atmcc1* were reported in a mutant line in *AtHDA19* (Cremona, 2010), which is involved in H3 and H4 deacetylation (Tian *et al.*, 2005). Indeed, Cremona (2010) observed univalents in meiosis I and unbalanced nuclei at the end of meiosis in *Athda19* microsporocytes.

### **1.5. Aims and activities of PhD thesis**

The aim of the present work is the identification of genes involved in plant meiotic processes, recombination and nuclear restitution that are of interest for applications in plant breeding. This work is partly supported by the European Project “MeioSYS” aiming at the systematic analysis of factors controlling meiotic recombination in higher plants.

The specific aims and activities of this PhD project are summarized as following:

- **identification of histone acetylases (HATs) and deacetylases (HDACs) with putative role in *Arabidopsis* meiosis/reproduction by *in silico* analysis;**
- **functional characterization of *Arabidopsis HDA7* gene by loss-of-function and gain-of-function strategies;**
- **Reverse genetics of putative meiotic genes affected by histone acetylation by screening of insertional lines;**
- **isolation of *PARALLEL SPINDLES LIKE (PSL)* genes in potato and evolutive analysis of PSLs in *Viridiplantae*.**

## 2. MATERIALS & METHODS

### 2.1. Plant materials and growth conditions

All *Arabidopsis* genotypes used in this study have the Columbia (Col-0) background. Plants were grown in a controlled growth room with 16 h/8 h of light/dark at 22°C/18°C. *In vitro* culture was performed as described by Weigel and Glazebrook (2002). Analysis of growth rate *in vitro* was performed as described by Tanaka and colleagues (2008) according to the growth stages defined by Boyes and colleagues (2001). The SALK and SAIL T-DNA lines used in this study were ordered from the NASC collection (<http://arabidopsis.info>) while the GK T-DNA lines from the GABI-Kat collection (Rosso *et al.*, 2003).

As regards potato, the previously described (Barone *et al.*, 1993) diploid clone of potato (named T710) coming from hybridization between *Solanum tuberosum* haploid USW3304 ( $2n = 2x = 24$ ) and *S. chacoense* ( $2n = 2x = 24$ ) has been used to isolate *PSL* genes.

### 2.2. Selection of candidate meiotic genes in *Arabidopsis thaliana*

#### 2.2.1. Microarray data analysis

*Arabidopsis* HATs and HDACs locus identifiers were downloaded from Chromatin Database (ChromDB, <http://chromdb.org>). The retrieved loci were used as query in Microarray Elements Search and Download tool ([www.arabidopsis.org](http://www.arabidopsis.org)) to get the corresponding Affymetrix ATH1 probesets. Affymetrix microarray data from reproductive and vegetative tissues was downloaded from NASCARRAY (<http://affy.arabidopsis.info>) and EBI ARRAY ([www.ebi.ac.uk/arrayexpress](http://www.ebi.ac.uk/arrayexpress)) databases (Table 2). Statistical analyses were then performed within R environment (<http://www.r-project.org>). Collected data were normalized by the median of the signal values. Expression values for each HAT/HDAC were selected with a spreadsheet editor. Two-Way Nested ANOVA was performed to identify differentially expressed genes between “reproductive” and “vegetative” groups ( $p < 0.05$ ;  $q < 0.05$ ). For each gene a fold change (FC) was calculated by raising 2 to the difference between the average signal of “reproductive” and “vegetative” groups.

**Table 2. List of microarray datasets used for the identification of HATs and HDACs differentially expressed in reproductive vs vegetative tissues. For each dataset, ID, database source, tissue and ecotype are reported.**

| ID                                      | Database   | Description                         | Ecotype | Group        |
|---|------------|-------------------------------------|---------|--------------|
| ATGE_31_A2                              | NASC ARRAY | Flowers stage 9                     | Col-0   | Reproductive |
| ATGE_31_B2                              | NASC ARRAY | Flowers stage 9                     | Col-0   | Reproductive |
| ATGE_31_C2                              | NASC ARRAY | Flowers stage 9                     | Col-0   | Reproductive |
| ATGE_32_A2                              | NASC ARRAY | Flowers stage 10/11                 | Col-0   | Reproductive |
| ATGE_32_B2                              | NASC ARRAY | Flowers stage 10/11                 | Col-0   | Reproductive |
| ATGE_32_C2                              | NASC ARRAY | Flowers stage 10/11                 | Col-0   | Reproductive |
| ATGE_33_A                               | NASC ARRAY | Flowers stage 12                    | Col-0   | Reproductive |
| ATGE_33_B                               | NASC ARRAY | Flowers stage 12                    | Col-0   | Reproductive |
| ATGE_33_C                               | NASC ARRAY | Flowers stage 12                    | Col-0   | Reproductive |
| E-GEOD-5449/GSE5449GSM124893            | EBI ARRAY  | Flower bud (anther stage 1-12)      | Col-0   | Reproductive |
| E-GEOD-5449/GSE5449GSM153864            | EBI ARRAY  | Flower bud (anther stage 1-12)      | Col-0   | Reproductive |
| E-GEOD-5449/GSE5449GSM153865            | EBI ARRAY  | Flower bud (anther stage 1-12)      | Col-0   | Reproductive |
| E-GEOD-680/GSE680GSM27359               | EBI ARRAY  | Floral buds                         | Ws-0    | Reproductive |
| Somerville_1-4_flower-GC5_Rep1_ATH1     | NASC ARRAY | Developed flowers and unopened buds | Col-0   | Reproductive |
| Somerville_1-5_flower-GC6_Rep2_ATH1     | NASC ARRAY | Developed flowers and unopened buds | Col-0   | Reproductive |
| Somerville_1-6_flower-GH5_Rep1_ATH1     | NASC ARRAY | Developed flowers and unopened buds | Col-0   | Reproductive |
| Somerville_1-7_flower-GH6_Rep2_ATH1     | NASC ARRAY | Developed flowers and unopened buds | Col-0   | Reproductive |
| Vizcay-Barrena_1-11_Ler-young_Rep3_ATH1 | NASC ARRAY | Young floral buds                   | Ler-0   | Reproductive |
| Vizcay-Barrena_1-3_Ler-young_Rep1_ATH1  | NASC ARRAY | Young floral buds                   | Ler-0   | Reproductive |
| Vizcay-Barrena_1-7_Ler-young_Rep2_ATH1  | NASC ARRAY | Young floral buds                   | Ler-0   | Reproductive |
| ATGE_7_A2                               | NASC ARRAY | Seedling, green part 7 days         | Col-0   | Vegetative   |
| ATGE_7_B2                               | NASC ARRAY | Seedling, green part 7 days         | Col-0   | Vegetative   |
| ATGE_7_C2                               | NASC ARRAY | Seedling, green part 7 days         | Col-0   | Vegetative   |
| ATGE_96_A                               | NASC ARRAY | Seedling, green part 7 days         | Col-0   | Vegetative   |
| ATGE_96_B                               | NASC ARRAY | Seedling, green part 7 days         | Col-0   | Vegetative   |
| ATGE_96_C                               | NASC ARRAY | Seedling, green part 7 days         | Col-0   | Vegetative   |
| ATGE_97_A                               | NASC ARRAY | Seedling, green part 7 days         | Col-0   | Vegetative   |
| ATGE_97_B                               | NASC ARRAY | Seedling, green part 7 days         | Col-0   | Vegetative   |
| ATGE_97_C                               | NASC ARRAY | Seedling, green part 7 days         | Col-0   | Vegetative   |
| ATGE_100_A                              | NASC ARRAY | Seedling, green part 7 days         | Col-0   | Vegetative   |
| ATGE_100_B                              | NASC ARRAY | Seedling, green part 7 days         | Col-0   | Vegetative   |
| ATGE_100_C                              | NASC ARRAY | Seedling, green part 7 days         | Col-0   | Vegetative   |
| ATGE_101_A                              | NASC ARRAY | Seedling, green part 7 days         | Col-0   | Vegetative   |
| ATGE_101_B                              | NASC ARRAY | Seedling, green part 7 days         | Col-0   | Vegetative   |
| ATGE_101_C                              | NASC ARRAY | Seedling, green part 7 days         | Col-0   | Vegetative   |
| RIKEN-GODA3A-M                          | NASC ARRAY | Seedling, 7 days                    | Ler-0   | Vegetative   |
| RIKEN-GODA3B-M                          | NASC ARRAY | Seedling, 7 days                    | Ler-0   | Vegetative   |
| RIKEN-GODA1A-M                          | NASC ARRAY | Seedling, 7 days                    | Ws-0    | Vegetative   |
| RIKEN-GODA1B-M                          | NASC ARRAY | Seedling, 7 days                    | Ws-0    | Vegetative   |
| E-GEOD-991/GSE991GSM15672               | EBI ARRAY  | Seedling, 7 days                    | Ler-0   | Vegetative   |
| E-GEOD-991/GSE991GSM15673               | EBI ARRAY  | Seedling, 7 days                    | Ler-0   | Vegetative   |
| E-GEOD-991/GSE991GSM15674               | EBI ARRAY  | Seedling, 7 days                    | Ler-0   | Vegetative   |
| CORNAH_1-4_A4-WSX_REP1_ATH1             | NASC ARRAY | Seedling                            | Ws-4    | Vegetative   |
| CORNAH_1-8_A4-WSX_REP2_ATH1             | NASC ARRAY | Seedling                            | Ws-4    | Vegetative   |
| CORNAH_1-12_A4-WSX_REP3_ATH1            | NASC ARRAY | Seedling                            | Ws-4    | Vegetative   |
| RENTE_1-3_WS2-CONTROL_REP1_ATH1         | NASC ARRAY | Seedling                            | Ws-2    | Vegetative   |

## 2.2.2. Identification of *Arabidopsis* HATs and HDACs most similar genes in other model organisms

Local databases of the proteomes of *Saccharomyces cerevisiae* ([www.yeastgenome.org](http://www.yeastgenome.org)), *Caenorhabditis elegans* ([www.wormbase.org](http://www.wormbase.org)), *Mus musculus* ([www.informatics.jax.org](http://www.informatics.jax.org)) and *Drosophila melanogaster* (<http://flybase.org>) were set up. After that, the protein sequences of *Arabidopsis* HATs and HDACs, which were downloaded from ChromDB, were blasted against each proteome by using BLAST+ (Altschul *et al.*, 1990). The most similar genes were

queried in each organism database to retrieve functional annotations and mutant phenotype descriptions.

### **2.3. *HDA7* in silico analysis**

Thousand base pairs upstream of the predicted start codon of *HDA7* (At5g35600) were analyzed with NSITE-PL (<http://linux1.softberry.com>) and Akiyama's TFSEARCHv1.3 (<http://molsun1.cbrc.aist.go.jp/research/db/TFSEARCH.html>) to detect putative regulatory motifs. The protein sequences of RPD3 HDACs from *Oryza sativa*, *Zea mays* and *Arabidopsis thaliana* were downloaded from ChromDB (<http://chromdb.org>). Aminoacid alignment and phylogenetic analysis were performed with MEGA 5 (Tamura *et al.*, 2007). For unrooted trees construction, the maximum likelihood method was used and bootstrap analysis was performed using 100 bootstrap replicates.

### **2.4. Analysis of gene coregulation**

The coregulation between *Arabidopsis* HDACs was checked by Expression Angler tool (<http://bar.utoronto.ca>) searching in AtGenExpress Tissue Set. The expression data of the experiments listed in Table 3 were selected to identify genes coregulated with *HDA7* during embryo development and in flowers at developmental stages from sporogenesis to fertilization. Both in the first and in the second coregulation analysis an r-value cut-off ranging from 0.75 to 1.0 and from -0.75 to -1.0 was used.

**Table 3. List of the microarray experiments selected to identify *HDA7* coregulated genes during embryo development and flower stages 9-15 (Smyth *et al.*, 1990).**

| Embryo Development |                       | Reproduction  |                           |
|--------------------|-----------------------|---------------|---------------------------|
| Experiment ID      | Tissue                | Experiment ID | Tissue                    |
| Lindsey_1-1        | Globular-stage embryo | GSE3056       | Ovary                     |
| Lindsey_1-2        | Globular-stage embryo | ATGE_31       | Flower Stage 9            |
| Lindsey_1-3        | Globular-stage embryo | ATGE_32       | Flower Stage 10/11        |
| Lindsey_1-4        | Globular-stage embryo | ATGE_33       | Flower Stage 12           |
| Lindsey_1-5        | Globular-stage embryo | ATGE_37       | Flowers Stage 12, Carpels |
| Lindsey_1-6        | Globular-stage embryo | ATGE_39       | Flower Stage 15           |
| Lindsey_1-7        | Heart-stage embryo    | ATGE_45       | Flowers Stage 15, Carpels |
| Lindsey_1-8        | Heart-stage embryo    |               |                           |
| Lindsey_1-9        | Heart-stage embryo    |               |                           |
| Lindsey_1-10       | Heart-stage embryo    |               |                           |
| Lindsey_1-11       | Heart-stage embryo    |               |                           |
| Lindsey_1-12       | Heart-stage embryo    |               |                           |
| Lindsey_1-14       | Torpedo-stage embryo  |               |                           |
| Lindsey_1-16       | Torpedo-stage embryo  |               |                           |
| Lindsey_1-18       | Torpedo-stage embryo  |               |                           |
| Lindsey_1-13       | Torpedo-stage embryo  |               |                           |
| Lindsey_1-15       | Torpedo-stage embryo  |               |                           |
| Lindsey_1-17       | Torpedo-stage embryo  |               |                           |
| Lindsey_1-19       | Torpedo-stage embryo  |               |                           |
| Lindsey_1-20       | Torpedo-stage embryo  |               |                           |
| Lindsey_1-21       | Torpedo-stage embryo  |               |                           |
| Lindsey_1-22       | Torpedo-stage embryo  |               |                           |
| Lindsey_1-23       | Torpedo-stage embryo  |               |                           |
| Lindsey_1-24       | Torpedo-stage embryo  |               |                           |
| Lindsey_1-25       | Torpedo-stage embryo  |               |                           |
| Lindsey_1-26       | Torpedo-stage embryo  |               |                           |
| Lindsey_1-27       | Torpedo-stage embryo  |               |                           |

## 2.5. amiRNA design and plasmid construction

The specific artificial microRNA to silence *HDA7* (amiHDA7) and the primers for subsequent cloning were designed with WMD3 tool according to the procedures and criteria described by Schwab and colleagues (2010) (<http://wmd3.weigelworld.org/cgi-bin/webapp.cgi>). The cloning of amiHDA7 was performed following the protocol described by Schwab and colleagues (2010) using the miR319a precursor-containing plasmid pRS300 as a template. As showed in Table 4, primers A and B were modified to allow the cloning with Gateway® Technology (Invitrogen, CA, USA). Predicted mature miRNA sequence to silence *HDA7* was 5'-UUAGACAAGUUGAAUGUGCCA-3'. Primers used in the

construction of amiHDA7 are listed in Table 4. The final PCR product was cloned into pK2GW7 binary vector (<http://gateway.psb.ugent.be>) with Gateway® Technology, using pDONR™/ZEO (Invitrogen, CA, USA) as donor, following the manufacturer instructions. The sequence of amiHDA7 was checked after cloning by nucleotide sequencing at Eurofins MWG Operon sequencing service (Germany).

**Table 4. Primers used to clone amiHDA7.**

| Primer         | Sequence (5'→3')   |
|----------------|--|
| HDA7_I_miR-s   | GATTAGACAAGTTGAATGTGCCACTCTCTTTTGTATTCCA                 |
| HDA7_II_miR-a  | AGTGGCACATTCAACTTGTCTAATCAAAGAGAATCAATGA                 |
| HDA7_III_miR*s | AGTGACACATTCAACATGTCTATTACAGGTCGTGATATG                  |
| HDA7_IV_miR*a  | GAATAGACATGTTGAATGTGCTCACTACATATATTCCCTA                 |
| ATTB1_A        | GGGGACAAGTTTGTACAAAAAAGCAGGCTCTGCAAGGCGATTAAGTTGGGTAAC   |
| ATTB2_B        | GGGGACCACTTTGTACAAGAAAGCTGGGTGCGGATAACAATTCACACAGGAAACAG |

## 2.6. *Arabidopsis* transformation

*Agrobacterium tumefaciens* GV3101 was used to transform *Arabidopsis* Col-0 plants with floral spray method as described by Chung and colleagues (2000). Transformants were selected on kanamycin added media (50 mg/ml) as described by Weigel and Glazebrook (2002).

## 2.7. Nucleic acid extraction

Bacterial plasmid DNA was isolated using QIAprep® Spin Miniprep Kit (QIAGEN, Germany). Genomic DNA was extracted using DNease Plant Mini Kit™ (QIAGEN, Germany). Total RNA from prebolting T710 buds and from *Arabidopsis* young leaves and inflorescences was isolated using RNeasy Plant Mini Kit™ (QIAGEN, Germany) and then treated with DNase I (Invitrogen, CA, USA) to remove residual genomic DNA following manufacturer instructions.

## 2.8. Expression analysis

Total RNA from *HDA7* leaves and buds was retrotranscribed with Superscript III™ Two-Step RT-PCR using Oligo(dT)<sub>12-18</sub> (Invitrogen, CA, USA) as primer for first strand cDNA synthesis. Gene-specific primers were designed using PRIMER EXPRESS software, ver. 2.0 (Applied Biosystems®, <http://www3.appliedbiosystems.com>) and are listed in Table 5. Real Time RT-PCR was carried out using Rotor-Gene™ 6000 (Corbett, UK) with FastStart SYBR® Green Master (Roche, ITA), *ADENOSINE PHOSPHORIBOSYL TRANSFERASE 1* (*APT1*) gene was used as reference.

**Table 5. Primers used for Real Time RT-PCR experiments.**

| Target Gene Model | Primer     | Sequence (5'->3')         |
|-------------------|------------|---------------------------|
| AT1G27450.1       | APT1_qRTF  | ATTGTTCCTCATGAGGAAGCC     |
|                   | APT1_qRTR  | CACCTACGTGCATCTCAATCGT    |
| AT5G35600.1       | HDA7_qRTF  | GCTGATTCTTTAGCTGGTGATCCGT |
|                   | HDA7_qRTR  | CCAGCAACGAGCAACATTTGGAAG  |
| AT5G63110.1       | HDA6_qRTF  | GGTCACGCTGATTGCCTTCGGTTC  |
|                   | HDA6_qRTR  | ACACCAGCAACGGGCAACATTTCCG |
| AT3G44680.1       | HDA9_qRTF  | GCGGGTTGCACCATGCCAAA      |
|                   | HDA9_qRTR  | ACGCTTCTTCAACCCCATCAC     |
| AT4G38130.1       | HDA19_qRTF | TGTCTGGTGATAGGTTGGGGTGTC  |
|                   | HDA19_qRTR | GCAACGGGCAACATTGCCGATAG   |
| AT4G22970.1       | AESP_qRTF  | TCATCGCGTAACAAGCCAGCTCA   |
|                   | AESP_qRTR  | GACAGGCGCAGCCCAATCA       |

## 2.9. Analysis of fertility associated traits

Silique length and seed set were assessed on 10 random siliques at stages 17-18 (Smyth *et al.*, 1990) after excision from *hda7-2*, *hda7<sup>oe</sup>* and wild type plants after removing of the peduncles. Pollen viability was determined by Alexander's staining (Alexander, 1969). Seed development within ovaries was observed with Leica Differential Interference Contrast (DIC) microscope as described by Meinke (1994). Ovules were observed with a Leica optical microscope equipped with fluorescence and a CCD camera, after dissection from buds at stage 13 (Smyth *et al.*, 1990), clarification in a mix of 85% lactic acid and phenol (2:1 w:w) for 30 minutes and staining with 4'-6-diamidino-2 phenylindole (DAPI) 10 mg/ml. As regards T-DNA insertional lines, screening was performed by looking at silique length and seed set in 24 plants per each line.

## 2.10. Potato *PSL* cloning and sequence analysis

*PSL1* genomic fragment was amplified by PCR with primers PS\_F1 and PS\_R1 and full sequence with primers PS\_F2 and PS\_R2 (Table 6). The coding region of *PSL* transcripts was amplified with PS\_CF and PS\_CR primers (Table 6). PCR products were cloned into PCR2.1 with T/A Cloning kit (Invitrogen, CA, USA). Nucleotide sequencing was carried out by Eurofins MWG Operon sequencing service (Germany). *PSL1* gene structure and cDNA predictions were carried out using FGESH online tool (<http://linux1.softberry.com>) selecting Tomato as organism. *In silico* translation of cDNA sequences was carried out using the Expsy Translation tool (<http://www.expsy.ch/tools/dna.html>).

**Table 6. Primers used to clone *PSL* in potato**

| Primer Name | Primer sequence (5->3')   | Purpose                          |
|-------------|---------------------------|----------------------------------|
| PS_F1       | ATGGCGGAAAAGCAAGAAT       | Cloning of PSL1 genomic sequence |
| PS_R1       | TTGGAAATCTTCTGCTGTCTCA    |                                  |
| PS_F2       | GGCTTAGCAAGTTCCACAGG      |                                  |
| PS_R2       | TTTGACATCTTTGATAAGAAGGG   |                                  |
| PS_CF       | CCTCTGTCTCTTTCTTCTCTCTCCC | Cloning of PSL cDNAs             |
| PS_CR       | ACCTAGCTAACTGTGCTGCCTGA   |                                  |

### 2.11. Identification of unannotated *PSL* genes

The PSL protein sequences were identified and collected (Table 7) by TBLASTN (Altschul *et al.*, 1990) search against the Phytozome v6 database (<http://www.phytozome.net>), SOL Genomic Network (SGN, <http://sgn.cornell.edu>) and Potato Genome Sequencing Consortium (PGSC, <http://potatogenomics.plantbiology.msu.edu/index.html>).

**Table 7. Description of sequence names, accession numbers, organisms and source databases used in evolutive study of PSLs.**

| Species                      | Database  | Accession                      | Protein |
|------------------------------|-----------|--------------------------------|---------|
| <b>DICOTS</b>                |           |                                |         |
| <b>Fabids</b>                |           |                                |         |
| <i>C. sativus</i>            | Phytozome | Cucsa.079920.1                 | CsPSL1  |
| <i>G. max</i>                | Phytozome | Glyma02g08210.1                | GmPSL1  |
| <i>G. max</i>                | Phytozome | Glyma02g08210.2                | GmPSL1a |
| <i>G. max</i>                | Phytozome | Glyma10g35930.1                | GmPSL4  |
| <i>G. max</i>                | Phytozome | Glyma10g35930.2                | GmPSL4a |
| <i>G. max</i>                | Phytozome | Glyma16g27290.1                | GmPSL2  |
| <i>G. max</i>                | Phytozome | Glyma16g27290.2                | GmPSL2a |
| <i>G. max</i>                | Phytozome | Glyma20g31660.1                | GmPSL3  |
| <i>M. esculenta</i>          | Phytozome | cassava24482.valid.m1          | MePSL1  |
| <i>M. truncatula</i>         | Phytozome | Medtr1g122320.1                | MtPSL1  |
| <i>P. persica</i>            | Phytozome | ppa000455m.g                   | PpSPL1  |
| <i>P. trichocarpa</i>        | GeneBank  | XM_002327195.1                 | PtPSL1  |
| <b>Lamiids</b>               |           |                                |         |
| <i>Mimulus guttatus</i>      | Phytozome | mgf021378m                     | MgPSL1  |
| <i>S. lycopersicum</i>       | SGN       | SL1.00sc02597_37.1.1           | SIPSL1  |
| <b>Malvids</b>               |           |                                |         |
| <i>A. thaliana</i>           | AGI       | At1g34355.1                    | AtPS1   |
| <i>A. lyrata</i>             | GeneBank  | XM_002891053.1                 | AIPSL1  |
| <i>B. rapa</i>               | Phytozome | AC232513_fgenesh               | BrPSL1  |
| <i>C. papaya</i>             | Phytozome | evm.model.supercontig_66.57    | CpPSL1  |
| <b>Rosids incertae sedis</b> |           |                                |         |
| <i>V. vinifera</i>           | GeneBank  | XM_002267100.1                 | VvPSL1  |
| <b>Stem eudicotyledons</b>   |           |                                |         |
| <i>A. coerulea</i>           | Phytozome | AcoGoldSmith_v1.001427m.g      | AcPSL1  |
| <b>MONOCOTS</b>              |           |                                |         |
| <b>Commelinids</b>           |           |                                |         |
| <i>B. distachyon</i>         | Phytozome | Bradi4g24400.1                 | BdPSL1  |
| <i>O. sativa</i>             | GeneBank  | NM_001072397.1                 | OsPSL1  |
| <i>S. italica</i>            | Phytozome | SiPROV000671m.g                | SiPSL1  |
| <i>S. bicolor</i>            | GeneBank  | XM_002450341.1                 | SbPSL1  |
| <b>ISOETOPSIDA</b>           |           |                                |         |
| <i>S. moellendorffii</i>     | Phytozome | fgenesh2_pg.C_scaffold_6000273 | SmPSL1  |

## 2.12. PSL molecular phylogenetic analysis

The PSL protein sequences were firstly aligned using MEGA 5. The best model for Maximum Likelihood phylogeny analysis was chosen testing all the available models in ProtTest version 2.4 (Abascal *et al.*, 2005) with slow optimization strategy and selecting the one with highest AICc value. The evolutionary history was then inferred by

using the Maximum Likelihood method using MEGA 5. The bootstrap consensus tree was inferred from 100 replicates.

### **2.13. PSL domain analysis**

The locations of FHA and PINc domains within PSL genes were detected using SMART (Schultz *et al.*, 1998). Secondary structure prediction was performed using domains from PSL sequences as input into the PSIPRED secondary structure prediction server (McGuffin *et al.*, 2000). The program MUSCLE (Edgar, 2004) was used to do multiple sequence alignments of FHA and PINc domains in PSL proteins, yRAD53p (NCBI:6325104) and hSMG6 (UniProt: Q86US8). Conservation of phosphothreonine-binding residues in FHA and of RNase activity residues in PINc were determined by alignment with yRAD53p and hSMG6, respectively.

### **2.14. Comparison of dN-dS values between PSL sequences**

The coding sequences of *PSLs* were obtained from the databases reported in Table 7. The terminal codons were manually removed, then the codon alignment was performed by MUSCLE using the default settings of MEGA 5. To select the best substitution model JmodelTest 0.1.1 (Posada, 2008, Guindon & Gascuel, 2003) was used with default settings. The codon alignment was then uploaded on Datamonkey 2010 server (Pond & Frost, 2005a, Pond *et al.*, 2005b) and dN-dS evaluated using GTR as substitution model, and SLAC (default settings except for Global dN-dS value = estimated with CI), FEL and REL (Pond & Frost, 2005c) algorithms. Codons subjected to evolutive pressure were identified with Integrative Selection Analysis selecting significance levels for SLAC  $p < 0.1$ , FEL  $p < 0.1$  and REL Bayes Factor  $< 50$ . Only codons with a significant dN-dS value according to all the three methods were reported.

### **2.15. Statistical analyses**

Chi-square test was used to analyze the segregation of *Arabidopsis* seedlings on selective media and to compare the frequencies of seedlings at different developmental stages in *Arabidopsis* wild type, *hda7-2* and *hda7<sup>oe</sup>*. T-test was used to compare the expression data of *HDA7*, *HDA6*, *HDA9* and *HDA19* in *Arabidopsis* wild type, *hda7-2* and *hda7<sup>oe</sup>*.



### 3. RESULTS

#### 3.1. Identification of histone acetylases (HATs) and deacetylases (HDACs) with putative role in *Arabidopsis* meiosis/reproduction by *in silico* analysis

Candidate plant meiotic genes were identified by looking at their expression profile and/or at the similarity to homologous genes in other model organisms. Based on emerging evidences that histone acetylation is involved in meiotic recombination and chromosome segregation, we focused our attention on histone acetylase (HAT) and deacetylase (HDAC) genes in *Arabidopsis thaliana*. The genome of this species was predicted to encode 12 HATs and 18 HDACs (Pandey *et al.*, 2002). A two step *in silico* analysis was performed to identify candidate HATs and HDACs with a meiotic role. Public microarray expression data of flower buds and seedlings were analyzed to select the genes differentially expressed at flower developmental stages corresponding to male and female sporogenesis and gametogenesis (Armstrong & Jones, 2003). As shown in Figure 3, 12 HDACs and 4 HATs are significantly up-regulated in *Arabidopsis* flower buds respect to seedlings. As shown in Table 8, *HDA7* and *HAG2* had the highest fold-change (FC), 2.25 and 1.83, among HDACs and HATs, respectively. On the other hand, 3 HDACs and 3 HATs, the latter belonging to RPD3 family, were down-regulated. Data for *HDA10* and *HDA17* was discarded because these two HDACs share the same probeset thus making impossible to quantify the expression values separately.

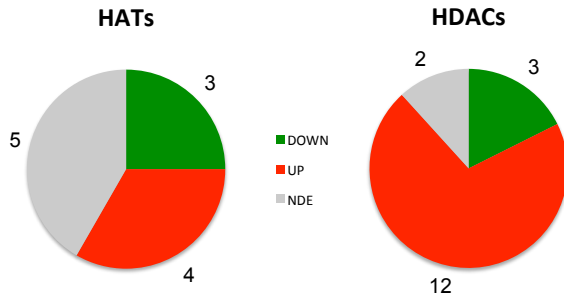


**Figure 3.** Distribution of up-regulated (red), down-regulated (green) and not differentially expressed (gray) HATs and HDACs in flower buds at stages 9-12 respect to seedlings. The number of genes for each class is shown outside of the pie-chart.

Afterward, HDACs and HATs from *Arabidopsis thaliana* were compared to those from model organisms *Mus musculus*, *Caenorhabditis elegans*, *Drosophila melanogaster* and *Saccharomyces cerevisiae*. Interestingly, we found that the number of genes in each family of HDACs and HATs is variable among the different organisms (Figure 4), the highest number occurring in *Arabidopsis* and mouse.

**Table 8. Summary of *in silico* analysis performed on HDAC (A) and HAT (B) genes. Genes, grouped according to families, are arranged in descending order of Final Score (FS). For each gene, Fold Change of the expression in flower buds respect to seedling, the most similar gene found in *M. musculus*, *D. melanogaster*, *S. cerevisiae*, *C. elegans* and the Homology Value (HV) are reported.**

**A**

| ID    | Locus     | Family | Fold Change | <i>M. musculus</i> | <i>D. melanogaster</i> | <i>S. cerevisiae</i> | <i>C. elegans</i> | HV   | FS   |
|-------|-----------|--------|-------------|--------------------|------------------------|----------------------|-------------------|------|------|
| HDA7  | At5g35600 |        | 2.25        | HDAC1              | RPD3                   | RPD3                 | HDA-1             | 3.00 | 5.25 |
| HDA6  | At5g63110 |        | 1.24        | HDAC1              | RPD3                   | RPD3                 | HDA-1             | 3.00 | 4.24 |
| HDA9  | At3g44680 |        | 1.23        | HDAC1              | RPD3                   | RPD3                 | HDA-3             | 3.00 | 4.23 |
| HDA19 | At4g38130 |        | 1.20        | HDAC1              | RPD3                   | RPD3                 | HDA-1             | 3.00 | 4.20 |
| HDA18 | At5g61070 |        | 2.16        | HDAC6              | HDAC6                  | HDA1                 | F41H10.6          | 1.00 | 3.16 |
| HDA10 | At3g44660 | RPD3   | -           | HDAC2              | N/A                    | HOS2                 | HDA-3             | 3.00 | 3.00 |
| HDA17 | At3g44490 |        | -           | HDAC1              | N/A                    | HOS2                 | HDA-3             | 3.00 | 3.00 |
| HDA15 | At3g18520 |        | 1.35        | HDAC6              | HDAC6                  | HDA1                 | F41H10.6          | 1.00 | 2.35 |
| HDA5  | At5g61060 |        | 1.15        | HDAC6              | HDAC6                  | HDA1                 | HDA-4             | 1.00 | 2.15 |
| HDA8  | At1g08460 |        | 0.76        | HDAC6              | HDAC6                  | HDA1                 | F41H10.6          | 1.00 | 1.76 |
| HDA14 | At4g33470 |        | 0.69        | HDAC10             | HDAC6                  | HDA1                 | F41H10.6          | 1.00 | 1.69 |
| HDA2  | At5g26040 |        | 0.63        | HDAC11             | HDACX                  | HOS2                 | C35A5.9           | 1.00 | 1.63 |
| SRT1  | At5g55760 | SIR2   | 1.23        | SIRT6              | SIRT6                  | HST2                 | SIR-2.4           | 2.00 | 3.23 |
| SRT2  | At5g09230 |        | NDE         | SIRT4              | SIRT4                  | HST1                 | SIR-2.2           | 2.00 | 2.00 |
| HDT3  | At5g03740 |        | 1.79        | N/A                | N/A                    | N/A                  | N/A               | 0.00 | 1.79 |
| HDT1  | At3g44750 | HDT    | 1.57        | N/A                | N/A                    | N/A                  | N/A               | 0.00 | 1.57 |
| HDT2  | At5g22650 |        | 1.55        | N/A                | N/A                    | N/A                  | N/A               | 0.00 | 1.55 |
| HDT4  | At2g27840 |        | NDE         | N/A                | N/A                    | N/A                  | N/A               | 0.00 | 0.00 |

**B**

| ID    | Locus     | Family                | Fold Change | <i>M. musculus</i> | <i>D. melanogaster</i> | <i>S. cerevisiae</i> | <i>C. elegans</i> | HV   | FS   |
|-------|-----------|-----------------------|-------------|--------------------|------------------------|----------------------|-------------------|------|------|
| HAG2  | At5g56740 |                       | 1.83        | HAT1               | CG2051                 | HAT1                 | SIR-2.4           | 2.00 | 3.83 |
| HAG1  | At3g54610 | GNAT                  | 1.34        | KAT2B              | PCAF                   | GCN5                 | PCAF-1            | 1.00 | 2.34 |
| HAG3  | At5g50320 |                       | NDE         | ELP3               | ELP3                   | ELP3                 | ELPC-3            | 0.00 | 0.00 |
| HAM1  | At5g64610 | MYST                  | 1.47        | MYST1              | MOF                    | ESA1                 | MYS-1             | 1.00 | 2.47 |
| HAM2  | At5g09740 |                       | NDE         | MYST1              | MOF                    | ESA1                 | MYS-1             | 1.00 | 1.00 |
| HAF1  | At1g32750 | TAF <sub>ii</sub> 250 | 1.12        | TAF1               | TAF1                   | TAF1                 | TAF-1             | 1.00 | 2.12 |
| HAF2  | At3g19040 |                       | NDE         | TAF1               | TAF1                   | TAF1                 | TAF-1             | 1.00 | 1.00 |
| HAC5  | At3g12980 |                       | 0.87        | CREBBP             | NEJ                    | N/A                  | CBP-1             | 1.00 | 1.87 |
| HAC4  | At1g55970 |                       | 0.86        | CREBBP             | N/A                    | N/A                  | CBP-1             | 1.00 | 1.86 |
| HAC2  | At1g67220 | CBP                   | 0.79        | EP300              | N/A                    | N/A                  | CBP-1             | 1.00 | 1.79 |
| HAC1  | At1g79000 |                       | NDE         | CREBBP             | N/A                    | N/A                  | CBP-1             | 1.00 | 1.00 |
| HAC12 | At1g16710 |                       | NDE         | CREBBP             | N/A                    | N/A                  | CBP-1             | 1.00 | 1.00 |

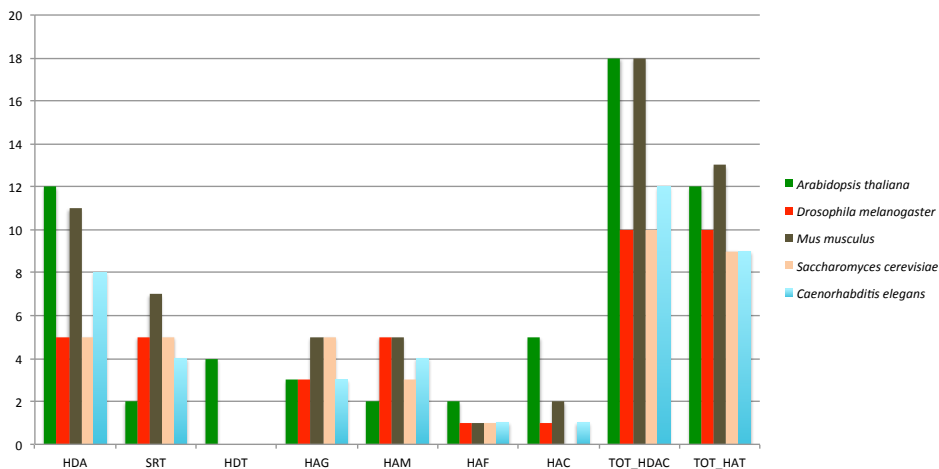


**Figure 4. Number of genes for each HAT and HDAC subgroup and total number of HATs and HDACs (TOT\_HAT and TOT\_HDAC) in *A. thaliana*, *D. melanogaster*, *M. musculus*, *S. cerevisiae* and *C. elegans*.**

The proteomes of each organism were then queried with *Arabidopsis* HATs and HDACs sequences in order to find the most similar genes. Their functions were checked on the basis of Gene Ontology annotations and of mutant phenotype as reported in public databases. Homology value (HV) equal to 1 was assigned for each organism in which the gene was demonstrated having a role in meiosis/reproduction. As shown in Table 8, 6 HDACs and 10 HATs of *Arabidopsis* are similar to at least one gene involved in the reproduction of other model organisms. Final Scores (FS) calculated by summing FC and HV values allowed to identify the most likely candidates with a role in meiosis/reproduction. In summary, *HAG2*, *HAG1*, *HAM1* and *HAF1* had the highest score among HATs and *HDA7*, *HDA6*, *HDA9* and *HDA19* had the highest score not only among HDACs but also among HATs. *HDA19* resulted to be required for meiotic recombination as evidenced by Cremona and colleagues (2010) thus confirming the effectiveness of *in silico* approach setup in this work.

### **3.2. Functional characterization of *Arabidopsis HDA7* gene by loss-of-function and gain-of-function strategies**

On the basis of *in silico* analysis, *HDA7* was chosen to assess its biological function by different strategies. RNA interference mediated by artificial miRNA (amiRNAi) was performed to silence *HDA7*, while.

the T-DNA line SALK\_002912C (hereinafter *hda7<sup>oe</sup>*) overexpressing *HDA7* (Cremona, 2010) was used as gain-of-function mutant. In *hda7<sup>oe</sup>*, a significant overexpression in leaf was confirmed by quantitative RT-PCR with a 245 fold-change respect to wild type.

### 3.2.1. *In silico* analysis of *HDA7*

*AtHDA7* (At5g35600) gene is composed by five exons and four introns ([www.arabidopsis.org](http://www.arabidopsis.org)) spanning about 1590 base pairs (bp). *In silico* analysis of 1000 bp upstream of the start codon was performed to identify putative regulatory motifs. As shown in Figure 5, eight motifs were identified between -893 and -12 bp from the ATG. The motif at position -245 is similar to the binding site of SBF-1 which is a repressor of transcription (Lawton *et al.*, 1991). On the other hand, the motifs ZC2 (recognized by chromatin remodellers with zinc-finger domains, Ponte *et al.*, 1994), the telobox (recognized by Athb homeodomain proteins, Sessa *et al.*, 1993), the W-box (recognized by WRKY transcription factors, Eulgem *et al.*, 2000), the BOX1\*, Tjaden *et al.*, 1995), the GCCAAG motif (Leah *et al.*, 1994) have been shown to be involved in transcriptional activation. These findings suggest that *AtHDA7* may be target of a complex transcriptional regulation.



**Figure 5. Schematic representation of *HDA7* gene structure and its promoter region.**

HDA7 is a 409 aminoacid long putative histone deacetylase of the Class I RPD3 family as evidenced by the Hist\_deacetyl domain (PF00850) which is characteristic of this family (Pandey *et al.*, 2002). Class I includes the homologues of RPD3 from yeast which preferentially deacetylates lysines 5 and 12 on H4 and lysines 9 and 18 on H3. The phylogenetic analysis of RPD3 HDACs from *Arabidopsis*, rice and maize revealed that HDA7 is related to OsHDA705 and ZmHDA108 (Figure 6). The phylogenetic tree, reported in Figure 7, taking into account separately HDACs from

RPD3 family of *Arabidopsis*, highlighted that HDA7 is closely related to HDA6 (At5g63110), HDA19 (At4g38130), HDA9 (At3g44680), HDA10 (At3g44660) and HDA17 (At3g44490). Despite their similarity, these proteins can be involved in different processes as it can be argued by their expression profiles. Indeed, HDA7, HDA10 and HDA17 are not significantly coregulated with any of the abovementioned histone deacetylases during *Arabidopsis* development as evidenced by ExpressionAngler tool (<http://bar.utoronto.ca/>). On the other hand, HDA6 is coregulated with HDA9 and HDA19 ( $r = 0.86$  and  $r = 0.91$ , respectively) and HDA9 is coregulated with HDA19 ( $r = 0.86$ ). These results suggest that HDA6, HDA9 and HDA19 could have at least partially redundant roles.

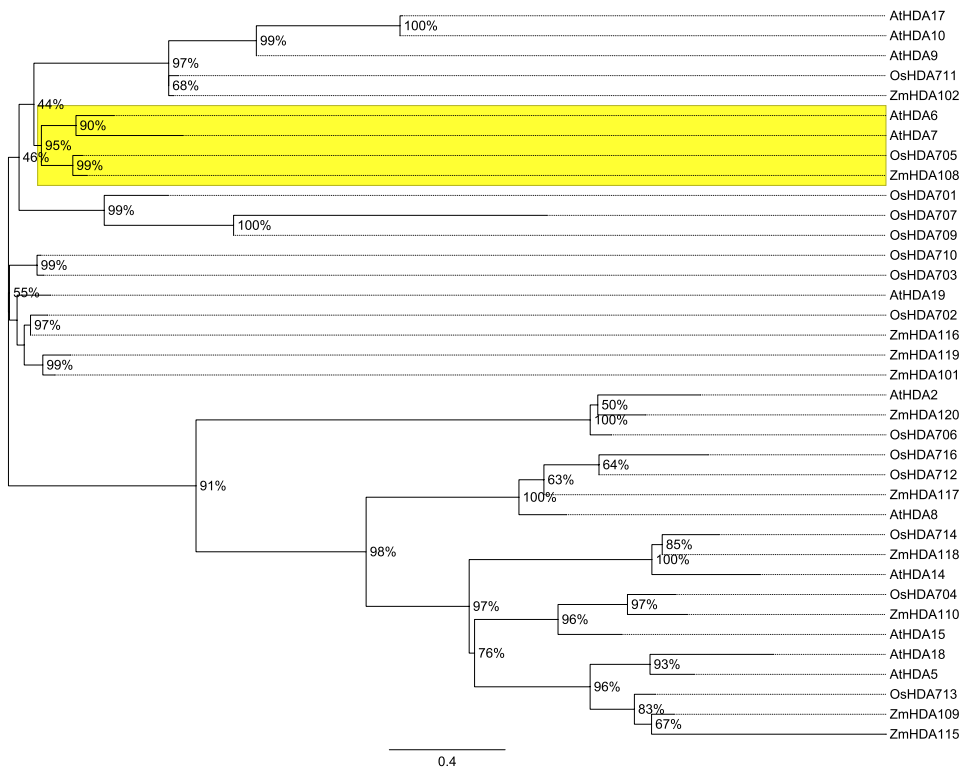


**Figure 6. Maximum-likelihood phylogenetic tree of *Arabidopsis thaliana* (At), *Oryza sativa* (Os) and *Zea mays* (Zm) RPD3 HDACs. Bootstrap values higher than 40% are shown. The clade including AtHDA7 is boxed in yellow. The branch lengths are measured in the number of substitutions per site.**

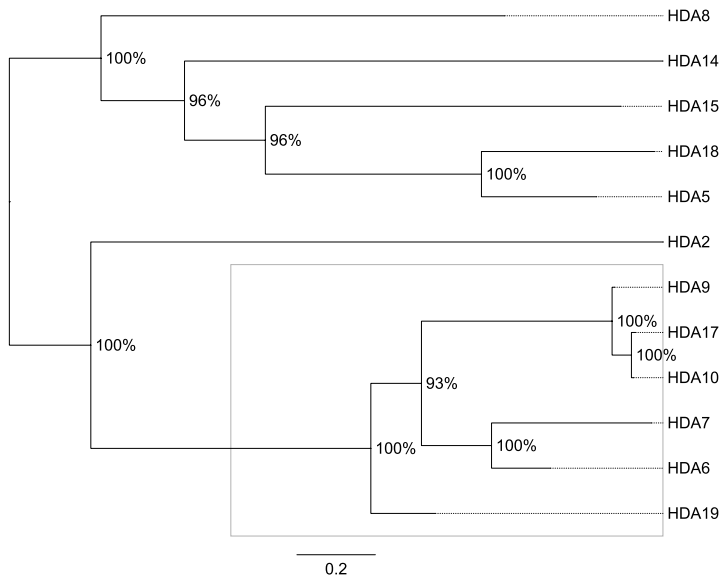


**Figure 7. Maximum-likelihood phylogenetic tree of *Arabidopsis* RPD3 HDACs. Bootstrap values higher than 50% are shown. The clade including HDA7 is outlined in gray. The branch lengths are measured in the number of substitutions per site.**

### 3.2.2. Analysis of *HDA7* mutants

Mutants characterized by *HDA7* silencing and *HDA7* overexpression (*hda7<sup>oe</sup>*) have been analyzed to assess the role of *HDA7* in *Arabidopsis* development and reproduction. In *hda7<sup>oe</sup>* mutant, all seedlings did not survive on selective media likely for the silencing of resistance gene. However, the presence of T-DNA was ascertained by PCR as showed by Cremona (2010).

To specifically silence *HDA7*, amiRNA designed with WMD3 tool (<http://wmd3.weigelworld.org/>) was cloned into the expression vector pK2GW7 (pK2GW7\_amiHDA7). After genetic transformation, 11 T<sub>0</sub> independent lines were selected by kanamycin resistance. Each line showed a 3:1 ratio of alive:dead seedlings on selective media by indicating a single T-DNA insertion. Segregation analysis of T<sub>2</sub> progenies evidenced that 8 lines were homozygous since they did not segregate on kanamycin. For the other 3 lines, a reduction of 11% of germination rate as well as a segregation distortion were observed on selective media with a ratio of alive:dead seedlings of 1:1 (Table 9).

**Table 9. Segregation analysis of T<sub>2</sub> amiRNAi-HDA7 lines on selective media. For each line the number of kanamycin resistant (Kan<sup>R</sup>) and susceptible (Kan<sup>S</sup>) seedlings, the observed ratio (Kan<sup>R</sup>:Kan<sup>S</sup>),  $\chi^2$ -value ( $p < 0.05$ ) in case of homozygous insertion T-DNA (A) and in case of 1:1 segregation ratio (B) are reported.**

| Line | Kan <sup>R</sup> :Kan <sup>S</sup> | Observed Ratio | $\chi^2$ -value <sup>a</sup> | $\chi^2$ -value <sup>b</sup> |
|------|------------------------------------|----------------|------------------------------|------------------------------|
| 1    | 58:0                               | 1:0            | 0                            | -                            |
| 2    | 74:2                               | 37:1           | 0.05                         | -                            |
| 3    | 75:0                               | 1:0            | 0                            | -                            |
| 4    | 92:0                               | 1:0            | 0                            | -                            |
| 5    | 76:4                               | 19:1           | 0.2                          | -                            |
| 6    | 70:0                               | 1:0            | 0                            | -                            |
| 7    | 60:0                               | 1:0            | 0                            | -                            |
| 8    | 60:0                               | 1:0            | 0                            | -                            |
| 9    | 48:45                              | 1.06:1         | 20.3*                        | 0.04                         |
| 10   | 52:53                              | 0.98:1         | 27.2*                        | 0                            |
| 11   | 27:23                              | 1.17:1         | 8.8*                         | 0.16                         |

To assess whether the segregation 1:1 was related to expression level of *HDA7*, the homozygous line 1 (hereinafter *hda7-1*) and segregating line 9 (hereinafter *hda7-2*) were selected to perform quantitative RT-PCR experiments. As shown in Figure 8, *HDA7* is down-regulated in both lines with a fold-change of 0.61 and 0.005 in *hda7-1* and *hda7-2*, respectively. Expression analysis was also performed in *hda7-2* on *HDA6*, *HDA9* and *HDA19* that are the HDACs closely related to *HDA7*. The fold changes of *HDA6*, *HDA9* and *HDA19* were 3.19, 2.57 and 0.8, respectively (Figure 9).

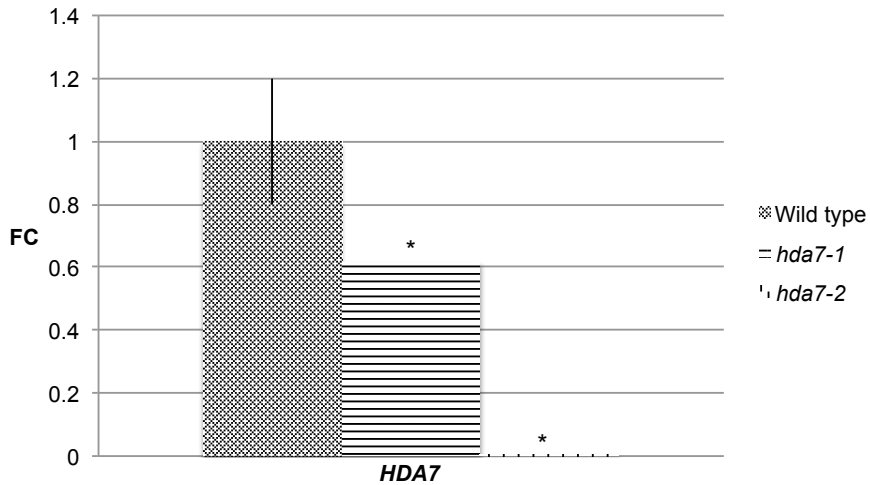


**Figure 8. Expression analysis of *HDA7* in *hda7-1* and *hda7-2* leaf respect to wild type. The fold change (FC) values are the average of three replicates, the standard error is reported as black vertical bars. Asterisks mark statistical significant differences between *hda7-1* and *hda7-2* respect to the control as verified by t-test ( $p < 0.05$ ).**

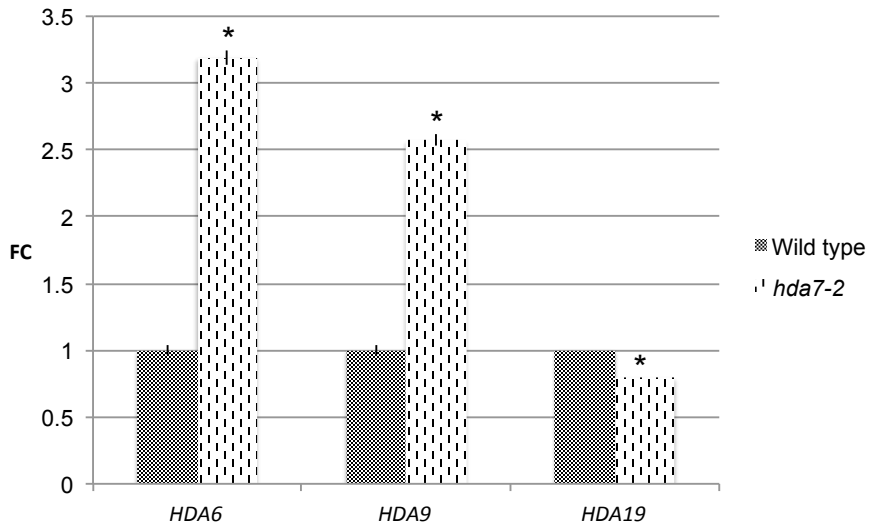


**Figure 9. Expression analysis of HDACs *HDA6*, *HDA9* and *HDA19* in *hda7-2* leaf respect to wild type. The fold change (FC) values are the average of three replicates, the standard error is reported as black vertical bars. Asterisks mark statistical significant differences between *hda7-2* and the control as verified by t-test ( $p < 0.05$ ).**

To assess whether *HDA7* has a role in plant development, *hda7-2* and *hda7<sup>oe</sup>* mutants have been analyzed for different aspects related to seed germination and plant growth. When the seeds of *hda7-2* and *hda7<sup>oe</sup>* lines were grown on media without selective agents reduced germination rate and delayed post-germination growth were observed. Indeed, the percentage of germinated seeds at 8 days after sowing (DAS) was 81.23% in *hda7-2* and 82.5% in *hda7<sup>oe</sup>* as compared to 99.63% in wild type. As regards post-germination growth, the seedlings/plants were scored at 4, 8, 12 and 15 DAS *in vitro* and grouped for growth stage according to Boyes and colleagues (2001). At 4 and 8 DAS, higher percentages of *hda7-2* seedlings, 13.16% and 21.81%, respectively, are at earlier developmental stages respect to wild type thus suggesting a reduced growth speed. At 12 DAS, the trend is confirmed while at 15 DAS, significant differences were not observed anymore (Figure 10). On the other hand, no significant changes in growth rate were observed in *hda7<sup>oe</sup>* *in vitro*.

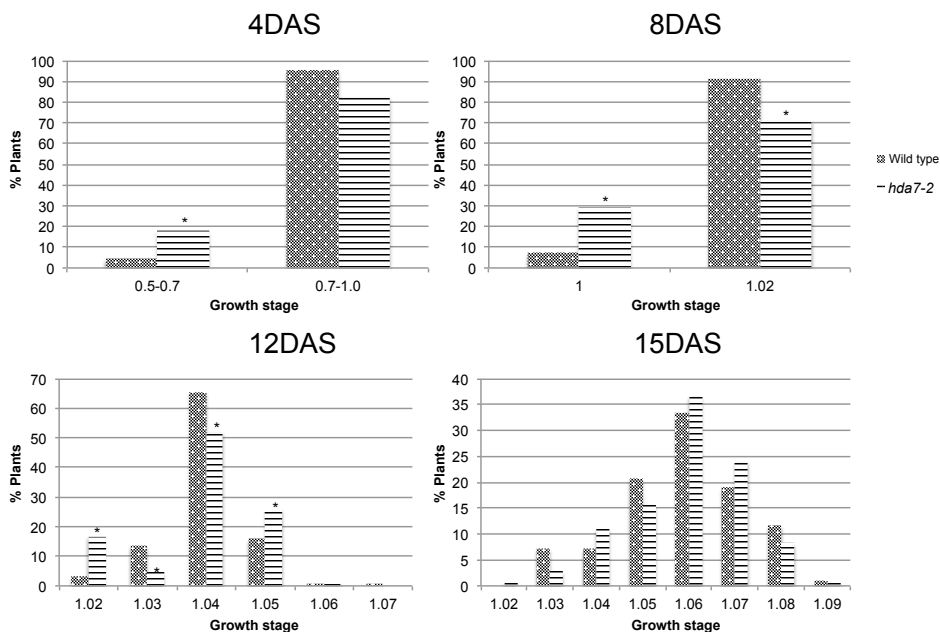


**Figure 10.** *In vitro* post-germination growth of *hda7-2* and wild type plants. The percentages of plants observed at 4, 8, 12 and 15 DAS are reported for each growth stage (Boyes *et al.*, 2001). Asterisks mark significant statistical differences between *hda7-2* and control ( $p < 0.05$ ).

Effects on post-germination growth were also observed in *hda7-2* and *hda7<sup>oe</sup>* plants grown on soil. As shown in Figure 11 at 21 DAS, 45% of control plants were at growth intermediate stages, 1.5, 1.6 and 1.7, while 31.6% of *hda7-2* and 25% of *hda7<sup>oe</sup>* plants were at the same stages. In *hda7-2*, 42.1% of plants were at 1.2 and 1.3 stages. On the other hand in *hda7<sup>oe</sup>*, 32.14% of plants were at 1.2, 1.3, 1.4 stages while 35.71% were at 1.8 and 1.9 stages. The different growth trends of *hda7-2* and *hda7<sup>oe</sup>* plants reported in Figure 13 showed that a significant higher number of *hda7<sup>oe</sup>* plants are developing faster than *hda7-2*.

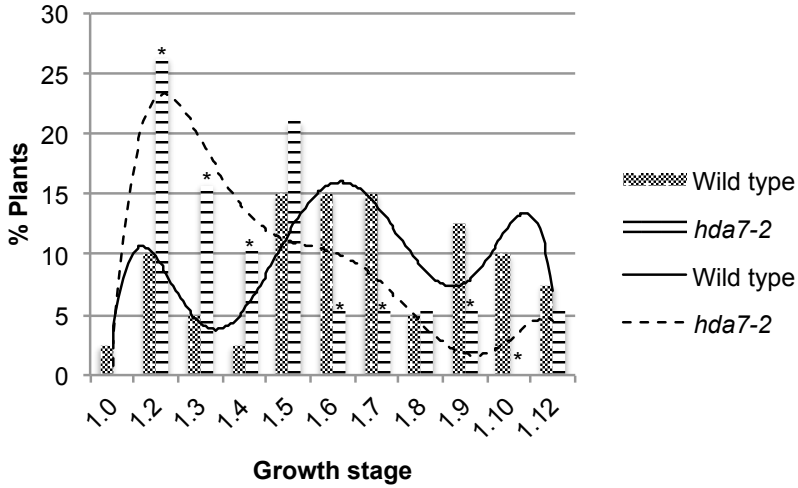


Figure 11. Post-germination growth of *hda7-2* and control plants in soil at 21 DAS. The percentage of plants is reported for each growth stage (Boyes et al., 2001). The growth trend lines of *hda7-2* and wild type are reported as dotted and continuous lines, respectively. Asterisks mark significant differences between *hda7-2* and control ( $p < 0.05$ ).

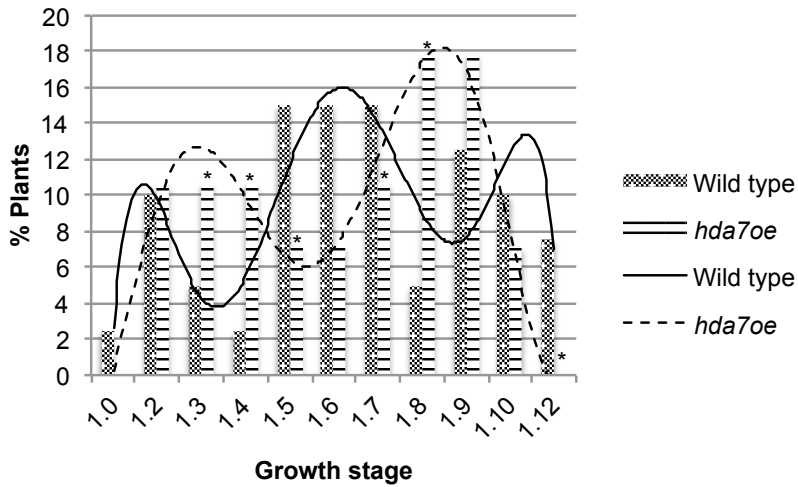


Figure 12. Post-germination growth of control and *hda7<sup>oe</sup>* plants in soil. The percentage of seedlings 21 DAS is reported for each growth stage (Boyes et al., 2001). The growth trendlines of control and *hda7<sup>oe</sup>* are reported as continuous and dotted lines, respectively. Asterisks mark significant statistical differences between *hda7<sup>oe</sup>* and control observed frequencies ( $p < 0.05$ ).

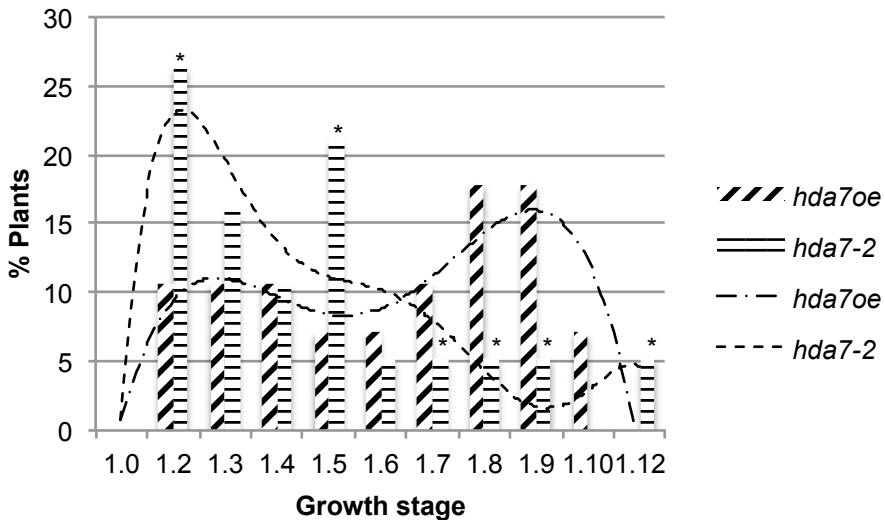
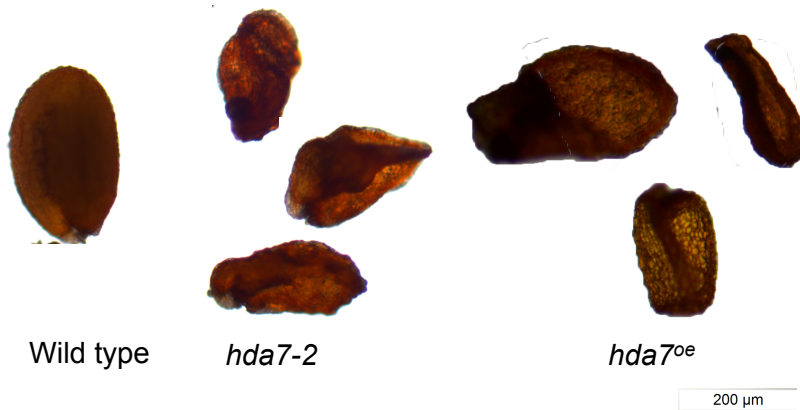


Figure 13. Post-germination growth of *hda7-2* and *hda7<sup>oe</sup>* plants in soil. The percentage of seedlings 21 DAS is reported for each growth stage (Boyes et al., 2001). The growth trendlines of *hda7-2* and *hda7<sup>oe</sup>* are reported as dotted and continuous-dotted lines, respectively. Asterisks mark significant statistical differences between *hda7<sup>oe</sup>* and *hda7-2* observed frequencies ( $p < 0.05$ ).

*In silico* analysis performed in this work evidenced that *HDA7* was significantly up-regulated in flowers respect to seedlings. For this reason, *hda7-2* and *hda7<sup>oe</sup>* plants were analyzed for traits associated to reproduction such as flowering time, length of siliques, number of seeds per siliques, pollen viability and ovule development. The flowering time of kanamycin positive plants evaluated as the mean number of leaves at bolting was not significantly different between wild type (19.1 leaves), *hda7-2* (19.1 leaves) and *hda7<sup>oe</sup>* (19.6 leaves) ( $p < 0.05$ ). The analysis of pollen viability by Alexander staining showed that both *hda7-2* and *hda7<sup>oe</sup>* plants were not different from the control. Despite male viability was not affected in *hda7* plants, the number of seeds per silique was significantly reduced of 20% in *hda7-2* ( $30.5 \pm 10$ ) respect to wild type ( $39.5 \pm 6$ ) ( $p < 0.05$ ) while it was unchanged in *hda7<sup>oe</sup>* ( $40.7 \pm 4$ ). Moreover, 25%

of *hda7-2* and 9% of *hda7<sup>oe</sup>* seeds were shrunken as shown in Figure 14.



**Figure 14. Shrunken seeds from *hda7-2* and *hda7<sup>oe</sup>* plants and a normal seed from wild type.**

To investigate about the possible cause/s of *hda7-2* semisterility, clarified ovaries after fertilization were analyzed by DIC microscopy. By this way, different defects affecting ovule and embryo development were observed. Indeed, as shown in Figure 15, defective ovules and ovary regions devoid of ovules were observed in *hda7-2* but not in the wild type. Moreover, additional investigations in *hda7-2* revealed that 14% of embryo sacs were collapsed (Figure 16). Delayed embryo development was also noticed as evidenced by the contemporary presence of heart, globular and pre-globular embryos in the same ovary. On the other hand, clarified *hda7<sup>oe</sup>* ovules and embryos appeared as the wild type. In agreement with the described defects, the length of mature siliques, which is an index of plant fertility, was significantly reduced of 14% in *hda7-2* respect to the wild type while it was unchanged in *hda7<sup>oe</sup>* as shown in Figure 17 ( $p < 0.05$ ).

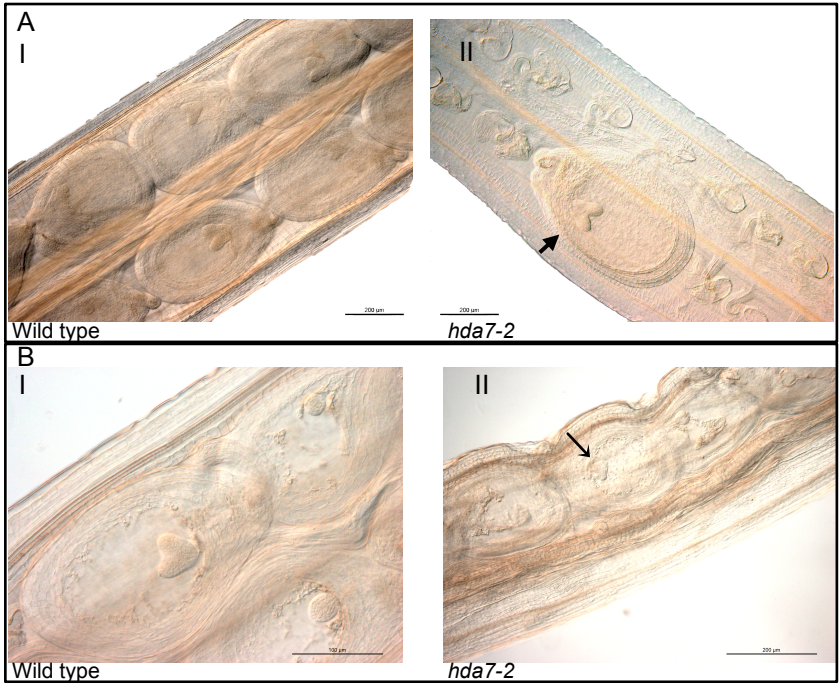


**Figure 15. Ovary segments in *hda7-2* and wild type. Defective ovules together with normal developing ovules (indicated by arrow) in *hda7-2* (AII). Normal ovules at the corresponding stage in wild type (AI). Part of ovary devoid of ovules together with embryos at heart stage (indicated by arrow) in *hda7-2* (BII). Normal ovules at the corresponding stage in wild type (BI). The scale bar is 100 μm in AI-AII-BI and 200 μm in BII.**

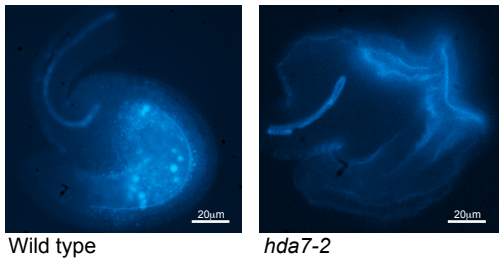


**Figure 16. Ovules from wild type and *hda7-2* plants: normal (left) and collapsed embryo sac.**

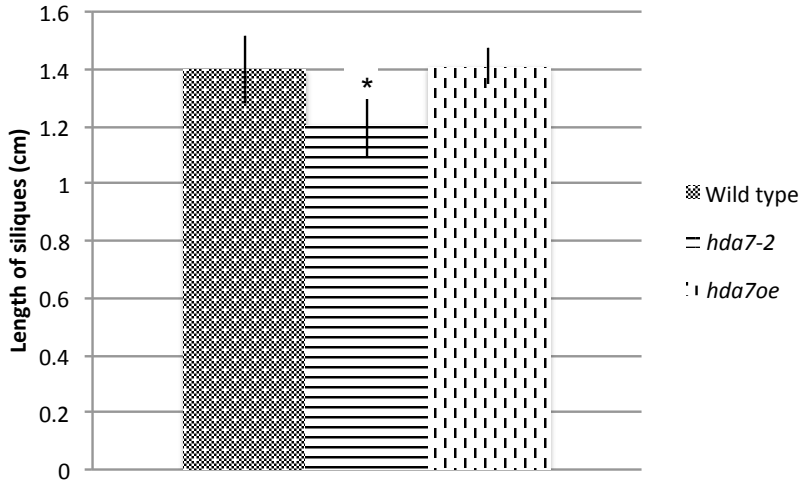


**Figure 17. Length of mature siliques in *hda7-2*, *hda7<sup>oe</sup>* and wild type plants. The asterisk marks the significant statistical difference between *hda7-2* and wild type as verified by t-test ( $p < 0.05$ ).**

On the basis of the pleiotropic effect of *HDA7* down-regulation affecting both vegetative and reproductive development, the Expression Angler tool (<http://bar.utoronto.ca/ntools>) was used to identify which genes were coregulated with *HDA7* in developing embryos and flowers at developmental stages from sporogenesis to fertilization. By this way, 589 and 317 genes were found to be positively coregulated with *HDA7* in embryos and flowers, respectively. The majority of *HDA7* coregulated genes in embryo resulted to be involved in protein metabolism, response to stress and developmental processes (Figure 18). Similarly, most of *HDA7* coregulated genes in flowers, ovaries and carpels resulted to be involved in protein metabolism, developmental processes and cell organization and biogenesis (Figure 19). The list of genes involved in developmental processes with the corresponding coregulation value with *HDA7* both in embryo and in flowers is reported in Table 10. The expression level of *ARABIDOPSIS HOMOLOG OF SEPARASE* (*AtAESP*), which is coexpressed with *HDA7* during embryo development, was assessed in inflorescences at developmental stages from sporogenesis to early embryogenesis. As showed in Figure 20, *AtAESP* resulted significantly downregulated in *hda7-2* respect to wild type with a fold change of 0.64.

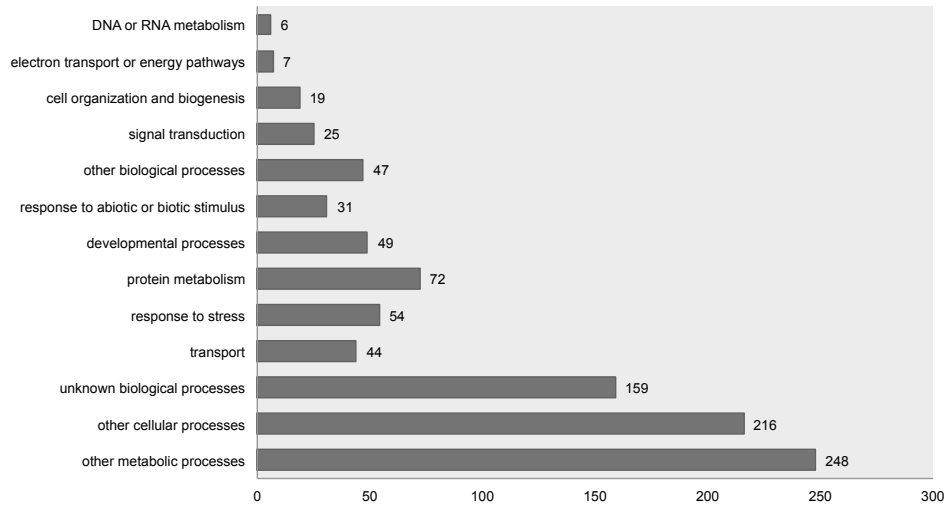


**Figure 18. Functional annotation of *HDA7* coregulated genes in developing embryos from globular to torpedo stage. The number of genes in each Biological Process category is reported on the right.**

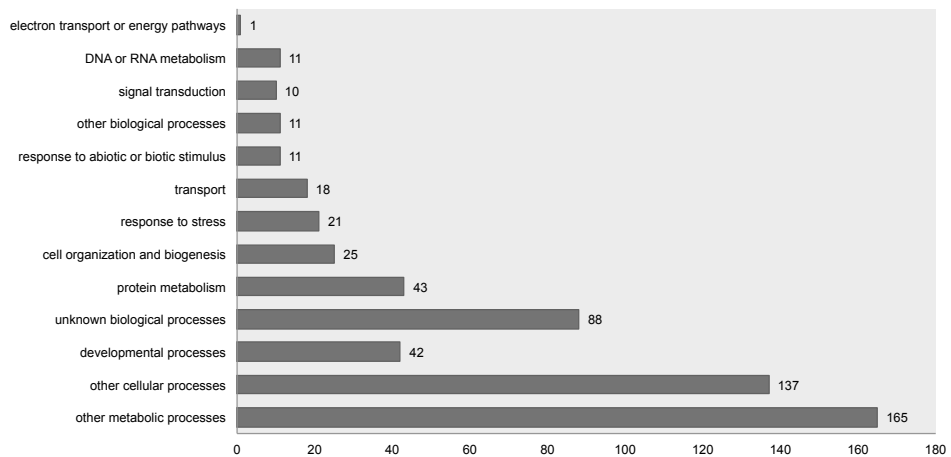


**Figure 19. Functional annotation of *HDA7* coregulated genes in ovaries, carpels and flowers from stage 9 to 15. The number of genes in each Biological Process category is reported on the right.**

**Table 10. List of genes involved in developmental processes which are coregulated with *HDA7* in embryos, from globular to torpedo stage, and in ovaries, carpels and flowers from stage 9 to stage 15. For each locus is reported the common name and the r-value.**

| Embryo    |            |         | Flower/Ovary/Carpel |            |         |
|-----------|------------|---------|---------------------|------------|---------|
| Locus     | Other Name | r-value | Locus               | Other Name | r-value |
| AT1G08090 | ACH1       | 0.877   | AT1G01280           | CYP703A2   | 0.788   |
| AT1G19180 | JAZ1       | 0.948   | AT1G02050           | LAP6       | 0.824   |
| AT1G19440 | KCS4       | 0.959   | AT1G04010           | ATPSAT1    | 0.827   |
| AT1G21210 | WAK4       | 0.946   | AT1G13710           | CYP78A5    | 0.877   |
| AT1G43170 | RPL3A      | 0.801   | AT1G22090           | EMB2204    | 0.832   |
| AT1G52240 | ROPGEF11   | 0.751   | AT1G62940           | ACOS5      | 0.814   |
| AT1G54330 | NAC020     | 0.885   | AT1G68540           | CCRL6      | 0.806   |
| AT1G61290 | ATSYP124   | 0.897   | AT1G68640           | PAN        | 0.806   |
| AT1G70940 | PIN3       | 0.76    | AT1G69500           | CYP704B1   | 0.788   |
| AT2G14210 | AGL44      | 0.841   | AT1G69560           | ATMYB105   | 0.767   |
| AT2G18800 | ATXTH21    | 0.852   | AT1G74030           | ENO1       | 0.803   |
| AT2G22860 | ATPSK2     | 0.885   | AT2G01830           | AHK4       | 0.761   |
| AT2G27300 | ANAC040    | 0.851   | AT2G16910           | AMS        | 0.808   |
| AT2G34790 | EDA28      | 0.941   | AT2G20570           | GLK1       | 0.766   |
| AT2G34830 | ATWRKY35   | 0.945   | AT2G21050           | LAX2       | 0.776   |
| AT2G37250 | ADK        | 0.915   | AT2G22840           | GRF1       | 0.844   |
| AT2G38810 | HTA8       | 0.943   | AT2G45190           | AFO        | 0.828   |
| AT2G44060 | F6E13.19   | 0.79    | AT3G02000           | ROXY1      | 0.824   |
| AT2G45890 | ATROPGEF4  | 0.799   | AT3G06300           | P4H2       | 0.86    |
| AT2G47270 | UPB1       | 0.796   | AT3G13220           | ABCG26     | 0.8     |
| AT3G01700 | AGP11      | 0.849   | AT3G13960           | ATGRF5     | 0.874   |
| AT3G05630 | PDLZ2      | 0.896   | AT3G25100           | CDC45      | 0.777   |
| AT3G10570 | CYP77A6    | 0.897   | AT3G28470           | ATMYB35    | 0.923   |
| AT3G12810 | PIE1       | 0.784   | AT3G42960           | ATA1       | 0.809   |
| AT3G13730 | CYP90D1    | 0.811   | AT3G57920           | SPL15      | 0.813   |
| AT3G20630 | ATUBP14    | 0.821   | AT3G61730           | RMF        | 0.83    |
| AT3G27810 | ATMYB21    | 0.847   | AT4G12920           | UND        | 0.847   |
| AT3G44350 | NAC061     | 0.916   | AT4G14080           | MEE48      | 0.802   |
| AT3G45640 | ATMAPK3    | 0.768   | AT4G20900           | TDM1       | 0.797   |
| AT3G52770 | ZPR3       | 0.824   | AT4G24960           | ATHVA22D   | 0.796   |
| AT3G53020 | RPL24      | 0.945   | AT4G34850           | LAP5       | 0.827   |
| AT3G56520 | T5P19.170  | 0.886   | AT4G35420           | DRL1       | 0.822   |
| AT3G57510 | ADPG1      | 0.875   | AT4G37740           | ATGRF2     | 0.838   |
| AT3G57670 | NTT        | 0.916   | AT5G09970           | CYP78A7    | 0.82    |
| AT4G14080 | MEE48      | 0.941   | AT5G10170           | ATMIPS3    | 0.834   |
| AT4G22970 | AESP       | 0.752   | AT5G14070           | ROXY2      | 0.909   |
| AT4G28110 | ATMYB41    | 0.784   | AT5G41090           | ANAC095    | 0.958   |
| AT4G32400 | ATBT1      | 0.866   | AT5G46590           | ANAC096    | 0.784   |
| AT5G06160 | ATO        | 0.808   | AT5G52000           | IMPA-8     | 0.797   |
| AT5G06760 | LEA4-5     | 0.937   | AT5G53660           | ATGRF7     | 0.857   |
| AT5G10420 | F12B17.230 | 0.798   | AT5G56110           | ATMYB103   | 0.866   |
| AT5G17260 | NAC086     | 0.844   |                     |            |         |
| AT5G18270 | ANAC087    | 0.77    |                     |            |         |
| AT5G24860 | ATFPF1     | 0.813   |                     |            |         |
| AT5G51310 | MWD22.26   | 0.809   |                     |            |         |
| AT5G60410 | ATSIZ1     | 0.806   |                     |            |         |
| AT5G61480 | PXY        | 0.805   |                     |            |         |
| AT5G65050 | AGL31      | 0.884   |                     |            |         |
| AT5G67180 | TOE3       | 0.937   |                     |            |         |

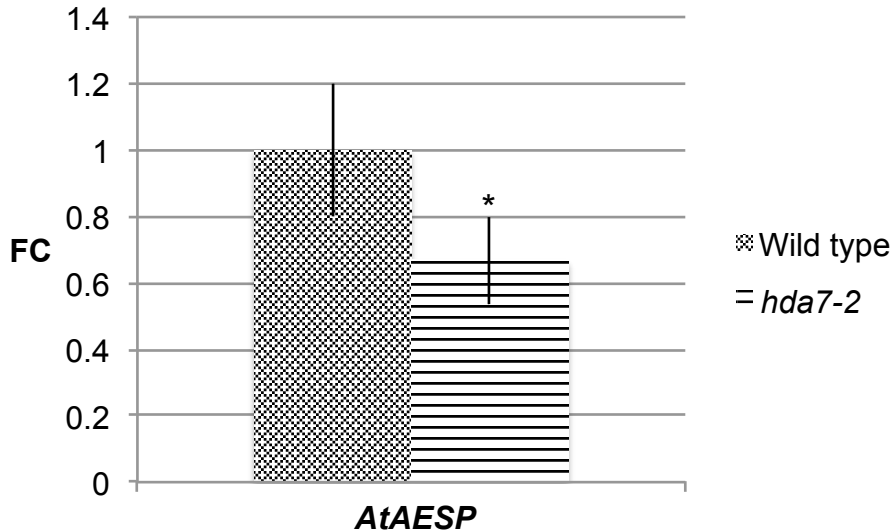


**Figure 20.** Expression analysis of *AtAESP* in *hda7-2* inflorescences (stages 1-15, Smyth *et al.* 1990) respect to wild type. The fold change (FC) values are the average of three replicates, the standard error is reported as black vertical bars. Asterisks mark statistical significant differences between *hda7-2* and the control as verified by t-test ( $p < 0.05$ ).

### 3.3. Reverse genetics of putative meiotic genes affected by histone acetylation by screening of insertional lines

The *Arabidopsis* putative histone acetylase *AtMCC1* was recently described as required for meiotic recombination and segregation (Perrella *et al.*, 2010). Laser Capture Microarray (LMM) experiments, conducted on the mutant overexpressing *AtMCC1*, allowed the identification of 150 genes affected by histone hyper-acetylation in *Atmcc1* microsporocytes (Barra, 2009). Among the 95 up-regulated genes, 16 genes were selected mostly among classes which are known to be required for meiosis in *Arabidopsis* or in other model organisms (Table 11). In particular, genes with a putative role in cell cycle, protein metabolism and chromosome dynamics were selected to investigate whether they had a function in *Arabidopsis* meiosis.

**Table 11. Genes affected by histone hyper-acetylation in *Atmcc1* mutant. For each locus, the description and the Fold Change of the expression between *Atmcc1* and wild type microdissected meiocytes are reported.**

| Locus     | Description                               | FC   |
|-----------|---|------|
| At1g76310 | CyclinB2;4                                | +1.6 |
| At4g37490 | CyclinB1;1                                | +1.6 |
| At5g03455 | CDC25 homolog                             | +1.6 |
| At1g28120 | Ubiquitin thioesterase otubain-like       | +2.9 |
| At1g53750 | 26S proteasome AAA-ATPase subunit (RPT1A) | +3.6 |
| At1g53780 | 26S proteasome AAA-ATPase subunit (RPT1B) | +3.6 |
| At3g60820 | 20S proteasome beta subunit               | +2.2 |
| At5g56150 | Ubiquitin-conjugating enzyme 30           | +2.1 |
| At4g08990 | DNA-methyltransferase                     | +1.5 |
| At1g65920 | Regulator of chromosome condensation      | +1.5 |
| At5g35600 | HDA7                                      | +2.6 |
| At4g09720 | RAB GTPase homolog G3A                    | +1.7 |
| At4g24860 | AAA-ATPase                                | +1.8 |
| At5g20690 | LRR protein                               | +1.6 |
| At5g25110 | CBL-interacting protein kinase 25         | +1.5 |
| At3g10020 | Unknown protein                           | +1.5 |

While for *HDA7* a strategy based on amiRNAi was chosen, we adopted a strategy based on the screening of insertional T-DNA lines obtained from *Arabidopsis* stock centers in order to get functional insights of the remaining 15 genes. Twenty-two lines were selected (Table 12) and for each one at least 24 plants were analyzed for reduced silique fertility without genotyping. Only for the line SALK\_073438, with an insertion in *AtCYCB2;4*, a reduced seed set was observed in 3 plants out of 24. While pollen viability was normal, aborted seeds and not fertilized ovules were observed inside the siliques of semisterile plants. However, when the SALK\_132430 with a T-DNA insertion in another region of *AtCYCB2;4* was analyzed, neither reduced seed set nor defective ovules/seeds were observed inside the siliques.

**Table 12. List of the genes analyzed by T-DNA lines. For each locus, the description, the selected lines and the T-DNA positions are reported.**

| Locus     | Description                               | Lines           | T-DNA Position |
|-----------|---|-----------------|----------------|
| At1g76310 | CyclinB2;4                                | SALK_132430     | 8th intron     |
|           |   | SALK_073438     | 8th exon       |
| At4g37490 | CyclinB1;1                                | GK-951A08       | 7th exon       |
| At5g03455 | CDC25 homolog                             | SALK_143282     | 2nd intron     |
|           |   | SALK_099759     | 1st exon       |
| At1g28120 | Ubiquitin thioesterase otubain-like       | SALK_058652     | 2nd exon       |
| At1g53750 | 26S proteasome AAA-ATPase subunit (RPT1A) | SALK_026158     | 3'-UTR         |
|           |   | SALK_041666     | 3'-UTR         |
| At1g53780 | 26S proteasome AAA-ATPase subunit (RPT1B) | SALK_106176C    | 8th exon       |
|           |   | SALK_121206     | 5th exon       |
| At3g60820 | 20S proteasome beta subunit               | SAIL_298_B07.v1 | 6th intron     |
| At5g56150 | Ubiquitin-conjugating enzyme 30           | SALK_116447     | 5'-UTR         |
|           |   | SALK_093835     | 8th intron     |
| At4g08990 | DNA-methyltransferase                     | SALK_048436     | 1st exon       |
|           |   | SALK_102231     | 10th exon      |
|           |   | SALK_006007     | 3rd exon       |
| At1g65920 | Regulator of chromosome condensation      | SALK_006007     | 3rd exon       |
| At4g09720 | RAB GTPase homolog G3A                    | SALK_139519C    | 4th exon       |
| At4g24860 | AAA-ATPase                                | SALK_011917C    | 3rd intron     |
|           |   | SALK_144667C    | 16th exon      |
| At5g20690 | LRR protein                               | SALK_129244     | 1st exon       |
| At5g25110 | CBL-interacting protein kinase 25         | SALK_079011     | 1st exon       |
| At3g10020 | Unknown protein                           | SALK_025645     | 1st exon       |

### 3.4. Isolation of *PARALLEL SPINDLES LIKE (PSL)* genes in potato and evolutive analysis of PSLs in *Viridiplantae*

In wild and cultivated species related to *Solanum tuberosum*, many genotypes are  $2n$  pollen producers because of a mutation in a gene termed *PARALLEL SPINDLES (PS)* which was not cloned, so far. Recently, d'Erfurth and colleagues (2008) showed that the phenotype of *Atps1* mutant in *Arabidopsis* is due to a mutation in a putative RNA-binding protein (AtPS1) characterized by a N-terminal FHA domain and a C-terminal PINc domain. Exploiting the information of *Arabidopsis* AtPS1 a homology based cloning of *PS LIKE (PSL)* genes in a diploid potato clone was performed. Indeed, using the predicted protein sequence of AtPS1, two ESTs were identified on DFCI Potato Gene Index (<http://compbio.dfci.harvard.edu/tgi>) named TC194262 and DN590600 corresponding to FHA and PINc domains, respectively. The primers designed on the abovementioned ESTs allowed to isolate in diploid potato a 3 Kbp genomic clone (*PSL1*) lacking UTR regions. In order to complete genomic sequence of *PSL1*, by querying Potato Genome Sequencing Consortium Database (<http://www.potatogenome.net/index.php>) and SOL Genomic Network (<http://solgenomics.net>) a 3 Kbp region of *S. phureja* v3 scaffold PGSC0003DMG402026117 (*phuPSL*) and a tomato BAC clone AC211085.1 (*SIPSL1*) sharing 97% and 93% of sequence identity with *PSL1*, respectively, were retrieved. Primers designed on the tomato sequence were used to isolate a potato 5.3 Kbp *PSL1* genomic region spanning 2 Kbp upstream of the start codon to about 200 bp downstream of the stop codon [GenBank:HQ418834]. *In silico* gene prediction showed a structure of *PSL1* composed by six exons and five introns (Figure 21A) and a 2.4 Kbp hypothetical *PSL1* cDNA (*PSL1\_pred*) with a GC content of 42% encoding a 92.5 kDa protein of 823 aminoacids (*PSL1\_pred*). Given the meiotic function of *AtPS1*, potato *PSL1* cDNA was isolated from pre-bolting buds. Seven different cDNAs ranging from 2.3 to 2.7 Kbp were isolated including *PSL1a* of 2.4 Kbp corresponding to *PSL1\_pred*. The sequence alignment between cDNAs and the genomic *PSL1* indicated the presence of different groups of related *PSL* sequences encoded by more than one locus (Figure 21A). In order to investigate the relationship between the different *PSL* cDNAs, we conducted a phylogenetic analysis that suggested the existence of three different loci named *PSL1*, *PSL2* and *PSL3* (Figure 21B). On the basis of sequence similarity, we assigned to

genomic *PSL1* the three cDNAs *PSL1a*, *PSL1b* and *PSL1c* [GenBank:HQ418835, GenBank:HQ418836 and GenBank:HQ418837], to *PSL3* *PSL3a*, *PSL3b* and *PSL3c* cDNAs [GenBank:HQ418839, GenBank:HQ418840 and GenBank:HQ418841] and the last cDNA to *PSL2* [GenBank:HQ418838]. Moreover, the distance measured as the number of different nucleotides among the seven cDNAs showed that *PSL2* was more similar to *PSL3* than to *PSL1* (Figure 21C). Based on the sequences of cloned *PSL* cDNAs, *PSL1b* and *PSL1c*, *PSL3a* and *PSL3b* are alternative splicing forms of *PSL1* and *PSL3* since they retained complete or partial introns causing the formation of premature stop codons (PTCs) (Figure 21A). Moreover, the cloned *PSL2* cDNA showed a PTC caused by the retention of the second intron. As a consequence, all the predicted *PSL* proteins, except *PSL1a* and *PSL3c*, had truncated or lacking PINc domain (Figure 21D). In order to evaluate whether the alternative splicing *PSL* variants were possible target of degradation through nonsense-mediated decay (NMD) we calculated the distance between PTCs and the successive exon-exon junction. Being this distance more than 50-55 nt according to Nagy and Maquat (1998) we could consider *PSL1b*, *PSL1c*, *PSL2*, *PSL3a* and *PSL3b* as target of NMD.

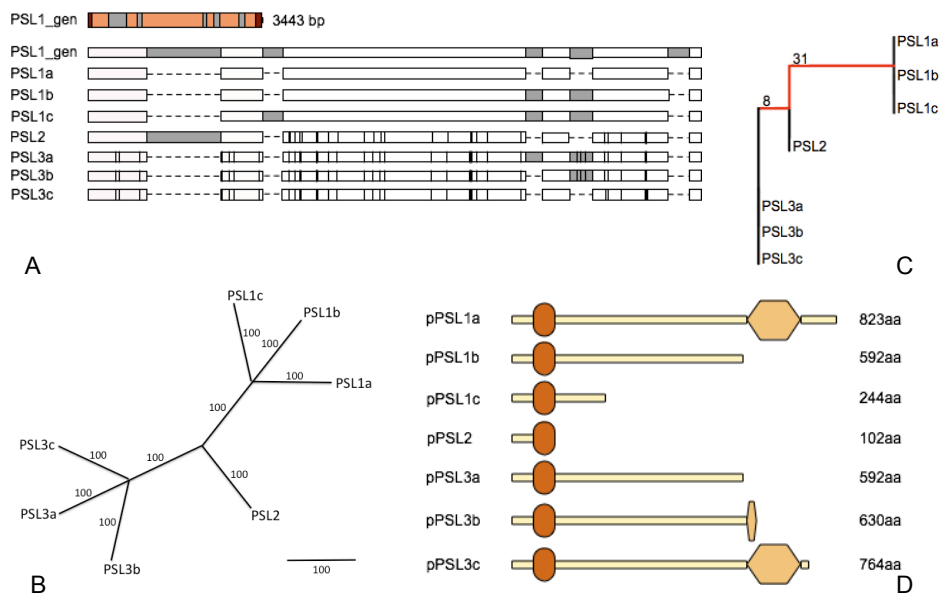


**Figure 21. Potato *PSL* gene family. (A) *PSL1* gene structure (*PSL1\_gen*) with UTRs reported in red, exons in orange and introns in gray is showed together with the schematic alignment of the cloned cDNAs and *PSL1\_gen* sequences, with exons in white, introns in gray and nucleotide differences respect to *PSL1\_gen* as vertical black lines. (B) Maximum Likelihood phylogenetic tree of *PSL* cDNAs is reported with bootstrap values for each node and branch lengths measured in bootstrap values. (C) The distance in terms of number of different nucleotides is reported for the cloned *PSL* cDNAs. (D) Schematic representation of *PSL* predicted proteins obtained after *in silico* translation of the corresponding cDNAs showing FHA and PINc domains as ovals and exagons, respectively.**

In order to investigate the evolution of *PSL* family, Interpro (<http://www.ebi.ac.uk/interpro>) was queried for proteins with both FHA and PINc domains. Interestingly, these domains were contemporary present only in plants, except for the multidrug-efflux transporter NAEGRDRAFT\_78193 from the amoeboid *Naegleria gruberi*. *PSL1a* sequence was blasted against Phytozome v6 database (<http://www.phytozome.net>) that contained the genomic sequences of 22 organisms and against SOL Genomics Network containing tomato genome assembly. Afterwards, 25 sequences of predicted *PSL* proteins were collected from 19 different organisms, as reported in Materials and Methods, since *Physcomitrella patens*, *Ricinus communis*, *Volvox carteri*, *Zea mays* and *Chlamydomonas reinhardtii* seemingly lack *PSL* genes. The sequences were then

aligned and the Maximum-Likelihood phylogenetic tree is shown in Figure 22. The distribution of PSLs is in agreement with the known phylogenetic relationships between species among dicots and monocots. Moreover, one *PSL* locus was found in the analyzed plant species, except for *Glycine max*. Indeed, four different *PSL* loci were identified in soybean and three of them encode alternative transcripts. Differently from potato, the alternative transcripts of soybean retain PINc domain being the splicing sites located at the 3'-end of mRNA (Figure 23).

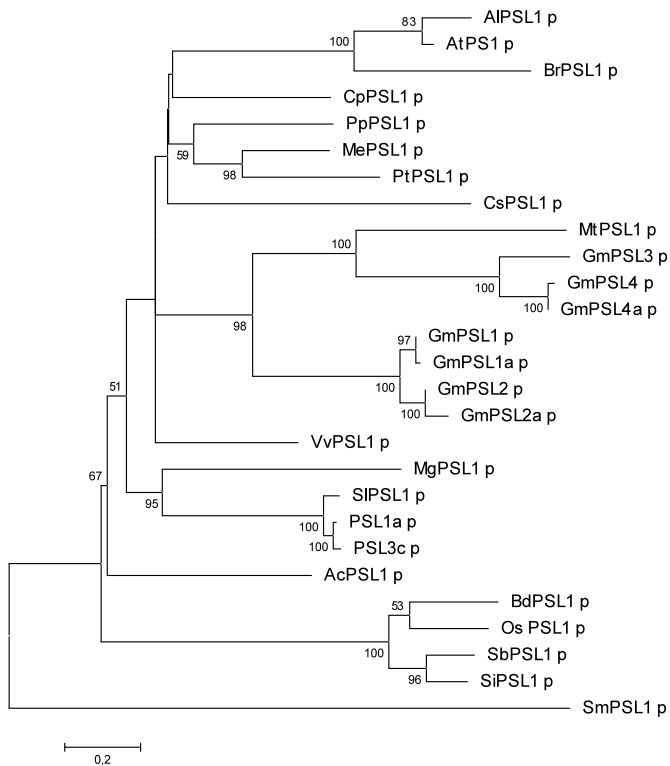


**Figure 22. Phylogenetic tree of plant PSL proteins. Maximum Likelihood phylogenetic tree of PSL predicted proteins from 20 plant species. Bootstrap values are shown for each node. The tree is drawn to scale, with branch lengths measured in the number of substitutions per site. At = *Arabidopsis thaliana*; Ac = *Aquilegia coerulea*; Al = *Arabidopsis lyrata*; Bd = *Brachypodium distachyon*; Br = *Brassica rapa*; Cp = *Carica papaya*; Cs = *Cucumis sativus*; Gm = *Glycine max*; Me = *Manihot esculenta*; Mg = *Mimulus guttatus*; Mt = *Medicago truncatula*; Os = *Oryza saliva*; Pp = *Prunus persica*; Pt = *Populus trichocarpa*; Sb = *Sorghum bicolour*; Si = *Setaria italica*; Sl = *Solanum lycopersicon*; Sm = *Selaginella moellendorffii*; Vv = *Vitis vinifera*.**

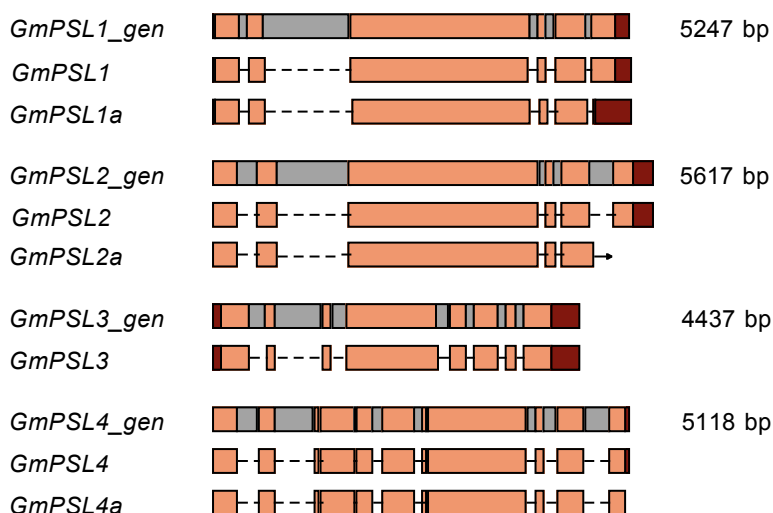


**Figure 23. Alternative splicing of *GmPSL* genes. *GmPSL1\_gen*, *GmPSL2\_gen*, *GmPSL3\_gen*, *GmPSL4\_gen* gene structures are reported with UTRs in red, exons in orange and introns in gray. The mRNAs are reported with UTRs in red, exons in orange and spliced introns as interrupted lines underneath each gene structure. Arrow indicates the lack of complete sequence.**

In order to assess the conservation degree of PSLs, we predicted and compared the secondary structure of FHA and PINc domains using SMART (<http://smart.embl-heidelberg.de>) and PSIPRED (<http://bioinf.cs.ucl.ac.uk/psipred>) tools. It is reported that FHA domain is 80-100 aminoacid (aa) long folded into a 11-stranded beta sandwich, which sometimes contains small helical insertions between the loops connecting the strands. However, in silico analysis of FHA displays only 8 beta-strands (b-strands) out of 11 including the residues involved in phosphopeptide recognition and stabilisation of domain architecture (Durocher et al., 2000). Using the above mentioned tools on yeast RAD53p [NCBI:6325104], a well characterized FHA containing protein (Durocher & Jackson, 2002), the identified FHA region was 52 aa covering 6 beta-strands. As shown in Figure 24, the length of the predicted FHA region in our dataset was 53 aa except for *Brassica rapa* (51 aa) and for *Glycine max* PSL2 (68 aa). While the majority of FHA domains showed 6 beta-strands, *Brassica rapa* FHA was predicted to be composed of 4 consecutive beta-strands followed by an alpha helical region. The group of monocots, *Brachypodium distachyon*, *Oryza sativa* and *Sorghum bicolor*, as well as dicot *Glycine max* (*GmPSL1*) showed a helical insertion between the 2nd and the 3rd beta-strand. In other

species this helical insertion was predicted at a low confidence value as estimated by PSIPRED. Afterward, the active sites in yRAD53p respect to those present in PSL<sup>FHA</sup> domains were compared as showed in Figure 25. It can be observed that glycine-5, arginine-6, serine-21 and histidine-24 in FHA domain are perfectly conserved. The arginine-19 seems to be absent in all plant sequences. In the analyzed species, asparagine-60 showed a substitution with histidine, characterized by a different polarity, except for soybean PSL4 glutamine-60 and *Brassica rapa* that seems to lack this site. Asparagine-66 is mostly substituted with serine that has similar polarity. Instead, AIPSL1, AtPSL1, GmPSL3 and GmPSL4 exhibited arginine-66 with different polarity while BrPSL1 glutamine-66 and MtPSL1 cysteine-66 both showing similar polarity of asparagine.

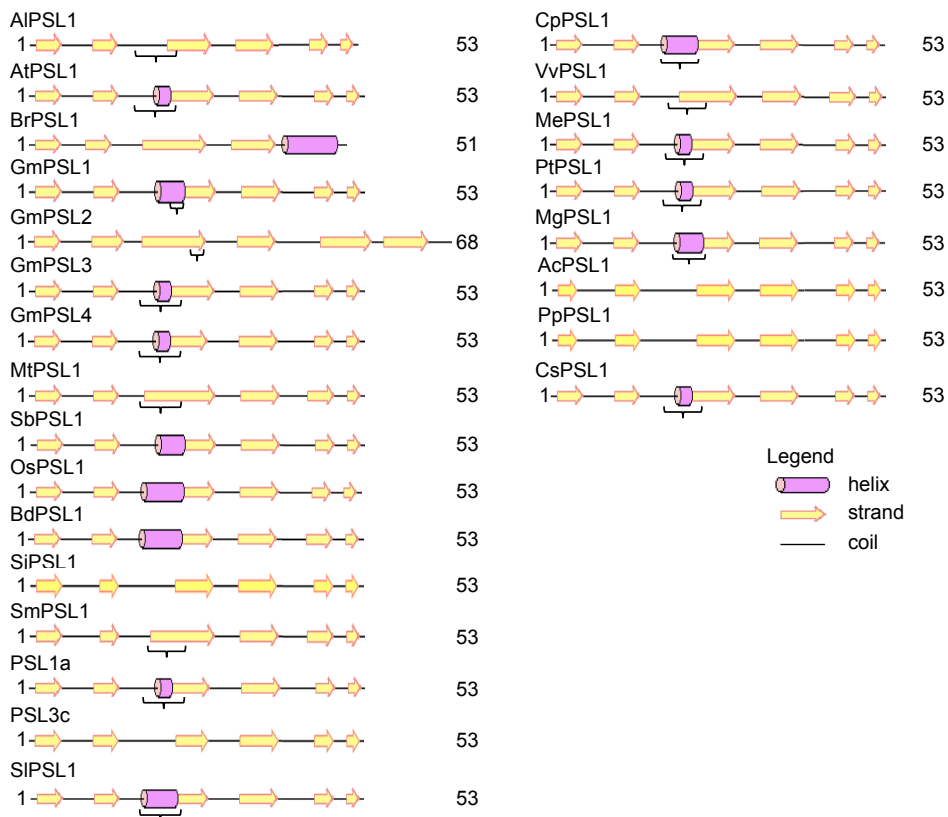


**Figure 24. Predicted secondary structures of PSLs<sup>FHA</sup>.** FHA domain predicted secondary structures of PSLs are reported with alpha-helices as violet tubes, beta-strands as yellow arrows and coiled regions as lines. Regions underlined with brackets show low significance as estimated by PSIPRED. The domain length is also reported. At = *Arabidopsis thaliana*; Ac = *Aquilegia coerulea*; Al = *Arabidopsis lyrata*; Bd = *Brachypodium distachyon*; Br = *Brassica rapa*; Cp = *Carica papaya*; Cs = *Cucumis sativus*; Gm = *Glycine max*; Me = *Manihot esculenta*; Mg = *Mimulus guttatus*; Mt = *Medicago truncatula*; Os = *Oryza saliva*; Pp = *Prunus persica*; Pt = *Populus trichocarpa*; Sb = *Sorghum bicolor*; Si = *Setaria italica*; Sl = *Solanum lycopersicon*; Sm = *Selaginella moellendorffii*; Vv = *Vitis vinifera*.



The analysis of PINc domain in our dataset started with the prediction of its secondary structure in human SMG6 (hSMG6) [UniProt:Q86US8]. It is reported that hSMG6<sup>PINc</sup> (hSMG6) is 182 aa folded into a 5-stranded parallel beta-sheets that is highly twisted and alpha-helices arranged on both sides of each beta-sheet for a total of 6. Three aspartate residues are essential for PINc activity in hSMG6, while a threonine or a serine in the sequence (T/S)XD might be involved in catalytic role on the basis of similarity with other PINc domains (Arcus *et al.*, 2004, Glavan *et al.*, 2006). SMART predicted a PINc domain of 152 aa lacking the first and the last alpha-helices while PSIPRED predicted 4 beta-sheets and 4 alpha helices in hSMG6. In our dataset the PINc domain ranged from a minimum of 123 aa in *Cucumis sativus* to a maximum of 162 aa in *Brachypodium distachyon* (Figure 26). In our prediction, the number of beta-sheets ranged from 3 in GmPSL3 and CsPSL1 to 9 in CpPSL1. The number of predicted alpha-helices ranged from 3 in CsPSL1, OsPSL1 and PSL3c to 7 in BdPSL1 and CpPSL1. Afterward, we compared the active residues of PINc in PSL proteins. The alignment between PINc domain of PSL proteins and hSMG6 is shown in Figure 27. BrPSL1, SmPSL1 and PSL3c show the three expected aspartate residues at positions 6, 194 and 233 of the alignment. SiPSL1 and SbPSL1 have a substitution of two aspartate residues with asparagine-6, glutammate-194. When a substitution occurs, the aspartate-194 is mostly replaced with glutammate-194 except for CpPSL1 showing a different polarity residue (lysine-194) and MgPSL1 showing an aliphatic residue (alanine-194). The aspartate-233 is widely conserved except in BdPSL1, OsPSL1 and SiPSL1 where it is substituted with a serine-233. Most of the PSL proteins show a catalytic serine-231 in the described pattern SXD (where X can be D, N, E or S in this study) instead of threonine-231 in hSMG6, PtPSL1, SiPSL1, SmPSL1 and VvPSL1. GmPSL3 and SbPSL1 are the only proteins lacking the C-terminal extremity of PINc being interrupted at leucine-203 and lysine-227, respectively, thus missing the catalytic threonine/serine-231 and aspartate-233.

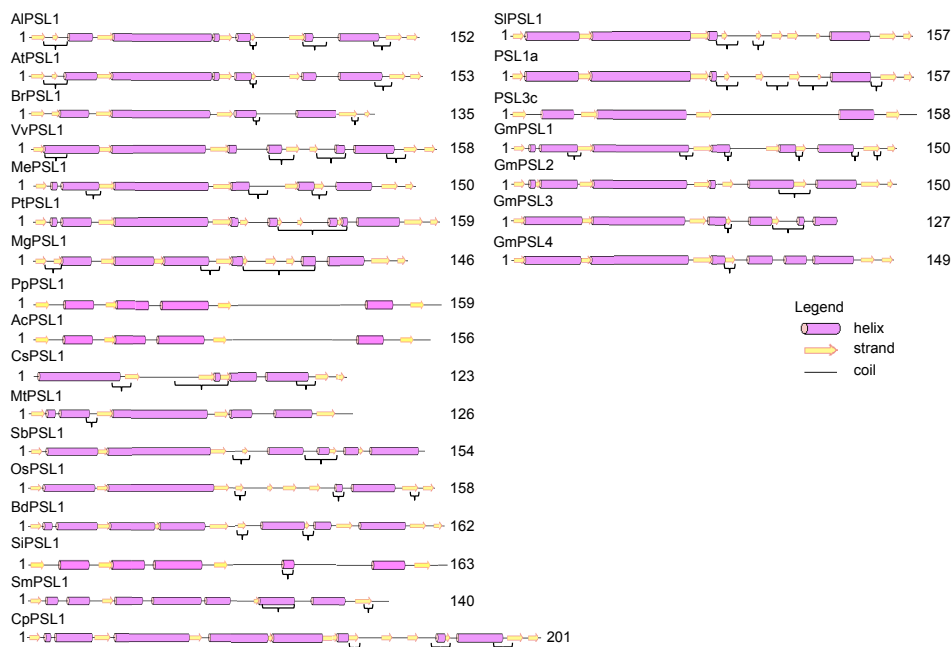


**Figure 26. Predicted secondary structure of PSLs<sup>PINc</sup>. PINc domain predicted secondary structures of PSLs are reported with alpha-helices as violet tubes, beta-strands as yellow arrows and coiled regions as lines. Regions underlined with brackets show low significance as estimated by PSIPRED. The domain length is also reported. At = *Arabidopsis thaliana*; Ac = *Aquilegia coerulea*; Al = *Arabidopsis lyrata*; Bd = *Brachypodium distachyon*; Br = *Brassica rapa*; Cp = *Carica papaya*; Cs = *Cucumis sativus*; Gm = *Glycine max*; Me = *Manihot esculenta*; Mg = *Mimulus guttatus*; Mt = *Medicago truncatula*; Os = *Oryza saliva*; Pp = *Prunus persica*; Pt = *Populus trichocarpa*; Sb = *Sorghum bicolour*; Si = *Setaria italica*; Sl = *Solanum lycopersicon*; Sm = *Selaginella moellendorffii*; Vv = *Vitis vinifera*.**

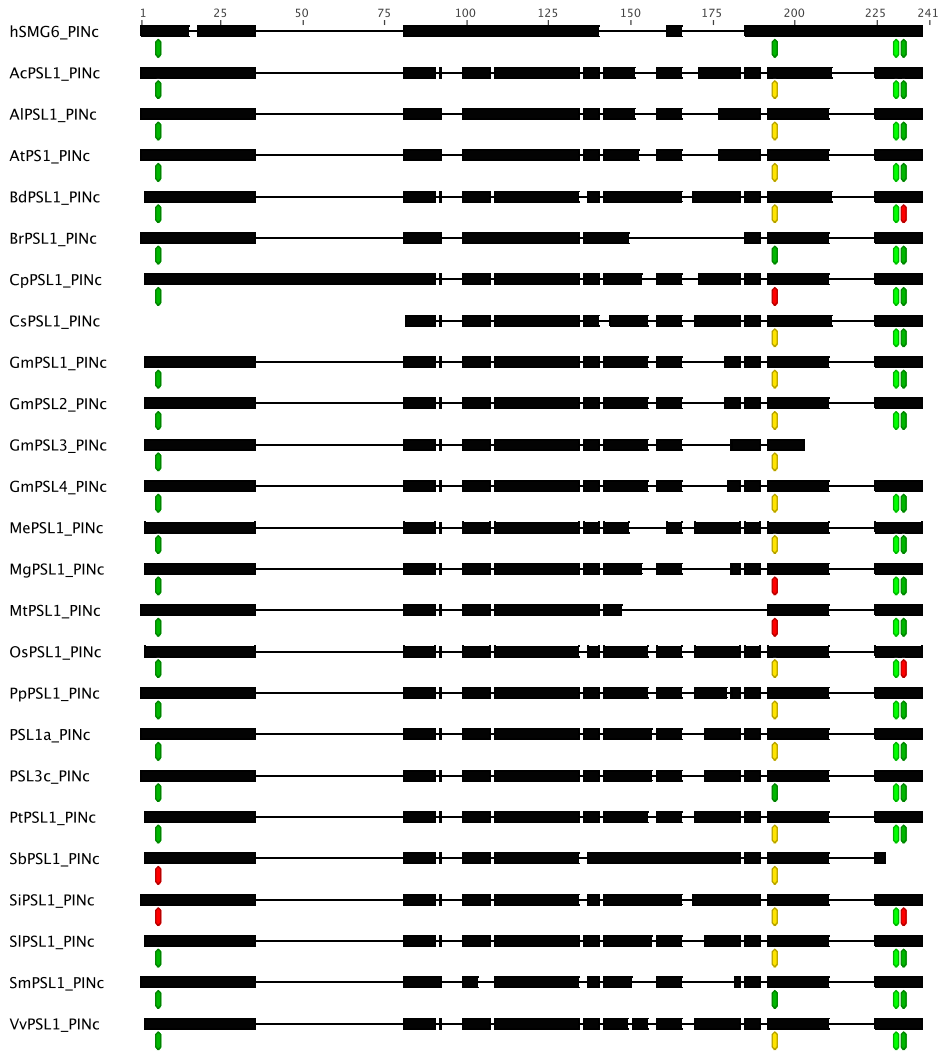


**Figure 27. Comparison of catalytic residues among PSLs<sup>PINC</sup> and hSMG6<sup>PINC</sup>. A schematic protein domain alignment of PSLs<sup>PINC</sup> and hSMG6<sup>PINC</sup> is reported showing the conservation of catalytic residues. Black lines represent gaps in the alignment. Active sites are labeled with a green octagon when the residues are conserved among PSLs<sup>PINC</sup> and hSMG6<sup>PINC</sup>. A yellow or a red octagon mark an amino acid substitution of same or different polarity, respectively. At = *Arabidopsis thaliana*; Ac = *Aquilegia coerulea*; Al = *Arabidopsis lyrata*; Bd = *Brachypodium distachyon*; Br = *Brassica rapa*; Cp = *Carica papaya*; Cs = *Cucumis sativus*; Gm = *Glycine max*; Me = *Manihot esculenta*; Mg = *Mimulus guttatus*; Mt = *Medicago truncatula*; Os = *Oryza saliva*; Pp = *Prunus persica*; Pt = *Populus trichocarpa*; Sb = *Sorghum bicolor*; Si = *Setaria italica*; Sl = *Solanum lycopersicon*; Sm = *Selaginella moellendorffii*; Vv = *Vitis vinifera*.**

In order to test whether positive selection occur at individual amino acid codons, the site specific models implemented in DataMonkey 2010 webserver (<http://www.datamonkey.org>) (Pond & Frost, 2005a) were used. The Integrative Selection Analysis of FEL, SLAC and FER algorithms evidenced no significant positive selected sites ( $dN-dS>0$ ). Conversely, 217 significant negative selected sites ( $dN-dS<0$ ) were identified. The region between FHA to PINc domains included few negative selected sites which were mostly located near the functional domains. The codons encoding the highly conserved active sites glycine-5, arginine-6, serine-21 and histidine-24 in FHA and aspartate-6, serine/threonine-231 and aspartate-233 in PINc were also subjected to negative selection (Figure 28). These observations which support the results obtained through sequence alignment evidence an occurrence of negative pressure upon non-synonymous mutations in *PSL* genes. In particular, the regions next to the functional domains and the codons for active sites were affected.

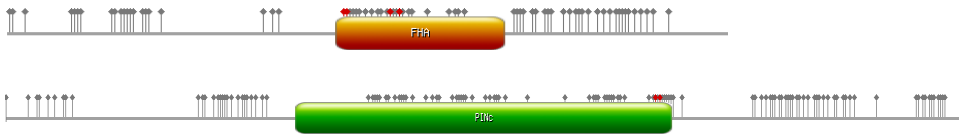


**Figure 28. Distribution of negatively selected codons in  $PSL^{FHA}$  and  $PSL^{PINc}$ . A schematic representation of FHA and PINc domains is reported showing negatively selected sites as gray diamonds. Red diamonds mark active sites subjected to negative selection.**

While the present work was being carried out, the Potato Genome Consortium published the genomic sequence of the doubled monoploid *S. tuberosum* Group *Phureja* clone DM1-3 516R44 (DM) (Xu *et al.*, 2011). In order to get more insights into *PSL* family in potato, *PSL1a*, *PSL2*, *PSL3c* cDNA sequences were blasted against the available potato genome sequence. Only the locus PGSC0003DMG402026117 was found to correspond to the abovementioned *phuPSL*. Same result was obtained by blasting the protein sequences of potato *PSLs*. The different genetic background of T710 and of the sequenced potato could be the cause of the different number of *PSL* loci. Moreover, it is possible that other *PSL* loci could be present in the 177 Mb which have not been sequenced in DM (Xu *et al.*, 2011). In contrast to a predicted *phuPSL* coding sequence (CDS) of 1845 nt reported to encode a 615 aa protein

lacking the N-terminal FHA domain, we found a CDS of 2472 nt encoding a complete PSL protein of 823 aa by aligning transcript and genomic sequences. Interestingly, when the *phuPSL* CDS was compared with the cloned *PSLs*, we found that it shared 98%, 92% and 80% of the nucleotide sequence with *PSL1a*, *PSL3c* and *PSL2*, respectively. In addition, RNAseq data produced by Potato Genome Consortium from different organs revealed that *phuPSL* is mainly expressed in reproductive organs as shown in Figure 29.

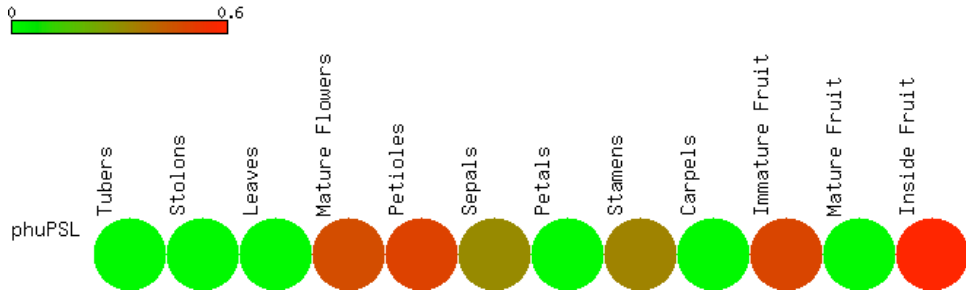


**Figure 29. Expression profile of *phuPSL*.** The expression values of *phuPSL* are shown in different organs as a HeatMap. The scale is in Fragments Per Kilobase of exon per Million fragments mapped (FPKM).



## 4. DISCUSSION

A strategy based on reverse genetics was applied to identify candidate genes with a meiotic function in model plant *Arabidopsis thaliana* and in crops. In *Arabidopsis*, the work was mainly focused on histone de-/acetylation (HDAC/HAT) for the increasing evidences about the crucial role in recombination. In the crops, based on *Arabidopsis AtPS1* gene, which appears responsible for 2n-pollen, PSL genes were isolated in potato and identified *in silico* in other plant species.

### 4.1. Identification of HATs/HDACs with putative role in *Arabidopsis* meiosis/reproduction

*In silico* analysis performed in this work identified HATs and HDACs which are both overexpressed in flowers during meiosis respect to seedlings and are similar to genes involved in sexual reproduction in other species. Indeed, genes with a meiotic function often show a specific expression pattern in reproductive organs. For instance, putative histone acetylase *AtMCC1* (Perrella *et al.*, 2010), histone deacetylase *AtHDA19* (Hollender & Liu, 2008, Cremona, 2010), *AtSPO11* and *RAD51* family members involved in meiotic recombination (Osakabe *et al.*, 2002, Hartung & Puchta, 2000), *AtASY1* and *AtZYP1* in Synaptonemal Complex (Caryl *et al.*, 2000, Higgins *et al.*, 2005) exhibited a peculiar expression profiling. Another feature of meiotic genes is that they often show primary sequence conservation in different organisms. This allowed the identification in *Arabidopsis* of *DMC1* (Klimyuk & Jones, 1997), *SPO11* (Hartung & Puchta, 2000) and *RAD51* (Osakabe *et al.*, 2002) genes which were homologues to yeast, *C. elegans* and human sequences, respectively. However, the homology-based-strategy does not allow the identification of genes which do not share similar protein sequence or are plant-specific.

*In silico* analysis performed in this study combined both the expression data and the similarity to other organisms respect to sequence and function in sexual reproduction. By this way, 4 HATs, *HAG1*, *HAG2*, *HAM1* and *HAF1*, and 4 HDACs, *HDA7*, *HDA6*, *HDA9* and *HDA19*, resulted the strongest candidates to have a role in *Arabidopsis* meiosis. For *HAG2* and *HAF1*, a functional analysis is not available, to date. Instead, *HAG1* (also known as *AtGCN5*) was

showed in *Arabidopsis* to affect several aspects of plant development, particularly in root and flower (Vlachonasios *et al.*, 2003, Bertrand *et al.*, 2003, Cohen *et al.*, 2009, Long *et al.*, 2006, Kornet & Scheres, 2009, Bond *et al.*, 2009). As regards sexual reproduction, flowering time was not affected in *Atgcn5* mutants, but several abnormalities were observed in flower development such as loss of whorl identity and termination of inflorescence meristem (Bertrand *et al.*, 2003) as well as reduced seed set in mature siliques (Vlachonasios *et al.*, 2003). However, the cause of reduced fertility was not deeply investigated. To date, it is unknown whether HAG1 has a meiotic role in *Arabidopsis*. For *HAM1*, Latrasse and colleagues (2008) showed that it plays a redundant role with *HAM2* in male and female gametophyte development. Indeed, while *ham1* and *ham2* mutants are similar to wild type, the double mutants *ham1/ham2* show pollen and ovule abortion leading to reduced fertility.

With regard to the 4 abovementioned HDACs, there is not information about the function of *HDA7* and *HDA9*. *HDA6* was proved to be involved in several aspects of plant development as well as in gene expression. Indeed, it was showed to be necessary to silence rDNA repeats and for nucleolar dominance (Probst *et al.*, 2004, Earley *et al.*, 2006), to establish DNA methylation in heterochromatic regions as well as in regions silenced by RNA dependent DNA Methylation (RdDM) (To *et al.*, 2011b, Aufsatz *et al.*, 2002). Moreover, *HDA6* silencing was showed to be involved in germination and post-germination growth together with *HDA9* and in conjunction with TSA treatments (Tanaka *et al.*, 2008), in leaf senescence by controlling the expression of Senescence Association Proteins (SAPs) which are induced by Jasmonic Acid (JA) (Wu *et al.*, 2008) and in flowering time by controlling the expression of the flowering repressor *FLC* in association with histone demethylase *FLD* (To *et al.*, 2011b). Chen and colleagues (2010b) also showed the involvement of *HDA6* in ABA-responsive expression of genes upon salt stress induced by NaCl treatment providing a link between *HDA6* and abiotic stress response. Successively, To and colleagues (To *et al.*, 2011a) showed also a *HDA6* function in cold acclimation. Despite having different biological roles, *hda6* mutant lines do not have obvious visible defects, except for a somewhat reduced fertility of the first flowers as reported by Aufsatz and colleagues (2002). Therefore, the role of *HDA6* in plant reproduction remains to be elucidated. *HDA19* is considered a global regulator of gene expression in

*Arabidopsis* (Fong *et al.*, 2006). Indeed its downregulation leads to induction and repression of 10.7% and 7.8% of the transcriptome in leaves and flower buds, respectively (Tian *et al.*, 2005). Moreover, knockout of *HDA19* obtained through RNAi and T-DNA insertion affects several developmental processes such as early senescence, serration of leaves, aerial rosette formation, flowers lacking sepals and petals and gaining extra stamens, infertility and delay of flowering (Tian & Chen, 2001, Tian *et al.*, 2003). When the causes of infertility were investigated, different phenotypes were observed in *hda19* plants such as abnormal flowers, shorter stamens which sometime were reduced in number or fused (Tian *et al.*, 2003). However, while Tian and colleagues (2003) found regular pollen in *hda19* plants, Cremona (2010) found about 40% of not viable pollen grains. Moreover, analysis of microsporogenesis revealed univalents in metaphase I and unbalanced spores at the end of meiosis (Cremona *et al.*, 2010). *HDA19* was also shown to be involved in embryo (Tanaka *et al.*, 2008) and seedling development in a temperature-sensitive way. Indeed, at 29°C *hda19* seedlings displayed several morphological defects (Long *et al.*, 2006). Finally, *HDA19* can be up-regulated in response to pathogens as showed by Zhou and colleagues (Zhou *et al.*, 2005). The data so far collected on the abovementioned HATs and HDACs of *Arabidopsis* highlight that *in silico* analysis performed in this study was effective to find genes involved in meiosis and/or in other aspects of sexual reproduction, as well. In this thesis the functional analysis of *HDA7* is reported. Indeed, *HDA7* resulted the strongest candidate among HDACs and HATs. However, other strong candidates such as *HDA6* and *HDA9* will be analyzed to assess their meiotic function.

#### **4.2. Functional characterization of *Arabidopsis* *HDA7* gene**

The function of the putative histone deacetylase *HDA7* was analyzed by means of *in silico* analysis and mutations inducing overexpression or silencing. *HDA7* overexpressing line (*hda7<sup>oe</sup>*) was previously identified by Cremona (2010) in a systematic screening of *Arabidopsis* T-DNA lines. As reported on TAIR, the T-DNA insertion is located in the promoter region of *HDA7*, 43 bases from the start codon. *In silico* analysis of the promoter region revealed that seven motifs associated to transcriptional activation and a SET-BINDING FACTOR-1 (SBF-1) motif, which is associated to repression of transcription (Lawton *et al.*, 1991), are located 1000 bps from *HDA7*

start codon. Interestingly, T-DNA insertion in *hda7<sup>oe</sup>* disrupt the association of five of the activating motifs as well as of SBF-1 but maintains the association with the activating GCCAAG motif (Leah *et al.*, 1994). Thus, the overexpression of *HDA7* in *hda7<sup>oe</sup>* could be the result of the interrupted association with the SBF-1 repressor motif. However, it is also possible that the other activating motifs are involved in a stringent transcriptional regulation that is abolished by T-DNA insertion.

To silence *HDA7* expression, amiRNAi approach was used. Indeed, amiRNAs were showed to efficiently silence multiple genes as well as single target genes in *Arabidopsis* (Schwab *et al.*, 2006). On the basis of the coregulation analysis we argued that *HDA7* might be not acting redundantly with other HDACs. Thus, amiRNA was designed to specifically silence *HDA7*. As previously stated, an altered phenotype was observed in *hda7-2* but not in *hda7-1* plants which could be linked to the higher expression of *HDA7* in *hda7-1*. This kind of variability was also observed in amiRNAi lines by Schwab and colleagues (2006) as well as by Alvarez and colleagues (2006) which reported strong, intermediate and weak phenotypes in transgenic plants overexpressing both natural and artificial miRNAs (Alvarez *et al.*, 2006). Moreover, the authors linked the intensity of the phenotypes with the expression levels of the miRNAs, and thus of their target genes, which is in agreement with our results. Interestingly, the downregulation as well as the upregulation of *HDA7* leads to multiple defects affecting both vegetative and reproductive development. Indeed, reduction of germination rate and altered post-germination growth were observed in *hda7-2* and *hda7<sup>oe</sup>* plants. Moreover embryo sac collapse and delayed embryo development were also observed in *hda7-2* plants. Effects on both vegetative and reproductive stages, arising from mutations in HATs and HDACs, were already reported in *Arabidopsis* for the abovementioned *HAG1*, *HDA6*, and *HDA19*. Moreover, the overexpression of the putative histone acetylase *AtMCC1* was showed to lead to defects in leaf development as well as in male and female meiosis (Perrella *et al.*, 2010). Knock-out lines of *HAC1* as well as the double mutants *hac1/hac5* and *hac1/hac12* showed reduced plant size, late flowering and semisterility (Han *et al.*, 2007). As regards *hag3* mutants, Nelissen and colleagues (2005) reported reduction of primary root growth and altered inflorescence architecture. *AtHD2A* was reported

to be required alone for seed (Wu *et al.*, 2000) and, together with *AtHD2B*, for leaf development (Tanaka *et al.*, 2008).

A reduction of about 20% in germination rate at 8 DAS and altered post-germination growth were observed both in *hda7-2* and *hda7<sup>oe</sup>* plants. Tanaka and colleagues (2008) studied the effect of TSA and of *HDA6/HDA19* silencing on germination rate and post-germination growth *in vitro* in *Arabidopsis*. A 10-15% reduction of germination rate was observed in wild type *Arabidopsis* seeds (Columbia and Wassilewskija strains) treated with TSA, an inhibitor of deacetylases. However, germination rate was not affected in *hda6* mutants (Tanaka *et al.*, 2008, Chen *et al.*, 2010b) as well as in the double *hda6/hda19* mutants (Wassilewskija background). Given that *hda7* has not an overlapping phenotype of seed germination with any of the already described HDACs mutants we can conclude that *HDA7* has a specific function in seed germination in *Arabidopsis*. Furthermore, the reduction of germination rate observed in *hda7* is similar to that reported by Tanaka and colleagues (2008) after seed treatment with TSA. This is furtherly supported by the observation that 25% and 9% of seeds were shrunken in *hda7-2* and *hda7<sup>oe</sup>*, suggesting that *HDA7* misregulation leads to seed abortion. The seed abortion observed in *hda7-2* can be explained by the delayed embryogenesis. Indeed, it is possible that delayed embryos arrest their development thus leading to seed failure. As regards *hda7<sup>oe</sup>*, the absence of obvious defects during embryo development and an higher percentage of not germinating seeds respect to the shrunken (20% vs 9%, respectively) suggest that other processes could be impaired during embryogenesis or germination respect to *hda7-2*. Tanaka and colleagues (2008) also showed that seeds of Columbia ecotype treated with TSA at a low concentration are characterized by a reduced post-germination growth at 7 DAS that normalizes at 14 DAS. On the contrary, seeds of Wassilewskija (Ws) ecotype are not affected by similar TSA treatment. Arrested post-germination growth was observed in *HDA6* repressed line, but only in conjunction with low concentrations of TSA, and in *hda6/hda19* double mutant. *Hda7-2* seedlings showed a reduced post-germination growth at 4, 8 and 12 DAS while post-germination growth defects were no longer visible at 15 DAS *in vitro*. Thus we can argue that *HDA7* plays its function early during *Arabidopsis* vegetative growth. Alternatively, balancing mechanisms could be triggered to normalize *in vitro* plant growth in the mutant. When *hda7-2* plants were grown on soil, most of the

seedlings at 21 DAS were developing slower than wild type while *hda7<sup>oe</sup>* showed both fast and slow growing seedlings. These data, together with the normal post-germination growth of *hda7<sup>oe</sup>* seedlings *in vitro*, suggest that complex interactions between environmental conditions and *HDA7* influence plant development as observed in temperature-sensitive *hda19* plants (Long *et al.*, 2006). The importance of histone de/acetylation for the initial steps of plant growth has been reported also for other HATs/HDACs in *Arabidopsis*. Indeed, *hag3* and *hda19* mutants were reported to grow slowly respect to wild type (Kojima *et al.*, 2011, Tian *et al.*, 2003). Moreover, Tian and colleagues (2001) reported premature dead of *hda19* seedlings (Tian & Chen, 2001). While *HD2A* silenced plants showed seed abortion (Wu *et al.*, 2000), *HD2A* and *HD2C* overexpressing plants showed aborted seed development and early germination, respectively (Zhou *et al.*, 2004, Sridha & Wu, 2006). Interestingly, Colville and colleagues (2011) showed that seed germination defects and post-germination growth in *hd2a* and *hd2c* knock-out plants are linked to response of seeds to sugars (Colville *et al.*, 2011). Indeed, the authors demonstrated that *HD2A* has a role in preventing germination while *HD2C* enhances germination in presence of glucose. However, the reduced seed germination observed in *hda7* plants is likely unlinked to sugar sensing, given that Colville and colleagues showed that *HDA7* is not induced by glucose in contrast to *HD2A* and *HD2C*. Histone de/acetylation was also proved to have an important role for proper timing of embryogenesis. Indeed, precocious embryo development was observed in double mutants for *HDA6* with *ARABIDOPSIS 6B-INTERACTING PROTEIN1-LIKE1* (*ASIL1*) or *ARABIDOPSIS 6B-INTERACTING PROTEIN1-LIKE2* (*ASIL2*) which prevent the expression of embryonic traits after seed germination (Willmann *et al.*, 2011). The involvement of histone deacetylases in seed development and production was also described in other plant species. In rice, downregulation of HDAC *OshDA703* led to sterility and altered seed morphology (Hu *et al.*, 2009). Moreover, Chung and colleagues (2009) were not able to recover homozygous mutants for rice *OshDAC1*, which is the closest homologue of *Arabidopsis HDA19*, suggesting its involvement either in embryo or in gametophyte development (Chung *et al.*, 2009), while Jang and colleagues (2003) reported increased growth rate in *OshDAC1* overexpressing lines (Jang *et al.*, 2003). However, studies concerning the relationship between histone de/acetylation and

embryogenesis were mostly performed in maize. Indeed, HDT and RPD3 histone deacetylases as well as histone acetylases were firstly isolated in crude extracts of maize embryos (López-Rodas *et al.*, 1991, Georgieva *et al.*, 1991, Kölle *et al.*, 1999). Lechner and colleagues (2000) reported a dynamic expression of two RPD3 HDACs in maize embryos (HD1B-I and HD1B-II) highlighting that histone deacetylation play a crucial role during embryogenesis (Lechner *et al.*, 2000). Successively, Varotto and colleagues (2003) showed that *ZmHDA108*, the closest homologue to *Arabidopsis HDA7*, is particularly abundant in embryos at 72 hours after germination, in endosperm at 3-8 days after pollination and in ears at early stage of development. Moreover, *ZmHDA108* protein is abundant in kernels at 3, 5, and 8 days after pollination (Varotto *et al.*, 2003). Even if there are not reports about the functional analysis of *ZmHDA108*, its expression profile suggests its involvement in embryo development. As regards other maize HDACs, Rossi and colleagues (2007) reported that *HDA101* overexpression and downregulation leads to normal germination but slow growing as indicated by a reduction of plant height.

Besides the abovementioned defects, *hda7-2* plants were characterized by other reproductive abnormalities. Flowering time was not affected by *HDA7* downregulation. Despite pollen viability was normal in *hda7-2*, it is not possible to exclude a change in the frequency or the distribution of COs in microsporocytes. Seed set decreased in *hda7-2* plants as a consequence of seed number reduction per silique (20%) due to embryo sac collapse (14%). These data support the view that *HDA7* has a role in the female germline development. Semisterility and gametophytic defects were described also by Latrasse and colleagues (2008) which showed that *ham1/ham2* plants were impaired both in male and female gametophyte development. Indeed, half of the mutant ovules and 40% of microspores aborted before the first mitotic division after meiosis causing reduced seed set and shorter siliques respect to wild type.

Even if further analyses are required to fully understand the causes of the observed defects, it can be argued that different processes are affected by *HDA7* mutation. Moreover, it remains to be elucidated whether *HDA7* exerts its function directly as a transcriptional regulator and/or indirectly as a chromatin modeler. Up-regulation of

both *HDA6* and *HDA9* and down-regulation of *HDA19* found in *hda7-2* suggest that many other genes could be affected by *HDA7* silencing. In this complex landscape, we can hypothesize that altered transcripts occur in *hda7-2* megagametophyte thereby affecting embryo development. This hypothesis is supported by the study of Pillot and colleagues (2010) that showed the requirement for embryo development of the transcripts produced in *Arabidopsis* female gametophyte (Pillot *et al.*, 2010). An alternative possibility is that *HDA7* is involved in the regulation of embryogenesis-related genes. Tanaka and colleagues (2008) ascribed seed abortion and delayed post-germination growth observed in plants treated with TSA to misregulation of several embryogenesis-related genes (*LEC1*, *LEC2*, *FUS3*, *ABI3*, *EtECP31*, *AtECP63*, *CRA*, *CRB* and *CRC*). However, to get some hints on the causes of the defects observed in *hda7*, we searched for genes coregulated with *HDA7* in embryos, ovaries and flowers. Among the significant coregulated genes none of the embryo-related investigated by Tanaka and colleagues (2008) was found. However, other genes that could affect both embryogenesis and ovule development were evidenced and discussed in the following paragraphs.

*AtAESP* encoding a separase was found to be essential for embryo development (Liu & Makaroff, 2006). Indeed, Liu and colleagues were not able to isolate homozygous *Ataesp* T-DNA lines thus suggesting embryo lethality which was then confirmed by a 25% reduction of seed set. Moreover, similarly to what observed in *hda7-2*, delayed embryogenesis and embryo development arrest at early globular stage were reported in *AtAESP/Ataesp* lines. Interestingly, Yang and colleagues (2011) showed delayed ovule development as well as 7% of ovule degeneration in *rws4* allele of *AtAESP*. Interestingly, *AtAESP* was downregulated in *hda7-2* suggesting that it could be involved in the ovule collapse and the delayed embryogenesis observed in the mutant.

In knockout lines of *AtUBP14* which encodes a protease involved in ubiquitin recovery from polyubiquitinated proteins, seed abortion associated to embryogenesis arrest at globular stage was described by Doelling and colleagues (2001) similarly to what was observed in *hda7-2* embryos. The authors also showed that *Atubp14* immature seeds had increased levels of both free multi-ubiquitin chains and ubiquitinated proteins, thus impairing embryo development. Moreover,

it is possible that AtUBP14 plays an important role as regulator of the transition from globular to heart staged embryo (Doelling *et al.*, 2001).

Another gene coregulated with *HDA7* and having a role in embryogenesis is *BRITTLE1*, which encodes a nucleotide carrier protein with a plastidial localization. Indeed, homozygous *Atbt1* T-DNA lines are embryo lethal and the seed produced by rescued homozygous plants are completely collapsed and empty (Kirchberger *et al.*, 2008). This phenotype resembles what was observed in *hda7-2*, therefore suggesting that *AtBT1* could be involved in seed and embryo defects.

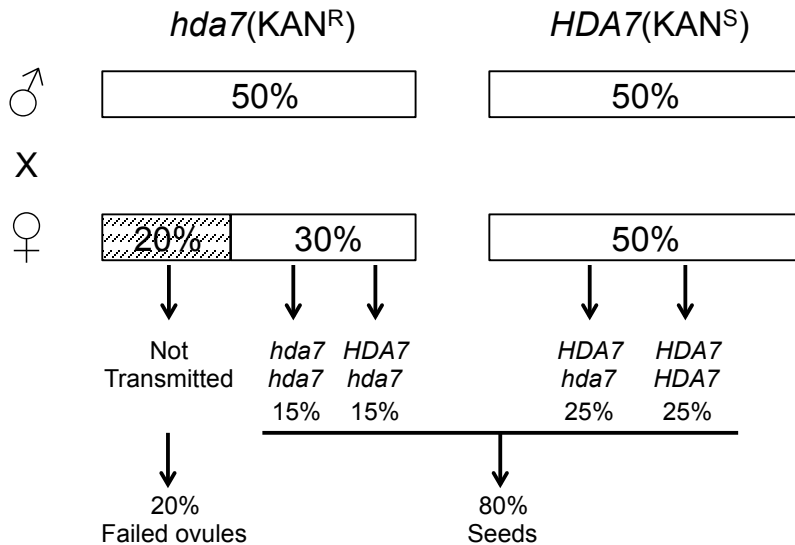
*ATO*, which encodes a protein homologue to human splicing factor SF3a60, was also found to be coregulated with *HDA7*. Moll and colleagues (2008) observed about 50% of infertile ovules and less than 10% of aborted seeds in *ato* mutants. However, the phenotype observed in *hda7* seems to exclude the involvement of *ATO*. Indeed, the authors attributed *ato* semisterility to reduced pollen tube attraction due to misspecification of synergid cells but there are not report of ovule collapse as observed in *hda7-2*.

Female gametophytic defects were also observed in *cdc45* (Prabhakar *et al.*, 2010) and *eno1/ppt1* (Prabhakar *et al.*, 2010) mutants. However, other defects impairing pollen development in *cdc45* and *eno1/ppt1* and vegetative growth suggest that these genes are not involved in *hda7* phenotype.

The different phenotype of *hda7-2* and *hda7<sup>oe</sup>* indicate either that different sets of genes are misregulated or that the same genes are differentially affected by *HDA7* up- or downregulation. Despite several *HDA7* coregulated genes could be involved in *hda7* phenotype, only transcriptional comparison of the mutants respect to wild type will be useful to understand the involved molecular mechanisms.

To give a genetic explanation of the distorted segregation ratio observed in the self-progeny from heterozygous *HDA7/hda7* line by kanamycin selection, we took into account the following observations. In *hda7-2* line, seed germination was affected: indeed, germination reduction ranging from 11% to 19% was seen on media with and without kanamycin whereas in wild type the seed germination was

complete. In the mutant, 46% of seedlings survive on kanamycin. Twenty per cent reduction was observed for the number of seeds per silique in the mutant confirmed through cytological analysis by the number of ovules with embryo sac collapse (14%). Based on the last observation, we can argue that *hda7* is a female gametophytic lethal mutation. However, it is not fully penetrant because the ovules carrying defective megagametophytes and, consequently, not developing into seeds are less than half. Although the transmission of *hda7* allele is reduced via female gametes, but not abolished, *hda7* homozygous plants should be expected at 18% but they were not recovered in self-progenies coming from *hda7-2* line (Figure 30). The hypothesis is that additional defects, likely during embryo development, affect seed development and germination, and seedling growth in *hda7/hda7*. Indeed, we observed shrunken seeds, germination reduction, excess of dead seedlings and growth delay.



| Phenotype                 | Expected (%) | Observed (%) | $\chi^2$ -value |
|---------------------------|--------------|--------------|-----------------|
| Seedling KAN <sup>R</sup> | 71 Alive     | 43 Alive     | 11*             |
| Seedling KAN <sup>S</sup> | 29 Dead      | 38 Dead      | 3               |
| No Germination (NG)       | 0 NG         | 19 NG        | -               |

**Figure 30. Expected allele frequencies in male and female gametes following meiosis and genotypes of self-progeny from *hda7/HDA7* plant considering female gametophytes carrying *hda7* as partially lethal. The table reports the expected and observed percentages of kanamycin resistant (KAN<sup>R</sup>), susceptible (KAN<sup>S</sup>) and not germinated seeds on kanamycin added media. \*Statistically different for  $p < 0.05$ .**

### 4.3. Reverse genetics of putative meiotic genes affected by histone acetylation

Perrella and colleagues (2010) showed that histone hyperacetylation mediated by *AtMCC1* overexpression leads to male and female meiotic defects in *Arabidopsis* (Perrella *et al.*, 2010). Successively, Barra and colleagues (2009) showed that *AtMCC1* overexpression leads to the differential expression of 150 genes in microspores as assessed by LMM. Cell cycle and ubiquitin-proteasome system genes as well as histone and DNA modifiers were enriched among the differentially expressed genes in *Atmcc1* and were subjected to functional analysis. Considering that silique semisterility is often

linked to meiotic defects (De Muyt *et al.*, 2009, Consiglio *et al.*, 2007), a screening based on silique fertility was performed on T-DNA insertion lines on 15 genes, while *HDA7*, which was the only histone deacetylase differentially expressed in *Atmcc1*, was analyzed as reported above. None of the analyzed T-DNA lines had a reproducible reduction of silique fertility. The lack of phenotype in the examined lines could be due to different causes. Firstly, some lines could lack the T-DNA insertion (Cremona, 2010). Moreover, the presence of the T-DNA insertion alone is not sufficient to cause gene knock-out because reduced expression levels (knock-down) as well as the expression of partial coding sequences (knock-about) can be enough to perform gene function (Krysan *et al.*, 1999). Secondly, in the case of functionally redundant genes, knock-out alleles may not show a phenotype (Sridha & Wu, 2006) which is possibly our case because most of the selected genes are members of multiple gene families. Finally, it is possible that the genes we have analyzed are not contributing to the meiotic defects observed in *Atmcc1*.

#### **4.4. Evolution of PARALLEL SPINDLES LIKE (PSL) in potato and *Viridiplantae***

*PSL* genes were isolated in a diploid potato ( $2n=2x=24$ ) and in other plant species through *in silico* analysis. The function of *PSL* in plants can be inferred from *Arabidopsis* study on *AtPS1* gene that appears responsible for the spindle orientation at meiosis II playing a regulatory function, likely via RNA decay (d'Erfurth *et al.*, 2008). In all the analyzed species, except soybean and potato, *PSL* loci appear as singleton behaving as resistant to duplication. It is known that angiosperms are mostly paleopolyploids (Bowers *et al.*, 2003), many having survived multiple duplication events (Paterson *et al.*, 2004, Paterson *et al.*, 2006). Analysis of genome sequences shows that some genes duplicate and persist as multiple copies after whole genome duplication (WGD) while other genes are iteratively returned to singleton status. Moreover, it seems that the singleton status is consistently restored for some functional gene groups like those involved in DNA repair or signal transduction (Doyle *et al.*, 2008). The evolutive history of potato and soybean could explain the expansion of *PSL* genes occurring in these species that have experienced recent WGD. In cultivated potato ( $2n=4x=48$ ), WGD is reported to have occurred about 10 million of years ago (*mya*) after the divergence from *Solanum lycopersicum* (Fawcett *et al.*, 2009). In

soybean ( $2n=2x=40$ ), which seems to be an ancient allopolyploid on the basis of two different centromeric repeat classes (Gill *et al.*, 2009), two rounds of WGD happened the latter aging 10-15 *mya* (Shoemaker *et al.*, 2006, Chang *et al.*, 2007). In addition, the location of the four soybean PSLs on different chromosomes reinforce their origin from WGD rather than tandem duplications. The evident feature of PSL proteins is the contemporary presence of FHA and PINc domains. FHA is reported as a phosphothreonine (pT) binding domain showing a 11 beta-sandwich secondary structure, also containing small helical insertions between the beta-strands (Durocher *et al.*, 2000). The FHA active sites are usually located in the loops connecting b3/b4, b4/b5 and b6/b7 strands. RAD53p<sup>FHA</sup> arginine-70, serine-85 and asparagine-107 (corresponding to arginine-6, serine-21 and asparagine-60 in Figure 25) are involved in the interaction with the phosphopeptide backbone. Arginine-83 (corresponding to arginine-19 in Figure 25) is the most important aminoacid for FHA binding specificity. Indeed, its conversion to glycine shifts the binding from pTXXD to pTXXI peptides in RAD53p<sup>FHA</sup> interaction experiments using surface plasmon resonance (Durocher *et al.*, 2000). Glycine-69 and histidine-88 (corresponding to glycine-5 and histidine-24 in Figure 25) stabilize the architecture of the binding site. The remaining conserved residue, asparagine-112 (corresponding to asparagine-65 in Figure 25), is remote from the peptide binding site and serves to tether the beta turn between b7/8 to b10 (Durocher & Jackson, 2002, Durocher *et al.*, 2000). The comparison of predicted secondary structure in our dataset showed a wide conservation among plant species regarding the number and the position of the beta-sheets and the presence of an helical insertion between the second and the third beta-sheet as a characteristic feature of monocot PSL proteins. The comparison of active sites showed that two PSL<sup>FHA</sup> residues involved in pT binding as well those involved in stabilisation of the architecture of the binding site are fully conserved except for asparagine-65 that is replaced with a different polarity residue (arginine) in AIPSL1, AtPS1, GmPSL3 and GmPSL4 with unknown possible effect on domain architecture. Moreover, as compared to RAD53p<sup>FHA</sup>, a conserved substitution in plants is a histidine instead of asparagine-60, known to be important for the selectivity of binding of phosphothreonine upon phosphoserine. The different polarity between these two residues might suggest a functional diversification of this active site. However,

the consequences of this substitution in PSL<sup>FHA</sup> domain in terms of ligand binding cannot be easily predicted and should be assessed by protein:protein interaction analysis. It is also intriguing the lack of arginine-19 in plants raising the question of binding selectivity for plant PSL<sup>FHA</sup>. As regards PINc domain, we made reference to human SMG6<sup>PINc</sup> which has RNase activity and it is composed of alternating beta-sheets and alpha-helices. It is reported that hSMG6 is involved in NMD together with hSMG5 and hSMG7 (Chang *et al.*, 2007). In *Arabidopsis*, *AtSMG7* was proved to be involved in NMD and to be required for meiotic spindle organization in meiosis II (Riehs *et al.*, 2008). As reported by Glavan and colleagues (2006), hSMG6 and other PINc domains show three conserved aspartic residues at positions 1251, 1353 and 1392 involved in Mg<sup>2+</sup> binding. Threonine or serine embedded in the motif (T/S) XD is proposed to be the catalytic site on the basis of sequence alignment of PIN domains and it is located at residue-1390 (corresponding to threonine-231 in Figure 27) in hSMG6<sup>PINc</sup>. Our results showed differences of secondary structures in PSL<sup>PINc</sup> domains even between phylogenetically close organisms. Moreover, the typical alternation between beta-sheets and alpha-helices does not seem to be respected. In spite of these differences, the active sites showed a wide conservation among plants. The aspartate-6 is conserved in all proteins except for SbPSL1 and SiPSL1 where an asparagine is present. This substitution maybe occurred after the divergence of BEP from PACCAD clades among *Poaceae* given its absence in *Oryza sativa*, *Brachypodium distachyon* and *Selaginella moellendorffii*. The residue-194 showed the major degree of variation among the species mostly characterized by glutamate instead of aspartate. This substitution is not related to phylogenesis, being glutamate present in both monocots and dicots while aspartate-194 is shared by the *Brassicaceae* BrPSL1, the *Selaginellaceae* SmPSL1 and the *Solanaceae* PSL3c. In *Carica papaya*, *Mimulus guttatus* and *Medicago truncatula* the change involved aminoacids with a different polarity such as lysine, alanine, and asparagine. The aspartate-233 is widely conserved among PSL proteins, except those of *Poaceae* OsPSL1, SiPSL1 and BdPSL1 showing a serine-233, likely a substitution occurred after the separation of monocots from dicots. GmPSL3 and SbPSL1 lack this residue due to PINc domain truncation at leucine-203 and lysine-227, respectively. As compared to hSMG6, the majority of plants showed a serine instead of

threonine-231 that is present only in PtPSL1, SiPSL1, SmPSL1 and VvPSL1. This substitution should not compromise the PINc activity since serine and threonine are the most represented residues at this position in PINc domains of different organisms (Arcus *et al.*, 2004). Based on the evidence that the three aspartate residues of PINc domain are crucial for RNase activity, we can argue that PSLs lacking one of these residues or showing aminoacid with different polarity (BdPSL1, CpPSL1, CsPSL1, GmPSL3, MgPSL1, MtPSL1, SbPSL1, SiPSL1, OsPSL1) have no enzymatic activity. However, we cannot exclude that they are partner of other proteins retaining RNase activity. Indeed, in human, it is known that hSMG5 lacking two aspartate residues respect to hSMG6 has no enzymatic activity but the interaction between hSMG5 and hSMG7 lead to a functional nuclease activity of SMG7–SMG5 complex (Glavan *et al.*, 2006).

Functional analysis of *Arabidopsis PS1* reinforced the evidence that the defects in meiotic spindle orientation in meiosis II led to the formation of diplopollen. Among the analyzed species, *Manihot esculenta* ( $2n=2x=36$ ) was reported to produce  $2n$  pollen but the cytological mechanisms underlying its formation were not deeply investigated (Ogburia & Yabuya, 2002). Since the predicted MePSL1 protein has FHA and PINc active sites similar to those of other species, it is likely that the mechanism leading to  $2n$  pollen in *Manihot esculenta* does not involve parallel spindles. In the potato genotype analyzed in this study, neither spindle defects nor  $2n$  pollen have been reported (Conicella *et al.*, 1991). In this genotype, we identified three PSL loci and seven transcripts. Based on AtPS1 characterized by FHA and PINc domains we can suspect that PSL1a and PSL3c, carrying both domains, are functional proteins. In addition, it can be speculated that PSL1a that evidences the same PINc active residues of AtPS1 is the strongest candidate for the regulation of spindle orientation in meiosis II. Functional analysis will be useful to answer to this issue providing at the same time an important tool for potato breeding. Indeed, gene complementation or silencing could be exploited to inhibit or induce parallel spindles in clones which produce or not  $2n$  pollen. The landscape of alternative splicing in potato PSL is not surprising since it has been already observed for genes involved in *Arabidopsis* meiosis. For instance, *AtSPO11-1*, involved in double strand breaks (DSBs) required for meiotic recombination, exhibits up to ten splicing forms showing PTCs (Hartung & Puchta, 2000). As inferred for *AtSPO11-1*, PSLs

are possible target of NMD that could act as a post-transcriptional regulatory pathway for the proper expression of PSL. Alternative splicing was observed also in *Glycine max* but the lack of PTCs exclude NMD regulation of PSL transcripts. Defining the ligands of FHA and PINc domains and proving PSL as a component in NMD are essential to link PSLs to plant evolution by polyploidization via  $2n$  gametes.

## 5. CONCLUDING REMARKS

The aim of the present work was the identification of genes involved in plant meiotic processes such as recombination and nuclear restitution, which are of interest for plant breeding, by using the model organism *Arabidopsis thaliana* and potato.

Most of the work performed in *Arabidopsis* was supported by the European Project “Systematic Analysis of Factors Controlling Meiotic Recombination in Higher Plants (MeioSYS)” which points to the identification and analysis of histone modifiers controlling frequency and distribution of meiotic crossovers in plants. Through an *in silico* analysis based on the identification of genes overexpressed in reproductive tissues and on similarity to genes involved in reproduction in other model organisms, the histone acetylases *HAG2*, *HAG1*, *HAM1* and *HAF1* and the histone deacetylases *HDA7*, *HDA6*, *HDA9* and *HDA19* have been identified as candidates for a meiotic role in *Arabidopsis*. In this PhD thesis, *HDA7* was functionally characterized by loss-of-function and gain-of-function mutants. Reduced seed set and embryo sac degeneration were observed in knock-down mutants allowing to conclude that *HDA7* is required for female gametophyte development. Moreover, *HDA7* has a role in embryo and plant development as highlighted by the reduced germination rate and the altered post-germination growth observed in knock-down and overexpressing mutants. Candidate genes which could be involved in *hda7* phenotype were also provided paving the way to a deeper understanding of the molecular role of *HDA7* in plant reproduction and development. The meiotic function of *HDA7* is currently under investigation to assess whether megasporogenesis defects are associated to embryo sac collapse and to verify if meiotic recombination is changed in microsporocytes.

The aim at identify meiotic genes affected by histone hyperacetylation by using *Atmcc1* mutant was not achieved. The screening of 22 T-DNA lines for reduced seed set did not produce any result. However this result does not rule out the possibility that the selected genes are involved in the meiotic defects observed in *Atmcc1*.

The work performed on the diploid potato clone T710 was aimed to the identification of *PSL* genes, which could be involved in  $2n$  pollen

production as showed for *Arabidopsis thaliana* *PS1*. By means of molecular and *in silico* analyses, the presence of at least three *PSL* loci in the potato genome was showed. Moreover, the candidate locus that likely has a role in  $2n$  pollen production was provided. The existence of *PSLs* throughout *Viridiplantae*, from mosses to higher plants, was also showed. *PSLs* occur mostly as singleton in the analyzed genomes except in soybean and potato both characterized by a recent whole genome duplication event. A useful insight into evolutionary conservation of FHA and PINc domains throughout plant *PSLs* was provided suggesting a fundamental role of these domains for *PSL* function. The work performed pave the way to the functional characterization of *PSL* genes and to the genetic manipulation of  $2n$  pollen production in several plants which could be very useful for plant breeding.

## 6. BIBLIOGRAPHY

- Abascal F, Zardoya R & Posada D (2005) ProtTest: selection of best-fit models of protein evolution. *Bioinformatics* 21:2104–2105.
- Ahn S-H, Henderson KA, Keeney S & Allis CD (2005) H2B (Ser10) phosphorylation is induced during apoptosis and meiosis in *S. cerevisiae*. *Cell Cycle* 4:780–783.
- Alexander MP (1969) Differential staining of aborted and nonaborted pollen. *Stain Technology* 44:117–122.
- Altschul SF, Gish W, Miller W, Myers EW & Lipman DJ (1990) Basic local alignment search tool. *Journal of Molecular Biology* 215:403–410.
- Alvarez JP, Pekker I, Goldshmidt A, Blum E, Amsellem Z & Eshed Y (2006) Endogenous and synthetic microRNAs stimulate simultaneous, efficient, and localized regulation of multiple targets in diverse species. *The Plant Cell* 18:1134–1151.
- Arabidopsis Genome Initiative (2000) Analysis of the genome sequence of the flowering plant *Arabidopsis thaliana*. *Nature* 408:796–815.
- Arcus VL, Bäckbro K, Roos A, Daniel EL & Baker EN (2004) Distant structural homology leads to the functional characterization of an archaeal PIN domain as an exonuclease. *The Journal of Biological Chemistry* 279:16471–16478.
- Armstrong SJ & Jones GH (2003) Meiotic cytology and chromosome behaviour in wild-type *Arabidopsis thaliana*. *Journal of Experimental Botany* 54:1–10.
- Aufsatz W, Mette MF, van der Winden J, Matzke M & Matzke AJM (2002) HDA6, a putative histone deacetylase needed to enhance DNA methylation induced by double-stranded RNA. *The EMBO Journal* 21:6832–6841.
- Bannister AJ & Kouzarides T (2011) Regulation of chromatin by histone modifications. *Cell Research* 21:381–395.
- Barone A, Carputo D & Frusciante L (1993) Selection of potato diploid hybrids for 2n gamete production. *Journal of Genetics and Breeding* 47:313–318.
- Barra L. PhD Thesis. School of Biotechnological Sciences XXII. University of Napoli Federico II.

- Bateman R & DiMichele W (1994) Heterospory: the most iterative key innovation in the evolutionary history of the plant kingdom. *Biological Reviews* 69:345–417.
- Baudat F, Buard J, Grey C, Fedel-Alon A, Ober C, Przeworski M, Coop G & de Massy B (2010) PRDM9 is a major determinant of meiotic recombination hotspots in humans and mice. *Science* 327:836–840.
- Benhamed M, Bertrand C, Servet C & Zhou D-X (2006) *Arabidopsis* GCN5, HD1, and TAF1/HAF2 interact to regulate histone acetylation required for light-responsive gene expression. *The Plant Cell* 18:2893–2903.
- Bertrand C, Bergounioux C, Domenichini S, Delarue M & Zhou D-X (2003) *Arabidopsis* histone acetyltransferase AtGCN5 regulates the floral meristem activity through the WUSCHEL/AGAMOUS pathway. *The Journal of Biological Chemistry* 278:28246–28251.
- Bond DM, Dennis ES, Pogson BJ & Finnegan EJ (2009) Histone acetylation, VERNALIZATION INSENSITIVE 3, FLOWERING LOCUS C, and the vernalization response. *Molecular Plant* 2:724–737.
- Borde V, Robine N, Lin W, Bonfils S, Géli V & Nicolas A (2009) Histone H3 lysine 4 trimethylation marks meiotic recombination initiation sites. *The EMBO Journal* 28:99–111.
- Bowers JE, Chapman BA, Rong J & Paterson AH (2003) Unravelling angiosperm genome evolution by phylogenetic analysis of chromosomal duplication events. *Nature* 422:433–438.
- Boyes DC, Zayed AM, Ascenzi R, McCaskill AJ, Hoffman NE, Davis KR & Görlach J (2001) Growth stage-based phenotypic analysis of *Arabidopsis*: a model for high throughput functional genomics in plants. *The Plant Cell* 13:1499–1510.
- Bretagnolle F & Thompson J (1995) Tansley review no-78 - Gametes with the somatic chromosome-number - Mechanisms of their formation and role in the evolution of autopolyploid plants. *The New Phytologist* 129:1–22.
- Brownfield L & Köhler C (2011) Unreduced gamete formation in plants: mechanisms and prospects. *Journal of Experimental Botany* 62:1659–1668.
- Burgess SM, Ajimura M & Kleckner N (1999) GCN5-dependent histone H3 acetylation and RPD3-dependent histone H4

- deacetylation have distinct, opposing effects on IME2 transcription, during meiosis and during vegetative growth, in budding yeast. *Proceedings of the National Academy of Sciences of the United States of America* 96:6835–6840.
- Capo A, Cammareri M, Rocca F & Errico A (2002) Evaluation for chipping and tuber soft rot (*Erwinia carotovora*) resistance in potato clones from unilateral sexual polyploidization (2x X 4x). *American Journal of Potato Research* 79:139-145.
- Carputo D, Basile B & Cardi T (2000) *Erwinia* resistance in backcross progenies of *Solanum tuberosum* x *S. tarijense* and *S. tuberosum* (+) *S. commersonii* hybrids. *Potato Research* 43:135-142.
- Caryl AP, Armstrong SJ, Jones GH & Franklin FC (2000) A homologue of the yeast HOP1 gene is inactivated in the *Arabidopsis* meiotic mutant *asy1*. *Chromosoma* 109:62–71.
- Caryl AP, Jones GH & Franklin FCH (2003) Dissecting plant meiosis using *Arabidopsis thaliana* mutants. *Journal of Experimental Botany* 54:25–38.
- Chang Y-F, Imam JS & Wilkinson MF (2007) The nonsense-mediated decay RNA surveillance pathway. *Annual Review of Biochemistry* 76:51–74.
- Chen C, Farmer AD, Langley RJ, Mudge J, Crow JA, May GD, Huntley J, Smith AG & Retzel EF (2010a) Meiosis-specific gene discovery in plants: RNA-Seq applied to isolated *Arabidopsis* male meiocytes. *BMC Plant Biology* 10:280.
- Chen L-T, Luo M, Wang Y-Y & Wu K (2010b) Involvement of *Arabidopsis* histone deacetylase *HDA6* in ABA and salt stress response. *Journal of Experimental Botany* 61:3345–3353.
- Chicheportiche A, Bernardino-Sgherri J, de Massy B & Dutrillaux B (2007) Characterization of Spo11-dependent and independent phospho-H2AX foci during meiotic prophase I in the male mouse. *Journal of Cell Science* 120:1733–1742.
- Chung MH, Chen MK & Pan SM (2000) Floral spray transformation can efficiently generate *Arabidopsis* transgenic plants. *Transgenic Research* 9:471–476.
- Chung PJ, Kim YS, Jeong JS, Park S-H, Nahm BH & Kim J-K (2009) The histone deacetylase *OsHDA1* epigenetically regulates the *OsNAC6* gene that controls seedling root growth in rice. *The Plant Journal* 59:764–776.

- Clayton AL, Hazzalin CA & Mahadevan LC (2006) Enhanced histone acetylation and transcription: a dynamic perspective. *Molecular Cell* 23:289–296.
- Cohen R, Schocken J, Kaldis A, Vlachonasios KE, Hark AT & McCain ER (2009) The histone acetyltransferase *GCN5* affects the inflorescence meristem and stamen development in *Arabidopsis*. *Planta* 230:1207–1221.
- Colville A, Alhattab R, Hu M, Labbe H, Xing T & Miki B (2011) Role of HD2 genes in seed germination and early seedling growth in *Arabidopsis*. *Plant Cell Reports* 30:1969–1979.
- Conicella C, Barone A, DELGIUDICE A, Frusciante L & Monti L (1991) Cytological evidences of SDR-FDR mixture in the formation of  $2n$  eggs in a potato diploid clone. *Theoretical and Applied Genetics* 81:59–63.
- Consiglio F, Carputo D, Monti L & Conicella C (2004) Exploitation of genes affecting meiotic non-reduction and nuclear restitution: *Arabidopsis* as a model? *Sexual Plant Reproduction* 17:97–105.
- Consiglio F, Carputo D, Frusciante L, Monti LM & Conicella C (2007). Meiotic mutations and crop improvement. *Plant Breeding Reviews* 6:163–214.
- Cremona G (2010) PhD Thesis. School of Biotechnological Sciences XXIII. University of Napoli Federico II.
- d'Erfurth I, Jolivet S, Froger N, Catrice O, Novatchkova M, Simon M, Jenczewski E & Mercier R (2008) Mutations in *AtPS1* (*Arabidopsis thaliana* *Parallel Spindle 1*) lead to the production of diploid pollen grains. *PLoS Genetics* 4:e1000274.
- d'Erfurth I, Jolivet S, Froger N, Catrice O, Novatchkova M & Mercier R (2009) Turning meiosis into mitosis. *PLoS Biology* 7:e1000124.
- d'Erfurth I, Cromer L, Jolivet S, Girard C, Horlow C, Sun Y, To JPC, Berchowitz LE, Copenhaver GP & Mercier R (2010) The cyclin-A *CYCA1;2/TAM* is required for the meiosis I to meiosis II transition and cooperates with *OSD1* for the prophase to first meiotic division transition. *PLoS Genetics* 6:e1000989.
- De Muyt A, Pereira L, Vezon D, Chelysheva L, Gendrot G, Chambon A, Lainé-Choinard S, Pelletier G, Mercier R, Nogué F & Grelon M (2009) A high throughput genetic screen identifies new early meiotic recombination functions in *Arabidopsis thaliana*. *PLoS Genetics* 5:e1000654.

- De Storme N & Geelen D (2011) The *Arabidopsis* mutant *jason* produces unreduced first division restitution male gametes through a parallel/fused spindle mechanism in meiosis II. *Plant Physiology* 155:1403–1415.
- Dirks R, Van Dun K, de Snoo CB, *et al.* (2009) Reverse breeding: a novel breeding approach based on engineered meiosis. *Plant Biotechnology Journal* 7:837–845.
- Doelling JH, Yan N, Kurepa J, Walker J & Vierstra RD (2001) The ubiquitin-specific protease UBP14 is essential for early embryo development in *Arabidopsis thaliana*. *The Plant Journal* 27:393–405.
- Doyle JJ, Flagel LE, Paterson AH, Rapp RA, Soltis DE, Soltis PS & Wendel JF (2008) Evolutionary genetics of genome merger and doubling in plants. *Annual Review of Genetics* 42:443–461.
- Durocher D & Jackson SP (2002) The FHA domain. *FEBS LETTERS* 513:58–66.
- Durocher D, Taylor IA, Sarbassova D, Haire LF, Westcott SL, Jackson SP, Smerdon SJ & Yaffe MB (2000) The molecular basis of FHA domain:phosphopeptide binding specificity and implications for phospho-dependent signaling mechanisms. *Molecular Cell* 6:1169–1182.
- Earley K, Lawrence RJ, Pontes O, Reuther R, Enciso AJ, Silva M, Neves N, Gross M, Viegas W & Pikaard CS (2006) Erasure of histone acetylation by *Arabidopsis HDA6* mediates large-scale gene silencing in nucleolar dominance. *Genes & Development* 20:1283–1293.
- Edgar RC (2004) MUSCLE: a multiple sequence alignment method with reduced time and space complexity. *BMC Bioinformatics* 5:113.
- Eulgem T, Rushton PJ, Robatzek S & Somssich IE (2000) The WRKY superfamily of plant transcription factors. *Trends in Plant Science* 5:199–206.
- Fawcett JA, Maere S & Van de Peer Y (2009) Plants with double genomes might have had a better chance to survive the Cretaceous-Tertiary extinction event. *Proceedings of the National Academy of Sciences of the United States of America* 106:5737–5742.
- Fischer JJ, Toedling J, Krueger T, Schueler M, Huber W & Sperling S

- (2008) Combinatorial effects of four histone modifications in transcription and differentiation. *Genomics* 91:41–51.
- Fong PM, Tian L & Chen ZJ (2006) *Arabidopsis thaliana* Histone Deacetylase 1 (AtHD1) is localized in euchromatic regions and demonstrates histone deacetylase activity *in vitro*. *Cell Research* 16:479–488.
- Game JC & Chernikova SB (2009) The role of RAD6 in recombinational repair, checkpoints and meiosis via histone modification. *DNA Repair* 8:470–482.
- Georgieva EI, López-Rodas G, Sendra R, Gröbner P & Loidl P (1991) Histone acetylation in *Zea mays*. II. Biological significance of post-translational histone acetylation during embryo germination. *The Journal of Biological Chemistry* 266:18751–18760.
- Gill N, Findley S, Walling JG, Hans C, Ma J, Doyle J, Stacey G & Jackson SA (2009) Molecular and chromosomal evidence for allopolyploidy in soybean. *Plant Physiology* 151:1167–1174.
- Glavan F, Behm-Ansmant I, Izaurralde E & Conti E (2006) Structures of the PIN domains of SMG6 and SMG5 reveal a nuclease within the mRNA surveillance complex. *The EMBO Journal* 25:5117–5125.
- Grossniklaus U & Schneitz K (1998) The molecular and genetic basis of ovule and megagametophyte development. *Seminars in Cell & Developmental Biology* 9:227–238.
- Guindon S & Gascuel O (2003) A simple, fast, and accurate algorithm to estimate large phylogenies by maximum likelihood. *Systematic Biology* 52:696–704.
- Hamant O, Ma H & Cande WZ (2006) Genetics of meiotic prophase I in plants. *Annual Review of Plant Biology* 57:267–302.
- Han S-K, Song J-D, Noh Y-S & Noh B (2007) Role of plant CBP/p300-like genes in the regulation of flowering time. *The Plant Journal* 49:103–114.
- Hartung F & Puchta H (2000) Molecular characterisation of two paralogous *SPO11* homologues in *Arabidopsis thaliana*. *Nucleic Acids Research* 28:1548–1554.
- Hayashi K, Yoshida K & Matsui Y (2005) A histone H3 methyltransferase controls epigenetic events required for meiotic prophase. *Nature* 438:374–378.

- Higgins JD, Sanchez-Moran E, Armstrong SJ, Jones GH & Franklin FCH (2005) The *Arabidopsis* synaptonemal complex protein ZYP1 is required for chromosome synapsis and normal fidelity of crossing over. *Genes & Development* 19:2488–2500.
- Hollender C & Liu Z (2008) Histone deacetylase genes in *Arabidopsis* development. *Journal of Integrative Plant Biology* 50:875–885.
- Hu Y, Qin F, Huang L, Sun Q, Li C, Zhao Y & Zhou D-X (2009) Rice histone deacetylase genes display specific expression patterns and developmental functions. *Biochemical and Biophysical Research Communications* 388:266–271.
- Iizuka M, Matsui T, Takisawa H & Smith MM (2006) Regulation of replication licensing by acetyltransferase Hbo1. *Molecular and Cellular Biology* 26:1098–1108.
- Jang I, Pakh Y, Song S, Kwon H, Nahm B & Kim J (2003) Structure and expression of the rice class-I type histone deacetylase genes *OshDAC1-3*: *OshDAC1* overexpression in transgenic plants leads to increased growth rate and altered architecture. *The Plant Journal* 33:531–541.
- Kaszás E & Cande WZ (2000) Phosphorylation of histone H3 is correlated with changes in the maintenance of sister chromatid cohesion during meiosis in maize, rather than the condensation of the chromatin. *Journal of Cell Science* 113:3217–3226.
- Kägi C & Gross-Hardt R (2007) How females become complex: cell differentiation in the gametophyte. *Current Opinion in Plant Biology* 10:633–638.
- Kik C (2002) Exploitation of Wild Relatives for the Breeding of Cultivated *Allium* species. *Allium Crop Science: Recent Advances*. (HD Rabinowitch) CABI Publishing, p 528.
- Kirchberger S, Tjaden J & Neuhaus HE (2008) Characterization of the *Arabidopsis* *Brittle1* transport protein and impact of reduced activity on plant metabolism. *The Plant Journal* 56:51–63.
- Kleckner N (1996) Meiosis: how could it work? *Proceedings of the National Academy of Sciences of the United States of America* 93:8167–8174.
- Klimyuk VI & Jones JD (1997) *AtDMC1*, the *Arabidopsis* homologue of the yeast *DMC1* gene: characterization, transposon-induced allelic variation and meiosis-associated expression. *The Plant*

Journal 11:1–14.

- Kojima S, Iwasaki M, Takahashi H, Imai T, Matsumura Y, Fleury D, Van Lijsebettens M, Machida Y & Machida C (2011) ASYMMETRIC LEAVES2 and Elongator, a histone acetyltransferase complex, mediate the establishment of polarity in leaves of *Arabidopsis thaliana*. *Plant & Cell Physiology* 52: 1259-1273.
- Kornet N & Scheres B (2009) Members of the GCN5 histone acetyltransferase complex regulate PLETHORA-mediated root stem cell niche maintenance and transit amplifying cell proliferation in *Arabidopsis*. *The Plant Cell* 21:1070–1079.
- Kouzarides T (2007) Chromatin modifications and their function. *Cell* 128:693–705.
- Kölle D, Brosch G, Lechner T, Pipal A, Helliger W, Taplick J & Loidl P (1999) Different types of maize histone deacetylases are distinguished by a highly complex substrate and site specificity. *Biochemistry* 38:6769–6773.
- Kranner I, Minibayeva FV, Beckett RP & Seal CE (2010) What is stress? Concepts, definitions and applications in seed science. *The New Phytologist* 188:655–673.
- Krysan PJ, Young JC & Sussman MR (1999) T-DNA as an insertional mutagen in *Arabidopsis*. *The Plant Cell* 11:2283–2290.
- Lareau LF, Brooks AN, Soergel DAW, Meng Q & Brenner SE (2007) The coupling of alternative splicing and nonsense-mediated mRNA decay. *Advances in Experimental Medicine and Biology* 623:190–211.
- Latrasse D, Benhamed M, Henry Y, Domenichini S, Kim W, Zhou D-X & Delarue M (2008) The MYST histone acetyltransferases are essential for gametophyte development in *Arabidopsis*. *BMC Plant Biology* 8:121.
- Lawton MA, Dean SM, Dron M, Kooter JM, Kragh KM, Harrison MJ, Yu L, Tanguay L, Dixon RA & Lamb CJ (1991) Silencer region of a chalcone synthase promoter contains multiple binding sites for a factor, SBF-1, closely related to GT-1. *Plant Molecular Biology* 16:235–249.
- Leah R, Skriver K, Knudsen S, Ruud-Hansen J, Raikhel NV & Mundy J (1994) Identification of an enhancer/silencer sequence directing

- the aleurone-specific expression of a barley chitinase gene. *The Plant Journal* 6:579–589.
- Lechner T, Lusser A, Pipal A, Brosch G, Loidl A, Goralik-Schramel M, Sendra R, Wegener S, Walton JD & Loidl P (2000) RPD3-Type histone deacetylases in maize embryos. *Biochemistry* 39:1683–1692.
- Lewis RA (2002) *CRC dictionary of agricultural sciences* (C Press). CRC Press.
- Li J, Lee GI, Van Doren SR & Walker JC (2000) The FHA domain mediates phosphoprotein interactions. *Journal of Cell Science* 113:4143–4149.
- Liu Z & Makaroff CA (2006) *Arabidopsis* separase AESP is essential for embryo development and the release of cohesin during meiosis. *The Plant Cell* 18:1213–1225.
- Long JA, Ohno C, Smith ZR & Meyerowitz EM (2006) TOPLESS regulates apical embryonic fate in *Arabidopsis*. *Science* 312:1520–1523.
- López-Rodas G, Georgieva EI, Sendra R & Loidl P (1991) Histone acetylation in *Zea mays*.I. Activities of histone acetyltransferases and histone deacetylases. *The Journal of Biological Chemistry* 266:18745–18750.
- Ma H (2005) Molecular genetic analyses of microsporogenesis and microgametogenesis in flowering plants. *Annual Review of Plant Biology* 56:393–434.
- Ma H (2006) A molecular portrait of *Arabidopsis* meiosis. *The Arabidopsis Book* 4:1–39.
- Martinez-Perez E & Moore G (2008) To check or not to check? The application of meiotic studies to plant breeding. *Current Opinion in Plant Biology* 11:222–227.
- McGuffin LJ, Bryson K & Jones DT (2000) The PSIPRED protein structure prediction server. *Bioinformatics* 16:404–405.
- Meinke DW (1994) Seed development in *Arabidopsis thaliana*. *Arabidopsis* vol. 27. (CSHL Press) p.253.
- Merker JD, Dominska M, Greenwell PW, Rinella E, Bouck DC, Shibata Y, Strahl BD, Mieczkowski P & Petes TD (2008) The histone methylase Set2p and the histone deacetylase Rpd3p repress meiotic recombination at the HIS4 meiotic recombination hotspot in *Saccharomyces cerevisiae*. *DNA Repair* 7:1298–1308.

- Mieczkowski PA, Dominska M, Buck MJ, Lieb JD & Petes TD (2007) Loss of a histone deacetylase dramatically alters the genomic distribution of Spo11p-catalyzed DNA breaks in *Saccharomyces cerevisiae*. *Proceedings of the National Academy of Sciences of the United States of America* 104:3955–3960.
- Mok DWS & Peloquin SJ (1975) The inheritance of three mechanisms of diplandroid ( $2n$  pollen) formation in diploid potatoes. *Heredity* 35:295–302.
- Moll C, Lyncker von L, Zimmermann S, Kägi C, Baumann N, Twell D, Grossniklaus U & Gross-Hardt R (2008) CLO/GFA1 and ATO are novel regulators of gametic cell fate in plants. *The Plant Journal* 56:913–921.
- Nagy E & Maquat LE (1998) A rule for termination-codon position within intron-containing genes: when nonsense affects RNA abundance. *Trends in Biochemical Sciences* 23:198–199.
- Nelissen H, Fleury D, Bruno L, Robles P, De Veylder L, Traas J, Micol JL, Van Montagu M, Inzé D & Van Lijsebettens M (2005) The *elongata* mutants identify a functional Elongator complex in plants with a role in cell proliferation during organ growth. *Proceedings of the National Academy of Sciences of the United States of America* 102:7754–7759.
- Nelissen H, De Groeve S, Fleury D, Neyt P, Bruno L, Bitonti MB, Vandebussche F, Van der Straeten D, Yamaguchi T, Tsukaya H, Witters E, De Jaeger G, Houben A & Van Lijsebettens M (2010) Plant Elongator regulates auxin-related genes during RNA polymerase II transcription elongation. *Proceedings of the National Academy of Sciences of the United States of America* 107:1678–1683.
- Ogburia M & Yabuya T (2002) A cytogenetic study of bilateral sexual polyploidization in cassava (*Manihot esculenta* Crantz). *Plant Breeding* 121:278-280.
- Ortiz R & Franco J (1997) Transfer of resistance to potato cyst nematode (*Globodera pallida*) into cultivated potato *Solanum tuberosum* through first division restitution  $2n$  pollen. *Euphytica* 85:219-226.
- Ortiz R, Simon P, Jansky S & Stelly D (2009) Ploidy manipulation of the gametophyte, endosperm and sporophyte in nature and for crop improvement: a tribute to Professor Stanley J. Peloquin (1921-2008). *Annals of Botany* 104:795–807.

- Osakabe K, Yoshioka T, Ichikawa H & Toki S (2002) Molecular cloning and characterization of RAD51-like genes from *Arabidopsis thaliana*. *Plant Molecular Biology* 50:71–81.
- Osman K, Higgins JD, Sanchez-Moran E, Armstrong SJ & Franklin FCH (2011) Pathways to meiotic recombination in *Arabidopsis thaliana*. *The New Phytologist* 190:523–544.
- Ott A, Trautshold B & Sandhu D (2011) Using microsatellites to understand the physical distribution of recombination on soybean chromosomes. *PLoS One* 6:e22306.
- Page SL & Hawley RS (2004) The genetics and molecular biology of the synaptonemal complex. *Annual Review of Cell and Developmental Biology* 20:525–558.
- Paigen K & Petkov P (2010) Mammalian recombination hot spots: properties, control and evolution. *Nature Reviews Genetics* 11:221–233.
- Pandey R, Müller A, Napoli CA, Selinger DA, Pikaard CS, Richards EJ, Bender J, Mount DW & Jorgensen RA (2002) Analysis of histone acetyltransferase and histone deacetylase families of *Arabidopsis thaliana* suggests functional diversification of chromatin modification among multicellular eukaryotes. *Nucleic Acids Research* 30:5036–5055.
- Parvanov ED, Petkov PM & Paigen K (2010) Prdm9 controls activation of mammalian recombination hotspots. *Science* 327:835.
- Paterson AH, Bowers JE & Chapman BA (2004) Ancient polyploidization predating divergence of the cereals, and its consequences for comparative genomics. *Proceedings of the National Academy of Sciences of the United States of America* 101:9903–9908.
- Paterson AH, Chapman BA, Kissinger JC, Bowers JE, Feltus FA & Estill JC (2006) Many gene and domain families have convergent fates following independent whole-genome duplication events in *Arabidopsis*, *Oryza*, *Saccharomyces* and *Tetraodon*. *Trends in Genetics* 22:597–602.
- Pawlowski WP (2010) Chromosome organization and dynamics in plants. *Current Opinion in Plant Biology* 13:640–645.
- Peloquin SJ, Boiteux LS & Carputo D (1999) Meiotic mutants in potato. Valuable variants. *Genetics* 153:1493–1499.

- Perrella G, Consiglio MF, Aiese-Cigliano R, Cremona G, Sanchez-Moran E, Barra L, Errico A, Bressan RA, Franklin FCH & Conicella C (2010) Histone hyperacetylation affects meiotic recombination and chromosome segregation in *Arabidopsis*. *The Plant Journal* 62:796–806.
- Peters AH, O'Carroll D, Scherthan H, Mechtler K, Sauer S, Schöfer C, Weipoltshammer K, Pagani M, Lachner M, Kohlmaier A, Opravil S, Doyle M, Sibilia M & Jenuwein T (2001) Loss of the Suv39h histone methyltransferases impairs mammalian heterochromatin and genome stability. *Cell* 107:323–337.
- Petes TD (2001) Meiotic recombination hot spots and cold spots. *Nature Reviews Genetics* 2:360–369.
- Pillot M, Baroux C, Vazquez MA, Autran D, Leblanc O, Vielle-Calzada J-P, Grossniklaus U & Grimanelli D (2010) Embryo and endosperm inherit distinct chromatin and transcriptional states from the female gametes in *Arabidopsis*. *The Plant Cell* 22:307–320.
- Pond SLK & Frost SDW (2005a) Datamonkey: rapid detection of selective pressure on individual sites of codon alignments. *Bioinformatics* 21:2531–2533.
- Pond SLK, Frost SDW & Muse SV (2005b) HyPhy: hypothesis testing using phylogenies. *Bioinformatics* 21:676–679.
- Pond KSL & Frost SDW (2005c) Not so different after all: a comparison of methods for detecting amino acid sites under selection. *Molecular Biology and Evolution* 22:1208–1222.
- Ponte I, Guillén P, Debón RM, Reina M, Aragay A, Espel E, Di Fonzo N & Palau J (1994) Narrow A/T-rich zones present at the distal 5'-flanking sequences of the zein genes Zc1 and Zc2 bind a unique 30 kDa HMG-like protein. *Plant Molecular Biology* 26:1893–1906.
- Posada D (2008) jModelTest: phylogenetic model averaging. *Molecular Biology and Evolution* 25:1253–1256.
- Prabhakar V, Löttgert T, Geimer S, Dörmann P, Krüger S, Vijayakumar V, Schreiber L, Göbel C, Feussner K, Feussner I, Marin K, Staehr P, Bell K, Flügge U-I & Häusler RE (2010) Phosphoenolpyruvate provision to plastids is essential for gametophyte and sporophyte development in *Arabidopsis thaliana*. *The Plant Cell* 22:2594–2617.
- Prigent C & Dimitrov S (2003) Phosphorylation of serine 10 in histone

- H3, what for? *Journal of Cell Science* 116:3677–3685.
- Probst AV, Fagard M, Proux F, Mourrain P, Boutet S, Earley K, Lawrence RJ, Pikaard CS, Murfett J, Furner I, Vaucheret H & Mittelsten Scheid O (2004) *Arabidopsis* histone deacetylase *HDA6* is required for maintenance of transcriptional gene silencing and determines nuclear organization of rDNA repeats. *The Plant Cell* 16:1021–1034.
- Ramanna M & Jacobsen E (2003) Relevance of sexual polyploidization for crop improvement - A review. *Euphytica* 133:3–18.
- Reddy KC & Villeneuve AM (2004) *C. elegans* HIM-17 links chromatin modification and competence for initiation of meiotic recombination. *Cell* 118:439–452.
- Riehs N, Akimcheva S, Puizina J, Bulankova P, Idol RA, Siroky J, Schleiffer A, Schweizer D, Shippen DE & Riha K (2008) *Arabidopsis* SMG7 protein is required for exit from meiosis. *Journal of Cell Science* 121:2208–2216.
- Rosenzweig C, Iglesias A, Yang XB, Epstein PR & Chivian E (2001) Climate change and extreme weather events; implications for food production, plant diseases, and pests. *Global Change and Human Health* 2:90–104.
- Rossi V, Locatelli S, Varotto S, Donn G, Pirona R, Henderson DA, Hartings H & Motto M (2007) Maize histone deacetylase *hda101* is involved in plant development, gene transcription, and sequence-specific modulation of histone modification of genes and repeats. *The Plant Cell* 19:1145–1162.
- Rosso MG, Li Y, Strizhov N, Reiss B, Dekker K & Weisshaar B (2003) An *Arabidopsis thaliana* T-DNA mutagenized population (GABI-Kat) for flanking sequence tag-based reverse genetics. *Plant Molecular Biology* 53:247–259.
- San-Segundo PA & Roeder GS (2000) Role for the silencing protein *Dot1* in meiotic checkpoint control. *Molecular Biology of the Cell* 11:3601–3615.
- Schultz J, Milpetz F, Bork P & Ponting CP (1998) SMART, a simple modular architecture research tool: identification of signaling domains. *Proceedings of the National Academy of Sciences of the United States of America* 95:5857–5864.
- Schwab R, Ossowski S, Riester M, Warthmann N & Weigel D (2006)

- Highly specific gene silencing by artificial microRNAs in *Arabidopsis*. *The Plant Cell* 18:1121–1133.
- Schwab R, Ossowski S, Warthmann N & Weigel D (2010) Directed gene silencing with artificial microRNAs. *Methods in Molecular Biology* 592:71–88.
- Sessa G, Morelli G & Ruberti I (1993) The Athb-1 and -2 HD-Zip domains homodimerize forming complexes of different DNA binding specificities. *The EMBO Journal* 12:3507–3517.
- Sharma GG, So S, Gupta A, Kumar R, Cayrou C, Avvakumov N, Bhadra U, Pandita RK, Porteus MH, Chen DJ, Cote J & Pandita TK (2010) MOF and histone H4 acetylation at lysine 16 are critical for DNA Damage Response and DSB Repair. *Molecular and Cellular Biology* 37:1363-1377.
- Shoemaker RC, Schlueter J & Doyle JJ (2006) Paleopolyploidy and gene duplication in soybean and other legumes. *Current Opinion in Plant Biology* 9:104–109.
- Smith E & Shilatifard A (2010) The chromatin signaling pathway: diverse mechanisms of recruitment of histone-modifying enzymes and varied biological outcomes. *Molecular Cell* 40:689–701.
- Smyth DR, Bowman JL & Meyerowitz EM (1990) Early flower development in *Arabidopsis*. *The Plant Cell* 2:755–767.
- Sollier J, Lin W, Soustelle C, Suhre K, Nicolas A, Géli V & La Roche Saint-André de C (2004) Set1 is required for meiotic S-phase onset, double-strand break formation and middle gene expression. *The EMBO Journal* 23:1957–1967.
- Sridha S & Wu K (2006) Identification of *AtHD2C* as a novel regulator of abscisic acid responses in *Arabidopsis*. *The Plant Journal* 46:124–133.
- Strahl BD & Allis CD (2000) The language of covalent histone modifications. *Nature* 403:41–45.
- Tachibana M, Nozaki M, Takeda N & Shinkai Y (2007) Functional dynamics of H3K9 methylation during meiotic prophase progression. *The EMBO Journal* 26:3346–3359.
- Tamura K, Dudley J, Nei M & Kumar S (2007) MEGA4: Molecular Evolutionary Genetics Analysis (MEGA) software version 4.0. *Molecular Biology and Evolution* 24:1596–1599.
- Tanaka M, Kikuchi A & Kamada H (2008) The *Arabidopsis* histone deacetylases *HDA6* and *HDA19* contribute to the repression of

- embryonic properties after germination. *Plant Physiology* 146:149–161.
- Tate JA, Soltis DE & Soltis PS (2005) Polyploidy in plants. *The Evolution of the Genome*. (TR Gregory) Elsevier, p. 371.
- Tian L & Chen ZJ (2001) Blocking histone deacetylation in *Arabidopsis* induces pleiotropic effects on plant gene regulation and development. *Proceedings of the National Academy of Sciences of the United States of America* 98:200–205.
- Tian L, Wang J, Fong MP, Chen M, Cao H, Gelvin SB & Chen ZJ (2003) Genetic control of developmental changes induced by disruption of *Arabidopsis* histone deacetylase 1 (*AtHD1*) expression. *Genetics* 165:399–409.
- Tian L, Fong PM, Wang JJ, Wei EN, Jiang H, Doerge RW & Chen JZ (2005) Reversible Histone acetylation and deacetylation mediate genome-wide, promoter-dependent and locus-specific changes in gene expression during plant development. *Genetics* 169:337–345.
- Tjaden G, Edwards JW & Coruzzi GM (1995) Cis elements and trans-acting factors affecting regulation of a nonphotosynthetic light-regulated gene for chloroplast glutamine synthetase. *Plant Physiology* 108:1109–1117.
- To TK, Nakaminami K, Kim J-M, Morosawa T, Ishida J, Tanaka M, Yokoyama S, Shinozaki K & Seki M (2011a) *Arabidopsis HDA6* is required for freezing tolerance. *Biochemical and Biophysical Research Communications* 406:414–419.
- To TK, Kim J-M, Matsui A, Kurihara Y, Morosawa T, Ishida J, Tanaka M, Endo T, Kakutani T, Toyoda T, Kimura H, Yokoyama S, Shinozaki K & Seki M (2011b) *Arabidopsis HDA6* regulates locus-directed heterochromatin silencing in cooperation with MET1. *PLoS Genetics* 7:e1002055.
- van Attikum H & Gasser SM (2009) Crosstalk between histone modifications during the DNA damage response. *Trends in Cell Biology* 19:207–217.
- van Steensel B (2011) Chromatin: constructing the big picture. *The EMBO Journal* 30:1885–1895.
- Varotto S, Locatelli S, Canova S, Pipal A, Motto M & Rossi V (2003) Expression profile and cellular localization of maize Rpd3-Type histone deacetylases during plant development. *Plant Physiology*

133:606–617.

- Vlachonasios KE, Thomashow MF & Triezenberg SJ (2003) Disruption mutations of ADA2b and GCN5 transcriptional adaptor genes dramatically affect *Arabidopsis* growth, development, and gene expression. *The Plant Cell* 15:626–638.
- Wagner CR, Kuervers L, Baillie DL & Yanowitz JL (2010) *xnd-1* regulates the global recombination landscape in *Caenorhabditis elegans*. *Nature* 467:839–843.
- Wahls WP & Davidson MK (2010) Discrete DNA sites regulate global distribution of meiotic recombination. *Trends in Genetics* 26:202–208.
- Wang C, Gao F, Wu J, Dai J, Wei C & Li Y (2010) *Arabidopsis* putative deacetylase *AtSRT2* regulates basal defense by suppressing *pad4*, *eds5* and *sid2* expression. *Plant & Cell Physiology* 51:1291–1299.
- Wei Y, Yu L, Bowen J, Gorovsky MA & Allis CD (1999) Phosphorylation of histone H3 is required for proper chromosome condensation and segregation. *Cell* 97:99–109.
- Weigel D & Glazebrook J (2002) *Arabidopsis: a laboratory manual* (C Press).
- Wijnker E & De Jong H (2008) Managing meiotic recombination in plant breeding. *Trends in Plant Science* 13:640–646.
- Willmann MR, Mehalick AJ, Packer RL & Jenik PD (2011) MicroRNAs Regulate the timing of embryo maturation in *Arabidopsis*. *Plant Physiology* 155:1871–1884.
- Wu K, Tian L, Malik K, Brown D & Miki B (2000) Functional analysis of HD2 histone deacetylase homologues in *Arabidopsis thaliana*. *The Plant Journal* 22:19–27.
- Wu K, Zhang L, Zhou C, Yu C-W & Chaikam V (2008) *HDA6* is required for jasmonate response, senescence and flowering in *Arabidopsis*. *Journal of Experimental Botany* 59:225–234.
- Xu C-R, Liu C, Wang Y-L, Li L-C, Chen W-Q, Xu Z-H & Bai S-N (2005) Histone acetylation affects expression of cellular patterning genes in the *Arabidopsis* root epidermis. *Proceedings of the National Academy of Sciences of the United States of America* 102:14469–14474.
- Xu X, Pan S, Cheng S, *et al.* (2011) Genome sequence and analysis of the tuber crop potato. *Nature* 475:189–195.

- Yamada T, Mizuno K-I, Hirota K, Kon N, Wahls WP, Hartsuiker E, Murofushi H, Shibata T & Ohta K (2004) Roles of histone acetylation and chromatin remodeling factor in a meiotic recombination hotspot. *The EMBO Journal* 23:1792–1803.
- Yamashita K, Shinohara M & Shinohara A (2004) Rad6-Bre1-mediated histone H2B ubiquitylation modulates the formation of double-strand breaks during meiosis. *Proceedings of the National Academy of Sciences of the United States of America* 101:11380–11385.
- Zhou C, Labbe H, Sridha S, Wang L, Tian L, Latoszek-Green M, Yang Z, Brown D, Miki B & Wu K (2004) Expression and function of HD2-type histone deacetylases in *Arabidopsis* development. *The Plant Journal* 38:715–724.
- Zhou C, Zhang L, Duan J, Miki B & Wu K (2005) *HISTONE DEACETYLASE19* is involved in jasmonic acid and ethylene signaling of pathogen response in *Arabidopsis*. *The Plant Cell* 17:1196–1204.
- Zinn KE, Tunc-Ozdemir M & Harper JF (2010) Temperature stress and plant sexual reproduction: uncovering the weakest links. *Journal of Experimental Botany* 61:1959–1968.



## **RESEARCH ACTIVITY IN FOREIGN LABORATORIES**

The identification of histone acetylases and deacetylases with putative role in *Arabidopsis* meiosis/reproduction by *in silico* analysis was performed in collaboration with Dr Dov Stekel at University of Nottingham (UK).



## APPENDIX

Perrella G., Consiglio F., **Aiese Cigliano R.**, Barra L., Cremona G., Sanchez-Moran E., Paino M., Errico A., Bressan R., Franklin F.C.H. and Conicella C. Histone hyperacetylation affects meiotic chromosome condensation, segregation, and chiasma distribution in *Arabidopsis*. *Plant Journal* 2010, 62 (5): 796-806.

**Aiese Cigliano R.**, Cremona G., Consiglio M.F., Conicella C. Functional biology in *Arabidopsis* to shed light on the molecular basis of  $2n$  gametes. *Minerva Biotechnologica* 2010, 22 (2): 1-2.

Cremona G., **Aiese Cigliano R.**, Consiglio M.F., Conicella C. Epigenetic control of meiotic recombination. *Minerva Biotechnologica* 2010, 22 (2): 25-26.

**Aiese Cigliano R.**, Sanseverino W., Cremona G., Consiglio M.F. and Conicella C. Evolution of *Parallel Spindles Like* genes in plants and highlight of unique domain architecture. *BMC Evolutionary Biology* 2011, 11 (1): 78-91.

**Aiese Cigliano R.**, Cremona G., Consiglio M.F., Conicella C. Insight into a meiotic role of the major histone H3 lysine 4 methyltransferase in *Arabidopsis*. *Minerva Biotechnologica* 2011, 23 (2): 53-55.

**Aiese Cigliano R.**, Consiglio M.F., Barra L., Conicella C. Looking for meiotic genes by cell-specific profiling in *Arabidopsis*. EMBO Conference on Meiosis (1<sup>st</sup>). 19-23 Settembre 2009, Isle sur la Sorgue (France). Poster Communication Abstract.

**Aiese Cigliano R.** Study of meiotic mutations for crop improvement. VIII Corso di genetica vegetale "Regulation of gene expression: from DNA to phenotype". 8-11 Giugno 2009, Assisi (Italia). Poster Communication Abstract.

Cremona G., Consiglio M.F., **Aiese Cigliano R.**, Conicella C. Changes in histone acetylation during male meiosis in *Arabidopsis thaliana*. EMBO Conference on Meiosis (1<sup>st</sup>). 19-23 Settembre 2009, Isle sur la Sorgue (France). Poster Communication Abstract.

**Aiese Cigliano R.**, Sanseverino W., Cremona G., Paparo R., Consiglio M.F., Conicella C. Analysis of *PARALLEL SPINDLES-LIKE*

gene family in plants. Proceedings of the 54th Italian Society of Agricultural Genetics Annual Congress Matera, Italy – 27/30 September, 2010 ISBN 978-88-904570-0-5. Poster Communication Abstract.

**Aiese Cigliano R.**, Perrella G., Cremona G., Paparo R., Consiglio M.F. and Conicella C. Histone acetylation controls meiotic crossover distribution in *Arabidopsis thaliana*. Proceedings of the 54th Italian Society of Agricultural Genetics Annual Congress Matera, Italy – 27/30 September, 2010 ISBN 978-88-904570-0-5. Abstract Oral Communication.

Cremona G., **Aiese Cigliano R.**, Consiglio M.F., Viotti A., Conicella C. Histone modification dynamics during male meiosis in *Arabidopsis thaliana*. Proceedings of the 54th Italian Society of Agricultural Genetics Annual Congress Matera, Italy – 27/30 September 2010 ISBN 978-88-904570-0-5. Poster Communication Abstract.

**Aiese Cigliano R.**, Cremona G., Paparo R., Consiglio M.F., Conicella C. A histone deacetylase is required for fertility, seed germination and seedling growth rate in *Arabidopsis*. Proceedings of the AGI-SIBV-SIGA Joint Congress Assisi, Italy – 19/22 September 2011 ISBN 978-88-904570-2-9. Poster Communication Abstract.

Cremona G., **Aiese Cigliano R.**, Paparo R., Consiglio M.F., Conicella C. Down-regulation of a histone deacetylase affects male meiosis in *Arabidopsis*. Proceedings of the AGI-SIBV-SIGA Joint Congress Assisi, Italy – 19/22 September 2011 ISBN 978-88-904570-2-9. Poster Communication Abstract.

**Aiese Cigliano R.**, Cremona G., Paparo R., Consiglio M.F., Conicella C. Insights into meiotic function of genes modifying histone acetylation in *Arabidopsis*. EMBO Conference on Meiosis. 17-21 Settembre 2011, Capaccio (Italy). Poster Communication Abstract.

Cremona G., **Aiese Cigliano R.**, Paparo R., Consiglio M.F. and Conicella C. Histone acetylation is required for meiotic recombination in *Arabidopsis*. EMBO Conference on Meiosis. 17-21 Settembre 2011, Capaccio (Italy). Poster Communication Abstract.

# Histone hyperacetylation affects meiotic recombination and chromosome segregation in Arabidopsis

Giorgio Perrella<sup>1,†</sup>, M. Federica Consiglio<sup>1,†</sup>, Riccardo Aiese-Cigliano<sup>1</sup>, Gaetana Cremona<sup>1</sup>, Eugenio Sanchez-Moran<sup>2</sup>, Lucia Barra<sup>1</sup>, Angela Errico<sup>3</sup>, Ray A. Bressan<sup>4</sup>, F. Christopher H. Franklin<sup>2</sup> and Clara Conicella<sup>1,\*</sup>

<sup>1</sup>CNR-IGV, Research Institute of Plant Genetics, Research Division, Portici, Via Università 133, 80055 Portici, Italy,

<sup>2</sup>School of Biosciences, University of Birmingham, Birmingham B15 2TT, UK,

<sup>3</sup>Department of Soil, Plant, Environmental and Animal Sciences, University of Naples 'Federico II', Via Università 100, 80055 Portici, Italy, and

<sup>4</sup>Department of Horticulture and Landscape Architecture, Purdue University, West Lafayette, IN, USA

Received 6 November 2009; revised 15 February 2010; accepted 17 February 2010; published online 8 April 2010.

\*For correspondence (fax +39 81 775 3579; e-mail conicell@unina.it).

<sup>†</sup>These authors contributed equally to this work.

## SUMMARY

In this study, the meiotic role of *MEIOTIC CONTROL OF CROSSOVERS1 (MCC1)*, a GCN5-related histone *N*-acetyltransferase, is described in Arabidopsis. Analysis of the over-expression mutant obtained by enhancer activation tagging revealed that acetylation of histone H3 increased in male prophase I. *MCC1* appeared to be required in meiosis for normal chiasma number and distribution and for chromosome segregation. Overall, elevated *MCC1* did not affect crossover number per cell, but has a differential effect on individual chromosomes elevating COs for chromosome 4, in which there is also a shift in chiasma distribution, and reducing COs for chromosome 1 and 2. For the latter there is a loss of the obligate CO/chiasma in 8% of the male meiocytes. The meiotic defects led to abortion in about half of the male and female gametes in the mutant. In wild type, the treatment with trichostatin A, an inhibitor of histone deacetylases, phenocopies *MCC1* over-expression in meiosis. Our results provide evidence that histone hyperacetylation has a significant impact on the plant meiosis.

**Keywords:** histone acetylation, meiosis, chromatin organization, chiasma, Arabidopsis.

## INTRODUCTION

Meiosis is a modified cell division programme essential to all the sexually reproducing eukaryotes. Starting with DNA replication and followed by two successive nuclear divisions, the major consequences of meiosis are a halving of chromosome number and the reassortment and segregation of genetic information guaranteed by homologous recombination (Zickler and Kleckner, 1998).

Histone modifications are increasingly recognized as playing important roles in meiotic recombination (Borde *et al.*, 2009; Buard *et al.*, 2009). In particular, histone acetylation was shown to be involved in meiotic recombination either by local analysis at hotspots in fission and budding yeast (Yamada *et al.*, 2004; Merker *et al.*, 2008) or by genome-wide analysis in *Saccharomyces cerevisiae* (Mieczkowski *et al.*, 2007). In fact, histones around the *ade6-M26* locus and *HIS4* locus, meiotic recombination hotspots in *Schizosaccharomyces pombe* and *S. cerevisiae* respectively, were highly acetylated during meiosis. Deletion of a

histone acetyltransferase (HAT), *SpGcn5*, required for *ade6-M26* hotspot-specific hyperacetylation, led to a partial decrease in DNA double-stranded breaks (DSBs) at this locus (Yamada *et al.*, 2004). Vice versa, loss-of-function of a histone deacetylase (HDAC), *ScRpd3p*, increases *HIS4* hotspot activity (Merker *et al.*, 2008). A mutation of the *SIR2* gene encoding a HDAC changes the genomic distribution of meiosis-specific DSBs in *S. cerevisiae*, elevating DSBs for 5% of yeast genes and reducing DSBs for 7% of the genes (Mieczkowski *et al.*, 2007). H3 and H4 acetylation enrichment was reported at the active mouse *PsmB9* hotspot. Interestingly, H3 acetylation was different in *PsmB9* and another hotspot, *Hlx1*, indicating distinct features between hotspots (Buard *et al.*, 2009). The function of histone acetylation might be direct in recruiting factors of meiotic recombination machinery and/or indirect by regulating chromatin structure at local and at higher-order levels (Hirota *et al.*, 2008). Indeed, histone acetylation has been demonstrated

*in vitro* to directly influence higher-order chromatin structure by inhibiting the formation of compact 30-nm chromatin fibres (Shogren-Knaak *et al.*, 2006). The observation that in budding yeast over 80% of histone H4 is acetylated at lysine 16 and most of the genome exists in a decondensed state is consistent with a role for histone acetylation in chromatin decompaction also *in vivo* (Lohr *et al.*, 1977; Smith *et al.*, 2003). In meiosis, a requirement for histone deacetylation in the condensation of metaphase chromosomes was reported in *Xenopus laevis* oocyte (Magnaghi-Jaulin and Jaulin, 2006). Histone acetylation can affect chromatin structure by altering the interactions of histones between adjacent nucleosomes or with the DNA (Kouzarides, 2007) and/or by collectively establishing a code recognized by downstream effector proteins and complexes (Strahl and Allis, 2000).

Histone deacetylation has been shown to be critical for chromosome segregation in TSA-treated mammalian oocytes. Indeed, histone hyperacetylation produced lagging chromosomes in mouse and pig (De La Fuente *et al.*, 2004; Akiyama *et al.*, 2006; Wang *et al.*, 2006).

Studies on histone acetylation dynamics in plant meiosis are sketchy. To date, histone acetylation patterns have been described in Arabidopsis mutants, *ask1* (Yang *et al.*, 2006) and *dsy10* (Boateng *et al.*, 2008). Different loss-of-function mutations in genes for individual HATs/HDACs have been identified in *Arabidopsis thaliana* whose genome has 18 genes encoding potentially functional HDACs and 12 putative HAT genes (Pandey *et al.*, 2002; see also <http://www.chromdb.org>). Analyses of HDAC T-DNA knockout and antisense lines, which in most cases displayed histone hyperacetylation, revealed a role for the HDACs in reproductive development. In particular, down-regulation of *AtHD1*, which is a global regulator of different developmental processes, induced delayed flowering, flower abnormalities, partial sterility and consequent seed set dropping (Tian *et al.*, 2003). Silencing of *AtHD2A*, a plant-specific HDAC, severely disturbed reproductive development causing seed abortion (Wu *et al.*, 2000). An *AtHDA6* mutant was reported to exhibit reduced fertility, but only in the first flowers (Aufsatz *et al.*, 2002). However, *AtHDA6* is reported to be involved in the silencing of transgenes, DNA repeats, and rDNA loci (Probst *et al.*, 2004) as well in jasmonate response, senescence, and flowering (Wu *et al.*, 2008). Among HATs, *AtGCN5* (GNAT family), *AtHAG4/HAM1* and *HAG5/HAM2* (MYST family) have been functionally characterized in Arabidopsis. Mutation of *AtGCN5* induced many defects on plant development including sterility or partial fertility with production of few seeds (Bertrand *et al.*, 2003; Vlachonasios *et al.*, 2003). Loss-of-function of either *HAM1* or *HAM2* did not display any abnormal phenotype while no double mutant could be recovered. Analysis of *HAM1/ham1*; *ham2/ham2* and *ham1/ham1*; *HAM2/ham2* plants indicate that these MYST members are required for gametophyte

development (Latrasse *et al.*, 2008). In all the aforementioned mutants except the last, the mechanism underlying the reduction of plant fertility remained unclear and, in particular, meiosis was not directly investigated.

In this study we have used an over-expression mutant of a GCN5-related histone *N*-acetyltransferase gene, *MEIOTIC CONTROL OF CROSSOVERS1* (*MCC1*), that was obtained by enhancer activation tagging (Perrella *et al.*, 2006) to investigate the interrelationship between histone hyperacetylation and meiotic events in Arabidopsis. Analysis of *mcc1* meicytes revealed hyperacetylation of histone H3 during male meiosis that was accompanied by defects in chromosome segregation and changes in crossover number and distribution in different chromosomes.

## RESULTS

### Phenotype of the *mcc1* mutant

We isolated the *b16* line following T-DNA mutagenesis by enhancer activation tagging in a screen for mutants with low seed-set (Perrella *et al.*, 2006). The line exhibited a significant reduction in fertility, producing on average 68% fewer seeds per silique ( $n = 40$ ;  $P \leq 0.01$ ) than wild-type plants. Based on our subsequent cytological characterization, *b16* was re-named *meiotic control of crossovers1* (*mcc1*). Analysis of F1 plants from a wild type  $\times$  *mcc1* cross confirmed that the mutation is dominant.

During vegetative development the mutant showed some changes respect to wild type. The rosette leaves did appear narrower and elongated (Figure S1a). Additionally, *mcc1* plants exhibited faster stem elongation (Figure S1b) and flowered about 6 days earlier than wild type ( $P \leq 0.001$ ). Analysis of *mcc1* anthers revealed a strong reduction in pollen viability (Figure S1d). Inspection of *mcc1* siliques indicated failure of seed development (Figure S1e). On average *mcc1* siliques were 17% shorter than wild type (Figure S1f). Prior to the onset of female meiosis ovule development in *mcc1* resembled that in wild type. Histological examination of *mcc1* gynoecea showed that following megasporogenesis the embryo sacs fail to differentiate in ~50% of *mcc1* ovules ( $n > 100$  ovules). Such that, at anthesis, the estimated number of fully developed ovules per gynoeceum was significantly less than in wild type ( $11.3 \pm 2.8$  versus  $22.6 \pm 4.8$ ;  $P \leq 0.005$ ) (Figure S2). However, the female lethality is not a gametophytic event because *MCC1* mutation inheritance was previously demonstrated to be sporophytic (Perrella *et al.*, 2006).

### Molecular characterization and expression of *MCC1*

Previously, we showed that the *mcc1* mutation cosegregated with a single T-DNA associated herbicide-resistance marker demonstrating tight genetic linkage of the two loci (Perrella *et al.*, 2006). A DNA fragment flanking the T-DNA insert in *mcc1* plants was obtained by thermal asymmetric

interlaced-PCR (TAIL PCR) (Liu *et al.*, 1995). This sequence was found to match the last exon of the predicted Arabidopsis gene At3g02960. However, the insertion of the T-DNA into the coding sequence of At3g02960 (Figure 1a) provoked no gene deregulation (Figure S3) making unlikely that the low seed set phenotype could be associated with it. As the T-DNA included multiple copies of the CaMV 35S enhancer (Weigel *et al.*, 2000), we tested whether the insertion caused an enhancement of the expression of the adjacent genes (Figure S3). RT-PCR analysis, performed on leaves and flower buds, indicated that only the expression of gene At3g02980 (*MCC1*), located 9.6 kb from the CaMV 35S enhancers, was elevated in the mutant compared with wild type (Figure 1b). This finding was confirmed by quantitative real-time RT-PCR, which revealed that the transcript level of *MCC1* was higher in mutant flower buds and leaf tissue compared with wild type by a factor of 3- and 1.5-fold respectively (Figure 1b).

*MCC1* has five exons and four introns (Genebank accession AC018363; F13E7.7) and encodes a predicted 247 amino acid protein containing a GCN5-related *N*-acetyltransferase domain (GenBank accession no. NM\_111168). Our RT-PCR

experiments, loaded on 2% agarose gel, revealed two transcripts (Figure S4a). The smallest transcript (GenBank accession EU598462) contains the full predicted ORF while the longest (GenBank accession no. EU598461) retains 30 nt of the second intron that causes a premature termination codon truncating the coding sequence at the 97th amino acid (Figure S4b). We found one *MCC1* homologue (At5g16800, 78% identical) in the Arabidopsis genome using a BLASTP search using the predicted *MCC1* sequence as the query.

To confirm that the low seed set phenotype of *mcc1* was due to enhanced expression of *MCC1*, we generated transgenic Arabidopsis plants expressing a genomic DNA fragment of At3g02980 under the control of a CaMV 35S promoter. Ninety-nine transformants were obtained that on visual inspection were found to have a large variability in seed set/silique. Eight independent transgenic lines that displayed a strong reduction in seed set were analysed further. The presence of the transgene with CaMV 35S promoter and kanamycin marker was confirmed by PCR and cytological examination revealed a reduction in pollen viability and male meiotic abnormalities similar to those described below in *mcc1* (Figure S5). When the C24 ecotype

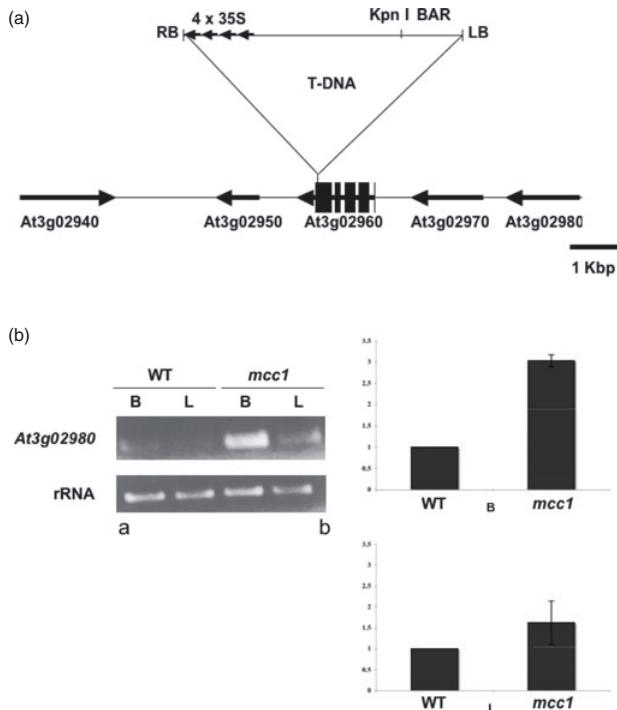


**Figure 1.** Chromosomal location of the T-DNA insertion and enhanced expression of the activated gene in *mcc1* mutant.

(a) Schematic representation of the T-DNA insertion site in the *mcc1* mutant. T-DNA is inserted within At3g02960 locus (exons are represented by black boxes), encoding a copper binding related protein. The four predicted genes, indicated by a black arrow, around T-DNA are At3g02950 encoding an unknown protein, MYB107 (At3g02940) encoding a putative transcription factor, EXL6 (At3g02970) encoding an exordium protein and At3g02980 encoding a GCN5-related *N*-acetyltransferase (GNAT) protein. BAR, Basta resistance. 4 × 35S denotes four copies of the 35S enhancer.

(b) Expression analyses of *MCC1*. (a) RT-PCR expression analysis of *MCC1* in wild type (WT) and *mcc1* bud (B) and leaf (L) tissue. The 18S rRNA is the control for *MCC1* expression. (b) Real time RT-PCR of relative expression of *MCC1* in wild type (WT) and *mcc1* in reproductive (B, bud) and somatic (L, leaf) tissue. The actin (*ACT2*) gene is used as the normalization control. Values are mean ± SE ( $n = 3$  experiments).

was transformed with the empty vector no effect on the phenotype was detected.

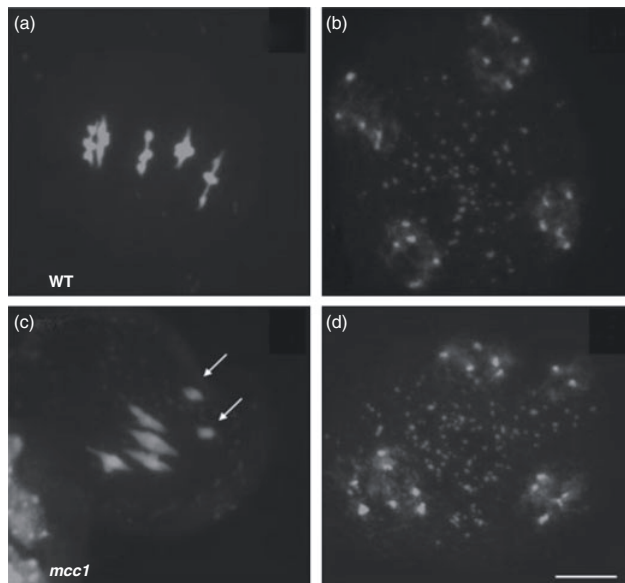
To perform loss-of-function of *MCC1*, T-DNA insertion lines SALK\_092359, SALK\_008970, and SALK\_135591 were analysed. The locus At3g02980 was tagged at the promoter (SALK\_092359, SALK\_008970) and at the third intron (SALK\_135591) (Figure S6a). Plants homozygous for the three independent mutant alleles had a phenotype resembling that of wild type. No difference in the expression level was seen for the *MCC1* gene between both lines SALK\_092359, and SALK\_008970 and the wild type with primers downstream of the insertion site (Figure S6b) revealing that *MCC1* is not disrupted in these two lines. In the case of line SALK\_135591, we failed to detect a transcript using primers spanning the insertion, although we detected a transcript using primers that were upstream of the insertion (Figure S6b). We hypothesized that either the truncated *MCC1* cDNA expressed in SALK\_135591 is functional or, alternatively, *MCC1* acts redundantly.

#### Occurrence of meiotic abnormality in *mcc1*

To investigate the basis of the reduced fertility phenotype in *mcc1* we conducted a cytological examination of meiosis using DAPI stained chromosome spread preparations from pollen mother cells (PMCs) at different meiotic stages (Figure 2). Earlier events of prophase I were not strikingly different from wild type PMCs isolated from anthers at a

comparable stage of development. At diplotene/diakinesis, the chromatin in *mcc1* was seemingly more relaxed in ~20% of the *mcc1* nuclei ( $n = 50$ ). The possibility that this might be indicative of a delay in prophase I progression was explored by conducting a time-course experiment using a 2-h pulse of bromo-deoxyuridine to label S-phase nuclei. Both *mcc1* and wild type took around 30 h to progress through prophase I. Although prophase I progression appeared not to be affected in *mcc1* the fate of those PMCs showing a strongly altered chromatin morphology is unclear (Figure 3). As the PMCs progressed beyond prophase I additional meiotic abnormalities became apparent. Inspection of chromosome spreads at metaphase I revealed the presence of univalent chromosomes in 8% of *mcc1* nuclei ( $n = 50$ ) (Figure 2c). Meiotic defects were also apparent at later meiotic stages. At anaphase I *mcc1* meiocytes showed lagging chromosomes (9%;  $n = 30$ ) and at telophase I uneven chromosome distribution was observed in 9% of PMCs ( $n = 50$ ) presumably due to the random segregation of the univalent chromosomes. Unsurprisingly, the defects were also observed in *mcc1* at the second meiotic division with missegregation at both anaphase II and telophase II (Figure 2d) and unequal sister chromatid distribution apparent in 21% of *mcc1* PMCs ( $n = 50$ ) giving rise to abnormal meiotic end products. However, that the frequency of these abnormalities was higher at meiosis II than meiosis I, cannot solely be explained by the univalent behaviour and is likely related

**Figure 2.** Microsporogenesis from wild-type (a, b) and *mcc1* (c, d) by DAPI staining in *Arabidopsis thaliana* ( $2n = 2x = 10$ ). Metaphase I showing four bivalents plus two univalents (arrows) in *mcc1* (c), and five bivalents in wild-type (a). Telophase II showing unbalanced chromosome number in two nuclei in *mcc1* (d), and four balanced nuclei in wild type (b) as estimated by the count of chromosome centres. Scale bar: 10  $\mu$ m.



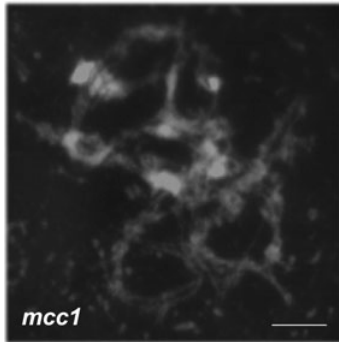


**Figure 3.** Pollen mother cell (PMC) in *mcc1* at mid-prophase I showing a strongly altered morphology of the chromosomes. Scale bar: 2  $\mu$ m.

to aberrant centromere function in sister chromatid segregation.

Female meiosis was also investigated in *mcc1*. This study revealed univalents at metaphase I (Figure S7) and chromosome segregation defects similar to those observed in male meiosis.

#### **MCC1 over-expression changes chiasma number per chromosome and chiasma distribution**

To establish whether *MCC1* affected meiotic recombination, chiasma frequency and distribution were evaluated in male meiosis (Table 1) at metaphase I after FISH with 4S and 5S rDNA probes (Figure 4) that allow the five chromosome pairs to be individually recognized as previously described

by Sanchez-Moran *et al.* (2001). Interestingly, the univalent chromosomes that occurred in 8% of *mcc1* nuclei was apparently not random, as all FISH observations revealed that this only involved the nucleolar acrocentric chromosome 2 (Figure 4). This finding was not seen in corresponding wild type nuclei ( $n = 50$ ), which is in complete agreement with previous results indicating that the mechanism that imposes the formation of a minimum of a single obligate CO/chiasma in Arabidopsis is very robust. Rather surprisingly, given the observation of the univalents, the mean number of chiasmata per cell was 7.9 in both *mcc1* and wild type ( $n = 50$  PMCs). Analysis of bivalent configuration, that is, 'rod versus ring,' where the chiasmata are restricted to a single arm or present in both arms respectively, revealed a significant decrease of 'ring' bivalents in *mcc1* in respect to wild type for chromosome 1 ( $P = 0.037$ ) and a significant increase for chromosome 4 ( $P = 0.033$ ). No significant changes were apparent on the remaining chromosomes. Analysis of chiasma localization in terms of distal versus proximal revealed an apparent increase of proximal COs on short arm of chromosome 3, but the increase was not statistically significant ( $P = 0.094$ ). For chromosome 4 in *mcc1* a significant increase ( $P = 0.002$ ) in the proportion of distal versus proximal chiasmata, 43 versus 23 respectively, was observed relative to wild type (29 versus 32). This was accompanied by a significant increase ( $P = 0.041$ ) in the relative proportion of chiasmata in the short arm. As mentioned above, the effect of this was to increase the overall occurrence of ring bivalents by 12% relative to wild type. Overall, it appears that elevated *MCC1* did not affect cross-over number per cell, but has a differential effect on individual chromosomes elevating COs for chromosome 4, in which there is also a shift in chiasma distribution, and

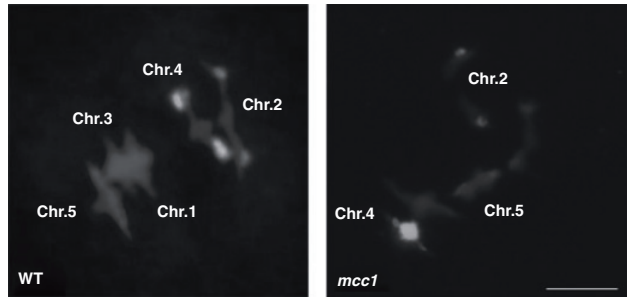
| Genotype    | Configurations                        |            | Chiasmata         |                   |                   |          |
|-------------|---------------------------------------|------------|-------------------|-------------------|-------------------|----------|
|             | Bivalents,<br>ring rod                | Univalents | Distal            | Proximal          | Short arm         | Long arm |
| Wild type   |                                       |            |                   |                   |                   |          |
| chr1        | 0.92, 0.08                            | –          | 1.48              | 0.58              | 0.92              | 1.14     |
| chr2        | 0.26, 0.74                            | –          | 0.78              | 0.48              | 0.34              | 0.92     |
| chr3        | 0.54, 0.46                            | –          | 1.08              | 0.46              | 0.54              | 1.00     |
| chr4        | 0.20, 0.80                            | –          | 0.58              | 0.64              | 0.24              | 0.98     |
| chr5        | 0.78, 0.22                            | –          | 1.36              | 0.46              | 0.78              | 1.04     |
| Total       | 2.70, 2.30                            | –          | 5.28              | 2.62              | 2.82              | 5.08     |
| <i>mcc1</i> |                                       |            |                   |                   |                   |          |
| chr1        | 0.84 <sup>a</sup> , 0.16 <sup>a</sup> | –          | 1.40              | 0.52              | 0.84              | 1.08     |
| chr2        | 0.22, 0.70                            | 0.08       | 0.72              | 0.42              | 0.30              | 0.84     |
| chr3        | 0.68, 0.32                            | –          | 1.10              | 0.62              | 0.68              | 1.04     |
| chr4        | 0.32 <sup>a</sup> , 0.68 <sup>a</sup> | –          | 0.86 <sup>b</sup> | 0.46 <sup>b</sup> | 0.38 <sup>a</sup> | 0.94     |
| chr5        | 0.84, 0.16                            | –          | 1.44              | 0.42              | 0.84              | 1.02     |
| Total       | 2.88, 2.02                            | 0.08       | 5.52              | 2.44              | 3.04              | 4.92     |

**Table 1** Average of pairing configurations per cell (rod versus ring), chiasmata per cell (distal versus proximal) and per bivalent arm (short versus long) in wild type and *mcc1* mutant ( $n = 50$  male meiocytes)

Data was analysed by chi-squared test.

<sup>a</sup> $P \leq 0.05$ ; <sup>b</sup> $P \leq 0.01$ .

**Figure 4.** FISH from wild type (WT) and *mcc1* at metaphase I in male meiosis. FISH was performed with the 5S rDNA (red) and 45S rDNA (green) probes. In WT, nucleolar chromosome 2 is a rod bivalent recognizable by 45S probes located on short arm; nucleolar chromosome 4 is a rod bivalent, as well, and shows 45S and 5S signals, both located on short arm. Chromosome 5 is a ring bivalent carrying only 5S. Chromosome 1 and 3 are ring bivalents without any signal and are distinguishable by size. In *mcc1*, the two univalents belong to chromosome 2 while chromosome 4 is configured as a ring bivalent. Scale bar: 5  $\mu$ m.



reducing COs for chromosome 1 and 2. In the latter this leads to the loss of the obligate CO/chiasma in some nuclei.

#### Synaptonemal complex (SC) appears normal in *mcc1*

Based on our observation that recombination was affected in *mcc1* we investigated whether SC was normal in the mutant. Immunolocalization studies were carried out on spread preparation of PMCs from the mutant at various stages throughout prophase I using Abs recognizing the axis-associated protein, ASY1 (Armstrong *et al.*, 2002) and the SC transverse element protein, ZYP1 (Higgins *et al.*, 2005). In wild type, immunolocalization of ASY1 indicates that the protein associates with the chromatin in G2 as numerous punctate foci. At the onset of leptotene there is a rapid, co-ordinated change in the distribution to a linear chromosome axis associated signal (Sanchez-Moran *et al.*, 2007). This finding coincides with the elaboration of the chromosome axes (Figures S8 and S9). In *mcc1* initial localization of ASY1 is indistinguishable from that in wild type (Figure S10a–c), but subsequently the axis transition appeared less coordinated (Figure S10d–i). This situation was manifested in the presence of nuclei at zygotene that exhibited stretches of linear ASY1 signal set against a diffuse chromatin-associated signal (Figure S10g–i). We have never observed this distribution of ASY1 in wild type material (Figure S9d–i). As prophase I progressed through zygotene to pachytene the ASY1 assumed a more typical linear signal running the length of the chromosome axes and there appears no substantive effect on the rate of progression of the PMCs through to pachytene (Figure S10j–l). At pachytene, ASY1 behaviour was accompanied by apparently normal SC formation based on immunolocalization of ZYP1 (Figure S11).

#### Hyperacetylation of histone H3 in *mcc1* male meiosis

Based on our findings that meiosis was defective in the mutant we surmised that if the prediction that MCC1 possesses histone acetyltransferase activity was correct, then evidence of histone hyperacetylation should be apparent in

*mcc1* PMCs. The level of histone acetylation in *mcc1* and wild type PMC spread preparations was quantified at pachytene by measuring the fluorescence signal intensity following dual-immunolocalization using an antibody (Ab) recognizing the lysine residues K9 and K14 on the tail of histone H3 (H3K9K14Ac) (Figure 5) and an anti-ASY1 Ab or, alternatively, anti-ZYP1 Ab (Figure S8). ASY1 and ZYP1 being well characterized for their spatial and temporal distribution during prophase I allow to identify unambiguously the PMC stage. The fluorescence signal arising from the anti-H3K9K14Ac Ab was consistently stronger in *mcc1* by a factor of 30% ( $n = 85$  nuclei) (Figure 5). This finding is consistent with *mcc1* PMCs exhibiting an elevated level of histone H3 acetylation.

#### Trichostatin A treatment phenocopies MCC1 over-expression

To obtain additional evidence that the meiotic defects described in *mcc1* were induced by the histone hyperacetylation, we treated wild type plants with trichostatin A (TSA), an inhibitor of histone deacetylases (Murphy *et al.*, 2000). Immunolocalization with anti-H3K9K14Ac Ab confirmed that the PMCs from the treated plants exhibited hyperacetylation

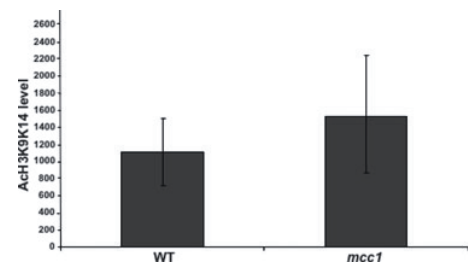


**Figure 5.** Level of histone acetylation in wild type and *mcc1* microsporocytes at pachytene ( $n = 85$  nuclei). It was measured by fluorescence intensity according to 'Step by Step AnalySIS' software. Data are means and SD.

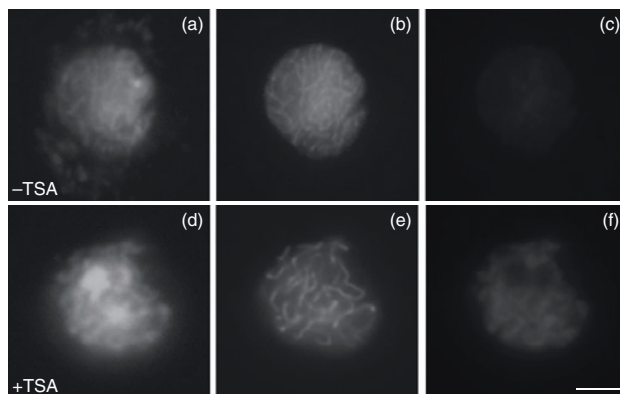


**Figure 6.** Dual immunolocalization of ASY1 (green; b, e), and H3K9K14Ac (red; c, f) to PMCs at zygonema with trichostatin A-treatment (+TSA, d–f) and without (–TSA, a–c). DNA was counterstained with DAPI (a, d). Higher level of histone acetylation is shown in TSA-treated sample (f) respect to untreated (c) at the same stage when ASY1 is visible as a continuous signal along chromosome axes (b, e). Scale bar: 5  $\mu$ m.

(Figure 6) indicating that deacetylation was inhibited starting at the lowest TSA concentration (10 ng/ml). The observation of DAPI-stained chromosome spreads in PMCs revealed that TSA treatment was able to phenocopy the meiotic defects of *mcc1* mutant. This factor included the presence of univalents at diakinesis (Figure 7c) leading to missegregation and unbalanced nuclei at the end of meiosis

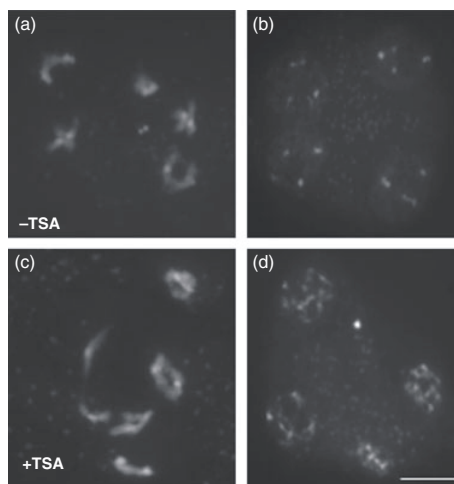


**Figure 7.** Meiosis from representative PMCs of wild type after the treatment with histone deacetylase inhibitor trichostatin A (+TSA, c, d) as compared with untreated PMCs (–TSA, a, b). In TSA-treated PMCs (10 ng/ml TSA), 2 univalents at diakinesis (c), and unbalanced nuclei at telophase II (d). Regular behaviour is shown by untreated PMCs (a, b). Scale bar: 10  $\mu$ m.

(Figure 7d). No meiotic irregularities were detected in untreated plants (Figure 7a,b). Thus, these results indicate that the effect of TSA treatment during meiosis is substantially the same as over-expression of *MCC1*.

#### DISCUSSION

Our analysis of the *A. thaliana* *mcc1* mutant where enhanced activation of a putative histone acetylase results in hyperacetylation of histone H3 in male meiosis has revealed compelling evidence of a link between histone de/acetylation and normal meiotic progression.

In *mcc1*, hyperacetylation has a clear effect on chiasma behaviour although not univocal for all the chromosomes. In particular, chromosome 1 shows a tendency ( $P < 0.05$ ) to form a single CO per bivalent instead of double COs typical of wild-type. CO assurance on chromosome 2 is defective, such that a proportion (8%) fails to form the obligate CO which is the minimum requirement to ensure accurate chromosome segregation at the first meiotic division (Lam *et al.*, 2005). Chromosome 4 formed a significantly greater proportion ( $P < 0.05$ ) of double COs per bivalent compared with wild type. Indeed, in this chromosome we observed a significant increase ( $P < 0.05$ ) in the proportion of chiasmata in the short arm (s.a.) relative to the long arm (l.a.) in *mcc1* (0.38 s.a./0.94 l.a.) compared with wild type (0.24 s.a./0.94 l.a.). CO increase was accompanied by a significant shift ( $P < 0.01$ ) toward distal chiasmata in the long arm of the chromosome 4. We propose that different chromosome features may underlie the differential response to hyperacetylation observed for chromosome 4 in *mcc1*. Apart from its smaller size, which may well be relevant, the key feature of chromosomes 4 is the presence of a large array of rDNA in the short arm (Copenhaver and Pikaard, 1996). Additionally, a cluster of CO hotspots has been mapped to the short arm of chromosome 4 adjacent to the

heterochromatic NOR (Drouaud *et al.*, 2006). It is therefore conceivable that hyperacetylation might enhance the activity of the pre-existing hotspot cluster on the short arm of chromosome 4 or, alternatively, induce novel recombination sites possibly located at NOR or flanking regions. Several previous studies lend support to this hypothesis. It is well documented that hyperacetylation of histone H3 or H4 occurs in recombinationally active chromosomal domains such as chicken immunoglobulin locus (Seo *et al.*, 2005), fission yeast *ade6-M26* (M26) locus (Yamada *et al.*, 2004), and mouse hotspot *Psmb9* (Buard *et al.*, 2009). Furthermore, mutation in the budding yeast histone deacetylase *RPD3* stimulates meiotic recombination at *HIS4* hotspot locus as measured through the double-stranded DNA breaks (DSBs), which are the earliest determinants of crossovers (Merker *et al.*, 2008). In contrast, histone hypoacetylation characterizes recombination-suppressed regions at rRNA gene clusters as well as at telomeres in budding yeast (Millar and Grunstein, 2006). When the histone deacetylase *SIR2* gene is deleted, an elevated rate of intrachromosomal recombination is observed in the rRNA genes (Gottlieb and Esposito, 1989). Consistent with this observation, the frequency of DSBs increases in rDNA and flanking regions in the *sir2* mutant (Mieczkowski *et al.*, 2007). Finally a study in *A. thaliana* showed that mutation of the histone deacetylase *HDA6* resulted in a loss of transcriptional silencing of repetitive sequences, chromatin decondensation and significant hyperacetylation localized to the NOR (Probst *et al.*, 2004). Although whether this had an effect during meiosis was not explored. That chromosome 2 behaves differently to chromosome 4 despite structural similarities, in terms of size and rDNA array, cannot readily be addressed at present. It is of interest that differences in the behaviour of the two chromosomes have previously been noted (Santos *et al.*, 2003). We assume that CO failure occurring on chromosome 2 as well as on chromosome 1 may be related to the number and relative distribution of CO hotspots along these chromosomes. However the distribution of hotspots on chromosome 1 and 2 has not yet been reported. Modifications in CO number and distribution could be related to changes in chromatin structure imposed by hyperacetylation. Indeed, over-expression of *MCC1* seems to have an effect on meiotic chromosome condensation that needs to be deeply investigated. In other organisms, hyperacetylation due to pharmacological inhibition of HDACs hampers the chromosome condensation during meiosis (Akiyama *et al.*, 2006; De La Fuente, 2006; Magnaghi-Jaulin and Jaulin, 2006; Wang *et al.*, 2006; Bui *et al.*, 2007), whereas over-expression of a deacetylase causes a premature chromatin condensation (Verdel *et al.*, 2003). In addition, the observation that *ASY1* behaviour appears abnormal would suggest that overexpression of *MCC1* affects chromatin organization since early meiosis.

Our analysis of *mcc1* evidences that histone de/acetylation is critical for ensuring the proper chromosome/sister chromatid segregation. Furthermore, this is supported by the observations of TSA-treated wild type meiocytes. A general requirement of histone deacetylation for proper segregation is illustrated in other organisms, in mitotic as well as in meiotic cells. For instance, hyperacetylation following treatment with histone deacetylase inhibitors results in chromosome segregation defects in fission yeast (Ekwall *et al.*, 1997), human (Cimini *et al.*, 2003) and tobacco (Li *et al.*, 2005) mitotic cells, as well as in mouse (De La Fuente *et al.*, 2004; Akiyama *et al.*, 2006) and porcine (Wang *et al.*, 2006) female meiosis. Evidence has been provided for the role of histone deacetylation in epigenetic control of centromeric heterochromatin (Ekwall *et al.*, 1997; Taddei *et al.*, 2001; Cimini *et al.*, 2003; De La Fuente *et al.*, 2004), in centromere cohesion (Eot-Houllier *et al.*, 2008) and kinetochore-microtubule attachment (Ishii *et al.*, 2008).

In *mcc1*, meiotic histone hyperacetylation influences negatively plant fertility by acting on male and female meiosis. In yeast, mutations in HATs produced meiotic arrest (Burgess *et al.*, 1999; Choy *et al.*, 2001), whereas TSA-dependent hyperacetylation caused apoptosis in murine male meiosis (Fenic *et al.*, 2004), and aneuploidy in female meiosis (Akiyama *et al.*, 2006) or inhibited the progression of meiotic maturation in half of the oocytes (De La Fuente *et al.*, 2004).

In conclusion, our findings point out that *MCC1* has a role in meiosis by influencing recombination and chromosome segregation. In a context of histone code hypothesis (Strahl and Allis, 2000; Jenuwein and Allis, 2001), it is likely that hyperacetylation driven by *MCC1* may alter the pattern of other histone modifications, methylation, phosphorylation and ubiquitination, especially at level of specialized sub-chromosomal domains.

## EXPERIMENTAL PROCEDURES

### Plant material and growth conditions

The Arabidopsis *mcc1* mutant was previously isolated from an enhancer activation tagging population (Perrella *et al.*, 2006) obtained after *Agrobacterium tumefaciens* floral transformation with strain GV3101 carrying the binary vector pSKI1015 (Koiwa *et al.*, 2002). C24 line homozygous for the chimeric *RD29A:LUC* reporter gene (Ishitani *et al.*, 1997) is the background of tagged T-DNA population and was used in this study as wild type. Plants were grown both in a controlled growth room with 16 h/8 h of light/dark at 22°C/18°C and in greenhouse. Phenotypic analysis was performed according to Boyes *et al.* (2001). Plant material was collected as described by Higgins *et al.* (2004).

### Nucleic acid extraction

Plant genomic DNA was isolated using the DNeasy Plant Mini Kit (QIAGEN). Bacterial plasmid DNA was isolated using QIAprep<sup>®</sup> Spin Miniprep Kit (QIAGEN, <http://www1.qiagen.com>). Total RNA from wild type and *mcc1* leaves and prebolving buds was extracted using the RNeasy Plant Mini Kit (QIAGEN) and then treated with DNase I

(Invitrogen, <http://www.invitrogen.com>) to remove residual genomic DNA.

#### Identification of T-DNA tagged locus

Genomic sequence flanking the T-DNA insertion in *mcc1* was determined by using the TAIL-PCR procedure of Liu *et al.* (1995) with primers corresponding to the nested regions internal to the left border and degenerated primers as listed in Table S1 online.

#### Identification of T-DNA insertion mutants

T-DNA insertion lines SALK\_092359, SALK\_008970, and SALK\_135591 were obtained from the ABRC and screened for homozygous progeny as described using specific primers and T-DNA primer suggested (Alonso *et al.*, 2003).

#### RT-PCR analysis

The SuperScript™ One-Step RT-PCR with Platinum *Taq* kit (Invitrogen) was used to amplify gene-specific products from total RNA. Primers designed to amplify the genes flanking the insertion site and 18S rRNA, used to equalize the RNA loading into RT-PCR reaction, are listed in Table S1 online.

#### Real-time RT-PCR analysis

The SuperScript III reverse transcriptase (Invitrogen) was used to synthesize first-strand cDNA from total RNA. Gene-specific primers were designed using PRIMER EXPRESS software, ver. 2.0 (Applied Biosystems®, <http://www3.appliedbiosystems.com>) and are listed in Table S1 online. Real-time PCR analysis was performed using the ABI PRISM 7000 instrument (Applied Biosystems®) and SYBR® Green PCR Master Mix (Applied Biosystem). Data were analysed through 7000 System SDS software ver. 1.2.3 (Applied Biosystems®). The amplification plots were analysed automatically calculating the baseline and the Ct values. Actin was used as endogenous control. Relative expression data were obtained by comparing wild type versus *mcc1* mutant samples.

#### MCC1 cloning and nucleic acid sequencing

The coding region of *MCC1* was amplified by RT-PCR by using SuperScript™ III Reverse Transcriptase (Invitrogen) with an oligo-dT (12–18) in C24 ecotype. The cDNA was subjected to PCR with gene-specific primers as listed in Table S1 online and cloned into PCR2.1 (Invitrogen). *MCC1* genomic fragment (corresponding to the region 14096–15414 of BAC clone F13E7) was amplified from C24 DNA by PCR with primers listed in Table S1 online and cloned into the binary vector pKYLX7135S<sup>2</sup> (Scharld *et al.*, 1987) to generate pKYLX7135S<sup>2</sup>-*MCC1*. Nucleotide sequencing was carried out by Eurofins MWG Operon sequencing service (Germany).

#### Recapitulation analysis

The construct pKYLX7135S<sup>2</sup>-*MCC1* was introduced into *Agrobacterium tumefaciens* strain GV3101, which was used to transform C24 ecotype as described by Koiva *et al.* (2002). The seed set/silique, the pollen viability, and the microsporogenesis were observed on T<sub>1</sub> transgenic plants harboring the overexpression construct to reconfirm the *MCC1* gene function.

#### Cytohistological analysis

Male meiosis was examined by light microscopy in 4'-6-diamidino-2 phenylindole (DAPI)-stained pollen mother cells (PMCs) as described by Ross *et al.* (1996). Female meiosis observation was performed according to Armstrong and Jones (2001). Chiasmata

were recorded at metaphase I in PMCs after fluorescence *in situ* hybridization (FISH) following the method of Sanchez-Moran *et al.* (2001). Fluorescence immunolocalization was carried out on chromosome spreadings in PMCs at prophase I as described by Armstrong *et al.* (2002). The following antibodies have been used: anti-ASY1 (rat, dilution 1:500), anti-ZYP1 (rabbit/rat, dilution 1:500), and anti-H3K9K14Ac (Upstate Biotechnology, catalogue no. 06-599; rabbit, dilution 1:500) (Armstrong *et al.*, 2002; Sanchez-Moran *et al.*, 2007). Slides were analyzed by fluorescence microscopy using a Nikon Eclipse T300 microscope. Image acquisition and analysis were conducted using 'Step by Step AnalySIS' software (Soft Imaging System GmbH, <http://www.soft-imaging.net>). The intensity of fluorescence was quantified by measuring the pixel value of fluorescence within a defined Region of Interest (ROI) using a 12-bit CCD camera.

Pollen viability was assessed by Alexander's staining (Alexander, 1969). For gynoecea observation, DAPI-stained longitudinal sections (8 µm) of buds collected at the floral stages 10–13, as defined by Smyth *et al.* (1990), corresponding to ovule stages 2–3 (Schneitz *et al.*, 1995), were performed according to paraffin-embedding procedure (Sharma and Sharma, 1980).

#### Bromodeoxyuridine (BrdU) pulse-labelling treatment

BrdU pulses were performed and detected using an anti-BrdU kit (Roche, <http://www.roche.com>) according to the technique described by Armstrong *et al.* (2003).

#### Trichostatin A treatment

The inflorescence stems from wild type and *mcc1* mutant were cut under water and placed in different concentrations of trichostatin A (Roche) (10, 100, 1000 ng/ml) as previously described for aminopeptidase inhibitor assay (Sanchez-Moran *et al.*, 2004). After 39 h the floral buds were fixed and PMCs analyzed as above reported.

#### Accession numbers

Sequence data from this article can be found in the Arabidopsis Genome Initiative or GenBank/EMBL databases under the following accession numbers: *MCC1*, At3g02980; EXP6, At3g02970; EST, At3g02950; MYB107, At3g02940; COBP, At3g02960; Actin, At3g18780; 18S rRNA, At3g41768.

#### ACKNOWLEDGEMENTS

The authors wish to thank Dr Maria Luisa Chiusano for helpful suggestions in bioinformatics. Valuable technical support was provided by Rosa Maisto, Elvira Lotti and Antonio Scafarto. We thank the ABRC for providing Arabidopsis seeds of the T-DNA insertion lines. This work was supported by the Italian Ministry of Research. Prof. FCH Franklin and Dr Eugenio Sanchez-Moran were funded by BBSRC. Contribution no. 345 from CNR-IGV, Research Institute of Plant Genetics, Research Division: Portici, Italy.

#### SUPPORTING INFORMATION

Additional Supporting Information may be found in the online version of this article:

**Figure S1.** Vegetative development and reproductive organs in *mcc1* mutant and wild type (WT).

**Figure S2.** Histological sections of gynoecea from *mcc1* and wild type.

**Figure S3.** RT-PCR analysis of genes surrounding the T-DNA insertion site in *mcc1*.

**Figure S4.** Different *MCC1* mRNA variants.

**Figure S5.** Microsporogenesis in 35S:*MCC1* plants.

**Figure S6.** Schematic representation of *MCC1* locus showing the T-DNA insertion sites in SALK lines.

**Figure S7.** Female meiosis from wild-type and *mcc1*.

**Figure S8.** Dual immunolocalization of ASY1 or ZYP1 and H3K9K14Ac to PMCs in *mcc1* and wild type.

**Figure S9.** Immunolocalization of ASY1 protein to early and mid-prophase I nuclei of wild type.

**Figure S10.** Immunolocalization of ASY1 protein to early and mid-prophase I nuclei of *mcc1* mutant.

**Figure S11.** Dual immunolocalization of ASY1 and ZYP1 to male mid-prophase I nuclei of wild type and *mcc1*.

**Table S1** Oligonucleotides used in this study.

Please note: As a service to our authors and readers, this journal provides supporting information supplied by the authors. Such materials are peer-reviewed and may be re-organized for online delivery, but are not copy-edited or typeset. Technical support issues arising from supporting information (other than missing files) should be addressed to the authors.

## REFERENCES

- Akiyama, T., Nagata, M. and Aoki, F. (2006) Inadequate histone deacetylation during oocyte meiosis causes aneuploidy and embryo death in mice. *Proc. Natl Acad. Sci. USA*, **103**, 7339–7344.
- Alexander, M.P. (1969) Differential staining of aborted and nonaborted pollen. *Stain Technol.* **44**, 117–122.
- Alonso, J.M., Stepanova, A.N., Leisse, T.J. et al. (2003) Genome-wide insertional mutagenesis of *Arabidopsis thaliana*. *Science*, **301**, 653–657.
- Armstrong, S.J. and Jones, G.H. (2001) Female meiosis in wild type *Arabidopsis thaliana* and in two meiotic mutants. *Sex. Plant Reprod.* **13**, 177–183.
- Armstrong, S.J., Caryl, A.P., Jones, G.H. and Franklin, F.C.H. (2002) *Asy1*, a protein required for meiotic chromosome synapsis, localizes to axis-associated chromatin in *Arabidopsis* and *Brassica*. *J. Cell Sci.* **115**, 3645–3655.
- Armstrong, S.J., Franklin, F.C.H. and Jones, G.H. (2003) A meiotic time-course for *Arabidopsis thaliana*. *Sex. Plant Reprod.* **16**, 141–149.
- Aufsatz, W., Mette, M.F., Van Der Winden, J., Matzke, M. and Matzke, A.J. (2002) HDA6, a putative histone deacetylase needed to enhance DNA methylation induced by double-stranded RNA. *EMBO J.* **21**, 6832–6841.
- Bertrand, C., Berguionoux, C., Domenichini, S., Delarue, M. and Zhou, D.X. (2003) *Arabidopsis* histone acetyltransferase ATGCN5 regulates the floral meristem activity through the WUSCHEL/AGAMOUS pathway. *J. Biol. Chem.* **278**, 28246–28251.
- Boateng, K.A., Yang, X., Dong, F., Owen, H.A. and Makaroff, C.A. (2008) SWI1 is required for meiotic chromosome remodeling events. *Mol. Plant*, **1**, 620–633.
- Borde, V., Robine, N., Lin, W., Bonfils, S., Géli, B. and Nicolas, A. (2009) Histone H3 lysine 4 trimethylation marks meiotic recombination initiation sites. *EMBO J.* **28**, 99–111.
- Boyes, D.C., Zaved, A.M., Ascenzi, R., McCaskill, A.J., Hoffman, N.E., Davis, K.R. and Görlach, J. (2001) Growth stage-based phenotypic analysis of *Arabidopsis*: a model for high throughput functional genomics in plants. *Plant Cell*, **13**, 1499–1510.
- Buard, J., Barthès, P., Grey, C. and de Massy, B. (2009) Distinct histone modifications define initiation and repair of meiotic recombination in the mouse. *EMBO J.* **28**, 2616–2624.
- Bui, H.T., Van Thuan, N., Kishigami, S., Wakayama, S., Hikichi, T., Ohta, H., Mizutani, E., Yamaoka, E., Wakayama, T. and Miyano, T. (2007) Regulation of chromatin and chromosome morphology by histone H3 modifications in pig oocytes. *Reproduction*, **133**, 371–382.
- Burgess, S.M., Ajimura, M. and Kleckner, N. (1999) GCN5-dependent histone H3 acetylation and RPD3-dependent histone H4 deacetylation have distinct, opposing effects on IME2 transcription, during meiosis and during vegetative growth, in budding yeast. *Proc. Natl Acad. Sci. USA*, **96**, 6835–6840.
- Choy, J.S., Toke, B.T., Huh, J.H. and Kron, S.J. (2001) Yng2p-dependent NuA4 histone H4 acetylation activity is required for mitotic and meiotic progression. *J. Biol. Chem.* **276**, 43653–43662.
- Cimini, D., Mattiuzzo, M., Torosantucci, L. and Degrossi, F. (2003) Histone hyperacetylation in mitosis prevents sister chromatid separation and produces chromosome segregation defects. *Mol. Biol. Cell*, **14**, 3821–3833.
- Copenhaver, G.P. and Pikaard, C.S. (1996) RFLP and physical mapping with an rDNA-specific endonuclease reveals that nucleolus organizer regions of *Arabidopsis thaliana* adjoin the telomeres on chromosomes 2 and 4. *Plant J.* **9**, 259–272.
- De La Fuente, R. (2006) Chromatin modifications in the germinal vesicle (GV) of mammalian oocytes. *Dev. Biol.* **292**, 1–12.
- De La Fuente, R., Viveiros, M.M., Burns, K.H., Adashi, E.Y., Matzuk, M.M. and Eppig, J.J. (2004) Major chromatin remodeling in the germinal vesicle (GV) of mammalian oocytes is dispensable for global transcriptional silencing but required for centromeric heterochromatin function. *Dev. Biol.* **275**, 447–458.
- Drouaud, J., Camilleri, C., Bourguignon, P.Y. et al. (2006) Variation in crossing-over rates across chromosome 4 of *Arabidopsis thaliana* reveals the presence of meiotic recombination 'hot spots.' *Genome Res.* **16**, 106–114.
- Ekwall, K., Olsson, T., Turner, B.M., Cranston, G. and Allshire, R.C. (1997) Transient inhibition of histone deacetylation alters the structural and functional imprint at fission yeast centromeres. *Cell*, **91**, 1021–1032.
- Eot-Houlier, G., Fulcrand, G., Watanabe, Y., Magnaghi-Jaulin, L. and Jaulin, C. (2008) Histone deacetylase 3 is required for centromeric H3K4 deacetylation and sister chromatid cohesion. *Genes Dev.* **22**, 2693–2744.
- Fenic, I., Sonnack, V., Failing, K., Bergmann, M. and Steger, K. (2004) In vivo effects of histone-deacetylase inhibitor trichostatin-A on murine spermatogenesis. *J. Androl.* **25**, 811–818.
- Gottlieb, S. and Esposito, R.E. (1989) A new role for a yeast transcriptional silencer gene, SIR2, in regulation of recombination in ribosomal DNA. *Cell*, **56**, 771–776.
- Higgins, J.D., Armstrong, S.J., Franklin, F.C. and Jones, G.H. (2004) The *Arabidopsis* MutS homolog ATMSH4 functions at an early step in recombination: evidence for two classes of recombination in *Arabidopsis*. *Genes Dev.* **18**, 2557–2570.
- Higgins, J.D., Sanchez-Moran, E., Armstrong, S.J., Jones, G.H. and Franklin, F.C. (2005) The *Arabidopsis* synaptonemal complex protein ZYP1 is required for chromosome synapsis and normal fidelity of crossing over. *Genes Dev.* **15**, 2488–2500.
- Hirota, K., Mizuno, K., Shibata, T. and Ohta, K. (2008) Distinct chromatin modulators regulate the formation of active and repressive chromatin at the fission yeast recombination hotspot *ade6-M26*. *Mol. Biol. Cell*, **19**, 1162–1173.
- Ishii, S., Kurasawa, Y., Wong, J. and Yu-Lee, L.Y. (2008) Histone deacetylase 3 localizes to the mitotic spindle and is required for kinetochore-microtubule attachment. *Proc. Natl Acad. Sci. USA*, **105**, 4179–4184.
- Ishitani, M., Xiong, L., Stevenson, B. and Zhu, J.K. (1997) Genetic analysis of osmotic and cold stress signal transduction in *Arabidopsis*: interactions and convergence of abscisic acid-dependent and abscisic acid-independent pathways. *Plant Cell*, **9**, 1935–1949.
- Jenuwein, T. and Allis, C.D. (2001) Translating the histone code. *Science*, **293**, 1074–1080.
- Koiva, H., Barb, A.W., Xiong, L. et al. (2002) C-terminal domain phosphatase-like family members (AtCPLs) differentially regulate *Arabidopsis thaliana* abiotic stress signaling, growth, and development. *Proc. Natl Acad. Sci. USA*, **99**, 10893–10898.
- Kouzarides, T. (2007) Chromatin modifications and their function. *Cell*, **128**, 693–705.
- Lam, S.Y., Horn, S.R., Radford, S.J., Housworth, E.A., Stahl, F.W. and Copenhaver, G.P. (2005) Crossover interference on nucleolus organizing region-bearing chromosomes in *Arabidopsis*. *Genetics*, **170**, 807–812.
- Latrasse, D., Benhamed, M., Henry, Y., Domenichini, S., Kim, W., Zhou, D.X. and Delarue, M. (2008) The MYST histone acetyltransferases are essential for gametophyte development in *Arabidopsis*. *BMC Plant Biol.* **8**, 121.
- Li, Y., Butenko, Y. and Graf, G. (2005) Histone deacetylation is required for progression through mitosis in tobacco cells. *Plant J.* **41**, 346–352.
- Liu, Y., Mitsukawa, N., Oosumi, T. and Whittier, R.F. (1995) Efficient isolation and mapping of *Arabidopsis thaliana* T-DNA insert junctions by thermal asymmetric intercalated PCR. *Plant J.* **8**, 457–463.
- Lohr, D., Kovacic, R.T. and Van Holde, K.E. (1977) Quantitative analysis of the digestion of yeast chromatin by staphylococcal nuclease. *Biochemistry*, **16**, 463–471.
- Magnaghi-Jaulin, L. and Jaulin, C. (2006) Histone deacetylase activity is necessary for chromosome condensation during meiotic maturation in *Xenopus laevis*. *Chromosome Res.* **14**, 319–332.

- Merker, J.D., Dominska, M., Greewell, P.W., Rinella, E., Bouck, D.C., Shibata, Y., Strahl, B.D., Mieczkowski, P. and Petes, T.D. (2008) The histone methylase Set2p and the histone deacetylase Rpd3p repress meiotic recombination at the HIS4 meiotic recombination hotspot in *Saccharomyces cerevisiae*. *DNA Repair*, **7**, 1298–1308.
- Mieczkowski, P.A., Dominska, M., Buck, M.J., Lieb, J.D. and Petes, T.D. (2007) Loss of a histone deacetylase dramatically alters the genomic distribution of Spo11p-catalyzed DNA breaks in *Saccharomyces cerevisiae*. *Nat Acad. Sci. USA*, **104**, 3955–3960.
- Millar, C.B. and Grunstein, M. (2006) Genome-wide patterns of histone modifications in yeast. *Nat. Rev. Mol. Cell Biol.* **7**, 657–666.
- Murphy, J.P., McAleer, J.P., Ugliarolo, A., Papile, J., Weniger, J., Bethelmie, F. and Tramontano, W.A. (2000) Histone deacetylase inhibitors and cell proliferation in pea root meristems. *Phytochemistry*, **55**, 11–18.
- Pandey, R., Muller, A., Napoli, C.A., Selinger, D.A., Plikaard, C.S., Richards, E.J., Bender, J., Mount, D.W. and Jorgensen, R.A. (2002) Analysis of histone acetyltransferase and histone deacetylase families of *Arabidopsis thaliana* suggests functional diversification of chromatin modification among multicellular eukaryotes. *Nucleic Acids Res.* **30**, 5036–5055.
- Perrella, G., Cremona, G., Consiglio, F., Errico, A., Bressan, R.A. and Conicella, C. (2006) Screening for mutations affecting sexual reproduction after activation tagging in *Arabidopsis thaliana*. *J. Appl. Genet.* **47**, 109–111.
- Probst, A.V., Fagard, M., Proux, F. et al. (2004) *Arabidopsis* histone deacetylase HDA6 is required for maintenance of transcriptional gene silencing and determines nuclear organization of rDNA repeats. *Plant Cell*, **16**, 1021–1034.
- Ross, K.J., Franz, P. and Jones, G.H. (1996) A light microscopic atlas of meiosis in *Arabidopsis thaliana*. *Chromosome Res.* **4**, 507–516.
- Sanchez-Moran, E., Armstrong, S.J., Santos, J.L., Franklin, C.H. and Jones, G.H. (2001) Chiasma formation in *Arabidopsis thaliana* accession Wasileskija and in two meiotic mutants. *Chromosome Res.* **9**, 121–128.
- Sanchez-Moran, E., Jones, G.H., Franklin, C.H. and Santos, J.L. (2004) A puromycin-sensitive aminopeptidase is essential for meiosis in *Arabidopsis thaliana*. *Plant Cell*, **16**, 2895–2909.
- Sanchez-Moran, E., Santos, J.L., Jones, G.H. and Franklin, C.H. (2007) ASY1 mediates AtDMC1-dependent interhomolog recombination during meiosis in *Arabidopsis*. *Genes Dev.* **21**, 2220–2233.
- Santos, J.L., Alfaro, D., Sanchez-Moran, E., Armstrong, S.J., Franklin, C.H. and Jones, G.H. (2003) Partial diploidization of meiosis in autotetraploid *Arabidopsis thaliana*. *Genetics*, **165**, 1533–1540.
- Schardl, C.L., Bvrd, A.D., Benzion, G., Altschuler, M.A., Hildebrand, D.F. and Hunt, A.G. (1987) Design and construction of a versatile system for the expression of foreign genes in plants. *Gene*, **61**, 1–11.
- Schneitz, K., Hülskamp, M. and Pruitt, R.E. (1995) Wild type ovule development in *Arabidopsis thaliana* – a light microscope study of cleared whole-mount tissue. *Plant J.* **7**, 731–749.
- Seo, H., Masuoka, M., Murofushi, H., Takeda, S., Shibata, T. and Ohta, K. (2005) Rapid generation of specific antibodies by enhanced homologous recombination. *Nat. Biotechnol.* **23**, 731–735.
- Sharma, A.K. and Sharma, A. (1980) Processing. In *Chromosome Techniques*. London: Butterworths and Co., pp. 71–90.
- Shogren-Knaak, M., Ishii, H., Sun, J.M., Pazin, M.J., Davie, J.R. and Peterson, C.L. (2006) Histone H4–K16 acetylation controls chromatin structure and protein interactions. *Science*, **311**, 844–847.
- Smith, C.M., Galken, P.R., Zhang, Z., Gottschling, D.E., Smith, J.B. and Smith, D.L. (2003) Mass spectrometric quantification of acetylation at specific lysines within the amino-terminal tail of histone H4. *Anal. Biochem.* **316**, 23–33.
- Smyth, D.R., Bowman, J.L. and Meyerowitz, E.M. (1990) Early flower development in *Arabidopsis*. *Plant Cell*, **8**, 755–767.
- Strahl, B.D. and Allis, C.D. (2000) The language of covalent histone modifications. *Nature*, **403**, 41–45.
- Taddei, A., Maison, C., Roche, D. and Almouzni, G. (2001) Reversible disruption of pericentric heterochromatin and centromere function by inhibiting deacetylases. *Nat. Cell Biol.* **3**, 114–120.
- Tian, L., Wang, J., Fong, M.P., Chen, M., Cao, H., Gelvin, S.B. and Chen, Z.J. (2003) Genetic control of developmental changes induced by disruption of *Arabidopsis* histone deacetylase 1 (*AtHD1*) expression. *Genetics*, **165**, 399–409.
- Verdel, A., Seigneurin-Berny, D., Faure, A.K., Eddahbi, M., Khochbin, S. and Nonchev, S. (2003) HDAC6-induced premature chromatin compaction in mouse oocytes and fertilised eggs. *Zygote*, **11**, 323–328.
- Vlachonasios, K.E., Thomashow, M.F. and Triezenberg, S.J. (2003) Disruption mutations of ADA2b and GCN5 transcriptional adaptor genes dramatically affect *Arabidopsis* growth, development, and gene expression. *Plant Cell*, **15**, 626–638.
- Wang, Q., Yin, S., Ai, J.S., Liang, C.G., Hou, Y., Chen, D.Y., Schatten, H. and Sun, Q.Y. (2006) Histone deacetylation is required for orderly meiosis. *Cell Cycle*, **5**, 766–774.
- Weigel, D., Ahn, J.H., Blázquez, M.A. et al. (2000) Activation tagging in *Arabidopsis*. *Plant Physiol.* **122**, 1003–1113.
- Wu, K., Tian, L., Malik, K., Brown, D. and Miki, B. (2000) Functional analysis of HD2 histone deacetylase homologues in *Arabidopsis thaliana*. *Plant J.* **22**, 19–27.
- Wu, K., Zhang, L., Zhou, C., Yu, C.W. and Chaikam, V. (2008) HDA6 is required for jasmonate response, senescence and flowering in *Arabidopsis*. *J. Exp. Bot.* **59**, 225–234.
- Yamada, T., Mizuno, K.I., Hirota, K., Kon, N., Wahls, W.P., Hartsuiker, E., Murofushi, H., Shibata, T. and Ohta, K. (2004) Roles of histone acetylation and chromatin remodeling factor in a meiotic recombination hotspot. *EMBO J.* **23**, 1792–1803.
- Yang, X., Timofejeva, L., Ma, H. and Makaroff, C.A. (2006) The *Arabidopsis* SKP1 homolog ASK1 controls meiotic chromosome remodeling and release of chromatin from the nuclear membrane and nucleolus. *J. Cell Sci.* **119**, 3754–3763.
- Zickler, D. and Kleckner, N. (1998) The leptotene–zygotene transition of meiosis. *Annu. Rev. Genet.* **32**, 619–697.



## Functional biology in *Arabidopsis* to shed light on the molecular basis of $2n$ gametes

R. AIESE CIGLIANO, G. CREMONA, M.F. CONSIGLIO, C. CONICELLA

It has been estimated that 30%–80% of the angiosperms are polyploids, including important economic crops such as wheat, banana, cranberry, potato, and alfalfa<sup>1</sup>. Several works postulate that polyploids originated from unreduced ( $2n$ ) gametes through various meiotic nuclear restitution mechanisms, some of which were identified in potato<sup>2,3</sup>. The formation of  $2n$  gametes has a variable expressivity and is suggested to be a polygenic trait under the control of mutated major loci. The malfunction of such loci has different genetic consequences that can be equivalent to a First Division Restitution (FDR) or to a Second Division Restitution (SDR). FDR mechanisms lead to unreduced nuclei carrying non-sister chromatids, and, therefore, transmit a high level of heterozygosity to the progeny. On the contrary, SDR mechanisms lead to unreduced nuclei carrying sister chromatids and to a relatively high level of homozygosity in the progeny. Besides the role in polyploid plant evolution,  $2n$  gametes are a significant tool in the development of new breeding strategies. Indeed, the production of  $2n$  gametes has been used in potato and alfalfa to transmit useful traits from diploid wild relatives to tetraploid cultivated genotypes through crossing schemes based on sexual polyploidization.

While molecular and functional analysis of the genes disrupted in the mutants that produce  $2n$  gametes is a difficult task due to the polyploidy of the involved species, the diploid wild crucifer *Arabidopsis thaliana*, a model for higher plants, has been successfully used to identify genes involved in meiotic nuclear restitution resulting in  $2n$  gametes.

The purpose of this review is to describe two ma-

CNR-IGV, Research Institute of Plant Genetics, Research Division: Portici, Portici, Italy

ior genes involved in  $2n$  gamete formation in *Arabidopsis thaliana*. The isolation of these genes is a milestone since it will surely help in the identification of candidate genes for  $2n$  gamete production in other plant species.

### Parallel Spindles 1 (AtPS1)

The product of normal microsporogenesis is a tetrahedron of haploid microspores following to a single round of DNA replication and two meiotic divisions. In potato, Mok and Peloquin<sup>2</sup> (1975), describing the cytological mechanism underlying the  $2n$  pollen production via FDR, showed that two parallel spindles occurred at second meiotic division instead of normally oriented spindles at 60°. This event leading to the formation of two groups of chromosomes moving to opposite poles resulted in a dyad of  $2n$  microspores. Based on genetic analysis, the authors suggested a single recessive mutation in a gene termed *Parallel Spindles* (*PS*).

The genomic complexity of *Solanum* species delayed functional studies on *PS* gene though its importance for potato breeding. More than thirty years elapsed before d'Erfurth and colleagues<sup>4</sup> provided

the first molecular analysis of unreduced pollen formation via FDR in *Arabidopsis* lines mutated in the gene *AtPSI*. The authors identified *AtPSI* gene using a bioinformatic tool on the basis of a good correlation with the expression pattern of known meiotic genes. Cytological analysis of *AtPSI* mutants showed that besides regular metaphase II-anaphase II spindles, parallel, fused or tripolar spindles mostly occurred explaining the appearance of unreduced dyads (65%) and tryads. Moreover, the analysis of *AtPSI* mutants in different ecotypes clearly showed that *AtPSI* acts as a major gene being the frequency of diploid gametes influenced by the genomic background. The *AtPSI* protein has two domains, a regulatory phosphopeptide recognition domain named ForkHead Associated domain (PHA), and a PINc domain, which is found in proteins involved in RNA processing. The authors suggest that *AtPSI* may directly control the orientation of metaphase spindles or be related to meiotic cell cycle control.

#### Omission of second division (AtOSD)

The most common mechanism leading to  $2n$  eggs is the omission of the second meiotic division (os). In normal megasporogenesis, a linear array of four haploid megaspores is formed after the first and second divisions. When os is present there is no second division, and the homologous chromosomes just segregate and of the resulting two  $2n$  megaspores, one gives rise to the  $2n$  female gametophyte and the other degenerates. Omission of the second division is genetically equivalent to a SDR mechanism and is simply inherited as a Mendelian recessive trait<sup>3</sup>. It has been detected in a large number of *Solanum* species as well as in maize (*elongate* gene) but so far, analogously to *PS*, it is not cloned in a crop.

Using the same approach leading to the identification of *AtPSI*, d'Erfurth and colleagues<sup>5</sup> found in *Arabidopsis* the gene *Omission of Second Divi-*

*sion (OSD)*. *Atosd* mutants are fertile plants producing 100% and 85% of unreduced pollen and ovules, respectively. According to this observation, they found the progeny deriving from selfing to be tetraploid (4x) for the 84% and triploid (3x) for the 16% as a consequence of bilateral and unilateral sexual polyploidization. Cytological analysis showed a total absence of meiosis II leading to SDR  $2n$ -megaspores. OSD is a UVI4-like protein not containing conserved known functional domains. The authors suggest its involvement in regulation of the transition from meiosis I to meiosis II.

#### Conclusions

The elegant work presented by d'Erfurth and colleagues<sup>4,5</sup> shed new light on the possible structure and function of *PS* and *OS* genes opening a breach toward the isolation and functional analysis of these genes in potato as well as in other important crops. Moreover, the strategy d'Erfurth and colleagues highlights the validity of using *Arabidopsis thaliana* as a model organism for complex processes such as unreduced gamete production. This will make it possible to synthesize new meiotic variants in crops species with economic and social benefits.

#### References

1. Consiglio MP, Carputo D, Frusciante L, Monti L, Conicella C. Meiotic mutations and crop improvement. In: Janick J, editor. Plant Breeding Reviews, 28. New Jersey: John Wiley & Sons; 2007. p.163-214.
2. Mok DWS, Peloquin SJ. Three mechanisms of  $2n$  pollen formation in diploid potatoes. Can J Genet Cytol 1975; 17:217-25.
3. Werner JE, Peloquin SJ. Occurrence and mechanisms of  $2n$  egg formation in  $2n$  potato. Genome 1991; 34: 975-82.
4. d'Erfurth I, Jolinet S, Froger N, Gatrice O, Novatchkova M, Simon M et al. Mutations in *AtPSI* (*Arabidopsis thaliana* Parallel Spindle I) lead to the production of diploid pollen grains. PLoS Genet 2008; 4(11): e1000277.
5. d'Erfurth I, Jolinet S, Froger N, Gatrice O, Novatchkova M, Mercier R. Turning meiosis into mitosis. PLoS Biol 2009;7:e1000124.

## Epigenetic control of meiotic recombination

G. CREMONA, R. AIESE CIGLIANO, M. F. CONSIGLIO, C. CONICELLA

CNR-IGV, Research Institute of Plant Genetics,  
Research Division, Portici (NA), Italy

Meiosis is a specialized cell cycle, essential for the sexual reproduction of higher organisms. During meiosis, diploid committed cells give rise to haploid gametes through the halving of genome content determined by a single round of DNA replication followed by two successive divisions, reductional and equational. During the first division, which is unique to meiotic cells, homologous chromosomes segregate. A correct segregation requires the establishment of connections between homologs and this is mediated in most species by reciprocal recombination events known as crossing over (CO) initiated by programmed formation of double-strand breaks (DSBs). In addition, COs increase genome diversity by reshuffling alleles over generations, thereby improving the efficacy of natural selection.

In eukaryotic organisms, COs do not occur randomly along chromosomal DNA but rather are clustered in small regions of elevated recombination activity. These so-called "hotspots" are surrounded by regions that are essentially devoid of recombination. The factors that determine hotspot locations are poorly understood. However, some evidence is increasingly pointing out that hot spot location is influenced by local chromatin structure<sup>1</sup> and higher order chromosome structure.

Chromatin is made-up of histones and DNA, both of which may be modified to affect the way in which they interact. Histones are responsible for the coiling of DNA into nucleosome, the basic subunit of chromatin, and are composed of a globular domain and amino-terminal extensions known as histone tails which residues can be post-

translationally modified by methylation, acetylation, phosphorylation, ubiquitylation and sumoylation. These post-translational modifications alter chromatin structure by affecting the interactions of histones between adjacent nucleosomes or with DNA and/or by collectively establishing a code recognized by downstream effector proteins and complexes. Thus, histones modifications assist in the formation of either condensed heterochromatic states or open euchromatic states.

Purpose of this review is to describe the main histone modifications, acetylation and methylation, that so far were demonstrated to be associated with meiotic recombination.

### Histone acetylation and meiotic recombination

Histone acetylation was shown to be involved in meiotic recombination either by local analysis at hotspots in different organisms or by genome-wide analysis in *Saccharomyces cerevisiae*. Enrichment of histone acetylation occurs in recombinationally active regions such as chicken immunoglobulin locus, fission yeast *ade6-M26* (M26) locus, budding yeast

HIS4 locus, and mouse hotspot *Psb99*<sup>1</sup>. Deletion of a histone acetylase, *Spgcn5*, required for *ade6-M26* hotspot-specific hyperacetylation, led at this locus to a partial decrease in the DNA double-strand breaks (DSBs). Vice versa, loss-of-function of a histone deacetylase, *ScRpd3p*, increases *HIS4* hotspot activity. In *S. cerevisiae*, histone hyperacetylation changes the genomic distribution of meiosis-specific DSBs, elevating DSBs for 5% of yeast genes and reducing DSBs for 7% of the genes.

*Arabidopsis thaliana mcc1* (meiotic control of CO) mutant overexpressing a histone acetylase has revealed compelling evidence of a link between histone acetylation and meiotic recombination in plants, as well<sup>2</sup>. Hyperacetylation has a clear effect on COs although not univocal for all the chromosomes. Overall, elevated *MCC1* did not affect CO number per cell, but has a differential effect on individual chromosomes elevating COs for chromosome 4, in which there is also a shift in CO location, and reducing COs for chromosome 1 and 2. For the latter there is a loss of the obligate CO in 8% of the male meiocytes<sup>2</sup>.

### Histone methylation and meiotic recombination

The trimethylation of lysine 4 of histone H3 (H3K4me3) has been shown to define the location of initiation sites for COs in yeast and mouse<sup>1,3</sup>. Indeed, DSB formation at well characterized hotspots is strongly reduced in the absence of Set1, the only H3K4 methylase in yeast<sup>3</sup>. Rad6, which mediates methylation of H3K4 through ubiquitylation of the H2B lysine 123, is also required for full levels of meiotic DSBs.

In mouse, a high level of H3K4me3 was correlated with high recombination activity at two distinct hotspots. Mouse *Prdm9* gene has been shown to trimethylate H3K4 and to be expressed specifically in germ cells during meiotic prophase I. Several experiments indicate that *Prdm9* is a strong candidate as the *trans*-acting factor that controls hotspot acti-

vation in mice as well as the factor that specifically binds to the 13-bp consensus motif that is common to many human hotspots<sup>4</sup>. However, no equivalent consensus element has been identified for mouse hotspots. So far, new insights have been provided to explain the heterogeneous distribution of DSBs along the chromosomes although the evolution of recombination initiation sites seems to be different between organisms.

### Conclusions

Although incomplete, the understanding of the relationship between meiotic recombination and histone modifications is rapidly increasing in yeast and metazoans. Strong evidences converge on the histone methylation as mark that defines a substantial number of hotspots. In contrast, the role of histone modifications in meiotic recombination remains largely unexplored in plants. *Arabidopsis*, as model plant, and the collections of mutants affected in recombination process will surely help to fill this gap. As example, analysis of *dsy10* mutant, which blocks recombination as well as homologue pairing and synapsis, showed that histone H3 deacetylation and H3K4me2 are absent during the early prophase I when recombination occurs<sup>5</sup>.

### References

1. Buard J, Barthe's P, Grey C, de Massy B. Distinct histone modifications define initiation and repair of meiotic recombination in the mouse. *EMBO J* 2009;28:2616-24.
2. Porrella G, Consiglio MF, Akese-Gigliano R, Cremona G, Sanchez-Moran E, Barra L, *et al*. Histone hyperacetylation affects meiotic recombination and chromosome segregation in *Arabidopsis*. *Plant J* 2010; DOI: 10.1111/j.1365-3113.2010.04191.x.
3. Borde V, Robine N, Lin W, Bonfils S, Géli V, Nicolas A. Histone H3 lysine 4 trimethylation marks meiotic recombination initiation sites. *EMBO J* 2009;28:99-111.
4. Baudat F, Buard J, Grey C, Fledel-Alon A, Ober C, *et al*. PRDM9 is a major determinant of meiotic recombination hotspots in humans and mice. *Science* 2010;327:836-40.
5. Boateng KA, Yang X, Dong F, Owen HA, Makaroff CA. SWI1 is required for meiotic chromosome remodeling events. *Mol Plant* 2008;4:620-33.

RESEARCH ARTICLE

Open Access

# Evolution of *Parallel Spindles Like* genes in plants and highlight of unique domain architecture<sup>#</sup>

Riccardo Aiese Cigliano<sup>1</sup>, Walter Sanseverino<sup>2</sup>, Gaetana Cremona<sup>1</sup>, Federica M Consiglio<sup>1</sup> and Clara Conicella<sup>1\*</sup>

## Abstract

**Background:** Polyploidy has long been recognized as playing an important role in plant evolution. In flowering plants, the major route of polyploidization is suggested to be sexual through gametes with somatic chromosome number ( $2n$ ). *Parallel Spindle1* gene in *Arabidopsis thaliana* (*AtPS1*) was recently demonstrated to control spindle orientation in the 2nd division of meiosis and, when mutated, to induce  $2n$  pollen. Interestingly, *AtPS1* encodes a protein with a FHA domain and PINc domain putatively involved in RNA decay (i.e. Nonsense Mediated mRNA Decay). In potato,  $2n$  pollen depending on parallel spindles was described long time ago but the responsible gene has never been isolated. The knowledge derived from *AtPS1* as well as the availability of genome sequences makes it possible to isolate potato *PSLike* (*PSL*) and to highlight the evolution of *PSL* family in plants.

**Results:** Our work leading to the first characterization of *PSLs* in potato showed a greater *PSL* complexity in this species respect to *Arabidopsis thaliana*. Indeed, a genomic *PSL* locus and seven cDNAs affected by alternative splicing have been cloned. In addition, the occurrence of at least two other *PSL* loci in potato was suggested by the sequence comparison of alternatively spliced transcripts. Phylogenetic analysis on 20 *Viridaplantae* showed the wide distribution of *PSLs* throughout the species and the occurrence of multiple copies only in potato and soybean. The analysis of *PSL*<sup>FHA</sup> and *PSL*<sup>PINc</sup> domains evidenced that, in terms of secondary structure, a major degree of variability occurred in PINc domain respect to FHA. In terms of specific active sites, both domains showed diversification among plant species that could be related to a functional diversification among *PSL* genes. In addition, some specific active sites were strongly conserved among plants as supported by sequence alignment and by evidence of negative selection evaluated as difference between non-synonymous and synonymous mutations.

**Conclusions:** In this study, we highlight the existence of *PSLs* throughout *Viridaplantae*, from mosses to higher plants. We provide evidence that *PSLs* occur mostly as singleton in the analyzed genomes except in soybean and potato both characterized by a recent whole genome duplication event. In potato, we suggest the candidate *PSL* gene having a role in  $2n$  pollen that should be deeply investigated. We provide useful insight into evolutionary conservation of FHA and PINc domains throughout plant *PSLs* which suggest a fundamental role of these domains for *PSL* function.

## Background

Polyploidy represents the occurrence of more than two complete sets of chromosomes in an organism and has long been recognized as playing an especially important role in plant evolution [1]. In flowering plants, polyploidy extent has been largely underestimated in terms

of its commonality. Indeed, major recent advances in genomic analysis has revealed that almost all angiosperms have experienced at least one round of whole genome duplication during their evolution.

The wide spreading of polyploidy throughout the angiosperms can be related to their highly plastic genome structure, as inferred from their tolerance to changes in chromosome number, genome size and epigenome [2]. Although information with regard to the modes of polyploidization is limited, the major route of

\* Correspondence: conicell@unina.it

<sup>1</sup>CNR - National Research Council of Italy, Institute of Plant Genetics, Research Division Portici, Via Università 133, 80055 Portici, Italy  
Full list of author information is available at the end of the article

polyploidization seems to be sexual through the functioning of gametes with somatic chromosome number ( $2n$  gametes) [3]. Indeed, sexual polyploidization as compared to asexual would explain better the success of polyploid species in terms of higher fitness and more genetic flexibility. The control of  $2n$  gamete formation has been generally attributed to the action of single recessive genes. These genes exhibit incomplete penetrance and variable expression that is significantly influenced by genetic, environmental and developmental factors [4]. The molecular mechanisms leading to  $2n$  gametes have only recently begun to be uncovered [5,6]. In particular, d'Erfurth and colleagues [7] isolated and characterized *Parallel Spindle1* gene in *Arabidopsis thaliana* (*AtPS1*) that controls diploid pollen formation through spindle orientation in the second division of meiosis. The occurrence of parallel spindles at meiosis II is a frequently found mechanism for  $2n$  pollen formation that was described in potato many decades ago [8,9]. In potato, *ps* mutants have been used for breeding purposes in order to introgress beneficial traits from diploid ( $2n = 2x = 24$ ) relatives into cultivated strains [10]. However, the gene *ps* leading to  $2n$  pollen via parallel spindles was not isolated, so far.

Interestingly, *AtPS1* is a protein which contains temporarily a ForkHead Associated domain (FHA), and a C-terminal PiIT N-terminus domain (PINc). So far, the FHA domain has been found in more than 5600 different proteins from prokaryotes to higher eukaryotes involved in several processes including cell cycle control, DNA repair, protein degradation, transcription and pre-mRNA splicing [11]. FHA domain was shown to recognize phosphothreonine-containing epitopes [12]. PINc domain has been found in more than 3600 proteins in all life kingdoms. PINc domain has RNA nuclease activity [13]. In eukaryotes, PINc-containing proteins, such as human SMG6 and SMG5, were linked to Nonsense-Mediated mRNA Decay (NMD), that recognizes and rapidly degrades mRNAs containing Premature translation Termination Codons (PTCs).

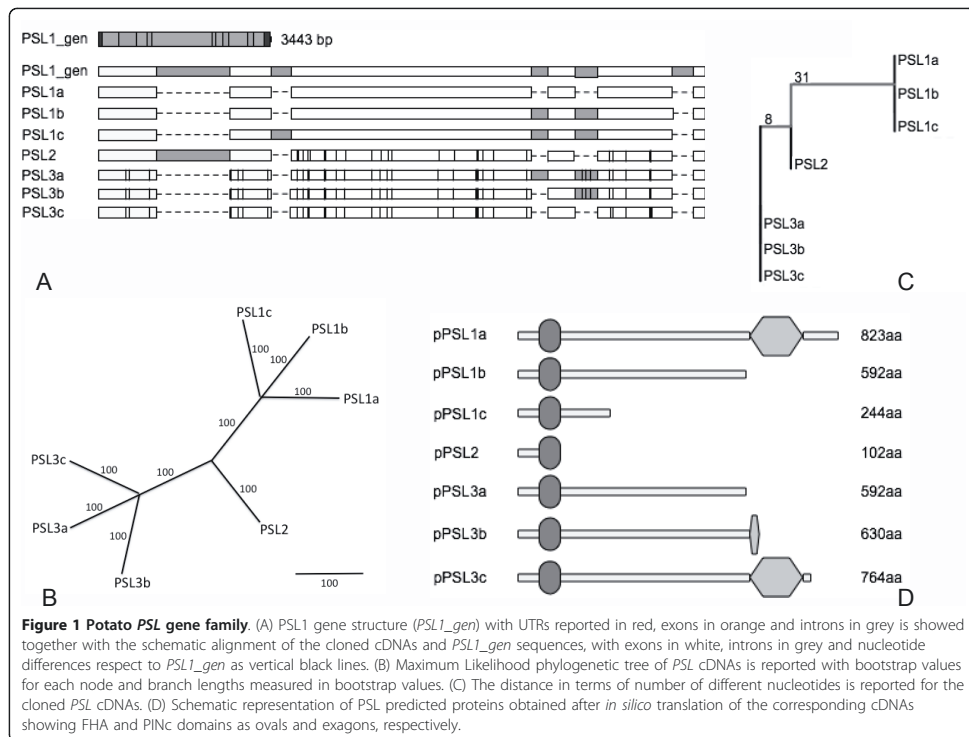
In this study, a sequence-homology-based strategy was carried out to isolate *PS* gene from a diploid potato. Through this approach, a genomic locus *PS-Like* (*PSL*) and seven cDNAs affected by alternative splicing have been cloned. The occurrence of at least two other *PSL* loci is suggested in potato. In order to shed light on the evolution and function of *PSL* genes in plants, a phylogenetic analysis of *PSL* genes was performed and FHA/PINc domains were compared. As far as we know, this is the first report about the isolation and characterization of *PSL* in a crop. We also demonstrate the conservation of this gene family throughout plants.

## Results

### Cloning and characterization of *PSL* genes in potato

Using the predicted protein sequence of *AtPS1*, two ESTs were identified on DFCI Potato Gene Index (<http://compbio.dfci.harvard.edu/tgi>) named TC194262 and DN590600 corresponding to FHA and PINc domains, respectively. The primers designed on the above mentioned ESTs allowed to isolate in diploid potato a 3 Kbp genomic clone (*PSL1*) lacking UTR regions. In order to complete genomic sequence of *PSL1*, by querying Potato Genome Sequencing Consortium Database (<http://www.potatogenome.net/index.php>) and SOL Genomic Network (<http://solgenomics.net>) we retrieved a 3 Kbp region of *S. phureja* v3 scaffold PGSC0003DMS000001829 (*phuPSL*) and a tomato BAC clone AC211085.1 (*SPSL1*) sharing 97% and 93% of sequence identity with *PSL1*, respectively. Primers designed on the tomato sequence were used to isolate a potato 5.3 Kbp *PSL1* genomic region spanning 2 Kbp upstream of the start codon to about 200 bp downstream of the stop codon [GenBank:HQ418834]. *In silico* gene prediction showed a structure of *PSL1* composed by six exons and five introns (Figure 1A) and a 2.4 Kbp hypothetical *PSL1* cDNA (*SPSL1\_pred*) with a GC content of 42% encoding a 92.5 kDa protein of 823 aminoacids (*pPSL1\_pred*).

Given the meiotic function of *AtPS1*, potato *PSL1* cDNA was isolated from pre-bolting buds. Seven different cDNAs ranging from 2.3 to 2.7 Kbp were isolated including *PSL1a* of 2.4 Kbp corresponding to *PSL1\_pred*. The sequence alignment between cDNAs and the genomic *PSL1* indicated the presence of different groups of related *PSL* sequences encoded by more than one locus (Figure 1A). In order to investigate the relationship between the different *PSL* cDNAs, we conducted a phylogenetic analysis that suggested the existence of three different loci named *PSL1*, *PSL2* and *PSL3* (Figure 1B). On the basis of sequence similarity, we assigned *PSL1a*, *PSL1b* and *PSL1c* cDNAs [GenBank:HQ418835, GenBank:HQ418836 and GenBank:HQ418837] to genomic *PSL1*, *PSL3a*, *PSL3b* and *PSL3c* cDNAs [GenBank:HQ418839, GenBank:HQ418840 and GenBank:HQ418841] to *PSL3* and the last cDNA to *PSL2* [GenBank:HQ418838]. Moreover, the distance measured as the number of different nucleotides among the seven cDNAs showed that *PSL2* was more similar to *PSL3* than to *PSL1* (Figure 1C). The nucleotide comparison between the predicted *phuPSL* cDNA and *PSL1a*, *PSL2* and *PSL3c* cDNAs showing a similarity of 98.5%, 99.1% and 99.6%, respectively, suggested that *phuPSL* locus corresponds to *PSL3* being the differences explained by the different genetic background.



Based on the sequences of cloned *PSL* cDNAs, *PSL1b* and *PSL1c*, *PSL3a* and *PSL3b* are alternative splicing forms of *PSL1* and *PSL3* since they retained complete or partial introns causing the formation of premature stop codons (PTCs) (Figure 1A). Moreover, the cloned *PSL2* cDNA showed a PTC caused by the retention of the second intron. As a consequence, all the predicted PSL proteins, except pPSL1a and pPSL3c, had truncated or lacking PINc domain (Figure 1D).

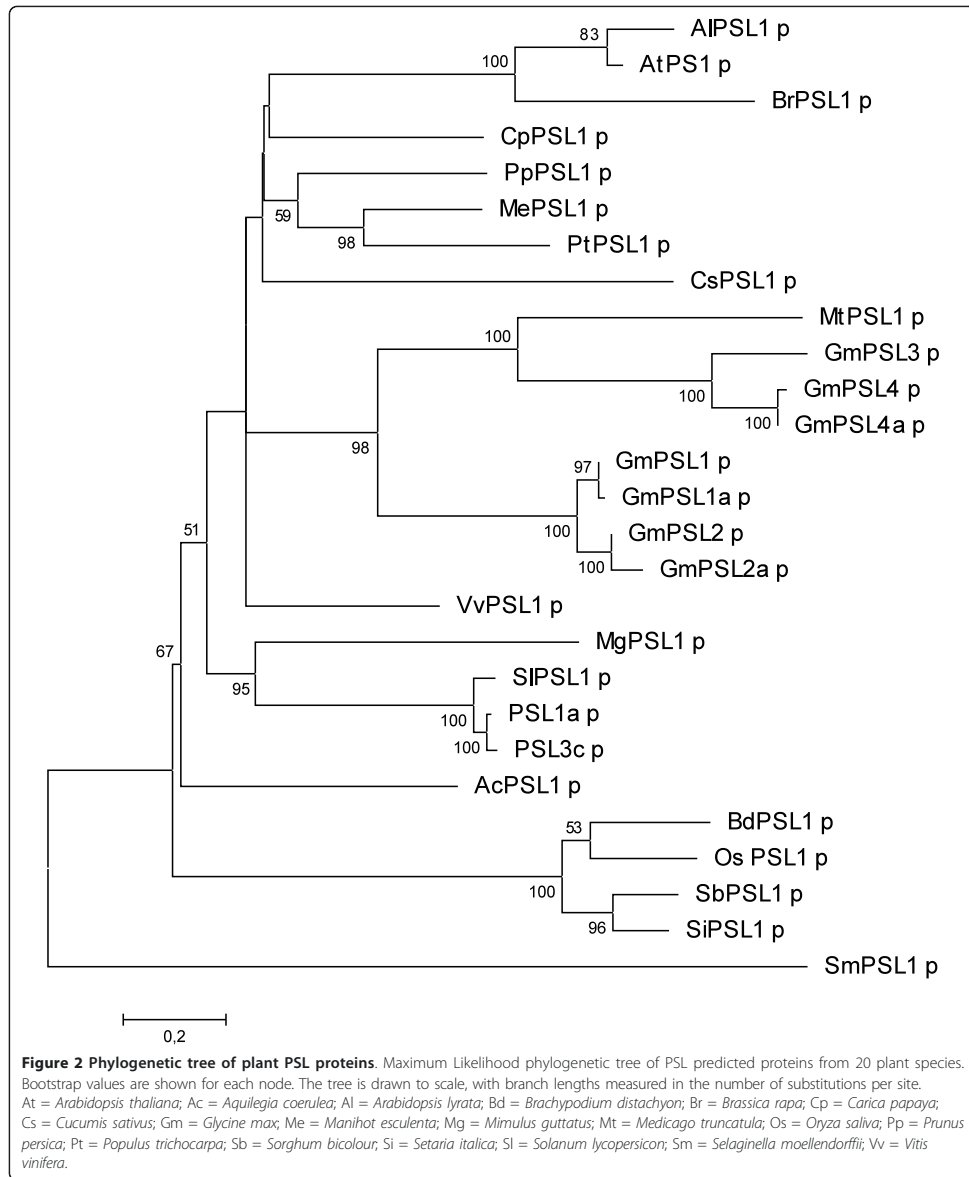
In order to evaluate whether the alternative splicing *PSL* variants were possible target of degradation through NMD we calculated the distance between PTCs and the successive exon-exon junction. Being this distance more than 50-55 nt according to Nagi and Maquat [14] we could consider *PSL1b*, *PSL1c*, *PSL2*, *PSL3a* and *PSL3b* as target of NMD.

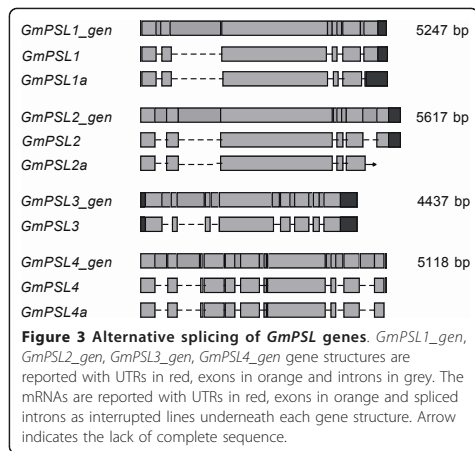
**Phylogenetic analysis of PSL genes in sequenced *Viridiaeplantae***

In order to investigate the evolution of *PSL* family, a phylogenetic analysis was performed by a search on

Interpro (<http://www.ebi.ac.uk/interpro>) for proteins with both FHA and PINc domains. Interestingly, these domains were contemporary present only in plants, except for the multidrug-efflux transporter NAEGR-DRAFT\_78193 from the amoeboid *Naegleria gruberi*.

*PSL1a* sequence was blasted against the Phytozome v6 database (<http://www.phytozome.net>) that contains the genomic sequences of 22 organisms and against the SOL Genomics Network containing the tomato genome assembly. Afterwards, 25 sequences of predicted PSL proteins were collected from 19 different organisms (Additional File 1), since *Physcomitrella patens*, *Ricinus communis*, *Volvox carteri*, *Zea mays* and *Chlamydomonas reinhardtii* seemingly lack *PSL* genes. The sequences were then aligned and the Maximum-Likelihood phylogenetic tree is shown in Figure 2. The distribution of PSLs is in agreement with the known phylogenetic relationships between species among dicots and monocots. Moreover, one *PSL* locus was found in the analyzed plant species, except for *Glycine max*. Indeed, four different *PSL* loci were identified in soybean and three of





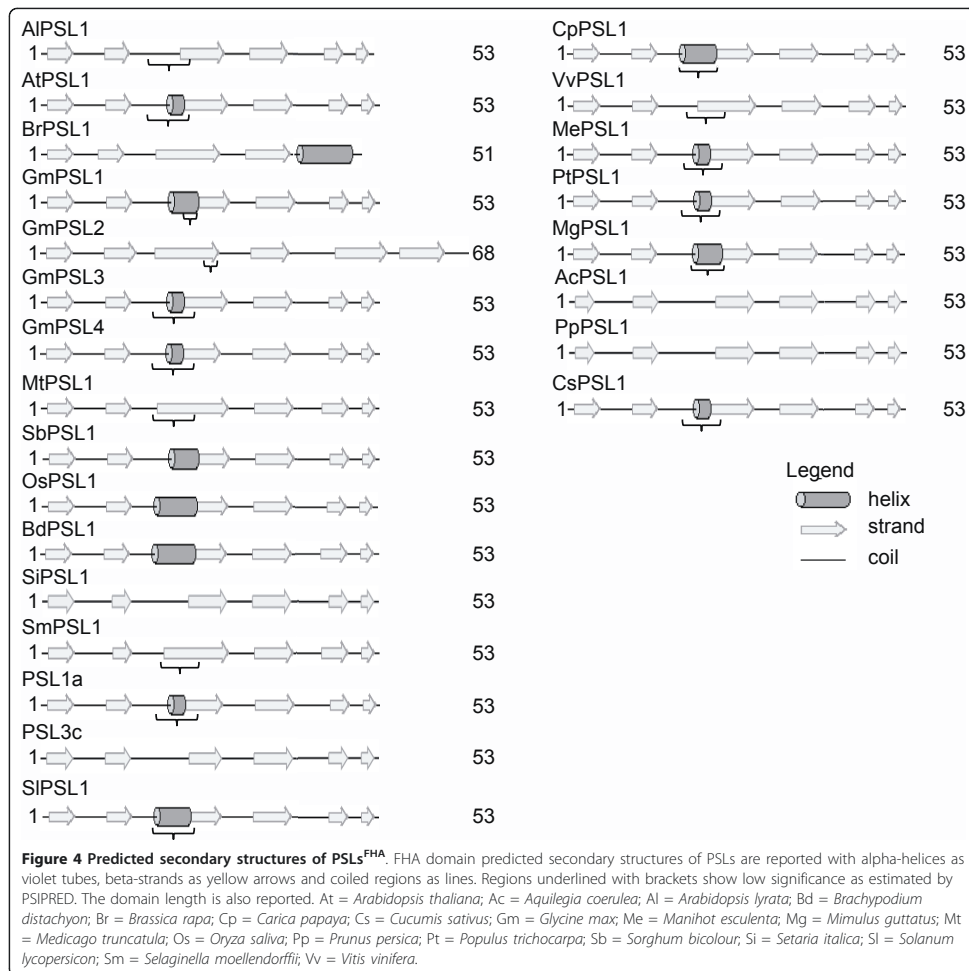
them encode alternative transcripts. Differently from potato, the alternative transcripts of soybean retain PINc domain being the splicing sites located at the 3'-end of mRNA (Figure 3).

#### Analysis of FHA and PINc secondary structure and active sites in PSL proteins

In order to assess the conservation degree of PSLs, we predicted and compared the secondary structure of FHA and PINc domains using the SMART (<http://smart.embl-heidelberg.de>) and PSIPRED (<http://bioinf.cs.ucl.ac.uk/psipred>) tools. It is reported that FHA domain is 80-100 aminoacid (aa) long folded into a 11-stranded beta sandwich, which sometimes contains small helical insertions between the loops connecting the strands. However, *in silico* analysis of FHA displays only 8 beta-strands (b-strands) out of 11 including the residues involved in phosphopeptide recognition and stabilisation of domain architecture [15]. Using the above mentioned tools on yeast RAD53p [NCBI:6325104], a well characterized FHA containing protein [12], the identified FHA region was 52 aa covering 6 beta-strands (data not shown). As shown in Figure 4, the length of the predicted FHA region in our dataset was 53 aa except for *Brassica rapa* (51 aa) and for *Glycine max* PSL2 (68 aa). While the majority of FHA domains showed 6 beta-strands, *Brassica rapa* FHA was predicted to be composed of 4 consecutive beta-strands followed by an alpha helical region. The group of monocots, *Brachypodium distachyon*, *Oryza sativa* and *Sorghum bicolor*, as well as dicot *Glycine max* (*GmPSL1*) showed a helical insertion between the [15]. Using the above mentioned tools on yeast RAD53p [NCBI:6325104], a well characterized FHA containing protein [12], the identified FHA region was 52 aa covering 6 beta-strands (data not shown). As shown in Figure 4, the length of the predicted FHA region in our dataset was 53 aa except for *Brassica rapa* (51 aa) and for *Glycine max* PSL2 (68 aa). While the majority of FHA domains showed 6 beta-strands, *Brassica rapa* FHA was predicted to be composed of 4 consecutive beta-strands followed by an alpha helical region. The group of monocots, *Brachypodium distachyon*, *Oryza sativa* and *Sorghum bicolor*, as well as dicot *Glycine max* (*GmPSL1*) showed a helical insertion between the

Afterward, we compared the active sites in yRAD53p with those present in PSL<sup>FHA</sup> domains through the protein alignment showed in Figure 5. It can be observed that glycine-5, arginine-6, serine-21 and histidine-24 in FHA domain are perfectly conserved. The arginine-19 seems to be absent in all plant sequences. In the analyzed species, asparagine-60 showed a substitution with histidine, characterized by a different polarity, except for soybean PSL4 glutamine-60 and *Brassica rapa* that seems to lack this site. Asparagine-66 is mostly substituted with the similar polar serine. Instead, AIPSL1, AtPSL1, GmPSL3 and GmPSL4 exhibited arginine-66 with different polarity while BrPSL1 glutamine-66 and MtPSL1 cysteine-66 both showing similar polarity of asparagine.

The analysis of PINc domain in our dataset started with the prediction of its secondary structure in human SMG6 (hSMG6) [UniProt:Q86U58]. It is reported that hSMG6<sup>PINc</sup> (hSMG6) is 182 aa folded into a 5-stranded parallel beta-sheets that is highly twisted and alpha-helices arranged on both sides of each beta-sheet for a total of 6. Three aspartate residues are essential for PINc activity in hSMG6, while a threonine or a serine in the sequence (T/S)XD might be involved in catalytic role on the basis of similarity with other PINc domains [16,17]. SMART predicted a PINc domain of 152 aa lacking the first and the last alpha-helices while PSIPRED predicted 4 beta-sheets and 4 alpha helices in hSMG6 (data not shown). In our dataset the PINc domain ranged from a minimum of 123 aa in *Cucumis sativus* to a maximum of 162 aa in *Brachypodium distachyon* (Figure 6). In our prediction, the number of beta-sheets ranged from 3 in GmPSL3 and CsPSL1 to 9 in CpPSL1. The number of predicted alpha-helices ranged from 3 in CsPSL1, OsPSL1 and PSL3c to 7 in BdPSL1 and CpPSL1. Afterward, we compared the active residues of PINc in PSL proteins. The alignment between PINc domain of PSL proteins and hSMG6 is shown in Figure 7 (refer to Additional file 2: Alignment of PSL<sup>PINc</sup> and hSMG6<sup>PINc</sup> residues to look at raw alignment). BrPSL1, SmPSL1 and PSL3c show the three expected aspartate residues at positions 6, 194 and 233 of the alignment. SiPSL1 and SbPSL1 have a substitution of two aspartate residues with asparagine-6, glutamate-194. When a substitution occurs, the aspartate-194 is mostly replaced with glutammate-194 except for CpPSL1 showing a different polarity residue (lysine-194) and MgPSL1 showing an alyphatic residue (alanine-194). The aspartate-233 is widely conserved except in BdPSL1, OsPSL1 and SiPSL1 where it is substituted with a serine-233. Most of the PSL proteins show a catalytic serine-231 in the described pattern SXD (where X can be D, N, E or S in this study) instead of threonine-231 in hSMG6, PtPSL1, SiPSL1, SmPSL1 and VvPSL1.



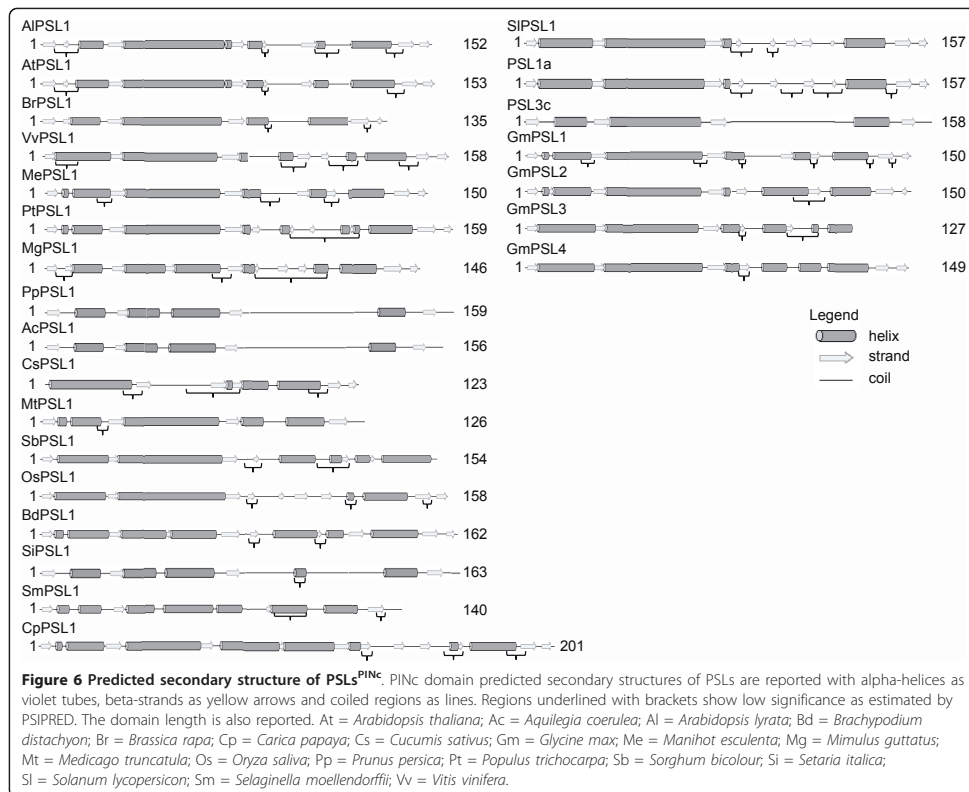
GmPSL3 and SbPSL1 are the only proteins lacking the C-terminal extremity of PINc interrupting at leucine-203 and lysine-227 respectively thus missing the catalytic threonine/serine-231 and the aspartate-233.

**Selective pressure among amino acid sites in the PSL family**

In order to test for presence of positive selection at individual amino acid codons, the site specific models implemented in DataMonkey 2010 webserver (<http://www.datamonkey.org>) [18] were used. The Integrative Selection Analysis of FEL, SLAC and FER algorithms

evidenced no significant positive selected sites ( $dN-dS > 0$ ). Conversely, 217 significant negative selected sites ( $dN-dS < 0$ ) were identified. The region between FHA to PINc domains included few negative selected sites which were mostly located near the functional domains. The codons encoding the highly conserved active sites glycine-5, arginine-6, serine-21 and histidine-24 in FHA and aspartate-6, serine/threonine-231 and aspartate-233 in PINc were also subjected to negative selection (Figure 8). These observations support the results obtained through sequence alignment and evidence an occurrence of negative pressure upon non-synonymous





mutations in *PSL* genes. In particular, the regions next to the functional domains and the codons for active sites were affected.

**Discussion**

In this work, we isolated *PSL* genes in a diploid potato ( $2n = 2x = 24$ ) and through *in silico* analysis we identified *PSL* in other plant species. The function of *PSL* in plants can be inferred from *Arabidopsis* study on *AtPSI* gene that appears responsible for the spindle orientation at meiosis II playing a regulatory function, likely via RNA decay [7].

In all the analysed species, except soybean and potato, *PSL* loci appear as singleton behaving as resistant to duplication. It is known that angiosperms are mostly paleopolyploids [19], many having survived multiple duplication events [20]. Analysis of genome sequences shows that some genes duplicate and persist as multiple copies after whole genome duplication (WGD) while

other genes are iteratively returned to singleton status. Moreover, it seems that the singleton status is consistently restored for some functional gene groups like those involved in DNA repair or signal transduction [21]. The evolutive history of potato and soybean could explain the expansion of *PSL* genes occurring in these species that have experienced recent WGD. In cultivated potato ( $2n = 4x = 48$ ), WGD is reported to have occurred about 10 million of years ago (*mya*) after the divergence from *Solanum lycopersicum* [22]. In soybean ( $2n = 2x = 40$ ), which seems to be an ancient allopolyploid on the basis of two different centromeric repeat classes [23], two rounds of WGD happened the latter aging 10-15 *mya* [24,25]. In addition, the location of the four soybean *PSLs* on different chromosomes reinforce their origin from WGD rather than tandem duplications.

The evident feature of *PSL* proteins is the contemporary presence of FHA and PINc domains. FHA is reported as a phosphothreonine (pT) binding domain

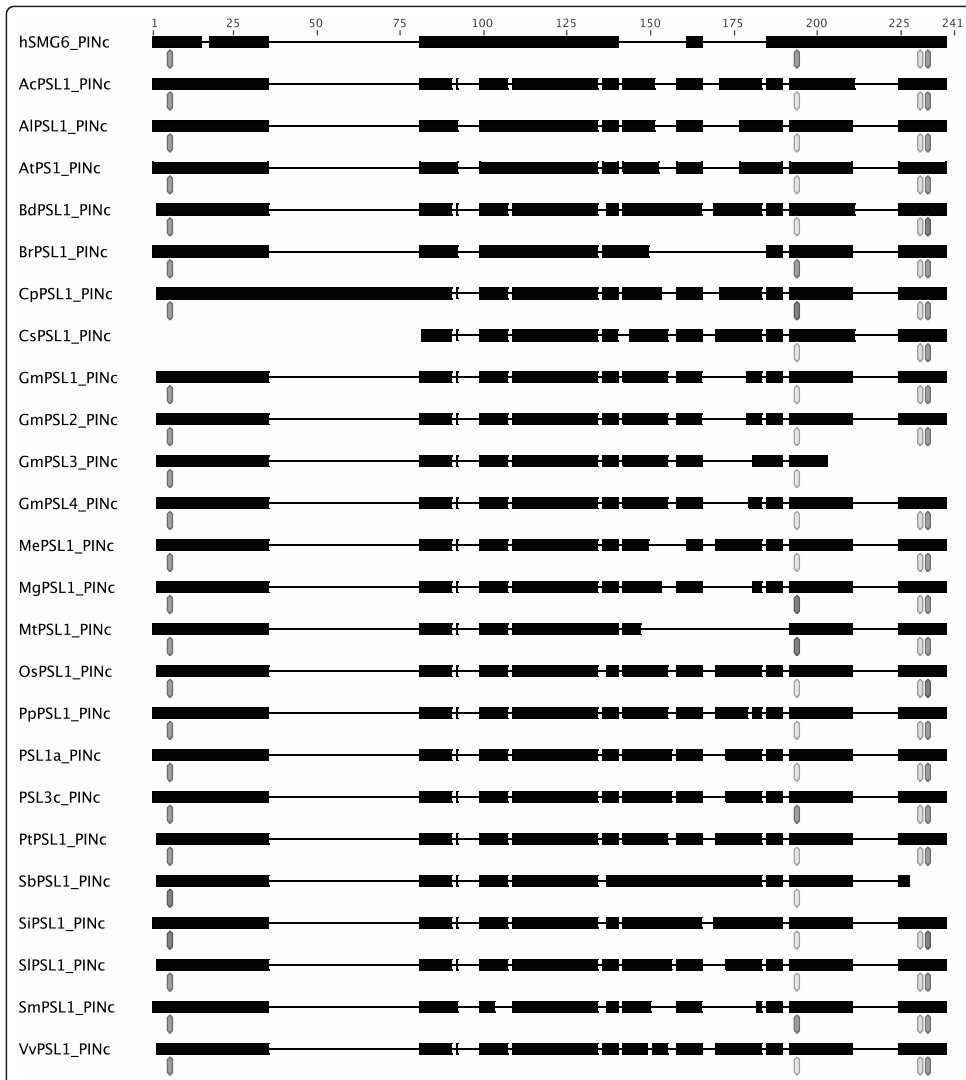
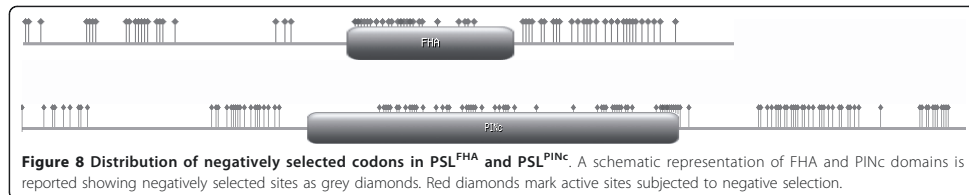


**Figure 7 Comparison of catalytic residues among PSLs<sup>PINC</sup> and hSMG6<sup>PINC</sup>.** A schematic protein domain alignment of PSLs<sup>PINC</sup> and hSMG6<sup>PINC</sup> is reported showing the conservation of catalytic residues. Black lines represent gaps in the alignment. Active sites are labeled with a green octagon when the residues are conserved among PSLs<sup>PINC</sup> and hSMG6<sup>PINC</sup>. A yellow or a red octagon mark an aminoacid substitution of same or different polarity, respectively. At = *Arabidopsis thaliana*; Ac = *Aquilegia coerulea*; Al = *Arabidopsis lyrata*; Bd = *Brachypodium distachyon*; Br = *Brassica rapa*; Cp = *Carica papaya*; Cs = *Cucumis sativus*; Gm = *Glycine max*; Me = *Manihot esculenta*; Mg = *Mimulus guttatus*; Mt = *Medicago truncatula*; Os = *Oryza saliva*; Pp = *Prunus persica*; Pt = *Populus trichocarpa*; Sb = *Sorghum bicolor*; Si = *Setaria italica*; Sl = *Solanum lycopersicon*; Sm = *Selaginella moellendorffii*; Vv = *Vitis vinifera*.



showing a 11 beta-sandwich secondary structure, also containing small helical insertions between the beta-strands [15]. The FHA active sites are usually located in the loops connecting b3/b4, b4/b5 and b6/b7 strands. RAD53p<sup>FHA</sup> arginine-70, serine-85 and asparagine-107 (corresponding to arginine-6, serine-21 and asparagine-60 in Figure 5) are involved in the interaction with the phosphopeptide backbone. Arginine-83 (corresponding to arginine-19 in Figure 5) is the most important aminoacid for FHA binding specificity. Indeed, its conversion to glycine shifts the binding from pTXXD to pTXXI peptides in RAD53p<sup>FHA</sup> interaction experiments using surface plasmon resonance [15]. Glycine-69 and histidine-88 (corresponding to glycine-5 and histidine-24 in Figure 5) stabilize the architecture of the binding site. The remaining conserved residue, asparagine-112 (corresponding to asparagine-65 in Figure 5), is remote from the peptide binding site and serves to tether the beta turn between b7/8 to b10 [12,15]. The comparison of predicted secondary structure in our dataset showed a wide conservation among plant species regarding the number and the position of the beta-sheets and the presence of an helical insertion between the second and the third beta-sheet as a characteristic feature of monocot PSL proteins. The comparison of active sites showed that two PSL<sup>FHA</sup> residues involved in pT binding as well those involved in stabilisation of the architecture of the binding site are fully conserved except for asparagine-65 that is replaced with a different polarity residue (arginine) in ALPSL1, AtPS1, GmPSL3 and GmPSL4 with unknown possible effect on domain architecture. Moreover, as compared to RAD53p<sup>FHA</sup>, a conserved substitution in plants is a histidine instead of asparagine-60, known to be important for the selectivity of binding of phosphothreonine upon phosphoserine. The different polarity between these two residues might suggest a functional diversification of this active site. However, the consequences of this substitution in PSL<sup>FHA</sup> domain in terms of ligand binding cannot be easily predicted and should be assessed by protein:protein interaction analysis. It is also intriguing the lack of arginine-19 in plants raising the question of binding selectivity for plant PSL<sup>FHA</sup>.

As regards PINc domain, we made reference to human SMG6<sup>PINc</sup> which has RNase activity and it is composed of alternating beta-sheets and alpha-helices. It is reported that hSMG6 is involved in NMD together with hSMG5 and hSMG7 [25]. In Arabidopsis, *AtSMG7* was proved to be involved in NMD and to be required for meiotic spindle organization in meiosis II [26]. As reported by Glavan and colleagues [17], hSMG6 and other PINc domains show three conserved aspartic residues at positions 1251, 1353 and 1392 (corresponding to aspartate-6, -194 and -233 in Additional File 2) involved in Mg<sup>2+</sup> binding. Threonine or serine embedded in the motif (T/S) XD is proposed to be the catalytic site on the basis of sequence alignment of PIN domains and it is located at residue-1390 (corresponding to threonine-231 in Figure 7) in hSMG6<sup>PINc</sup>.

Our results showed differences of secondary structures in PSL<sup>PINc</sup> domains even between phylogenetically close organisms. Moreover, the typical alternation between beta-sheets and alpha-helices does not seem to be respected. In spite of these differences, the active sites showed a wide conservation among plants. The aspartate-6 is conserved in all proteins except for SbPSL1 and SiPSL1 where an asparagine is present. This substitution maybe occurred after the divergence of BEP from PACCAD clades among *Poaceae* given its absence in *Oryza sativa*, *Brachypodium distachyon* and *Selaginella moellendorffii*. The residue-194 showed the major degree of variation among the species mostly characterized by glutamate instead of aspartate. This substitution is not related to phylogenesis, being glutamate present in both monocots and dicots while aspartate-194 is shared by the *Brassicaceae* BrPSL1, the *Selaginellaceae* SmPSL1 and the *Solanaceae* PSL3c. In *Carica papaya*, *Mimulus guttatus* and *Medicago truncatula* the change involved aminoacids with a different polarity such as lysine, alanine, and asparagine. The aspartate-233 is widely conserved among PSL proteins, except those of *Poaceae* OsPSL1, SiPSL1 and BdPSL1 showing a serine-233, likely a substitution occurred after the separation of monocots from dicots. GmPSL3 and SbPSL1 lack this residue due to PINc domain truncation at leucine-203 and lysine-227, respectively. As compared to hSMG6,

the majority of plants showed a serine instead of threonine-231 that is present only in PtPSL1, SiPSL1, SmPSL1 and VvPSL1. This substitution should not compromise the PINc activity since serine and threonine are the most represented residues at this position in PINc domains of different organisms [16]. Based on the evidence that the three aspartate residues of PINc domain are crucial for RNase activity, we can argue that PSLs lacking one of these residues or showing aminoacid with different polarity (BdPSL1, CpPSL1, CsPSL1, GmPSL3, MgPSL1, MtPSL1, SbPSL1, SiPSL1, OsPSL1) have no enzymatic activity. However, we cannot exclude that they are partners of other proteins retaining RNase activity. Indeed, in human, it is known that hSMG5 lacking two aspartate residues respect to hSMG6 has no enzymatic activity but the interaction between hSMG5 and hSMG7 led to a functional nuclease activity of SMG7-SMG5 complex [17].

Functional analysis of *Arabidopsis* *PS1* reinforced the evidence that the defects in meiotic spindle orientation in meiosis II led to the formation of diplopollen. Among the analysed species, *Manihot esculenta* ( $2n = 2x = 36$ ) was reported to produce  $2n$  pollen but the cytological mechanisms underlying its formation were not deeply investigated [27]. Since the predicted MePSL protein has FHA and PINc active sites similar to those of other species, it is likely that the mechanism leading to  $2n$  pollen in *Manihot esculenta* does not involve parallel spindles.

In the potato genotype analysed in this study, neither spindle defects nor  $2n$  pollen have been reported [28]. In this genotype, we identified three *PSL* loci and seven transcripts. Based on AtPS1 characterized by FHA and PINc domains we can suspect that PSL1a and PSL3c, carrying both domains, are functional proteins. In addition, it can be speculated that PSL1a that evidences the same PINc active residues of AtPS1 is the strongest candidate for the regulation of spindle orientation in meiosis II. The landscape of alternative splicing in potato *PSL* is not surprising since it has been already observed for genes involved in *Arabidopsis* meiosis. For instance, *AtSPO11-1*, involved in double strand breaks (DSBs) required for meiotic recombination, exhibits up to ten splicing forms showing PTCs [29]. As inferred for *AtSPO11-1*, *PSLs* are possible target of NMD that could act as a post-transcriptional regulatory pathway for the proper expression of *PSL*. Alternative splicing was observed also in *Glycine max* but the lack of PTCs exclude NMD regulation of *PSL* transcripts. Defining the ligands of FHA and PINc domains and proving *PSL* as a component in NMD are essential to link *PSLs* to plant evolution by polyploidization via  $2n$  gametes.

## Conclusions

In this study, we show that *PSLs* are common genes across *Virididaeplantae*. We provide evidence that *PSLs* occur mostly as singleton in the analyzed genomes except in soybean and potato both characterized by a recent event of whole genome duplication. We provide useful insight into evolutionary preservation of FHA and PINc domains throughout plant *PSL* genes, suggesting a fundamental role of these domains for *PSL* function. FHA appeared to be highly conserved, while PINc secondary structure and specific active sites showed a less conserved landscape, suggesting a functional diversification among *PSL* genes.

## Methods

### Plant material

A previously described [30] diploid clone of potato (named T710) coming from hybridization between *Solanum tuberosum* haploid USW3304 ( $2n = 2x = 24$ ) and *S. chacoense* ( $2n = 2x = 24$ ) has been used to isolate *PSL* genes.

### Potato *PSL* cloning and sequence analysis

Plant genomic DNA was isolated from leaves using the DNeasy Plant Mini Kit (QIAGEN <http://www1.qiagen.com>). Bacterial plasmid DNA was isolated using QIAprep Spin Miniprep Kit (QIAGEN). Total RNA from prebolting buds was extracted using the RNeasy Plant Mini Kit (QIAGEN) and then treated with DNase I (Invitrogen, <http://www.invitrogen.com>) to remove residual genomic DNA. Primer pairs for cloning designed with PRIMER3 (<http://frodo.wi.mit.edu/cgi-bin/primer3/primer3.cgi>) are listed in Additional file 3: Primers used in this study.

*PSL1* genomic fragment was amplified by PCR with primers PS\_F1 and PS\_R1 and full sequence with primers PS\_F2 and PS\_R2. The coding region of *PSL* transcripts was amplified by RT-PCR by using SuperScript<sup>TM</sup> III Reverse Transcriptase (Invitrogen) with an oligo-dT<sub>12-18</sub> (Invitrogen). The cDNA was subjected to PCR with PS\_CF and PS\_CR primers (Additional File 3). PCR products have been cloned into PCR2.1 with T/A Cloning kit (Invitrogen). Nucleotide sequencing was carried out by Eurofins MWG Operon sequencing service (Germany).

*PSL1* gene structure and cDNA predictions were carried out using FGENESH online tool (<http://linux1.softberry.com/berry.phtml?topic=fgenesh&group=programs&subgroup=gfind>) selecting Tomato as organism. *In silico* translation of cDNA sequences was carried out using the ExPasy Translation tool (<http://www.expasy.ch/tools/dna.html>).

### Identification of unannotated *PSL* genes

The *PSL* protein sequences were identified and collected by TBLASTN [31] search against the Phytozome v6 database (<http://www.phytozome.net/>), SGN (SOL Genomic Network, <http://sgn.cornell.edu/>) and Potato Genome Sequencing Consortium (PGSC, <http://potatogenomics.plantbiology.msu.edu/index.php?p=blast>).

### Molecular Phylogenetic analysis by Maximum Likelihood method

The *PSL* protein sequences were firstly aligned by MUSCLE [32] using the default settings of MEGA5 [33]. The best model for Maximum Likelihood phylogeny analysis was chosen testing all the available models in ProtTest version 2.4 [34] with slow optimization strategy and selecting the one with highest AICc value. The evolutionary history was then inferred by using the Maximum Likelihood method according to Jones *et al.* w/freq. model [35]. The bootstrap consensus tree was inferred from 100 replicates [36]. Initial tree(s) for the heuristic search were obtained automatically as following. When the number of common sites is <100 or less than one fourth of the total number of sites, the maximum parsimony method was used, otherwise BIONJ method with MCL distance matrix was used. A discrete Gamma distribution was used to model evolutionary rate differences among sites (4 categories, +G, parameter = 1.3900). The rate variation model allowed for some sites to be evolutionarily invariable ([+I], 9.0566% sites). All ambiguous positions were removed for each sequence pair. Evolutionary analyses were conducted in MEGA5.

### PSL domain analysis

The locations of FHA and PINc domains within *PSL* genes were detected using SMART [37]. Secondary structure prediction was performed using domains from *PSL* sequences as input into the PSIPRED secondary structure prediction server [38]. The program MUSCLE [32] was used to do multiple sequence alignments of FHA and PINc domains in *PSL* proteins, yRAD53p [NCBI:6325104] and hSMG6 [UniProt: Q86US8]. Conservation of phosphothreonine-binding residues in FHA and of RNase activity residues in PINc were determined by alignment with yRAD53p and hSMG6, respectively.

### Comparison of dN-dS values between *PSL* sequences

The coding sequences of *PSL*s were obtained from the databases reported in Additional File 1. The terminal codon was manually removed, then the codon alignment was performed by MUSCLE [32] using the default

settings of MEGA5 [33] (Tamura *et al.*, personal communication). To select the best substitution model we used JmodelTest 0.1.1 [39,40] with default settings. The GTR [41] model was selected as the best fitting as evidenced by AICc values.

The codon alignment was then uploaded on Data-Monkey 2010 server [18,42] and dN-dS evaluated using GTR as substitution model, and SLAC (default settings except for Global dN/dS value = estimated with CI), FEL and REL [43] algorithms. Codons subjected to evolutionary pressure were identified with Integrative Selection Analysis selecting significance levels for SLAC  $p < 0.1$ , FEL  $p < 0.1$  and REL Bayes Factor  $< 50$ . Only codons with a significant dN-dS value according to all the three methods were reported.

### Note

#Contribution n 358 from CNR - National Research Council of Italy, Institute of Plant Genetics, Research Division Portici.

### Additional material

**Additional file 1: *PSL* sequences used in this study.** Description of sequence names, accession numbers, organisms and source databases used in this study.

**Additional file 2: Alignment of *PSL*<sup>PINc</sup> and *hSMG6*<sup>PINc</sup> residues.** The protein domain alignment of *PSL*<sup>PINc</sup> and *hSMG6*<sup>PINc</sup> is reported showing the conservation of catalytic residues. Dotted lines represent gaps in the alignment. Active sites are labeled with a green octagon when the residues are conserved among *PSL*<sup>PINc</sup> and *hSMG6*<sup>PINc</sup>. A yellow or a red octagon mark an aminoacid substitution of same or different polarity, respectively.

**Additional file 3: Primers used in this study.** Primers used for the isolation of *PSL* genomic clone and cDNAs

### Acknowledgements

We wish to thank Ms. Rosa Paparo for helpful technical assistance, Prof. Domenico Carputo and Dr. Raphael Mercier for useful comments on the manuscript. This work was partially funded by Galileo Grant from University Italy-France.

### Author details

<sup>1</sup>CNR - National Research Council of Italy, Institute of Plant Genetics, Research Division Portici, Via Università 133, 80055 Portici, Italy. <sup>2</sup>DISSPAPA, Dept. of Soil, Plant and Environmental Sciences, University of Naples "Federico II", Via Università 100, 80055 Portici, Italy.

### Authors' contributions

RAC performed the molecular research and the protein domain analysis, participated in phylogenetic analysis, study design and drafted the manuscript. WS carried out the phylogenetic analysis and participated in bioinformatic analysis design. GC participated in molecular analysis. FMC performed the molecular analysis design and revised the manuscript. CC conceived of and coordinated the study, and revised the manuscript. All authors read and approved the final manuscript.

Received: 26 November 2010 Accepted: 24 March 2011  
Published: 24 March 2011

## References

1. Tate JA, Soltis DE, Soltis PS: **Polyploidy in Plants**. In *The Evolution of the Genome*. Edited by: Gregory T. Elsevier Inc; 2005:371-414.
2. Leitch AR, Leitch IJ: **Genomic plasticity and the diversity of polyploid plants**. *Science* 2008, **320**:481-483.
3. Bretagnolle F, Thompson J: **Tansley Review No-78 - Gametes with the somatic chromosome-number - mechanisms of their formation and role in the evolution of autopolyploid plants**. *New Phytol* 1995, **129**(1):1-22.
4. Consiglio F, Carputo D, Frusciante L, Monti LM, Conicella C: **Meiotic mutations and crop improvement**. In *Plant Breeding reviews*. Volume 28. Edited by: Janick J. Purdue University, John Wiley; 2007:163-203.
5. Mercier R, Vezon D, Bullier E, Motamayor J, Sellier A, Lefeuvre F, Pelletier G, Horlow C: **SWITCH1 (SW1): a novel protein required for the establishment of sister chromatid cohesion and for bivalent formation at meiosis**. *Gene Dev* 2001, **15**(14):1859-1871.
6. Ravi M, Marimuthu MPA, Siddiqi I: **Gamete formation without meiosis in Arabidopsis**. *Nature* 2008, **451**:1121-1124.
7. d'Erfurth I, Jolivet S, Froger N, Catrice O, Novatchkova M, Simon M, Jenczewski E, Mercier R: **Mutations in APT51 (Arabidopsis thaliana parallel spindle 1) lead to the production of diploid pollen grains**. *PLoS Genet* 2008, **4**:e1000274.
8. Fukuda Y: **Cytological studies on the development of pollen grains in different races of solanum**. *Bot Mag Tokyo* 1927, **41**:459-474.
9. Mok D, Peloquin J: **The inheritance of three mechanisms of diplandroid (2n pollen) formation in diploid potatoes**. *Heredity* 1975, **35**:1-8.
10. Peloquin SJ, Boiteux LS, Carputo D: **Meiotic mutants in potato. Valuable variants**. *Genetics* 1999, **153**:1493-1499.
11. Li J, Lee GI, Van Doren SR, Walker JC: **The FHA domain mediates phosphoprotein interactions**. *J Cell Sci* 2000, **113**:4143-4149.
12. Durocher D, Jackson SP: **The FHA domain**. *FEBS Lett* 2002, **513**:58-66.
13. Lareau LF, Brooks AN, Soergel DAW, Meng Q, Brenner SE: **The coupling of alternative splicing and nonsense-mediated mRNA decay**. *Adv Exp Med Biol* 2007, **623**:190-211.
14. Nagy E, Maquat LE: **A rule for termination-codon position within intron-containing genes: when nonsense affects RNA abundance**. *Trends Biochem Sci* 1998, **23**(6):198-199.
15. Durocher D, Taylor IA, Sarbassova D, Haire LF, Westcott SL, Jackson SP, Smerdon SJ, Yaffe MB: **The molecular basis of FHA domain: phosphopeptide binding specificity and implications for phospho-dependent signaling mechanisms**. *Mol Cell* 2000, **6**(5):1169-1182.
16. Arcus VL, Bäckbro K, Roos A, Daniel EL, Baker EN: **Distant structural homology leads to the functional characterization of an archaeal PIN domain as an exonuclease**. *J Biol Chem* 2004, **279**(16):16471-16478.
17. Glavan F, Behm-Ansmant I, Izaurralde E, Conti E: **Structures of the PIN domains of SMG6 and SMG5 reveal a nuclease within the mRNA surveillance complex**. *The EMBO Journal* 2006, **25**(21):5117-5125.
18. Pond SLK, Frost SDW: **Datamonkey: rapid detection of selective pressure on individual sites of codon alignments**. *Bioinformatics* 2005, **21**(10):2531-2533.
19. Bowers JE, Chapman BA, Rong J, Paterson AH: **Unravelling angiosperm genome evolution by phylogenetic analysis of chromosomal duplication events**. *Nature* 2003, **422**(6930):433-438.
20. Paterson AH, Bowers JE, Chapman BA: **Ancient polyploidization predating divergence of the cereals, and its consequences for comparative genomics**. *Proc Natl Acad Sci USA* 2004, **101**(26):9903-9908.
21. Doyle JJ, Flagel LE, Paterson AH, Rapp RA, Soltis DE, Soltis PS, Wendel JF: **Evolutionary genetics of genome merger and doubling in plants**. *Annu Rev Genet* 2008, **42**:443-461.
22. Fawcett JA, Maere S, Van de Peer Y: **Plants with double genomes might have had a better chance to survive the Cretaceous-Tertiary extinction event**. *Proc Natl Acad Sci USA* 2009, **106**(14):5737-5742.
23. Gill N, Findley S, Walling JG, Hans C, Ma J, Doyle J, Stacey G, Jackson SA: **Molecular and chromosomal evidence for allopolyploidy in soybean**. *Plant Physiol* 2009, **151**(3):1167-1174.
24. Shoemaker RC, Schlueter J, Doyle JJ: **Paleopolyploidy and gene duplication in soybean and other legumes**. *Curr Opin Plant Biol* 2006, **9**(2):104-109.
25. Chang Y-F, Imam JS, Wilkinson MF: **The nonsense-mediated decay RNA surveillance pathway**. *Annu Rev Biochem* 2007, **76**:51-74.
26. Riehs N, Akimcheva S, Puizina J, Bulankova P, Idol RA, Siroky J, Schleiffer A, Schweizer D, Shippen DE, Riha K: **Arabidopsis SMG7 protein is required for exit from meiosis**. *J Cell Sci* 2008, **121**:2208-2216.
27. Ogburia M, Yabuya T, Adachi T: **A cytogenetic study of bilateral sexual polyploidization in cassava (*Manihot esculenta* Crantz)**. *Plant Breeding* 2002, **121**:278-280.
28. Conicella C, Barone A, Giudice A, Frusciante L, Monti LM: **Cytological evidences of SDR-FDR mixture in the formation of 2n eggs in a potato diploid clone**. *Theor Appl Genet* 1991, **81**(1):59-63.
29. Hartung F, Puchta H: **Molecular characterisation of two paralogous SPO11 homologues in Arabidopsis thaliana**. *Nucleic Acids Res* 2000, **28**(7):1548-1554.
30. Barone C, Frusciante L: **Selection of potato diploid hybrids for 2n gamete production**. *Journal of Genetics and Breeding* 1993, **47**:313-318.
31. Altschul SF, Lipman DJ: **Protein database searches for multiple alignments**. *Proc Natl Acad Sci USA* 1990, **87**(14):5509-5513.
32. Edgar RC: **MUSCLE: multiple sequence alignment with high accuracy and high throughput**. *NAR* 2004, **32**(5):1792-1797.
33. Tamura K, Dudley J, Nei M, Kumar S: **MEGA4: Molecular Evolutionary Genetics Analysis (MEGA) software version 4.0**. *Mol Biol Evol* 2007, **24**:1596-1599.
34. Abascal F, Zardoya R, Posada D: **ProtTest: Selection of best-fit models of protein evolution**. *Bioinformatics* 2005, **21**:2104-2105.
35. Jones DT, Taylor WR, Thornton JM: **The rapid generation of mutation data matrices from protein sequences**. *Comput Appl Biosci* 1992, **8**(3):275-282.
36. Felsenstein J: **Confidence limits on phylogenies: An approach using the bootstrap**. *Evolution* 1985, **39**:783-791.
37. Schultz J, Milpetz F, Bork P, Ponting CP: **SMART, a simple modular architecture research tool: identification of signaling domains**. *Proc Natl Acad Sci USA* 1998, **95**(11):5857-5864.
38. McGuffin LJ, Bryson K, Jones DT: **The PSIPRED protein structure prediction server**. *Bioinformatics* 2000, **16**(4):404-405.
39. Posada D: **jModelTest: Phylogenetic Model Averaging**. *Mol Biol Evol*.
40. Guindon S, Gascuel O: **A simple, fast and accurate method to estimate large phylogenies by maximum-likelihood**. *Syst Biol* 2003, **52**:696-704.
41. Tavaré S: **Some Probabilistic and Statistical Problems in the Analysis of DNA Sequences**. In *Lectures on Mathematics in the Life Sciences* Edited by: AMS 1986, **17**:57-86.
42. Pond SLK, Muse SV: **HyPhy: hypothesis testing using phylogenies**. *Bioinformatics* 2005, **21**(5):676-679.
43. Pond SLK, Frost SDW: **Not So Different After All: A Comparison of Methods for Detecting Amino Acid Sites Under Selection**. *Mol Biol Evol* 2005, **22**(5):1208-1222.

doi:10.1186/1471-2148-11-78

Cite this article as: Cigliano et al.: Evolution of Parallel Spindles Like genes in plants and highlight of unique domain architecture<sup>®</sup>. *BMC Evolutionary Biology* 2011 **11**:78.

Submit your next manuscript to BioMed Central and take full advantage of:

- Convenient online submission
- Thorough peer review
- No space constraints or color figure charges
- Immediate publication on acceptance
- Inclusion in PubMed, CAS, Scopus and Google Scholar
- Research which is freely available for redistribution

Submit your manuscript at  
www.biomedcentral.com/submit





# Insight into a meiotic role of the major histone H3 lysine 4 methyltransferase in *Arabidopsis*

R. AIESE CIGLIANO, G. CREMONA, M. F. CONSIGLIO, C. CONICELLA

## Introduction

Research Division, CNR-IGV, Research Institute of Plant Genetics, Portici, Naples, Italy

The life cycle in plants with sexual reproduction is characterized by the alternance of diploid ( $2n$ ) and haploid ( $n$ ) state occurring by the halving and restoration of the chromosome number. In this process, meiosis is crucial and leads to the formation of spores and subsequently of haploid gametophytes. Homologous recombination, one of the key features of meiosis, ensures chromosome segregation and allows the formation of new gene combinations. Given its importance, meiosis is a tightly regulated process which requires a perfect timing of gene expression, chromatin remodeling and chromosome dynamics.

Chromatin is a DNA-protein complex that can be dynamically modified to respond to internal and external stimuli. The complex interaction between DNA and histones gives rise to the main unit of chromatin, the nucleosome, whose positioning and distribution affect several DNA-based-processes such as transcription, replication and repair. A key factor for the regulation of such molecular processes is the post-translational modification of histones. Indeed, histones can be modified by an array of epigenetic marks such as acetylation, methylation, ubiquitination. Lysine methylation is one of the most studied histone modifications in several organisms. Each lysine residue can be mono-, di- and trimethylated (me1, me2 and me3) with different biological effects depending on the ability of DNA-binding proteins to selectively recognize each of them. Histone methylation at lysine 4 (H3K4) and lysine 36 (H3K36) are commonly recognized as marks able to activate transcription and to in-

duce an "open-state" of chromatin. On the contrary, methylation at lysine 9 (H3K9) and lysine 27 (H3K27) play important roles in transcription suppression and heterochromatin formation. In particular, a remarkable importance of H3K4me3 has been recognized since this mark defines the sites for the formation of DNA Double Strand Breaks which are the first step of meiotic recombination in yeast and mouse.

*Arabidopsis* genome encodes at least 40 histone methyltransferases (HMTs) and only few of them have been extensively studied ([www.arabidopsis.org](http://www.arabidopsis.org)). H3K4 methylation was linked to flowering time, cell wall regulation, response to abiotic stresses and reproduction. Recently, Guo and colleagues<sup>1</sup> and Berr and colleagues<sup>2</sup> reported SDG2 as the major histone H3K4 methyltransferase in *Arabidopsis*. Indeed, *sdg2* lines show pleiotropic defects both at sporophytic and gametophytic level influencing plant size, flowering time, cell cycle and the development of pollen, ovule and embryo. Among the reproductive anomalies affecting *sdg2-1* mutant, Berr and colleagues<sup>2</sup> reported a complete female sterility and the formation of triads, dyads and monads at the end of male meiosis. Moreover, the authors observed irregular positioning of both sperm nuclei and vegetative nucleus in mature pollen. Berr and colleagues<sup>2</sup> by performing Agilent microarray on premeiotic buds found a relationship between the gametophytic defects and the

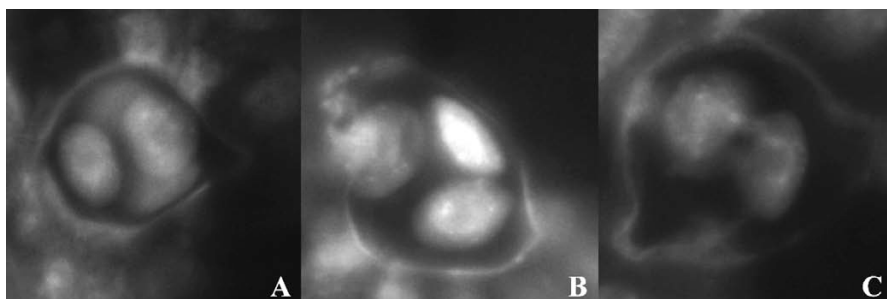


Figure 1.—Meiotic products of *Arabidopsis* wild-type (A) and *Atmcc1* mutant (B-C): a tetrad (A), a triad (B) and a dyad (C). All the photographs were taken with a fluorescence microscope with a magnification of 1000x after DAPI staining.

misregulation of known gametophytic genes (i.e. *BT*, *SPL/NZZ*). However, no hypothesis was made about the causes of meiotic product defects. A further analysis of the microarray data from Berr and colleagues<sup>2</sup> was performed in this study in order to get new insights into SDG2 activity and to identify the effectors of the meiotic defects observed in *sdg2* mutant lines.

### Materials and methods

#### Data Analysis

Microarray datasets (GSE18513) based on Agilent array were downloaded as \*.txt files from NCBI GEO (<http://www.ncbi.nlm.nih.gov/geo/>). GeneSpringGX ([www.agilent.com](http://www.agilent.com)) was used for quantile normalization of the expression values. The normalized expression values file was analysed with MEV<sup>3</sup>. T-test was performed between wt and *sdg2-1* setting wt and *sdg2-1* duplicates as “group 1” and “group 2”, respectively. Only genes resulted differentially expressed with a p-value < 0.05 were considered.

### Results and Discussion

In order to evidence whether a transcriptional effect of *sdg2* mutation was related to the defects observed at the end of male meiosis, we performed an analysis of the Agilent microarray data produced by

Berr and colleagues<sup>2</sup>. Our analysis showed 1331 up-regulated and 1104 down-regulated genes in *sdg2* flower buds corresponding to 8.4% of the genes spotted on Agilent’s Whole Arabidopsis Gene Expression Microarray (G2519F, V4, 4x44K). Berr and colleagues<sup>2</sup> found 452 down-regulated and 273 up-regulated genes. The discrepancy with our results can be explained by the different parameters used for the statistical analyses.

Our analysis showed the misregulation of genes known to have a meiotic function in *Arabidopsis*. Indeed, *ATMCC1* was up-regulated while *TES* appeared down-regulated. *ATMCC1* encodes a GCN5-like histone acetyltransferase and when overexpressed leads to defects both at sporophytic and gametophytic level. Female and male partial sterility, crossover failure and chromosome segregation defects were reported in *Atmcc1* mutant<sup>4</sup>. As showed in Figure 1, triads, dyads and monads were observed at the end of male meiosis in *Atmcc1* microsporocytes<sup>4</sup> as well as in *sdg2-1* mutant<sup>2</sup>. Seemingly, histone methylation and acetylation cooperate to ensure the regular formation of the meiotic products.

Mutations in *TES* were described by Spielman and colleagues<sup>5</sup> which showed its involvement in male meiotic cytokinesis, leading to the formation of coenocytic tetrads and of a variable number of generative and vegetative nuclei inside pollen grains. Berr and colleagues<sup>2</sup> reported that cytokinesis was not affected in *sdg2* meiocytes since apparently normal walls occurred among the microspores inside tetrads. Moreover, the altered position of generative and vegetative

**Looking for meiotic genes by cell-specific profiling in *Arabidopsis***

*Riccardo Aiese Cigliano, Federica Consiglio, Lucia Barra, Gaetana Cremona, Clara Conicella  
CNR-Institute of Plant Genetics*

Meiosis is a modified cell division program essential to all the sexually-reproducing eukaryotes. In plants, understanding and manipulation of the meiotic process could have important implications for plant breeding. So far, more than 50 genes have been identified in *Arabidopsis thaliana* through the mutagenized populations and homologues of meiotic genes identified in other model organisms such as *Drosophila*, *C. elegans*, yeast and mouse. Combination of the single cell technology and gene expression analysis through Laser Microdissection Microarray (LMM) could be an innovative approach to find new genes involved in plant meiosis. Given the tight regulation of meiotic genes and the proven role of histone acetylation for transcription during meiosis, our aim is to find genes differentially expressed during meiosis in response to a perturbation of histone acetylation. Transcripts of microsporocytes were analysed by LMM in *meiotic chromosome condensation 1* (*mcc1*) *Arabidopsis* mutant with hyperacetylated histones. About 150 differentially expressed genes were found in *mcc1* meiocytes in comparison to the wild type. Functional clusters, proved to be involved in meiosis in other organisms, were identified by using "DAVID tool" (<http://david.abcc.ncifcrf.gov>). One gene cluster is related to the ubiquitin-proteasome system (UPS) including subunits of proteasome 26S, of SKP1-Cullin-F-box (SCF) complex and a deubiquitinating enzyme. Among these genes there is ASK1, a member of SCF complex, previously described in *Arabidopsis* as essential for meiotic early nuclear reorganization events. Another interesting gene cluster is related to cell cycle genes including cyclins and Cell-Division-Cycle. We are focusing on a subset of 20 genes related to UPS and cell cycle, and including unknown genes, as well. Twenty-five putative knock-out lines for these genes obtained from public *Arabidopsis* Stock Centers are being screened for semisterile phenotype possibly associated to meiotic defects.

Presented by: **Aiese Cigliano, Riccardo**

## **Study of meiotic mutations for crop improvement**

Riccardo Aiese Cigliano

CNR-Institute of Plant Genetics, UOS Portici

Understanding and manipulating the meiotic process in plants could have its major impact on plant breeding. To give an example, the incorporation of beneficial traits into a crop rely on the ability of the chromosomes from the crop and the species carrying the desired trait to undergo meiotic recombination.

The first aim of our research is to find new genes involved in meiosis in the model organism *Arabidopsis thaliana*. Using the innovative approach of Laser Microdissection Microarray (LMM) on meiocytes we identified 150 loci differentially regulated in a semisterile mutant over-expressing a histone acetylase. Among the 150 loci we selected 16 genes involved in different biological processes as the ubiquitin-proteasome system or the cell cycle. Recently, evidence from works on plants and other model organisms indicates that these genes are important in the meiotic process. We are performing a screening for fertility on mutant lines carrying a T-DNA insertion in the selected genes.

Our second aim is to identify the *PARALLEL SPINDLES (PS)* gene in potato. This gene determines the production of unreduced pollen grains by a First Division Restitution (FDR) mechanism having as genetic consequences maximization of heterozygosity and sexual polyploidization. We designed primers on potato EST sequences showing high sequence identity with *AtPSI* gene previously identified in *Arabidopsis thaliana*. These primers will be used to clone the genomic and the cDNA sequences of *PS* gene from flower buds of a diploid potato genotype that doesn't produce unreduced pollen. Subsequently, we will characterize the function of *StPS* gene by silencing its expression through PTGS and expressing its cDNA in an another diploid potato genotype that produces unreduced pollen grains.

**Changes in histone acetylation during male meiosis in *Arabidopsis thaliana***

*Gaetana Cremona, Federica Consiglio, Riccardo Aiese Cigliano, Clara Conicella  
CNR-Institute of Plant Genetics, UOS Portici*

Epigenetic states, and particularly histone modifications are increasingly recognized as playing important roles in chromosome organization during meiosis. Histone acetylation may influence chromatin structure by altering the interactions of histones between adjacent nucleosomes or with the DNA and/or by collectively establishing a code recognized by downstream effector proteins and complexes. In some mammalian oocytes, the equilibrium between the acetylation/deacetylation state of the chromatin is shifted dramatically during meiosis. To date, histone acetylation dynamics was not exhaustively investigated in plant meiosis. Only brief descriptions have been reported relatively to some stages in plant meiotic mutants. However, studies performed in other organisms indicate that histone acetylation play a role in meiotic progression, meiotic recombination, and chromosome segregation. In the present study, we investigated the acetylation state in all stages of male meiosis in *Arabidopsis thaliana* using a panel of antibodies specific for acetylated forms of histone H3 and H4. In particular, immunocytochemical experiments were performed by antibodies raised against acetylated lysine 9 and 14 of histone H3 (Ac-H3K9K14) and acetylated lysine 5 and 16 of histone H4 (Ac-H4K5, Ac-H4K16) in Col-O ecotype. The results showed that the patterns of histone acetylation in male meiocytes were meiosis stage- dependent and lysine residue-specific.

Presented by: **Cremona, Gaetana**

## ANALYSIS OF *PARALLEL SPINDLES-LIKE* GENE FAMILY IN PLANTS

AIESE CIGLIANO R.\*, SANSEVERINO W.\*\*\*, CREMONA G.\*, PAPARO R.\*, CONSIGLIO M.F.\*, CONICELLA C.\*

\*) CNR-IGV, Institute of Plant Genetics, Research Division Portici, Via Università 133, 80055 Portici (Italy)

\*\*) Department of Soil, Plant, Environment and Animal Production Sciences, University of Naples Federico II, Via Università 100, 80055 Portici (Italy)

### *Potato, PS, 2n gametes, sexual polyploidization*

Polyploidy was estimated to occur in angiosperms from 30% to 80% of the species that include also important economic crops such as wheat, banana, potato, and alfalfa. Several works postulate that polyploids originated from genetic mutations leading to diploid ( $2n$ ) gametes. Furthermore,  $2n$  gametes emerged as a significant tool in the development of new breeding strategies. For instance,  $2n$  gametes have been used in potato to transmit useful traits from diploid wild relatives to tetraploid cultivated genotypes (*Solanum tuberosum*) through crossing schemes based on sexual polyploidization.

In *Solanum* spp., different cytological mechanisms leading to meiotic nuclear restitution were identified and a single recessive mutation in a gene termed *PARALLEL SPINDLES* (*PS*) was suggested to be responsible of one of these mechanisms causing  $2n$  gametes. However, the genomic complexity of *Solanum* species delayed functional study of *PS* gene. Recently, d'Erfurth and colleagues (PLoS Genet 2008, 4) provided the first molecular analysis of *PS* homologue (*AtPS1*) in *Arabidopsis* mutants displaying diploid pollen.

Taking advantage of the characterization of *AtPS1* gene a sequence-homology-based strategy was employed to isolate *PS-like* sequences in a diploid ( $2n = 2x = 24$ ) potato clone. We isolated seven cDNAs and one genomic clone sharing 33-37% and 44% of nucleotide identity with *AtPS1* cDNA and genomic sequences, respectively. Molecular and phylogenetic analysis of potato *PS-like* sequences confirmed a more complicated landscape of this family respect to *Arabidopsis* in which only one locus has been identified. Indeed, differentially spliced cDNAs were found and the existence of at least three different *PS-like* loci was inferred. Moreover, preliminary analysis of *PS-like* genes in different plant families showed a various degree of complexity. For instance, in *Glycine max* four loci were identified on public databases. Further bioinformatic studies will be carried out to get more hints about the evolution of *PS-like* gene family.

## **HISTONE ACETYLATION CONTROLS MEIOTIC CROSSOVER DISTRIBUTION IN *ARABIDOPSIS THALIANA***

AIESE CIGLIANO R., PERRELLA G., CREMONA G., PAPARO R., CONSIGLIO M.F., CONICELLA C.

Institute of Plant Genetics (IGV) – CNR, Portici, Via Università 133, 80055 Portici (Italy)

*Histone acetylation, meiosis, Arabidopsis, chiasmata*

Traditional plant breeding techniques are based on genetic exchange (crossovers) during homologous recombination in meiosis which creates new combinations of alleles. The frequency and distribution of meiotic crossovers (COs), affecting the number of loci that recombine, are a major constraint to future crop improvement. In cereal crops, for example, COs are predisposed to the ends of the chromosomes such that about 30-50% of the genes rarely recombine.

Post-translational modifications of histones during meiosis are being recognized as playing important roles in chromosome structure, recombination and segregation in several organisms but in spite of their importance the precise function and regulation are sketchy in plants.

Following activation tagging approach, a dominant mutation in *Arabidopsis thaliana* was isolated leading to the over-expression of the histone acetylase *MEIOTIC CONTROL OF CROSSOVERS 1 (MCC1)* (Perrella et al. 2010, Plant J 62(5): 796-806). Enhanced expression of *MCC1* caused histone hyperacetylation in male meiosis as revealed by immunolocalization with H3K9K14Ac antibody. Moreover, *mcc1* exhibited an early flowering, a reduced fertility with siliques carrying few seeds and a lower terminal height as compared to wild type. Cytological analysis of microsporogenesis showed meiotic defects such as aberrant chromosome condensation at diakinesis and univalent chromosomes at metaphase I. At meiosis II, the disjunction of sister chromatids occurred asynchronously in *mcc1* and migration of the chromatids towards the poles was irregular giving rise to an unequal sister chromatid distribution at telophase II. Female meiosis was also investigated in *mcc1* revealing defects similar to those observed in male meiosis. Fluorescent *in situ* hybridization on male meiocytes with 45S and 5S rDNA probes indicated that the univalents were exclusively nucleolar chromosome 2. Furthermore, analysis of chiasma frequency showed that elevated *MCC1* did not affect crossover number per cell, but has a differential effect on individual chromosomes elevating COs for chromosome 4, in which there is also a shift in chiasma distribution, and reducing COs for chromosome 1 and 2. The observed meiotic defects led to abortion in about half of the male and female gametes in the mutant.

In wild type, the treatment with the inhibitor of histone deacetylases, trichostatin A, phenocopies *MCC1* over-expression in meiosis.

Our work demonstrated for the first time in plant that histone acetylation has a significant impact on the control of meiotic recombination. For this reason, we started a systematic analysis of genes involved in histone modifications and chromatin remodeling in order to identify factors controlling meiotic recombination in higher plants.

**HISTONE MODIFICATION DYNAMICS DURING MALE MEIOSIS IN  
*ARABIDOPSIS THALIANA***

CREMONA G. \*, AIESE CIGLIANO R. \*, CONSIGLIO M.F. \*, VIOTTI A. \*\*, CONICELLA C. \*

\*) CNR-IGV, Institute of Plant Genetics, Research Division Portici, Via Università 133, 80055 Portici (Italy)

\*\*) CNR-IBBA, Institute of Biology and Agricultural Biotechnology, Via Bassini 15, 20133 Milano (Italy)

*Acetylation, methylation, immunofluorescence*

Epigenetic states, and particularly histone post-translational modifications, i.e. phosphorylation, acetylation, methylation and ubiquitination, are increasingly recognized as playing important roles in chromatin organization during meiosis. These modifications can alter chromatin structure by affecting the interaction of histones between adjacent nucleosomes or with DNA and/or even by collectively establishing a histone code recognized by downstream effector proteins and complexes.

Histone acetylation and methylation involve the modification of different lysine residues mainly in the amino terminal region of H3 and H4 histone proteins. Histone acetylation plays a role in meiotic progression, recombination, and chromosome segregation, as evidenced in yeast and mammals. Moreover, cytological observations in mammalian oocytes showed that the equilibrium between the acetylation and deacetylation state of the chromatin shifted during meiosis. Similarly, histone methylation is essential for several aspects of meiotic chromosome pairing and recombination. Observations of mammalian oocytes revealed that, in contrast to acetylation, histone methylation appears to be relatively stable during meiosis.

To date, histone acetylation and methylation dynamics were not deeply investigated in plant meiosis and only brief descriptions have been reported relatively to some stages in plant meiotic mutants. In the present study, we investigated histones H3 and H4 acetylation and H3 methylation during male meiosis in *Arabidopsis thaliana* to infer relationships between histone marks and crucial meiotic events. In particular, immunocytochemical experiments were performed by antibodies raised against acetylated lysine (K) at both residues 9 and 14 or only residue 9 of histone H3 (H3K9/14ac, H3K9ac), and acetylated K5 or K16 of histone H4 (H4K5ac, H4K16ac) in Col-0 ecotype. Moreover and preliminarily, the occurrence of methylated lysine was investigated using an antibody against trimethylated K4 of histone H3 (H3K4me3). The results showed that the patterns of histone acetylation in male meiocytes were meiotic stage-dependent and lysine residue-specific, while the distribution of H3K4me3 was stable during the stages of meiosis so far examined.

**A HISTONE DEACETYLASE IS REQUIRED FOR FERTILITY, SEED GERMINATION AND SEEDLING GROWTH RATE IN *ARABIDOPSIS***

AIESE-CIGLIANO R., CREMONA G., PAPARO R., CONSIGLIO M.F., CONICELLA C.

CNR-Institute of Plant Genetics, UOS Portici, Via Università 133, 80055 Portici (Italy)

*Arabidopsis*, epigenetics, reproduction

Histone post-translational modifications (HPTMs) play a fundamental role in many aspects of plant development and interaction with environmental stimuli. In *Arabidopsis*, several works underlined the involvement of histone de-/acetylation in the determination of flowering time, organ identity, flower morphology and fertility. Based on *in silico* analysis which looked for histone acetylases/deacetylases (HATs/HDACs) preferentially expressed in *Arabidopsis* flower buds and orthologous genes involved in sexual reproduction in other organisms, a HDAC (hereinafter named *HDAC1*) was identified as the strongest candidate for a reproduction role in *Arabidopsis*. In this work, the function of this gene was investigated by reverse genetics. Plants over-expressing *HDAC1* (hereinafter *oeHDAC1*) as well as lines silenced by artificial miRNA (hereinafter *amiHDAC1*) have been analyzed. Both *oeHDAC1* and *amiHDAC1* show a drop in seed germination and changes of seedling growth rate. Moreover, *amiHDAC1* plants exhibit additional defects affecting plant reproduction. Indeed, delayed embryo development, seed abortion and silique semisterility were observed as well as abnormal ovules and defects in bivalent disjunction during microsporogenesis. Further molecular, biochemical and cytological analyses are being carried out to investigate the role of *HDAC1* in *Arabidopsis* reproduction.

The research leading to these results has received funding from the European Community's Seventh Framework Programme FP7/2007-2013 under grant agreement n. KBBE-2009-222883.

**DOWN-REGULATION OF A HISTONE DEACETYLASE AFFECTS MALE MEIOSIS IN *ARABIDOPSIS***

CREMONA G., AIESE-CIGLIANO R., PAPARO R., CONSIGLIO M.F., CONICELLA C.

CNR-Institute of Plant Genetics, UOS Portici, Via Università 133, 80055 Portici (Italy)

*Arabidopsis thaliana, histone acetylation, microsporogenesis*

Recent studies showed that histone post-translational modifications (HPTMs) are associated to meiotic events including homologous recombination, cohesion, chromosome segregation. Our previous work in *Arabidopsis* evidenced that histone acetylation is required for meiotic recombination and chromosome segregation in male meiosis (Perrella et al. *Plant J* 2010, 62: 796). Histone acetylation is a reversible process carried out by two classes of enzymes known as histone acetylases (HATs) and histone deacetylases (HDACs). In this work, we focused our attention on a HDAC recognized as a global regulator that is involved in different physiological and developmental processes in *Arabidopsis*. Down-regulation of this HDAC mediated by antisense RNA and T-DNA insertion caused male and female sterility. In order to elucidate the mechanisms underlying the reduction of plant fertility the functional role of this HDAC was investigated in male meiosis in T-DNA mutant characterized by lower expression level and transcript rearrangement as compared to wild type. Different abnormalities affecting pairing, recombination and chromosome segregation have been observed in the mutant. As compared to wild type meiocytes, homologous chromosomes appeared not fully synapsed in pachytene. At diplotene/diakinesis, two univalents were observed in 17% of male meiocytes indicating a failure of the obligate CO for one chromosome pair. At later stages, uneven chromosome distribution was evidenced, as well. It is likely that the meiotic defects are depending on the histone hyperacetylation caused by HDAC down-regulation.

**Insights into meiotic function of genes modifying histone acetylation in *Arabidopsis***

Riccardo Aiese Cigliano, Gaetana Cremona, Rosa Paparo, Federica Consiglio, Clara Conicella  
CNR-Institute of Plant Genetics, UOS Portici

Histone post-translational modifications (HPTMs) play a fundamental role in meiotic chromosome pairing, recombination and segregation as demonstrated in different organisms including mouse, yeast and human. The relationships between meiotic events and HPTMs are less known in plants. *Arabidopsis* genome is predicted to encode 12 histone acetylases (HATs), 18 histone deacetylases (HDACs), 40 histone methyltransferases (HMTs) and 4 histone ubiquitinases. On the basis of *in silico* analysis, we identified different candidates among HDACs that could have a meiotic role in *Arabidopsis*. To investigate the function of these genes *in vivo* we are silencing them by RNAi approach mediated by amiRNA (see also Cremona *et al.*, *this meeting*). Here, we report the preliminary analysis of a HDAC showing that its down-regulation leads to delay in embryo and plant development as well as some defects in microsporogenesis. As regards HATs, recently we demonstrated in the *Arabidopsis* mutant over-expressing a novel histone acetylase (*AtMCC1*) that histone hyper-acetylation affected meiotic recombination and chromosome segregation (Perrella *et al. Plant J* 2010, 62: 796). To investigate whether histone hypo-acetylation influences meiotic events, we silenced the expression of both *AtMCC1* and its paralogue (*At5g16800*). In this mutant, plant development seems to be unaffected while plant fertility and pollen viability drop-off. Further molecular, biochemical and cytological analyses are being carried out on HDAC and HAT mutants.

**Histone acetylation is required for meiotic recombination in *Arabidopsis***

Gaetana Cremona, Riccardo Aiese-Cigliano, Rosa Paparo, Federica Consiglio, Clara Conicella  
CNR-Institute of Plant Genetics, UOS Portici

Histone post-translational modifications (HPTMs) are crucial in meiosis. Indeed, recent studies highlighted HPTMs as associated to essential meiotic events including homologous recombination, cohesion, chromosome segregation. In *Arabidopsis*, by investigating over-expression of HAT GCN5-related gene (*AtMCC1*) in male meiosis we demonstrated that *AtMCC1* is required for meiotic recombination and chromosome segregation (Perrella *et al. Plant J* 2010, 62: 796). Histone acetylation is a reversible process carried out by two classes of enzymes known as histone acetylases (HATs) and histone deacetylases (HDACs). Here, we gain an insight into the functional role of a HDAC in *Arabidopsis* male meiosis (see also Aiese-Cigliano *et al.*, this meeting). We focused on a HDAC that was global regulator involved in many physiological and developmental processes. Down-regulation of this HDAC by antisense inhibition and T-DNA insertion leads to male and female sterility but the mechanisms underlying the reduction of plant fertility remain to be elucidated. Here, a dominant mutation dependent on T-DNA insertion was analyzed. RT-PCR indicated that HDAC gene was expressed in the mutant at a lower level than in wild type. Furthermore, a transcript rearrangement was evidenced by sequencing. Different abnormalities were observed in the mutant microsporogenesis. In particular, pairing, recombination and chromosome segregation were affected. As compared to wild type meiocytes, homologous chromosomes appeared not fully synapsed in pachytene. At diplotene/diakinesis, two univalents were observed in 17% of male meiocytes indicating a failure of the obligate CO for one chromosome pair. At later stages, uneven chromosome distribution was evidenced, as well. It is likely that the meiotic defects are due to a histone hyperacetylation caused by the HDAC down-regulation.